UC Santa Cruz
UC Santa Cruz Electronic Theses and Dissertations

Title
How Oceanography Influences The Foraging Behavior Of A Twilight Zone Predator, The Elephant Seal

Permalink
https://escholarship.org/uc/item/5rm2z0x5

Author
Keates, Theresa Rebecca

Publication Date
2022

Copyright Information

Peer reviewed|Thesis/dissertation

UNIVERSITY OF CALIFORNIA
SANTA CRUZ

**HOW OCEANOGRAPHY INFLUENCES THE FORAGING BEHAVIOR OF
A TWILIGHT ZONE PREDATOR, THE ELEPHANT SEAL**

A dissertation submitted in partial satisfaction
of the requirements for the degree of

DOCTOR OF PHILOSOPHY

in

OCEAN SCIENCES

by

Theresa R Keates

December 2022

The Dissertation of Theresa R Keates is
approved:

_____
Professor Daniel Costa, chair

_____
Professor Raphael Kudela

_____
Professor Jerome Fiechter

_____
Elliott Hazen, Ph.D.

_____
Steven Bograd, Ph.D.

_____
Peter Biehl
Vice Provost and Dean of Graduate Studies

Table of Contents

List of Tables

List of Figures

Abstract

How Oceanography Influences The Foraging Behavior Of A Twilight Zone Predator,
The Elephant Seal

By

Theresa R Keates

In a rapidly changing ocean that remains largely undersampled, physical and biological observations are crucial to understanding, predicting, and mitigating effects of anthropogenic stressors. Animals instrumented with oceanographic sensors offer valuable supplements to datasets from more traditional oceanographic methods while simultaneously offer information about the oceanography of areas significant to the animals. Marine predator foraging behavior relative to physical or biological features such as fronts, eddies, and phytoplankton blooms can be used to infer oceanographic influences on the distribution of pelagic prey. This dissertation applies tracking data from adult female northern elephant seals (*Mirounga angustirostris*) and southern elephant seals (*Mirounga leonina*) with *in situ* temperature, salinity, and chlorophyll fluorescence collected by instruments carried by the seals to investigating relationships between oceanographic features and the foraging behavior of these wide-ranging mesopelagic predators at basin- to submesoscales.

Chapter 1 investigated the behavior of northern elephant seals when they encountered eddies. This project used a 17-year dataset of time-depth recorders and concluded that while eddies are a minor feature of their habitat, seals do derive foraging benefits from both cyclonic and anticyclonic eddies. Our observations

suggest that physical prey aggregation is a more likely mechanism making eddies beneficial to foraging seals than bottom-up energetic enhancement of the food web resulting from nutrient injection.

Chapter 2 combined tracking data from northern and southern elephant seals to compare their behavior relative to the oceanographic conditions they encountered. This first direct comparison between the at-sea behavior of these two closely related species showed comparable movement and diving behavior and further, very similar relationships between behavior and temperature, salinity, and mixed layer depths encountered. Both seal populations were more responsive to horizontal variability in physical conditions during the post-molt trip than during the post-breeding trip and showed these inter-trip differences in behavior despite the seasonal offset in when the trips occur in their relative hemispheres. We conclude that these species employ similar strategies in two contrasting ocean basins, indicating that the mesopelagic prey field may be driven by similar oceanographic properties and seasonal resource pulses in both ocean basins.

Chapter 3 used *in situ* chlorophyll fluorescence data collected by seal-borne instruments and remotely sensed chlorophyll data to test whether elevated chlorophyll concentrations were associated with enhanced foraging behavior in northern elephant seals. We found that real-time chlorophyll data, despite having the advantage of containing subsurface data, did not predict seal foraging behavior. Instead, remotely sensed chlorophyll data from 2-4 months prior to seal presence was associated with

elevated foraging behavior. This effect was especially strong during the post-molt season when less of the seals' range was contained elevated chlorophyll but had several months prior. These chapters illuminate the interplay between intrinsic and extrinsic drivers of behavior and the role of spatiotemporal scale linking physics to biology in the open ocean.

Acknowledgements

There is no way for me to acknowledge in brief all the people I have to thank for their contributions over the last six years, but I will make an attempt. Thank you to my advisor, Dan Costa, for making an exception and taking on a Master's student – who ended up sticking around, as you predicted. The opportunities you have given me have been truly life-changing, from working with wild elephant seals to traveling to international conferences. Thank you to the rest of my committee, Raphe, Jerome, Steven, and Elliott, for each offering valuable perspectives and advice along the way. It's from your diverse expertise I was able to pursue the interdisciplinary research questions I was fascinated by.

Thank you to Rachel and Caitie, who I have chosen as my big sisters whether they want to be or not. Rachel, you helped me find my feet when I first arrived in the lab (and again and again since) and have been the best coworker in field work and data crunching I could have asked for. Aside from the science, you have always been there for over the last six years and I don't know if I could have done this without you. Many runs and many cookie bakings helped me keep my sanity. Caitie, you gave me so much great advice and made me feel understood when things were hard. Your spirit and perseverance encourage me to be better. All of our work parties featuring laughter, snacks, and naps in blanket nests I will cherish forever.

Luis, thank you for being a selfless mentor and sharing with me such singular opportunities such as a research trip to the Antarctic Peninsula. I learned so much from you, at work and possibly even more over drinks – an observation I'm sure you'd approve of. Hope, thanks for reading most things I ever wrote and listening to most talks I ever practiced, and improving every single one of them. I loved the time we spent together on bikes, you inspired me to test my physical and intellectual limits and I have appreciated your friendship since day one of graduate school orientation so much. Thank you Laney for being the most kind, open, and generous friend I could have found in a roommate connected through mutual acquaintances from thousands

of miles apart. Logan and Arina, field working with you was always such a joy. You are both such humble high achievers and I am so excited to see where you go next. Chris, I've loved our many paddle adventures, always featuring a beer. Jason, you have been so incredibly supportive and helpful as I navigate career decisions (also often featuring beer) and I'm so excited to be your neighbor in a few weeks.

Ena and Tori, some of my oldest friends, you helped me see there is a world outside of graduate school and I am so grateful for your steadfast friendship even if our busy lives mean we don't always see each other very often. Kaitlyn, I'm glad we get to be in each other's lives through our various adventures since our undergrad, may this continue the rest of our lives. Lena, we've known each other since childhood and it's been so fun to end up on our PhD journeys in the same place. Thank you to my family, especially my parents and my sister Pauline, for your unconditional love and support and enthusiasm for whatever I decide to do next in life.

This is a very incomplete list, but every member of my Santa Cruz community and those residing geographically further afield – thank you. A big hug to all of you.

- Theresa

Introduction

Physical and biological observations of the rapidly changing ocean are crucial to understanding, predicting, and mitigating effects of anthropogenic stressors. A variety of oceanographic variables (*e.g.* temperature, salinity, and chlorophyll fluorescence) are routinely measured by a large array of sampling platforms from Argo floats to satellites; further sampling methods and platforms are needed to better meet global ocean observing needs. Deploying tracking tags on marine megafauna (or "biologging") offers a valuable supplement to more traditional ocean observing methods by providing data from remote regions at relatively low cost (Miloslavich et al., 2018). The ocean observational potential of biologging is twofold: first, such technology remotely documents movements and behaviors of animals that are inherently difficult to observe directly in their natural habitat, thus providing insight into their ecology, and second, these behavioral observations coupled with *in situ* environmental data at fine scales can document organismal relationships to their environment in unprecedented detail (*e.g.* Bograd et al. 2010, Costa et al. 2012, Hussey et al. 2015, Harcourt et al. 2019).

Marine predator foraging behavior relative to physical or biological features such as fronts, eddies, or phytoplankton assemblages can be used to infer oceanographic influences on the distribution of pelagic prey. Oceanographic features such as fronts, eddies, and phytoplankton blooms can be roughly documented on a global scale using remote sensing, but an increased understanding of their ecological significance across

trophic levels benefits marine spatial management and prediction of climate change effects on marine ecosystems (eg. Woodson and Litvin 2015). Biologging is a powerful tool to investigate biological hotspots in the pelagic ocean and address the ecological significance of oceanographic features by both documenting their structure *in situ* and representing their ecological importance through their behavior (Palacios et al., 2006). Many marine predators associate with oceanographic features such as fronts and eddies (Bost et al., 2009; Godø et al., 2012; Olson et al., 1994), including basking sharks (Miller et al., 2015), blue sharks (Braun et al., 2019), white sharks (Gaube et al., 2018), king penguins (Cotté et al., 2007), seabirds (eg. Bost et al. 2009, Tew Kai et al. 2009), albacore tuna (Snyder et al., 2017; Zainuddin et al., 2008), loggerhead sea turtles (Kobayashi et al., 2008; Polovina et al., 2006), leatherback sea turtles (Lambardi et al., 2008), cetaceans (Davis et al., 2002; Woodworth et al., 2012), northern fur seals (Nordstrom et al., 2013; Ream et al., 2005), Antarctic fur seals (Guinet et al., 2001; Lea and Dubroca, 2003), southern elephant seals (Bailleul et al., 2010b; Bost et al., 2009; Campagna et al., 2006; Cotté et al., 2015; Gordine et al., 2019; Massie et al., 2016), and northern elephant seals (Abrahms et al., 2017; Simmons et al., 2007). Several large marine predators have been found to associate with elevated primary productivity, including humpback whales (Trudelle et al., 2016), tuna (Walli et al., 2009), Cape gannets (Grémillet et al., 2008), Antarctic fur seals (Guinet et al., 2001; Lea and Dubroca, 2003) and southern elephant seals (Cotté et al., 2015). Most such studies rely on remotely sensed oceanographic data (eg. Davis et al. 2002, Lea and Dubroca 2003, Bradshaw et al. 2004a, Ream et al. 2005,

Palacios et al. 2006, Simmons et al. 2007, Zainuddin et al. 2008, Lambardi et al. 2008, Woodworth et al. 2012, Scales et al. 2014b, Tosh et al. 2015, Cotté et al. 2015, Sousa et al. 2016, Lee et al. 2017, Ballard et al. 2019) and commonly identify oceanographic features using satellite-derived sea surface temperature (Belkin and O'Reilly, 2009; Liu and Levine, 2016; Miller, 2009; Miller et al., 2015; Miller and Christodoulou, 2014; Scales et al., 2014a; Ullman and Cornillon, 2000), sea surface height (Abrahms et al., 2018; Bailleul et al., 2010b; Charrassin et al., 2008; Cotroneo et al., 2013; Nordstrom et al., 2013; Prants et al., 2014), or ocean color (Belkin and O'Reilly, 2009; Miller, 2009; Miller et al., 2015). While invaluable for providing large-scale context, remotely sensed data are broad in resolution and only document the near-surface ocean.

Deriving oceanographic data directly from biologging instruments can provide valuable insights into physical-biological coupling at meso- to submesoscales. Biological resources in the open ocean are patchily distributed (Haury et al., 1978; Mackas et al., 1985; Steele, 1978), with ultimate implications for predator ecology (*e.g.* Benoit-Bird et al., 2013) as well as resource management (Scales et al., 2018). Pelagic organisms operate in three dimensions and may respond to shorter-lived and/or subsurface features that are undetectable using remotely sensed data alone. Subsurface hydrographic properties may be especially important to deep-diving predators whose prey may be further removed from near-surface oceanographic processes. Only a handful of studies to date have investigated predator foraging behavior in relation to hydrographic features identified *in situ*, and all mammal

studies of this kind are limited to the Southern Ocean (Bailleul et al., 2007; Biuw et al., 2007; Dragon et al., 2010; Jaud et al., 2012; Vacquié-Garcia et al., 2015), with one North Pacific example examining tuna crossing fronts in the California Current System (Snyder et al., 2017). This dissertation furthers the understanding of physical effects on mesopelagic biology by evaluating environmental influences on the behavior of a mesopelagic predator, utilizing *in situ*, remotely sensed, and modeled oceanographic data.

Biologging instruments with oceanographic sensors, such as Conductivity-Temperature-Depth Satellite Relay Data Loggers (CTD-SRDLs, Boehme et al. 2009), have been deployed extensively in the Southern Ocean over the last decade to describe physical oceanography (Boehme et al., 2008a, 2008b; Charrassin et al., 2008) and seal distribution relative to their physical environment (eg. Bailleul et al., 2007; Biuw et al., 2007; Bradshaw et al., 2004; Guinet et al., 2014). These CTD tags have been deployed on northern elephant seals (*Mirounga angustirostris*) at Año Nuevo Reserve and San Nicolas Island since 2009 with great potential for far-reaching applications spanning physical oceanography to trophic ecology. Older time-depth recorders that record temperature have not been used as extensively for oceanographic applications but nonetheless provide valuable data to profile ocean features at high horizontal resolution, as they measure temperature during every dive a seal makes. These instruments were deployed on adult female northern elephant seals at Año Nuevo Reserve and San Nicolas Island in California and San Benito

Island in Mexico. Instruments were deployed on southern elephant seals (*Mirounga leonina*) at Kerguelen Islands and Macquarie Island.

Long-term demographic and tracking studies on closely related northern elephant seals in the North Pacific and southern elephant seals in the Southern Ocean show similar life histories in two distant ocean basins (Hindell, 2018; Hindell et al., 2016; Le Boeuf et al., 2000; Robinson et al., 2012). Between on-land fasting periods to breed and to molt, adult females undergo two foraging trips annually. They spend two to three months at sea after breeding (between November and January in southern elephant seals; between February and April in northern elephant seals) and about 8 months after molting (between March and October in southern elephant seals; between June and January in northern elephant seals) (Hindell and Burton, 1988; Le Boeuf and Laws, 1994). They predominately spend this time in the open ocean (Bailleul et al., 2010a; Hindell et al., 2021, 1991; Kienle et al., 2022; Le Boeuf et al., 2000; Robinson et al., 2012) diving continuously and heavily utilizing the mesopelagic zone (McMahon et al., 2019; Naito et al., 2017; Robinson et al., 2012). The diet of female seals is dominated by mesopelagic fishes, especially myctophids, and some squid (Bailleul et al., 2010a; Banks et al., 2014; Bradshaw et al., 2003; Cherel et al., 2008; Ducatez et al., 2008; Goetsch et al., 2018; Guinet et al., 2014; Naito et al., 2013; Yoshino et al., 2020).

The mesopelagic zone remains mysterious and poorly understood. Observations of these depths, especially in offshore regions, are logistically challenging; indirect

observations through animal tracking studies offer promising new insights. The biomass of the mesopelagic zone is thought to be huge, though uncertainty in estimates are large, ranging from 1,000 million tons (Gjøsæter and Kawaguchi 1980, Lam and Pauly 2005) to an order of magnitude higher (Irigoien et al., 2014). The biota of the mesopelagic plays a large role in active transport of carbon to depth (Irigoien et al., 2014): in oligotrophic areas in can account for up to 40% of the carbon export while in highly productive areas, the mesopelagic community may mediate between 10-15% of the carbon export (Davison et al., 2013). Given some developing interest in commercial exploitation of mesopelagic fish, primarily for fishmeal (eg. Valinassab, Pierce, & Johannesson 2007, Gjøsæter and Kawaguchi 1980, see also citations in St. John et al. 2016) and upcoming deep-sea mining activities will have thus far poorly defined consquences on this depth zone (Drazen et al., 2020), understanding this ecosystem is imperative to inform future management (St. John et al., 2016).

Mesopelagic biomass correlates to primary productivity, demonstrating that at large scales, this deep-water environment is coupled to the surface ocean (Davison et al., 2013; Irigoien et al., 2014; Proud et al., 2017). Mesopelagic predator tracking can shed new light on the spatiotemporal dynamics of this dependency at finer scales, improving our ability to predict subsurface manifestations of near-surface processes that are easier to observe.

These chapters use extensive tracking datasets of adult female northern elephant seals (*Mirounga angustirostris*) and southern elephant seals (*Mirounga leonina*) to investigate relationships between basin- to mesoscale oceanographic features and the foraging behavior of these wide-ranging mesopelagic predators. The environmental influences on the spatial and temporal distribution of foraging elephant seals allows inference of distribution of their poorly understood prey. This research will contribute to our understanding of physical and biological surface-to-deep-ocean coupling, assisting prediction of the biological effects of changing ocean conditions.

Chapter 1 identified and tracked eddies in northeast Pacific that northern elephant seals encounter, characterized the three-dimensional extent, approximate age, and rotational direction of those eddies, and determined whether these eddies are associated with a behavior change in seals. We hypothesized that seals would show heightened foraging behavior when they encountered eddies, that this effect would be stronger in association with anticyclonic eddies than cyclonic eddies, and that older eddies would elicit a stronger behavioral response than younger eddies as they would have had more time to accumulate a denser prey field. Chapter 2 leverages tracking data from closely related northern and southern elephant seals to compare oceanographic influences to foraging behavior while also comparing the two species' behavior at sea for the first time. Because adult females of both species are morphologically similar and rely on the same kinds of prey, we aimed to infer oceanographic drivers of the prey field operating in the northeast Pacific and the Southern Ocean. We expected similar ranges in behavior in both species, but salinity

to be a stronger driver of behavior in southern elephant seals due to the more distinct water masses in the Southern Ocean relative to the northeast Pacific and that fronts would be a stronger influence on foraging behavior in the Southern Ocean. Chapter 3 combines an *in situ* chlorophyll fluorescence dataset collected by instrumented elephant seals and additionally incorporates remotely sensed ocean color data to explore relationships between primary productivity and the foraging behavior of this deep-water predator. We expected weak relationships between foraging behavior and concurrent chlorophyll concentrations measured by seal-borne instruments due to the time it would take for surface productivity to translate to higher trophic levels within the mesopelagic zone. This would result in a weaker, more spatiotemporally diffuse relationship, which we expected to see evidence of using remotely sensed chlorophyll data collected prior to seal presence. These chapters strengthen our understanding of physical and biological surface-to-mid-ocean coupling in two ocean basins, which helps predict biological consequences of changing ocean conditions.

References

Abrahms, B., Hazen, E.L., Bograd, S.J., Brashares, J.S., Robinson, P.W., Scales, K.L., Crocker, D.E., Costa, D.P., 2017. Climate mediates the success of migration strategies in a marine predator. Ecol. Lett. doi:10.1111/ele.12871

Abrahms, B., Scales, K.L., Hazen, E.L., Bograd, S.J., Schick, R.S., Robinson, P.W., Costa, D.P., 2018. Mesoscale activity facilitates energy gain in a top predator. Proc. Natl. Acad. Sci. B 285. doi:10.1098/rspb.2018.1101

Bailleul, F., Authier, M., Ducatez, S., Roquet, F., Charrassin, J.B., Cherel, Y., Guinet, C., 2010a. Looking at the unseen: Combining animal bio-logging and stable isotopes to reveal a shift in the ecological niche of a deep diving predator. Ecography (Cop.). 33, 709–719. doi:10.1111/j.1600-0587.2009.06034.x

Bailleul, F., Charrassin, J.-B., Monestiez, P., Roquet, F., Biuw, M., Guinet, C., 2007. Successful foraging zones of southern elephant seals from the Kerguelen Islands in relation to oceanographic conditions. Philos. Trans. R. Soc. B Biol. Sci. 362, 2169–2181. doi:10.1098/rstb.2007.2109

Bailleul, F., Cotté, C., Guinet, C., 2010b. Mesoscale eddies as foraging area of a deep-diving predator, the southern elephant seal. Mar. Ecol. Prog. Ser. 408, 251–264. doi:10.3354/meps08560

Ballard, G., Schmidt, A.E., Toniolo, V., Veloz, S., Jongsomjit, D., Arrigo, K.R., Ainley, D.G., 2019. Fine-scale oceanographic features characterizing successful

Adélie penguin foraging in the SW Ross Sea. Mar. Ecol. Prog. Ser. 608, 263–277.

Banks, J., Lea, M.A., Wall, S., McMahon, C.R., Hindell, M.A., 2014. Combining bio-logging and fatty acid signature analysis indicates spatio-temporal variation in the diet of the southern elephant seal, Mirounga leonina. J. Exp. Mar. Bio. Ecol. 450, 79–90. doi:10.1016/j.jembe.2013.10.024

Belkin, I.M., O'Reilly, J.E., 2009. An algorithm for oceanic front detection in chlorophyll and SST satellite imagery. J. Mar. Syst. 78, 319–326. doi:10.1016/j.jmarsys.2008.11.018

Benoit-Bird, K.J., Battaile, B.C., Nordstrom, C.A., Trites, A.W., 2013. Foraging behavior of northern fur seals closely matches the hierarchical patch scales of prey. Mar. Ecol. Prog. Ser. 479, 283–302. doi:10.3354/meps10209

Biuw, M., Boehme, L., Guinet, C., Hindell, M., Costa, D., Charrassin, J.-B., Roquet, F., Bailleul, F., Meredith, M., Thorpe, S., Tremblay, Y., McDonald, B., Park, Y.-H., Rintoul, S.R., Bindoff, N., Goebel, M., Crocker, D., Lovell, P., Nicholson, J., Monks, F., Fedak, M.A., 2007. Variations in behavior and condition of a Southern Ocean top predator in relation to *in situ* oceanographic conditions. Proc. Natl. Acad. Sci. U. S. A. 104, 13705–10. doi:10.1073/pnas.0701121104

Boehme, L., Lovell, P., Biuw, M., Roquet, F., Nicholson, J., Thorpe, S.E., Meredith, M.P., Fedak, M., 2009. Technical note: Animal-borne CTD-Satellite Relay Data Loggers for real-time oceanographic data collection. Ocean Sci. 5, 685–695.

doi:10.5194/os-5-685-2009

Boehme, L., Meredith, M.P., Thorpe, S.E., Biuw, M., Fedak, M., 2008a. Antarctic

circumpolar current frontal system in the South Atlantic: Monitoring using

merged Argo and animal-borne sensor data. J. Geophys. Res. Ocean. 113, 1–19.

doi:10.1029/2007JC004647

Boehme, L., Thorpe, S.E., Meredith, M.P., 2008b. Monitoring Drake Passage with

elephant seals : Frontal structures and snapshots of transport. Limnol. Oceanogr.

53, 2350–2360.

Bograd, S.J., Block, B.A., Costa, D.P., Godley, B.J., 2010. Biologging technologies:

New tools for conservation. Introduction. Endanger. Species Res. 10, 1–7.

doi:10.3354/esr00269

Bost, C.A., Cotté, C., Bailleul, F., Cherel, Y., Charrassin, J.B., Guinet, C., Ainley,

D.G., Weimerskirch, H., 2009. The importance of oceanographic fronts to

marine birds and mammals of the southern oceans. J. Mar. Syst. 78, 363–376.

doi:10.1016/j.jmarsys.2008.11.022

Bradshaw, C.J.A., Higgins, J., Michael, K.J., Wotherspoon, S.J., Hindell, M.A., 2004.

At-sea distribution of female southern elephant seals relative to variation in

ocean surface properties. ICES J. Mar. Sci. 61, 1014–1027.

doi:10.1016/j.icesjms.2004.07.012

Bradshaw, C.J.A., Hindell, M.A., Best, N.J., Phillips, K.L., Wilson, G., Nichols, P.D.,

2003. You are what you eat: describing the foraging ecology of southern elephant seals (Mirounga leonina) using blubber fatty acids. Proc. R. Soc. B Biol. Sci. 207, 1283–1292. doi:10.1098/rspb.2003.2371

Braun, C.D., Gaube, P., Sinclair-Taylor, T.H., Skomal, G.B., Thorrold, S.R., 2019. Mesoscale eddies release pelagic sharks from thermal constraints to foraging in the ocean twilight zone. Proc. Natl. Acad. Sci. 201903067. doi:10.1073/pnas.1903067116

Campagna, C., Piola, A.R., Rosa Marin, M., Lewis, M., Fernández, T., 2006. Southern elephant seal trajectories, fronts and eddies in the Brazil/Malvinas Confluence. Deep. Res. Part I Oceanogr. Res. Pap. 53, 1907–1924. doi:10.1016/j.dsr.2006.08.015

Charrassin, J.-B., Hindell, M., Rintoul, S.R., Roquet, F., Sokolov, S., Biuw, M., Costa, D.P., Boehme, L., Lovell, P., Coleman, R., Timmermann, R., Meijers, A., Meredith, M., Park, Y.-H., Bailleul, F., Goebel, M., Tremblay, Y., Bost, C.-A., McMahon, C.R., Field, I.C., Fedak, M.A., Guinet, C., 2008. Southern Ocean frontal structure and sea-ice formation rates revealed by elephant seals. Proc. Natl. Acad. Sci. U. S. A. 105, 11634–11639. doi:10.1073/pnas.0800790105

Cherel, Y., Ducatez, S., Fontaine, C., Richard, P., Guinet, C., 2008. Stable isotopes reveal the trophic position and mesopelagic fish diet of female southern elephant seals breeding on the Kerguelen Islands. Mar. Ecol. Prog. Ser. 370, 239–247. doi:10.3354/meps07673

Costa, D.P., Breed, G. a., Robinson, P.W., 2012. New insights into pelagic

    migrations: Implications for ecology and conservation. Annu. Rev. Ecol. Evol.

    Syst. 43, 73–96. doi:10.1146/annurev-ecolsys-102710-145045

Cotroneo, Y., Budillon, G., Fusco, G., Spezie, G., 2013. Cold core eddies and fronts

    of the Antarctic Circumpolar Current south of New Zealand from *in situ* and

    satellite data. J. Geophys. Res. Ocean. 118, 2653–2666. doi:10.1002/jgrc.20193

Cotté, C., D'Ovidio, F., Dragon, A.C., Guinet, C., Lévy, M., 2015. Flexible

    preference of southern elephant seals for distinct mesoscale features within the

    Antarctic Circumpolar Current. Prog. Oceanogr. 131, 46–58.

    doi:10.1016/j.pocean.2014.11.011

Cotté, C., Park, Y.H., Guinet, C., Bost, C.A., 2007. Movements of foraging king

    penguins through marine mesoscale eddies. Proc. R. Soc. B Biol. Sci. 274,

    2385–2391. doi:10.1098/rspb.2007.0775

Davis, R.W., Ortega-Ortiz, J.G., Ribic, C.A., Evans, W.E., Biggs, D.C., Ressler, P.H.,

    Cady, R.B., Leben, R.R., Mullin, K.D., Bernd, W., 2002. Cetacean habitat in the

    northern oceanic Gulf of Mexico. Deep Sea Res. 49, 121–142.

    doi:10.1016/S0967-0637(01)00035-8

Davison, P.C., Checkley, D.M., Koslow, J.A., Barlow, J., 2013. Carbon export

    mediated by mesopelagic fishes in the northeast Pacific Ocean. Prog. Oceanogr.

    116, 14–30. doi:10.1016/j.pocean.2013.05.013

Dragon, A.C., Monestiez, P., Bar-Hen, A., Guinet, C., 2010. Linking foraging behaviour to physical oceanographic structures: Southern elephant seals and mesoscale eddies east of Kerguelen Islands. Prog. Oceanogr. 87, 61–71. doi:10.1016/j.pocean.2010.09.025

Drazen, J.C., Smith, C.R., Gjerde, K.M., Haddock, S.H.D., Carter, G.S., Anela Choy, C., Clark, M.R., Dutrieux, P., Goetze, E., Hauton, C., Hatta, M., Anthony Koslow, J., Leitner, A.B., Pacini, A., Perelman, J.N., Peacock, T., Sutton, T.T., Watling, L., Yamamoto, H., 2020. Midwater ecosystems must be considered when evaluating environmental risks of deep-sea mining. Proc. Natl. Acad. Sci. U. S. A. 117, 17455–17460. doi:10.1073/pnas.2011914117

Ducatez, S., Dalloyau, S., Richard, P., Guinet, C., Cherel, Y., 2008. Stable isotopes document winter trophic ecology and maternal investment of adult female southern elephant seals (Mirounga leonina) breeding at the Kerguelen Islands. Mar. Biol. 155, 413–420. doi:10.1007/s00227-008-1039-3

Gaube, P., Braun, C.D., Lawson, G.L., McGillicuddy, D.J., Penna, A. Della, Skomal, G.B., Fischer, C., Thorrold, S.R., 2018. Mesoscale eddies influence the movements of mature female white sharks in the Gulf Stream and Sargasso Sea. Sci. Rep. 8, 7363. doi:10.1038/s41598-018-25565-8

Godø, O.R., Samuelsen, A., Macaulay, G.J., Patel, R., Hjøllo, S.S., Horne, J., Kaartvedt, S., Johannessen, J.A., 2012. Mesoscale eddies are oases for higher trophic marine life. PLoS One 7, 1–9. doi:10.1371/journal.pone.0030161

Goetsch, C., Conners, M.G., Budge, S.M., Mitani, Y., Walker, W.A., Bromaghin, J.F., Simmons, S.E., Reichmuth, C., Costa, D.P., 2018. Energy-rich mesopelagic fishes revealed as a critical prey resource for a deep-diving predator using Quantitative Fatty Acid Signature Analysis. Front. Mar. Sci. 5, 1–19. doi:10.3389/fmars.2018.00430

Gordine, S.A., Fedak, M.A., Boehme, L., 2019. The importance of Southern Ocean frontal systems for the improvement of body condition in southern elephant seals. Aquat. Conserv. Mar. Freshw. Ecosyst. 29, 283–304. doi:10.1002/aqc.3183

Grémillet, D., Lewis, S., Drapeau, L., Van Der Lingen, C.D., Huggett, J.A., Coetzee, J.C., Verheye, H.M., Daunt, F., Wanless, S., Ryan, P.G., 2008. Spatial match-mismatch in the Benguela upwelling zone: Should we expect chlorophyll and sea-surface temperature to predict marine predator distributions? J. Appl. Ecol. 45, 610–621. doi:10.1111/j.1365-2664.2007.01447.x

Guinet, C., Dubroca, L., Lea, M.A., Goldsworthy, S., Cherel, Y., Duhamel, G., Bonadonna, F., Donnay, J.P., 2001. Spatial distribution of foraging in female antarctic fur seals Arctocephalus gazella in relation to oceanographic variables: A scale-dependent approach using geographic information systems. Mar. Ecol. Prog. Ser. 219, 251–264. doi:10.3354/meps219251

Guinet, C., Vacquie-Garcia, J., Picard, B., Bessigneul, G., Lebras, Y., Dragon, A.C., Viviant, M., Arnould, J.P.Y., Bailleul, F., 2014. Southern elephant seal foraging

success in relation to temperature and light conditions: Insight into prey

distribution. Mar. Ecol. Prog. Ser. 499, 285–301. doi:10.3354/meps10660

Harcourt, R., Sequeira, A.M.M., Zhang, X., Roquet, F., Komatsu, K., Heupel, M.,

McMahon, C., Whoriskey, F., Meekan, M., Carroll, G., Brodie, S.,

Simpfendorfer, C., Hindell, M., Jonsen, I., Costa, D.P., Block, B., Muelbert, M.,

Woodward, B., Weise, M., Aarestrup, K., Biuw, M., Boehme, L., Bograd, S.J.,

Cazau, D., Charrassin, J.-B., Cooke, S.J., Cowley, P., de Bruyn, P.J.N.,

Jeanniard du Dot, T., Duarte, C., Eguíluz, V.M., Ferreira, L.C., Fernández-

Gracia, J., Goetz, K., Goto, Y., Guinet, C., Hammill, M., Hays, G.C., Hazen,

E.L., Hückstädt, L.A., Huveneers, C., Iverson, S., Jaaman, S.A.,

Kittiwattanawong, K., Kovacs, K.M., Lydersen, C., Moltmann, T., Naruoka, M.,

Phillips, L., Picard, B., Queiroz, N., Reverdin, G., Sato, K., Sims, D.W.,

Thorstad, E.B., Thums, M., Treasure, A.M., Trites, A.W., Williams, G.D.,

Yonehara, Y., Fedak, M.A., 2019. Animal-Borne Telemetry: An Integral

Component of the Ocean Observing Toolkit. Front. Mar. Sci. 6.

doi:10.3389/fmars.2019.00326

Haury, L.R., McGowan, J.A., Wiebe, P.H., 1978. Patterns and processes in the time-

space scales of plankton distributions, in: Steele, J.H. (Ed.), Spatial Pattern in

Plankton Communities. Plenum Press, New Y, pp. 277–328.

Hindell, M.A., 2018. Elephant Seals: Mirounga angustirostris and M. leonina, in:

Encyclopedia of Marine Mammals. pp. 303–307. doi:10.1016/b978-0-12-

804327-1.00115-1

Hindell, M.A., Burton, H.R., 1988. Seasonal Haul-Out Patterns of the Southern
Elephant Seal (Mirounga leonina L.), at Macquarie Island. J. Mammal. 69, 81–
88.

Hindell, M.A., Burton, H.R., Slip, D.J., 1991. Foraging areas of southern elephant
seals, mirounga leonina, as inferred from water temperature data. Mar. Freshw.
Res. 42, 115–128. doi:10.1071/MF9910115

Hindell, M.A., McMahon, C.R., Bester, M.N., Boehme, L., Costa, D., Fedak, M.A.,
Guinet, C., Herraiz-Borreguero, L., Harcourt, R.G., Huckstadt, L., Kovacs,
K.M., Lydersen, C., McIntyre, T., Muelbert, M., Patterson, T., Roquet, F.,
Williams, G., Charrassin, J.B., 2016. Circumpolar habitat use in the southern
elephant seal: Implications for foraging success and population trajectories.
Ecosphere 7, 1–27. doi:10.1002/ecs2.1213

Hindell, M.A., McMahon, C.R., Jonsen, I., Harcourt, R., Arce, F., Guinet, C., 2021.
Inter- and intrasex habitat partitioning in the highly dimorphic southern elephant
seal. Ecol. Evol. 1–14. doi:10.1002/ece3.7147

Hussey, N.E., Kessel, S.T., Aarestrup, K., Cooke, S.J., Cowley, P.D., Fisk, A.T.,
Harcourt, R.G., Holland, K.N., Iverson, S.J., Kocik, J.F., Flemming, J.E.M.,
Whoriskey, F.G., 2015. Aquatic animal telemetry: A panoramic window into the
underwater world. Science (80-.). 348, 1255642. doi:10.1126/science.1255642

Irigoien, X., Klevjer, T.A., Røstad, A., Martinez, U., Boyra, G., Acuña, J.L., Bode, A., Echevarria, F., Gonzalez-Gordillo, J.I., Hernandez-Leon, S., Agusti, S., Aksnes, D.L., Duarte, C.M., Kaartvedt, S., 2014. Large mesopelagic fishes biomass and trophic efficiency in the open ocean. Nat. Commun. 5, 3271. doi:10.1038/ncomms4271

Jaud, T., Dragon, A.-C., Garcia, J.V., Guinet, C., 2012. Relationship between chlorophyll a concentration, light attenuation and diving depth of the southern elephant seal Mirounga leonina. PLoS One 7, e47444. doi:10.1371/journal.pone.0047444

Kienle, S.S., Friedlaender, A.S., Crocker, D.E., Mehta, R.S., Costa, D.P., 2022. Trade-offs between foraging reward and mortality risk drive sex-specific foraging strategies in sexually dimorphic northern elephant seals. R. Soc. Open Sci. 9. doi:10.1098/rsos.210522

Kobayashi, D.R., Polovina, J.J., Parker, D.M., Kamezaki, N., Cheng, I.J., Uchida, I., Dutton, P.H., Balazs, G.H., 2008. Pelagic habitat characterization of loggerhead sea turtles, Caretta caretta, in the North Pacific Ocean (1997-2006): Insights from satellite tag tracking and remotely sensed data. J. Exp. Mar. Bio. Ecol. 356, 96–114. doi:10.1016/j.jembe.2007.12.019

Lam, V., Pauly, D., 2005. Mapping the global biomass of mesopelagic fishes. Sea around Us Proj. Newsl. July/Augus, 4.

Lambardi, P., Lutjeharms, J.R.E., Mencacci, R., Hays, G.C., Luschi, P., 2008.

Influence of ocean currents on long-distance movement of leatherback sea turtles in the Southwest Indian Ocean. Mar. Ecol. Prog. Ser. 353, 289–301. doi:10.3354/meps07118

Le Boeuf, B.J., Crocker, D.E., Costa, D.P., Blackwell, S.B., Webb, P.M., Houser, D.S., 2000. Foraging ecology of northern elephant seals. Ecol. Monogr. 70, 353–382. doi:10.1890/0012-9615(2000)070[0353:FEONES]2.0.CO;2

Le Boeuf, B.J., Laws, R.M. (Eds.), 1994. Elephant seals: population ecology, behavior, and physiology. . University of California Press, Berkeley.

Lea, M.A., Dubroca, L., 2003. Fine-scale linkages between the diving behaviour of Antarctic fur seals and oceanographic features in the southern Indian Ocean. ICES J. Mar. Sci. J. du … 60, 990–1002. doi:10.1016/S1054

Lee, J.F., Friedlaender, A.S., Oliver, M.J., DeLiberty, T.L., 2017. Behavior of satellite-tracked Antarctic minke whales (Balaenoptera bonaerensis) in relation to environmental factors around the western Antarctic Peninsula. Anim. Biotelemetry 5, 23. doi:10.1186/s40317-017-0138-7

Liu, X., Levine, N.M., 2016. Submesoscale frontal dynamics enhances phytoplankton chlorophyll in the North Pacific Subtropical Gyre. Geophys. Res. Lett. 43, 1651–1659. doi:10.1002/2015GL066996

Mackas, D.L., Denman, K.L., Abbott, M.R., 1985. Plankton patchiness: biology in the physical vernacular. Bull. Mar. Sci. 37, 653–674.

Massie, P.P., McIntyre, T., Ryan, P.G., Bester, M.N., Bornemann, H., Ansorge, I.J., 2016. The role of eddies in the diving behaviour of female southern elephant seals. Polar Biol. 39, 297–307. doi:10.1007/s00300-015-1782-0

McMahon, C.R., Hindell, M.A., Charrassin, J.-B., Corney, S., Guinet, C., Harcourt, R., Jonsen, I., Trebilco, R., Williams, G., Bestley, S., 2019. Finding mesopelagic prey in a changing Southern Ocean. Sci. Rep. 9, 1–11. doi:10.1038/s41598-019-55152-4

Miller, P., 2009. Composite front maps for improved visibility of dynamic sea-surface features on cloudy SeaWiFS and AVHRR data. J. Mar. Syst. 78, 327–336. doi:10.1016/j.jmarsys.2008.11.019

Miller, P.I., Christodoulou, S., 2014. Frequent locations of oceanic fronts as an indicator of pelagic diversity: Application to marine protected areas and renewables. Mar. Policy 45, 318–329. doi:10.1016/j.marpol.2013.09.009

Miller, P.I., Scales, K.L., Ingram, S.N., Southall, E.J., Sims, D.W., 2015. Basking sharks and oceanographic fronts: Quantifying associations in the north-east Atlantic. Funct. Ecol. 29, 1099–1109. doi:10.1111/1365-2435.12423

Miloslavich, P., Bax, N.J., Simmons, S.E., Klein, E., Appeltans, W., Aburto-Oropeza, O., Anderson-García, M., Batten, S.D., Benedetti-Cecchi, Lisandro Checkley, D.M.J., Chiba, S., Duffty, J.E., Dunn, D.C., Fischer, A., Gunn, J., Kudela, R., Marsac, F., Muller-Karger, F.E., Obura, D., Shin, Y.-J., 2018. Essential Ocean Variables for sustained observations of marine biodiversity and ecosystems.

Glob. Chang. Biol. doi:10.1111/gcb.14108

Naito, Y., Costa, D.P., Adachi, T., Robinson, P.W., Fowler, M., Takahashi, A., 2013.
Unravelling the mysteries of a mesopelagic diet: A large apex predator
specializes on small prey. Funct. Ecol. 27, 710–717. doi:10.1111/1365-
2435.12083

Naito, Y., Costa, D.P., Adachi, T., Robinson, P.W., Peterson, S.H., Mitani, Y.,
Takahashi, A., 2017. Oxygen minimum zone: An important oceanographic
habitat for deep-diving northern elephant seals , Mirounga angustirostris. Ecol.
Evol. 1–12. doi:10.1002/ece3.3202

Nordstrom, C.A., Battaile, B.C., Cotté, C., Trites, A.W., 2013. Foraging habitats of
lactating northern fur seals are structured by thermocline depths and
submesoscale fronts in the eastern Bering Sea. Deep. Res. Part II Top. Stud.
Oceanogr. 88–89, 78–96. doi:10.1016/j.dsr2.2012.07.010

Olson, D., Hitchcock, G., Mariano, A., Ashjian, C., Peng, G., Nero, R., Podesta, G.,
1994. Life on the Edge: Marine Life and Fronts. Oceanography 7, 52–60.
doi:10.5670/oceanog.1994.03

Palacios, D.M., Bograd, S.J., Foley, D.G., Schwing, F.B., 2006. Oceanographic
characteristics of biological hot spots in the North Pacific: A remote sensing
perspective. Deep. Res. Part II Top. Stud. Oceanogr. 53, 250–269.
doi:10.1016/j.dsr2.2006.03.004

Polovina, J., Uchida, I., Balazs, G., Howell, E.A., Parker, D., Dutton, P., 2006. The

    Kuroshio Extension Bifurcation Region: A pelagic hotspot for juvenile

    loggerhead sea turtles. Deep. Res. Part II Top. Stud. Oceanogr. 53, 326–339.

    doi:10.1016/j.dsr2.2006.01.006

Prants, S. V., Budyansky, M. V., Uleysky, M.Y., 2014. Identifying Lagrangian fronts

    with favourable fishery conditions. Deep. Res. Part I Oceanogr. Res. Pap. 90,

    27–35. doi:10.1016/j.dsr.2014.04.012

Proud, R., Cox, M.J., Brierley, A.S., 2017. Biogeography of the global ocean's

    mesopelagic zone. Curr. Biol. 27, 113–119. doi:10.1016/j.cub.2016.11.003

Ream, R.R., Sterling, J.T., Loughlin, T.R., 2005. Oceanographic features related to

    northern fur seal migratory movements. Deep. Res. Part II Top. Stud. Oceanogr.

    52, 823–843. doi:10.1016/j.dsr2.2004.12.021

Robinson, P.W., Costa, D.P., Crocker, D.E., Gallo-Reynoso, J.P., Champagne, C.D.,

    Fowler, M.A., Goetsch, C., Goetz, K.T., Hassrick, J.L., Hückstädt, L.A., Kuhn,

    C.E., Maresh, J.L., Maxwell, S.M., McDonald, B.I., Peterson, S.H., Simmons,

    S.E., Teutschel, N.M., Villegas-Amtmann, S., Yoda, K., 2012. Foraging

    behavior and success of a mesopelagic predator in the northeast Pacific Ocean:

    insights from a data-rich species, the northern elephant seal. PLoS One 7.

    doi:10.1371/journal.pone.0036728

Scales, K.L., Hazen, E.L., Jacox, M.G., Castruccio, F., Maxwell, S.M., Lewison,

    R.L., Bograd, S.J., 2018. Fisheries bycatch risk to marine megafauna is

intensified in Lagrangian coherent structures. Proc. Natl. Acad. Sci. 201801270. doi:10.1073/pnas.1801270115

Scales, K.L., Miller, P.I., Embling, C.B., Ingram, S.N., Pirotta, E., Votier, S.C., 2014a. Mesoscale fronts as foraging habitats: composite front mapping reveals oceanographic drivers of habitat use for a pelagic seabird. J. R. Soc. Interface 11, 20140679. doi:10.1098/rsif.2014.0679

Scales, K.L., Miller, P.I., Hawkes, L.A., Ingram, S.N., Sims, D.W., Votier, S.C., 2014b. On the front line: Frontal zones as priority at-sea conservation areas for mobile marine vertebrates. J. Appl. Ecol. 51, 1575–1583. doi:10.1111/1365-2664.12330

Simmons, S.E., Crocker, D.E., Kudela, R.M., Costa, D.P., 2007. Linking foraging behaviour of the northern elephant seal with oceanography and bathymetry at mesoscales. Mar. Ecol. Prog. Ser. 346, 265–275. doi:10.3354/meps07014

Snyder, S., Franks, P.J.S., Talley, L.D., Xu, Y., Kohin, S., 2017. Crossing the line: Tunas actively exploit submesoscale fronts to enhance foraging success. Limnol. Oceanogr. Lett. doi:10.1002/lol2.10049

Sousa, L.L., Queiroz, N., Mucientes, G., Humphries, N.E., Sims, D.W., 2016. Environmental influence on the seasonal movements of satellite ☐ tracked ocean sunfish Mola mola in the north ☐ east Atlantic. Anim. Biotelemetry. doi:10.1186/s40317-016-0099-2

St. John, M.A., Borja, A., Chust, G., Heath, M., Grigorov, I., Mariani, P., Martin, A.P., Santos, R.S., 2016. A dark hole in our understanding of marine ecosystems and their services: Perspectives from the mesopelagic community. Front. Mar. Sci. 3, 1–6. doi:10.3389/fmars.2016.00031

Steele, J.H., 1978. Spatial pattern in plankton communities, NATO Conference Series, Marine Sciences IV. Plenum Press, New York, NY.

Tew Kai, E., Rossi, V., Sudre, J., Weimerskirch, H., Lopez, C., Hernandez-Garcia, E., Marsac, F., Garçon, V., 2009. Top marine predators track Lagrangian coherent structures. Proc. Natl. Acad. Sci. U. S. A. 106, 8245–8250. doi:10.1073/pnas.0811034106

Tosh, C.A., de Bruyn, P.J.N., Steyn, J., Bornemann, H., van den Hoff, J., Stewart, B.S., Plötz, J., Bester, M.N., 2015. The importance of seasonal sea surface height anomalies for foraging juvenile southern elephant seals. Mar. Biol. 162, 2131–2140. doi:10.1007/s00227-015-2743-4

Trudelle, L., Cerchio, S., Zerbini, N., Geyer, Y., Mayer, F., Jung, J., Hervé, M.R., Adam, O., 2016. Influence of environmental parameters on movements and habitat utilization of humpback whales in the Madagascar breeding ground. R. Soc. Open Sci. 3.

Ullman, D.S., Cornillon, P.C., 2000. Evaluation of front detection methods for satellite-derived SST data using *in situ* observations. J. Atmos. Ocean. Technol. 1667–1675.

Vacquié-Garcia, J., Guinet, C., Laurent, C., Bailleul, F., 2015. Delineation of the
    southern elephant seal's main foraging environments defined by temperature and
    light conditions. Deep. Res. Part II Top. Stud. Oceanogr. 113, 145–153.
    doi:10.1016/j.dsr2.2014.10.029

Valinassab, T., Pierce, G.J., Johannesson, K., 2007. Lantern fish (Benthosema
    pterotum) resources as a target for commercial exploitation in the Oman Sea. J.
    Appl. Ichthyol. 23, 573–577. doi:10.1111/j.1439-0426.2007.01034.x

Walli, A., Teo, S.L.H., Boustany, A., Farwell, C.J., Williams, T., Dewar, H., Prince,
    E., Block, B.A., 2009. Seasonal movements, aggregations and diving behavior of
    Atlantic bluefin tuna (Thunnus thynnus) revealed with archival tags. PLoS One
    4. doi:10.1371/journal.pone.0006151

Woodson, C.B., Litvin, S.Y., 2015. Ocean fronts drive marine fishery production and
    biogeochemical cycling. Proc. Natl. Acad. Sci. 112, 1710–1715.
    doi:10.1073/pnas.1417143112

Woodworth, P.A., Schorr, G.S., Baird, R.W., Webster, D.L., Mcsweeney, D.J.,
    Hanson, M.B., Andrews, R.D., Polovina, J.J., 2012. Eddies as offshore foraging
    grounds for melon-headed whales (Peponocephala electra). Mar. Mammal Sci.
    28, 638–647. doi:10.1111/j.1748-7692.2011.00509.x

Yoshino, K., Takahashi, A., Adachi, T., Costa, D.P., Robinson, P.W., Peterson, S.H.,
    Hückstädt, L.A., Holser, R.R., Naito, Y., 2020. Acceleration-triggered animal-
    borne videos show a dominance of fish in the diet of female northern elephant

seals. J. Exp. Biol. jeb.212936. doi:10.1242/jeb.212936

Zainuddin, M., Saitoh, K., Saitoh, S.I., 2008. Albacore (Thunnus alalunga) fishing

ground in relation to oceanographic conditions in the western North Pacific

Ocean using remotely sensed satellite data. Fish. Oceanogr. 17, 61–73.

doi:10.1111/j.1365-2419.2008.00461.x

Chapter 1: Foraging behavior of a mesopelagic predator, the northern elephant seal, in northeastern Pacific eddies

Theresa R Keates, Elliott L Hazen, Rachel R Holser, Jerome Fiechter, Steven J

Bograd, Patrick W Robinson, Juan Pablo Gallo-Reynoso, Daniel P Costa

1.1 Abstract

The role of mesoscale features in structuring trophic transfer in the mesopelagic

zone is poorly understood. Deploying sensors on marine animals, or "biologging," is

a powerful tool to infer the organism's behavior and simultaneously collect high-

resolution oceanographic data to describe physical-biological interactions. We

investigated whether mesoscale eddies are used by a mesopelagic predator, the

northern elephant seal (*Mirounga angustirostris*), and if so, what mechanisms might

create beneficial foraging conditions in association with eddies. We hypothesized

seals would increase their foraging behavior in both cyclonic and anticyclonic eddies

due to nutrient enhancement and physical aggregation of prey and that seals would

dive deeper in anticyclonic eddies in response to a deeper prey field. We used

tracking data and continuous *in situ* temperature measurements from 221 adult female

northern elephant seals collected between 2004 and 2019. These predators primarily

targeted myctophid fishes and squid throughout the northeast Pacific mesopelagic

zone, foraging between approximately 400 – 800 m. Eddy encounters were identified

using remotely sensed sea level anomaly data and confirmed visually with collocated

sea level anomaly, *in situ* temperature, and *in situ* temperature anomaly. Over more

than 30,000 days of data and >3 million temperature casts collected by seals, we

found 129 high confidence encounters with anticyclonic eddies and 83 with cyclonic eddies. Overall, seals traveled more slowly and in a less directed manner while associated with eddies, particularly anticyclonic eddies, suggesting increased foraging behavior, especially in the California Current. Elephant seals spent more time at the edges of cyclonic eddies than their center. In contrast, they utilized both the interior and edge of anticyclonic eddies. This suggests that the aggregation of prey at the frontal region of an eddy is an important mechanism, whereas nutrient upwelling associated with an eddy play a more minor role in enhancing the seals' prey field. Seal foraging behavior was not influenced by eddy age, size, amplitude, or rotational speed. The large sample size in this study showed considerable variation between individual behavioral responses, suggesting caution when extrapolating individual behavior to a population level. Our data show that both cyclonic and anticyclonic eddies can affect the seals' prey field as demonstrated by enhanced foraging behavior. Still, the variation in behavioral responses resulting from individual foraging strategies, eddy histories, and possible spatiotemporal mismatches between eddy physics and biological responses relevant to mesopelagic predators merit further investigation.

1.2 Introduction

Understanding the biological significance of mesoscale oceanographic features is ecologically valuable, benefitting both marine spatial management and prediction of climate change effects on marine ecosystems (*e.g.* Palacios et al. 2006, Woodson and Litvin 2015). Growing evidence suggests that marine predators use eddies, mesoscale

features which can maintain physically distinct conditions from their surroundings altering phytoplankton (Gaube et al., 2013) and zooplankton assemblages (Atwood et al., 2010; Bakun, 2006; Mackas et al., 2005). However, the influence of eddies on higher-trophic level organisms in the mesopelagic zone (200 to 1,000 meters below the surface) is challenging to document and only beginning to be understood. Deploying sensors on marine animals, or "biologging," is a powerful tool used to collect oceanographic observations and simultaneously assess the relationship between an organism's behavior and its dynamic oceanographic environment below the surface (Harcourt et al., 2019). Using this methodology, inferences about mesopelagic biota through the perspective of a diving predator offer new insights into the influence of eddies on deep-water organisms.

Eddy energetics can significantly enhance upper ocean mixing, renewing nutrients in surface waters and stimulating primary production (Flierl and McGillicuddy, 2002; Martin and Richards, 2001; Peterson et al., 2005). Entrainment of coastal water within eddies and subsequent movement offshore can transport nutrients and less mobile organisms (Flierl and McGillicuddy, 2002; Johnson et al., 2005). In addition, the edges of eddies can act as fronts and aggregate small organisms (Bakun, 2006; Legal et al., 2007; Schmid et al., 2020; Zhang et al., 2015). Higher trophic levels can be influenced by eddies including micronekton (Boyd et al., 1986; Della Penna et al., 2021; Della Penna and Gaube, 2020; Godø et al., 2012) and larger predators such as loggerhead sea turtles (Chambault et al., 2019; Polovina et al., 2006), leatherback sea turtles (Lambardi et al., 2008), albacore tuna (Zainuddin et al., 2008), king penguins

(Cotté et al., 2007), northern fur seals (Pelland et al., 2014; Ream et al., 2005), and Steller sea lions (Lander et al., 2020). Some studies have observed eddy influences on mesopelagic micronekton community through acoustics (Della Penna et al., 2021; Della Penna and Gaube, 2020) but it remains a major challenge to document mid-trophic level mesopelagic organisms' association with eddies at larger spatiotemporal scales. About a quarter of eddies worldwide extend to depths of 1000 m or more (Petersen et al., 2013), suggesting that they can directly impact the mesopelagic zone, and mesopelagic predators such as blue and white sharks (Braun et al., 2019; Gaube et al., 2018), melon-headed whales (Woodworth et al., 2012), and southern elephant seals (Bailleul et al., 2010; Campagna et al., 2006; Massie et al., 2016) associate with eddies. A closely related species, the northern elephant seal (*Mirounga angustirostris*), pursues mesopelagic prey in the northeast Pacific, where such mesopelagic predator studies relating foraging to eddies have not yet been conducted.

Adult female northern elephant seals range throughout the northeast Pacific, primarily targeting myctophid fish and squid (Goetsch et al., 2018; Naito et al., 2017, 2013; Yoshino et al., 2020). Elephant seals forage nearly non-stop during biannual offshore foraging trips (Adachi et al., 2021), the first lasting approximately 10 weeks after breeding in the winter and the second 8 months after molting in the spring (Robinson et al., 2012). Northern elephant seals are the only mesopelagic predator in the northeast Pacific for which a large dataset of tracking data exist, and previous work relating their foraging behavior to mesoscale oceanography has relied on remotely sensed data (Abrahms et al., 2018; Simmons et al., 2007). The northeast

Pacific within the elephant seals' range contains fewer large eddies than the western basin (Cheng et al., 2014; Roden, 1991), but the Gulf of Alaska and California Current are nonetheless significant eddy hotspots, with fewer eddies occurring in the North Pacific Transition Zone (Cheng et al., 2014). Eddies in these regions are on average 160 km across and persist for approximately 125 days, though they can persist for up to 3 years (Cheng et al., 2014; Crawford et al., 2000; Stegmann and Schwing, 2007). This study system therefore offers a valuable opportunity to investigate the relationship between eddy characteristics and the foraging behavior of a predator in the mesopelagic zone.

Subsurface oceanographic data derived from biologging instruments can improve our understanding of physical-biological interactions at fine scales (*e.g.* Bograd et al. 2010, Costa et al. 2012, Hussey et al. 2015). Many time-depth recorders designed primarily to study animal behavior also continuously sample temperature, providing high horizontal resolution of temperature by collecting profiles during every dive an animal makes. Northern elephant seals appear to derive foraging benefits from mesoscale activity (Abrahms et al. 2018) and these continuous *in situ* temperature measurements can provide the first description of potentially relevant mesoscale features and the seals' behavioral changes at fine scales. These observations can increase our understanding of mesopelagic dynamics in the northeast Pacific where observations are limited.

We evaluated the importance of mesoscale eddies for a population of northern elephant seals using a 15-year data set of 221 records of behavioral and *in situ* temperature data. Both cyclonic eddies and anticyclonic eddies were expected to enhance foraging opportunities due to nutrient upwelling and advection of productive coastal waters, respectively. We expected seals to make deeper dives within anticyclonic eddies due to mesopelagic prey being physically driven deeper within these downwelling, warm-core eddies (Godø et al., 2012; Samuelsen et al., 2012). In contrast, we expected shallower dives within cyclonic eddies due to colder water and increased productivity at shallower depths. Finally, we expected that prey would be more abundant within older eddies as they would have had more time to accumulate biomass.

1.3 Methods

1.3.1 Elephant seal tracking

221 adult female northern elephant seals carried satellite tags (Mk10, n=55, or SPOT, n=147,– Wildlife Computers, Redmond, WA; or CTD-SRDLs – Sea Mammal Research Unit, St. Andrews, Scotland, n=19) and time-depth-temperature recorders (Mk9, n=166, or integrated into Mk10, n=55, Wildlife Computers) between 2004 and 2019. Seals were instrumented at Año Nuevo State Park, California, USA (37.11°N, -122.33°W, n=201) and Islas San Benito, Mexico (28.30°N, -115.37°W; n=20). Northern elephant seals from both colonies exhibit comparable behavior at sea (Kienle, 2019; Robinson et al., 2012). For instrument deployment and recovery, seals were chemically immobilized following established protocols (Robinson et al., 2012).

Satellite transmitting tags were attached to the head and time-depth-recorders, if separate, to the dorsal side between the axilla and sternum. All animal handling protocols were authorized by the University of California Santa Cruz Institutional Animal Care and Use Committee and conducted under National Marine Fisheries Service permit numbers 786-1463, 87-143, 14636, 17952, and 19108, and under Dirección General de Vida Silvestre permit numbers NÚMS/SGPA/DGVS/05734-2004 and NÚMS/SGPA/DGVS/05321-2005.

Pressure and temperature data were collected by the Mk9 or Mk10 instruments, which measure pressure with an accuracy of ± 1% of reading from which depth can be estimated at 0.5 m resolution and temperature at a resolution of 0.05°C and accuracy ± 0.1°C. Depth and temperature readings were collected at least every 8 seconds throughout deployment, a sampling interval previously demonstrated to be sufficient to resolve thermal features using these instruments (Simmons et al., 2009). While the smaller number of CTD-SRDLs (n=15) deployed also collected temperature data, they are programmed to do so only approximately 4 times per day, providing far lower horizontal resolution than the continuously-recording Mk9 or Mk10s. As such, we did not use the CTD-SRDL temperature data to identify eddy encounters at the fine scales required for this study. Depth data were zero offset corrected using a custom-written toolbox in MATLAB (Robinson et al., 2012). Previous evaluations of the temperature data collected by these instruments showed stability over time (Simmons et al., 2009), but out of caution, deep-water temperature measurements (>800 m) over time were visually inspected for signs of drift.

Temperature measurements from the down- and up-casts from an individual dive were combined and interpolated to 1 m intervals using a Piecewise Cubic Hermite Interpolating Polynomial from the Gibb's Sea Water Oceanographic Toolbox in MATLAB (McDougall and Barker, 2011).

All seals were tracked using the Argos system (https://www.argos-system.org/); a subset of seals were additionally tracked with Fastloc® GPS. Where available, Argos error ellipse data were retained for the highest quality uncertainty estimates; these data were not available for older Argos data predating the implementation of a Kalman filter by the data provider. Erroneous locations on land were first filtered out by cross-referencing seal locations to bathymetry data (see Section 2.4). GPS and Argos location estimates were then further refined using the foieGras R package (version 0.7-7.9276, https://github.com/ianjonsen/foieGras), which uses a continuous time sate-space model incorporating location error estimates to filter the tracking data (Jonsen et al., 2020). We used a correlated random walk model and imposed a speed filter of 3 m/s. All analyses in R were carried out in version 4.1.1 (R Core Team, 2022). Locations were interpolated to one-hour intervals and assigned to each temperature cast based on time. Any interpolated locations with a standard error ≥ 30 km were omitted. These hourly interpolated locations were used to identify proximity to eddies (see Section 2.3); for statistical models, 12-hour mean locations were used.

1.3.2 Behavioral Metrics

The northern elephant seal dataset offers both lateral movement and vertical diving data. We used transit rate (horizontal velocity), which performs well as a simple proxy for northern elephant seal foraging behavior (Robinson et al., 2010). Lower transit rate is related to presumed higher foraging activity and higher transit rate to presumed lower foraging activity. Average transit rate as displacement over time was derived from the interpolated tracks over 12-hour intervals. As an additional indication of behavioral state, movement persistence was derived from the foieGras state-space model for each 12-hour window. This metric describes autocorrelation in direction and speed, ranging continuously between 0, indicating low persistence and frequent changes in direction and/or speed, likely foraging, to 1, indicating high persistence and infrequent changes in direction and/or speed, likely traveling (Jonsen et al., 2019).

Elephant seals exhibit drift dives that can be used as a metric of changes in body composition (fatter seals more buoyant and leaner seals less buoyant) and thus foraging success on the order of a few days to a week (Biuw et al., 2003; Crocker et al., 1997; Robinson et al., 2010; Webb et al., 1998). For all seal tracks in this study, daily average drift rate was calculated across all drift dives identified each day, then the change in drift rate was calculated over four-day intervals. Maximum dive depth, bottom time (the time that vertical velocity remains below 20% of ascent and descent rates), and number of "wiggles" (small vertical inflections likely associated with prey pursuit (Robinson et al., 2010)) were determined for each individual dive using a

custom-written toolbox in MATLAB (Robinson et al., 2012). For diving behavioral

analyses relative to eddies, we removed dives shallower than 100 m and all drift

dives, as seals are unlikely to be foraging during these dives. We retained the

temperature data from all dives regardless of likely behavior for eddy identification in

section 2.3. As most elephant seals exhibit diel differences in dive depth, likely

reflecting vertical migration of the prey field (Robinson et al., 2012), dive depth,

bottom time, and number of wiggles were analyzed separately for daytime and

nighttime dives. Daytime dives were distinguished from nighttime dives by

calculating a solar elevation angle for the dives' location and date using the

SolarAzEl function in MATLAB (Koblick, 2021). Daytime was designated as solar

elevation >0.

1.3.3 Eddy Identification

Each day of the trip, eddies within 50 km of a seal's location were first identified

as potential eddy encounters using the Mesoscale Eddy Trajectory Atlas (META2.0),

produced by SSALTO/DUACS and distributed by AVISO (Chelton et al., 2011).

Eddy encounters were confirmed visually using several metrics: (1) *in situ*

temperature, (2) *in situ* temperature anomaly, (3) sea level anomaly (SLA), and (4)

comparison of *in situ* observations to eddy characteristics derived from the META.

Temperature anomalies throughout the water column were calculated by subtracting

climatological data (World Ocean Atlas 2018 monthly climatology 1955-2017, ¼°

resolution) from the *in situ* temperature data collected by the seal tags. SLA data were

obtained from Copernicus (1/4° resolution, dataset ID DATASET-DUACS-REP-

GLOBAL-MERGED-ALLSAT-PHY-L4). Eddy encounters were only retained if all data sources agreed: the SLA data showed an elevation/depression consistent with the eddy polarity (cyclonic or anticyclonic) and approximate eddy amplitude determined from the META and the seal-derived data showed an appropriate warm/cold anomaly and/or deepening/shoaling of the mixed layer (Fig. 1.1). For each retained eddy association, the time at which the seal entered and exited the eddy was visually determined from the *in situ* temperature and temperature anomaly data (seals collected on average 104 temperature profiles per day, enabling high horizontal resolution for this determination).

Eddy characteristics for the retained eddy encounters were derived from the META: eddy radius, eddy age, eddy rotational speed, eddy amplitude, and eddy polarity. For each eddy a seal encountered, we referenced the META to find the first day that particular eddy was identified and calculated the age of the eddy at the time of the seal encounter as the time difference between the first detection of the eddy and the day the seal encountered it. To normalize eddy age across eddies to assess the influence of eddy intensification and decay phases on seal behavior, we additionally represented eddy age at the time of a seal's encounter as a percentage of the eddy's observed lifespan (0%: first day eddy was identified in the META, 100%: last day eddy was documented in the META). Across all eddies in the study area, eddy rotational speed and amplitude tended to increase to a maximum during the first quartile if the eddy's lifespan and decrease again during the third quartile (Fig. 1.S2). We calculated and mapped the kernel density of eddies and hourly seal locations per

square kilometer using the kernel density tool in ArcMap 10.7.1 using a geodesic method for distance calculations.

To compare diving behavior within an eddy to the outside of an eddy, we considered the dive parameters of interest (i.e., maximum dive depth, bottom time, and the number of wiggles). We pulled those parameters from dives made while the seal was within the eddy as well as dives covering an equal cumulative amount of time divided evenly between pre- and post-eddy encounter, with buffers in time (2 days pre-/post-encounter) and space (at least 0.1 degree from the eddy center) to ensure the animal was no longer associating with the eddy. The temporal buffer was expanded if the dives made before or after the eddy encounter in question were within 1 day of a potential encounter with another eddy (i.e., an eddy within 50 km of the seal, whether or not we could verify that the seal actually traversed the eddy) while keeping the time window of outside-of-eddy seal behavior unchanged. Differences in diving behavior within an eddy compared to behavior before and after the eddy encounter were determined using two-sample t-tests for each individual eddy encounter.

1.3.4 Additional oceanographic parameters

In situ sea surface temperature (SST) was calculated for each individual dive as the mean of *in situ* temperature collected in the upper 5 m of the water column. Mixed layer depth (MLD) was determined by applying the temperature-based algorithm presented in Holte and Talley (2009) to the *in situ* temperature data. Remotely-sensed

observational gridded 1/25° finite-sized Lyapunov exponents (FSLE) were extracted

from AVISO (d'Ovidio et al., 2004) and the mean, maximum, and standard deviation

of FSLE extracted within a 5 pixel radius (approximately 25 km) ± 2 days per day of

seal data. FSLEs characterize the confluence of fluid parcels and are often used to

identify Lagrangian structures; the FLSE will have higher values on fronts on the

edges of eddies, with lower values in the center of eddies and more quiescent parts of

the ocean with low dispersion (*e.g.* d'Ovidio et al., 2004). Seafloor topography data at

1/60° resolution based on satellite altimetry and ship depth soundings were

downloaded from the NOAA CoastWatch ERDDAP server (dataset ID usgsCeSS111,

Smith and Sandwell, 1997) and a bathymetric depth was assigned to seal dives by

calculating the mean of bathymetric depth over a 2 km square to account for the error

associated with Argos-derived locations. Dives made in areas where water depth was

shallower than 500 m were excluded from further analyses to focus on mid-water

foraging on pelagic prey.

Given the seals' large and oceanographically variable range, data were divided into

three subregions: the Gulf of Alaska, California Current, and North Pacific Transition

Zone (Fig. 1.2). The California Current region was designated as south of 48°N,

below variable positions of the North Pacific Current's southern bifurcation

(Cummins and Freeland, 2007; Sydeman et al., 2011). In the absence of a well-

defined division between the California Current and the interior of the subtropical

gyre circulation (Cummins and Freeland, 2007), we used a western cut-off at -135°W,

following the edge of an abundance of cyclonic eddies typical of eddies formed in the

California Current (Stegmann and Schwing, 2007). The North Pacific Transition

Zone was then designated as west of -135°W and between 28°N and 48°N between

the subarctic frontal zone and subtropical frontal zone, taking into consideration

interannual variability of the North Pacific Current (Cummins and Lagerloef, 2004;

Roden, 1991; Sydeman et al., 2011; Yuan and Talley, 1996). Finally, observations

were assigned to the Gulf of Alaska if they were north of the North Pacific Current,

approximated at 48°N (Cummins and Freeland, 2007). These subregional

designations incorporated the major hotspots of eddy and seal activity (Figure S1).

To evaluate the relationship between the mixed layer depth and the depth of the

ferricline, we extracted iron profiles from a biogeochemical model

(https://resources.marine.copernicus.eu/product-

detail/GLOBAL_MULTIYEAR_BGC_001_029029) at monthly resolution within 2°

latitude and longitude of every eddy encounter. As this model is not data assimilating,

it does not resolve specific eddies matching those the seals encounter in space in time.

Instead, we used these data to determine the vertical iron distribution typical for the

location and time without the perturbation of an eddy. For each iron profile, we first

calculated the scaled first derivative of the iron concentration by depth, then found the

depths containing the 75th percentile of the derivative to identify the depth region of

most rapid change. As this depth zone of rapid iron increase typically spanned

sections of 100 – 250 m, we assigned a ferricline "upper boundary" by identifying the

10th percentile of the depths associated with the iron change and a ferricline "lower

boundary" as the 90th percentile of the depths associated with rapid concentration

change. We additionally determined a "middle" using the 50th percentile. Profiles

with iron concentrations >= 0.6 nmol/kg near the surface were assigned as having no

ferricline as that concentration approximates the deep water iron concentration in the

North Pacific (https://www.mbari.org/science/upper-ocean-systems/chemical-sensor-

group/periodic-table-of-elements-in-the-ocean/). We then compared the median of the

modeled ferricline upper boundary, middle, and upper boundary for each eddy

encounter to the MLD calculated from the *in situ* temperature data both inside the

eddies.

1.3.5 Statistical Analysis

We tested the influence of eddy encounters on five behavioral variables: transit rate

(horizontal speed) and movement persistence (a continuous variable between 0,

suggesting convoluted movement likely associated with foraging, and 1 suggesting

directed movement which is likely travel) from the entire trip, and dive depth, dive

bottom time, and number of wiggles averaged over an eddy encounter (see Section

2.2 for detailed descriptions of behavioral metrics). We did this using generalized

additive mixed models (GAMMs) in the "mgcv" package version 1.8-36 in R (Wood,

2017). While at sea, elephant seals must gain sufficient energy to recover energy

stores lost during their fasting period on land and prepare for the next fasting period

(Costa et al., 1986). Consequently, elephant seal at-sea behavior is strongly driven by

internal factors. To account for this, we tested the influence of season (which of the

two annual foraging trips a seal was undergoing), days since leaving the colony

(representing their internal schedule of maximizing energy intake and the need to

return to land to breed or molt), and drift rate (to represent past foraging success) on movement and diving behavior. We retained the intrinsic variables that explained the greatest amount of behavioral variance and were not colinear with one another (all retained variables had Pearson correlation coefficients ≤ 0.15). Subsequent addition of oceanographic variables to the intrinsic model tested further behavioral modulation by the local environment: eddies, mixed layer depth, sea surface temperature, FSLE, bathymetric depth, and distance from shore. For MLD and SST from *in situ* data, we calculated the mean and standard deviation within 12-hour periods to match the timescale of the response variable. We also included latitude and longitude in the model due to the large geographic range covered and to account for spatial autocorrelation.

Using this full model, the effect of eddies on seal behavior was assessed using the difference in explanatory power (R^2 deviance) between a model containing eddy category (Table 1.1) and a model without this factor. When models resulted in a negative R^2, we reported these as $R^2=0$ to indicate no explanatory power. Models built to assess the influence of eddies also contained oceanographic parameters representing water column mixing, temperature, and mesoscale activity metrics that can be associated with eddies but which seals will also encounter elsewhere (Table 1.1). This was designed to test whether seal behavior was influenced specifically by mesoscale eddies or by oceanographic phenomena that, while characteristic of an eddy, could also represent other features such as fronts or jets.

GAMMs testing movement persistence were fit with a Gamma distribution while the diving behavior (dive depth, bottom time, and number of wiggles) and transit rate models were run with a Gaussian distribution. Individual seal was included as a random effect. The resulting models were evaluated for homogeneity (residuals vs. fitted), independence (residuals vs. covariates), and normality of residuals. They were additionally tested for spatial autocorrelation by calculating Moran's I using the package "ape" version 5.5 in R (Paradis and Schliep, 2019) (Table 1.S4). Model outputs were visualized using the package "mgcViz" version 0.1.9 in R (Fasiolo et al., 2020).

To assess the amount of time seals spent in relative positions within the eddies, we used histograms of hourly seal locations relative to distance from eddy center represented as a percentage of the eddy radius, i.e., 100% represented the eddy edge, below 100% was inside the eddy, and above 100% was outside of the eddy. These data omitted locations with standard errors greater than 15 km to increase confidence in satellite-based locations and omitted transit rates faster than 6 km/h to remove data unlikely associated with foraging behavior.

1.4. Results
1.4.1 Eddy Encounters
Of 221 seals tracked between 2004 and 2019, 119 individuals encountered eddies: 129 encounters with anticyclonic eddies and 83 encounters with cyclonic eddies (Fig. 1.2 & 1.3), compared to a nearly equal availability of eddies of either polarity in the total eddy field (50.6% cyclonic, 49.4% anticyclonic). The tracks of these seals were

retained for further analyses. Seals spent 3.1 ± 7.4 (mean ± sd) days within an eddy with no difference between cyclonic and anticyclonic eddies (3.1 ± 6.9 days in anticyclonic eddies, 3.1 ± 8.2 days in cyclonic eddies, t-test p=0.96). All 221 tracked seals collectively collected 3.2 million temperature casts during 30,786 days at sea of which 733 were classified as within eddies, accounting for 2.4% of the seals' time. They spent a cumulative 478 days (65.2% of in-eddy time) in anticyclonic eddies and 255 days (34.8 % of in-eddy time) in cyclonic eddies (Table 1.S1). Just under half of the eddy-encountering seals (48.7%) encountered more than one eddy; no seal was observed to visit the same eddy a second time.

The area of highest kernel density of seal locations was in the California Current radiating out from the colonies, which overlaps with one eddy hotspot (Fig. 1.S1). The other eddy hotspot, the coastal Gulf of Alaska, had a very low density of seals. Compared to all eddies identified in the META in the region during this time, eddies encountered by seals were on average significantly older (157 ± 132 days vs. 73 ± 79 days for all eddies), larger (in both radius, 70.4 ± 13.7 km vs. 67.1 ± 16.3 km for all eddies, and amplitude, 6.07 ± 4.03 cm vs. 3.94 ± 2.99 cm for all eddies), and had rotational speed (14.4 ± 6.8 cm/s vs. 9.8 ± 5.8 cm/s for all eddies) (t-test, p<0.001, Fig. 1.4).

None of the eddies had MLDs deep enough to reach the lower boundary of the modeled ferricline; only one eddy's MLD reached the vertical center of the ferricline. About one quarter (25.1%) of the observed eddy MLDs reached the upper boundary of the modeled ferricline, about 2/3 cyclonic eddies and 1/3 anticyclonic eddies.

1.4.2 Horizontal Movement Behavior

After retaining the intrinsic variables explaining the greatest amount of behavioral

variance, we came up with a null model for seal behavior (transit rate, movement

persistence, and diving) including the season of the foraging trip (post-breeding or

post-molt) and the timing within the foraging trip (days since leaving the colony). The

addition of eddy category to the horizontal movement behavior models increased

explanatory power (R^2) of the null model. It also increased explanatory power when

the model included oceanographic variables characteristic of but not exclusively

related to eddies that could induce a behavioral effect, such as a change in MLD

(Table 1.1). Overall, elephant seals exhibited reduced transit rate (mean reduction by

38.4%) within eddies compared to outside of eddies, suggesting enhanced foraging

behavior (Fig. 1.5). Similar trends were observed for movement persistence (Fig.

1.S4). Visualizations of full model outputs can be found in the Supplementary

Material (Fig. 1.S3 and Fig. 1.S4).

The strongest influence of eddies on transit rate occurred in the California Current,

where the addition of eddy category to the models resulted in the highest increase to

explanatory power (Tables 1.2 and 1.S2). In the California Current, both transit rate

(Fig. 1.5 C, mean reduction 27.1 %) as lower within eddies, with a particularly strong

decrease in association with anticyclonic eddies (transit rate on average 29.4% lower

in anticyclonic eddies than cyclonic eddies). This was the only subregion to contain a

large sample size of both eddy types and eddy polarity did not appreciably improve

explanatory power of models describing transit rate. Being in an eddy did not increase

explanatory power for transit rate in the North Pacific Transition Zone (Table 1.2, Fig. 1.5 B). In the Gulf of Alaska, though eddy encounters had a mean reduction of 65.8% in transit rate, eddy encounters only increased the explanatory power of the transit rate models by a very small amount (Tables 1.2 and 1.S2). The same relative trends were observed in movement persistence reductions across regions (Figure 1.S4, Table 1.S3). Change in drift rate was not well explained by eddy encounters.

Eddy characteristics (age, life stage, radius, amplitude, or rotational speed) did very little to further explain transit rate or movement persistence in association with either cyclonic or anticyclonic eddies within any region. The number of days since the start of the trip (normalized to trip length) explained the largest amount of variability in both transit rate and movement persistence in the models (Table 1.S2-1.S3). There was a weak linear effect of normalized eddy age in anticyclonic eddies in the Gulf of Alaska and the California Current, in which transit rate was slower in association with older eddies (Table 1.S7). Absolute eddy age did not increase the explanatory power of the behavioral models (Table 1.S7).

When encountering cyclonic eddies, the number of hourly seal locations peaked around the edges of the eddies (Fig. 1.6 top). When encountering anticyclonic eddies, locations were spread through the interior and across the edges of the eddies, a pattern especially pronounced in the Gulf of Alaska and the California Current (Fig. 1.6 bottom).

Season (post-breeding or post-molt) increased the explanatory power of the transit

rate models (R^2 deviance 0.031). Models testing the influence of eddies for each

season separately showed a stronger behavioral response to eddies during the post-

molt trip than the post-breeding trip (R^2 deviance post-breeding 0, R^2 deviance post-

molt 0.009).

1.4.3 Diving Behavior

Diving behavior (maximum dive depth, bottom time, and the number of wiggles)

was poorly explained by intrinsic models, in contrast to the two-dimensional

behavioral metrics. Being in an eddy did not increase the explanatory power of

intrinsic models for any dive behavior (Table 1.S8-1.S9). Once within an eddy,

average nighttime dive depths were not different between eddy polarities; average

daytime dive depth was slightly deeper in anticyclonic eddies (580 ± 97 m) than

cyclonic eddies (557 ± 137 m), which is unlikely biologically meaningful (Table

1.S5, Fig. 1.S5). Bottom time and the number of wiggles were not different between

eddy polarities (Table 1.S5, Fig. 1.S5).

Just over half the eddy encounters elicited a significant change (two-sample t-test,

$p<0.05$) in average dive depth with approximately equal proportions of behavioral

responses in opposite directions (increase and decrease) (Table 1.S6). Just under half

showed a difference in bottom time, also with comparable proportions of opposite

behavioral responses. Fewer than 40% of eddy encounters showed a significant

difference in the average number of wiggles. These proportions changed by 4.6 $\pm$

2.5% (mean ± sd) using the different temporal buffers around eddy associations

considered (1 day, 2 days, and 5 days), showing low sensitivity to buffer choice.

1.5. Discussion

Our findings indicate that mesoscale eddies affect northern elephant seal foraging

behavior, though with a high degree of individual variability. Seals decreased their

transit rate and movement persistence when encountering eddies, behavioral

responses associated with foraging (Jonsen et al., 2019; Robinson et al., 2010),

suggesting that eddies may increase the density or abundance of mid trophic-level

organisms in the mesopelagic zone. Across the study area, seals transited more slowly

and showed lower movement persistence through anticyclonic eddies than through

cyclonic eddies. While these two-dimensional movement patterns of seals suggest

increased searching behavior, they cannot confirm increased prey capture. Foraging

success can be estimated from changes in drift rate, but its temporal resolution did not

match the resolution needed to identify energy gain while in an eddy. Encounters with

mesoscale eddies lasted on average ~ 3 days (with some exceptions of long eddy

associations), while changes in drift rate are detectable over a few days to a week

(Biuw et al. 2003).

The northern elephant seals tracked in this study spent only a small fraction of

their time at sea associated with mesoscale eddies. Previous work on southern

elephant seals (*Mirounga leonina*), a closely related mesopelagic predator, found

similar patterns, with mesoscale eddies also not a major habitat feature to most

southern elephant seal populations. These studies observed behavioral responses to

both cyclonic and anticyclonic eddies, though similarly with a high degree of individual variability (Bailleul et al., 2010; Bost et al., 2009; Campagna et al., 2006; D'Ovidio et al., 2013; Dragon et al., 2010). Northern elephant seals in this study encountered eddies that were on average larger, older, and of higher energy than the background eddy field. This may indicate that those eddies were more important to seals or reflect the eddies we were able to identify from the *in situ* temperature data. The eddy encounters we identified are likely a subset of the actual number of eddy encounters by seals, as we only retained high confidence encounters visible in both remotely sensed SLA and *in situ* temperature data. Seals encountered more anticyclonic eddies than cyclonic eddies, while the background eddy field contained approximately equal numbers of each, though this could be an artifact of our eddy detection method if anticyclonic eddies were more readily identified from the *in situ* temperature data. Seals usually did not spend an extended amount of time associated with eddies and we did not observe repeated visits to the same eddy. We found only one example of a seal that could be considered an eddy specialist, having spent approximately 30% of her time associated with eddies. However, when seals did encounter eddies, they usually changed their behavior.

Eddies had the greatest influence on seal behavior in the Gulf of Alaska and the California Current. The Gulf of Alaska is a major eddy hotspot in the Northeast Pacific with many long-lived anticyclonic eddies (Cheng et al., 2014). However, while visited by about half of the seals (153 of 221), only 7.6% of the total days at sea for all seals were spent within in the Gulf of Alaska. Therefore, a small fraction of the

adult female northern elephant seal population is likely to encounter Gulf of Alaska eddies. In contrast, all seals pass through the California Current at the very least upon leaving and returning to the colony. This boundary current forms another Northeast Pacific eddy hotspot (Cheng et al., 2014) and is therefore the most likely subregion where elephant seals would encounter eddies.

Both cyclonic and anticyclonic eddies triggered behavioral responses in seals. The only subregion with a near-equal number of encounters with both eddy types to best enable a comparison in seal behavior between eddy polarities was the California Current. Seal transit rate and movement persistence were not significantly different between cyclonic and anticyclonic eddies in the California Current, offering little evidence that these eddies of opposite polarity within the same subregion differ in the biological relevance to seals. The small number of encounters with cyclonic eddies in the North Pacific Transition Zone and the Gulf of Alaska precluded comparing behavioral responses to either polarity in those subregions. As there were differences in transit rate and movement persistence between cyclonic and anticyclonic eddies in the full dataset, these effects are therefore likely attributable to eddies differing across regions due to a variety of factors beyond their rotational direction. The additional eddy properties we considered (eddy age, radius, amplitude, and rotational speed) did little to further explain seal behavior. Biological factors that we were not able to test such as ecosystem state at the eddies' origin or trophic processes occurring throughout the eddy's lifespans may be relevant to foraging elephant seals.

In the absence of direct observations of the mesopelagic prey field, the trends in elephant seal behavior allow us to infer some possible mechanisms. Elephant seals may forage in eddies due to an increase in prey availability because of nutrient upwelling, altered mixing, advection of nutrient- and organism-enriched water, and/or aggregating prey items physically or behaviorally. Much of the offshore northeast Pacific is characterized as a high-nutrient low-chlorophyll (HNLC) region, where phytoplankton growth is limited by iron (Boyd et al., 2004; Martin et al., 1989). Eddies that inject nutrients from deep water or horizontally advect nutrients can increase local primary production. Enhancement of the base of the food web can then translate up trophic levels. Interestingly, elephant seals showed little interest in the center of cyclonic eddies where notable nutrient upwelling occurs. They also exhibited stronger foraging behavior in relation to anticyclonic eddies that generally downwell in their center (Gaube et al., 2014; McGillicuddy and Robinson, 1997; Palacios et al., 2006), using both the center and edges of these eddies. These behavioral patterns suggest that nutrient enhancement alone does not increase mesopelagic prey abundance or availability via trophic transfer. It is possible that vertical nutrient supply may not be occurring very frequently in this HNLC region, as few eddies in this study had MLDs deep enough to penetrate the ferricline and resupply iron to the surface. Alternatively, if eddy-induced nutrient upwelling does occur, it may not be operating at the spatiotemporal scales relevant to elephant seals.

In addition to vertical processes, a large component of the biological importance of large-scale anticyclonic eddies in the northeast Pacific, especially in the Gulf of

Alaska, is in the horizontal direction: the stimulation of primary production by transporting nutrients offshore can result in elevated chlorophyll concentrations that persist across multiple seasons (Crawford et al., 2005; Johnson et al., 2005). As a result, it is not uncommon to find enhanced chlorophyll concentrations within these anticyclonic eddies (Crawford et al., 2007; Gaube et al., 2014, 2013). In fact, in the Gulf of Alaska, over half of surface chlorophyll may be found within anticyclonic eddies that cover only 10% of the area (Crawford et al., 2007). The optical complexity commonly associated with anticyclonic eddies in this region for this reason makes it more likely that prey shifting deeper as hypothesized would be due to thermal and/or nutrient availability factors rather than visual predator avoidance. On the other hand, anticyclonic eddies in the California Current tend to subduct coastal nutrients advected offshore and limit primary production (Gruber, 2011), and at least some eddies in the Transition Zone in this study did not form near the coast and therefore could not have advected coastal nutrients, making horizontal nutrient movement a less likely mechanism in these regions. In oligotrophic waters, such as are found through much of the North Pacific Transition Zone, anticyclonic eddies' reduced stratification could increase convective mixing in their center and stimulate primary production as a deep chlorophyll maximum (Dufois et al., 2016). As an alternative or complementary mechanism to nutrient input, the entrainment of coastal water within eddies can advect planktonic organisms with limited mobility (Flierl and McGillicuddy, 2002), facilitating energy transfer through trophic levels and creating a pelagic community distinct from the eddy's surroundings. Greater prey availability

within an eddy can then in turn attract more mobile species (Godø et al., 2012). It is likely some prey advection occurs inside these anticyclonic eddies as seals utilized the center and edges of these eddies. While we cannot rule out nutrient input as an influential mechanism in anticyclonic eddies, elephant seals more frequently targeting the edges of cyclonic eddies, likely taking advantage of aggregation at the eddy edges, rather than the center, which are usually nutrient-enriched, we hypothesize that nutrient input is a minor component of prey enhancement of interest to this mesopelagic predator at eddies.

Small scale currents at mesoscale features such as eddies may also physically entrain predators in a "quasi-planktonic" way (Della Penna et al., 2016). This effect may also be occurring here, but identifying seal trajectories and speeds relative to circulation at such small scales was not possible given the location errors inherent with Argos-based tracking. If the horizontal advection of plankton or the upwelling of nutrients were important mechanisms, we would expect older eddies to be more relevant to foraging seals as it would take time to develop an enhanced higher trophic level biomass in response. Seals on average showed stronger behavioral response to anticyclonic eddies, which tend to be longer-lived and have greater propagation distances than cyclonic eddies (Chelton et al., 2011), potentially allowing more time for the development of biological communities distinct from the eddy's immediate surroundings. However, anticyclonic eddies encountered by seals were not significantly older than the encountered cyclonic eddies nor were they further from their origin sites. We observed only a weak negative relationship between seal transit

rate and normalized eddy age, and no relationship to absolute eddy age, in anticyclonic eddies. Eddies continually exchange water with their surroundings, which can reduce anomalous conditions within them with time (D'Ovidio et al., 2013; Gaube et al., 2014; Olson, 1986). Despite this, our observations agree more strongly with observations of the maintenance of altered biological conditions throughout the eddy's lifespan, such as Schmid et al. (2020) who observed sustained enhanced plankton concentrations within an eddy relative to its surroundings and Mackas et al. (2005) who saw a continuing development of the zooplankton community as the eddy was colonized by organisms from its surroundings. There remains a dearth of data on mid- to high trophic levels throughout the lifespan of eddies. Elephant seals showed foraging behavior throughout the eddies' lifespans, including young eddies.

Elephant seals not showing a preference for the upwelling-dominant interiors of cyclonic eddies and the limited likelihood of iron recirculation in the eddies we observed suggest a deemphasis on bottom-up processes in favor of alternative physical and/or biological mechanisms that enhance prey availability. Fronts develop on the edges of eddies, physically aggregating organisms or inducing frontal upwelling (Bakun, 2006; Legal et al., 2007; Schmid et al., 2020; Zhang et al., 2015), which can leave a biomass minimum in eddy centers (Godø et al., 2012). Modeling indicates that biomass increases at eddy edges are likely due in greater part to biological rather than physical mechanisms (Samuelsen et al., 2012), highlighting the importance of considering multiple possible drivers beyond physics. Seals heavily used the edges of cyclonic eddies and, to a lesser extent, the edges of anticyclonic

eddies, suggesting that frontal dynamics may be important in enhancing their prey field.

These potential ecological pathways leading to enhanced foraging opportunities for predators within eddies are difficult to disentangle and expectations of biology within eddies based on eddy polarity are often generalizations. For example, while anticyclonic eddies are traditionally associated with low primary productivity, nutrient injection can still occur in anticyclones. The decay of an anticyclonic eddy can reverse the dominant direction of vertical water exchange (Flierl and McGillicuddy, 2002; Franks et al., 1986), and some foraging animals may benefit from this productivity increase fueled by this upwelling (Chambault et al., 2019). Vertical nutrient input can also occur as a result of reduced stratification or eddy-induced Ekman pumping in high-wind conditions, in which the dominant up- and downwelling patterns in cyclonic and anticyclonic eddies, respectively, are counteracted due to wind stress curl opposite of the eddy polarity (Dufois et al., 2016; Flierl and McGillicuddy, 2002; Franks et al., 1986). Certain eddies in the Gulf of Alaska have been documented to have an upwelled iron flux comparable in magnitude to dust deposition, the primary mechanism by which iron is delivered to the offshore North Pacific (Xiu et al., 2011).

Observations of biological responses to eddies are mixed. For instance, in contrast to the biomass minimum observation in the center of an anticyclonic eddy in Godø et al. (2012), a recent study acoustically sampled eddies in the North Atlantic and found the most intense mesopelagic acoustic backscatter in the interior of anticyclonic

eddies, which strongly decreased towards their edges (Della Penna and Gaube, 2020).

In our study, the variability in seal behavior suggests that some but not all eddies

encountered by contained enhanced mesopelagic prey fields. There may also be a

spatiotemporal mismatch between some physical processes within eddies and the

occurrence of higher trophic level prey items (*e.g.* Abrahms et al., 2019; Bailleul et

al., 2010; Barlow et al., 2021; Cotté et al., 2015; Guinet et al., 2001; Visser et al.,

2011).

We observed a high degree of individual variability in behavioral responses to

eddies, highlighting that small sample sizes cannot necessarily be extrapolated to

population-level trends. When encountering eddies, the diving behavior of individual

seals was quite variable. This suggests that the prey field did not shift vertically or

that prey abundance increased in a predictable way in cyclonic or anticyclonic eddies.

In addition to reflecting eddy variability, the range in behavioral responses can result

from individual differences between seals' diving behavior and responsiveness to

environmental cues are modulated by numerous confounding factors, such as predator

avoidance, experience, and specialized foraging strategies (Abrahms et al., 2017;

Beltran et al., 2021; Bradshaw et al., 2004). When the same seal encountered different

eddies of the same polarity, the best test for individual specialization available in this

dataset, behavioral responses were often inconsistent, suggesting further proximate

internal or external factors influence behavioral decisions. Northern elephant seals

forage over a vast region and can have variable diets (Goetsch et al., 2018). As such,

individuals may show a wide range of foraging behaviors (Le Boeuf et al., 2000;

Maxwell et al., 2012; Robinson et al., 2012) and respond differently to ocean dynamics. Such behavioral plasticity can buffer them from environmental changes (Abrahms et al., 2017; Goetsch et al., 2018; Holser, 2020), in contrast to other pinnipeds such as California sea lion (*Zalophus californianus*) (McHuron et al., 2018). Foraging within eddies is one of many foraging strategies employed by this species and most likely a result of opportunistic encounters. Only one seal in this study spent more than 20% of her foraging trip associated with eddies, so extended associations with these mesoscale features appear to be a viable but uncommon foraging strategy for northern elephant seals.

Eddies result in anomalous temperatures in their interiors relative to their immediate surroundings. As endothermic animals that maintain a large temperature gradient between their core and the ambient water, the temperature differences due to eddies are unlikely to have a direct effect on the seals the way they may on sharks (Braun et al., 2019; Gaube et al., 2018). The temperature anomalies within eddies (-0.55°C to 0.90°C) were an order of magnitude smaller than the vertical temperature gradients encountered during a typical deep dive (often 10°C or more). Thermal effects on the seals' prey are not well understood. Alewijnse et al. (2021) found very little effect of temperature on the metabolic rate of myctophids in the Southern Ocean. While we cannot assume myctophids in the North Pacific are physiologically equivalent, this result suggests that extremely cold temperatures are unlikely to disadvantage myctophids. On the other end of the spectrum, the warm cores of anticyclonic eddies may increase growth and reproduction of mesopelagic organisms

by increasing metabolic rates (Della Penna and Gaube, 2020; Proud et al., 2017), potentially increasing prey biomass. Determining whether the timescale of anticyclonic eddies' interaction with mesopelagic biota is sufficient for this positive thermal effect to influence a predator would likely require more direct sampling of mesopelagic organisms than is possible with predator tracking alone.

In agreement with a preference of southern elephant seals for (sub)mesoscale features during the post-molt trip but not the post-breeding trip documented in (Cotté et al., 2015), we observed a stronger reduction in transit rate and movement persistence during the post-molt trip than during the post-breeding trip. The northern elephant seals in this study did encounter eddies during the post-breeding trip so this does not seem to be an availability difference (127 eddy encounters during post-breeding, 88 post-molt). It is challenging to determine whether this seasonal difference in behavior is due to an internal or external influence. We have no way to directly test whether the wintertime eddies encountered during the post-breeding trip were of poorer foraging quality, but there was no significant difference in age or size of eddies between seasons. As internal factors such as trip timing explained more variability in behavior in our models than environmental factors, we hypothesize that this is the case here as well. The more muted behavioral response to the eddies encountered during the post-breeding trip may be due to the shorter nature of that trip, during which seals show faster transit rate and higher movement persistence. Perhaps the precise timing required discourages the seals from associating with mesoscale

features. If so, this illustrates a confounding factor of behavior in attempting to assess oceanographic effects on a prey field through the eyes of a predator.

Seal behavior suggests that physical-biological mechanisms such as frontal aggregation and behavioral attraction are likely required to increase seals' foraging potential within eddies; trophic transfer originating with nutrient enhancement is likely insufficient. Both cyclonic and anticyclonic eddies can contain distinct populations of mesopelagic fish larva which are physically retained by eddies (Atwood et al., 2010; Contreras-Catala et al., 2012; Daudén-Bengoa et al., 2020; Muhling et al., 2007; Nishimoto and Washburn, 2002). This study contributes to a growing body of evidence suggesting an enhancement of adult mesopelagic fish populations (Della Penna and Gaube, 2020; Devine et al., 2021; Fennell and Rose, 2015), helping connect the dots from eddies to higher trophic levels in the mesopelagic. Previous studies of mesopelagic predator foraging behavior in relation to eddies have been limited to small sample sizes of animals and eddies (sample sizes 1 to ~ 40) (Bailleul et al., 2010; Campagna et al., 2006; Dragon et al., 2010; Massie et al., 2016). We show here that mesoscale eddies are one type of oceanographic feature that may enhance foraging opportunities for northern elephant seals at sea when encountered.

Biological resources in the open ocean are patchily distributed (Benoit-Bird et al., 2013; Haury et al., 1978; Mackas et al., 1985; Steele, 1978) with implications for predator ecology as well as resource management (*e.g.* Santora et al. 2012, Scales et

al. 2014, 2018). The non-uniform distribution of prey items can be influenced by mesoscale features such as eddies. Our long-term northern elephant seal tracking suggests that Northeast Pacific eddies' biological relevance can extend to the mesopelagic zone and to a higher trophic level predator. While other predators in the Northeast Pacific such as northern fur seals (*Callorhinus ursinus)* (Pelland et al., 2014; Ream et al., 2005) and Steller sea lions (*Eumetopias jubatus*) (Lander et al., 2020) also use eddies, elephant seals are the first to demonstrate the relevance of eddies to the mesopelagic prey field in this region. Life in the mesopelagic zone is extremely abundant but poorly understood and vulnerable to anthropogenic pressures such as climate change and resource extraction (Caiger et al., 2021; Gjøsæter and Kawaguchi, 1980; Irigoien et al., 2014; Lam and Pauly, 2005; Martin et al., 2020). Investigating physical-biological mechanisms across trophic levels at these depths is therefore a research priority.

1.6. Conclusion

Our data show evidence of eddies affecting the seals' prey field, presumably through prey aggregation processes as seals used the edges of eddies more heavily than the interiors, with bottom-up processes playing a smaller role. Anticyclonic eddies triggered the strongest behavioral responses. The variability in behavioral responses suggests there is likely complexity in eddies' biological characteristics not well captured by their physical characteristics and some spatiotemporal mismatch between eddy physics and elephant seal prey species. These physical-biological mechanisms require further investigation and are especially relevant as the ocean

undergoes unprecedented rapid change and its effects on deep sea biology and pelagic

predators remain challenging to predict.

1.7 References

Abrahms, B., Hazen, E.L., Aikens, E.O., Savoca, M.S., Goldbogen, J.A., Bograd, S.J., 2019.
Memory and resource tracking drive blue whale migrations. Proc. Natl. Acad. Sci. 1–6.
https://doi.org/10.1073/pnas.1819031116

Abrahms, B., Hazen, E.L., Bograd, S.J., Brashares, J.S., Robinson, P.W., Scales, K.L.,
Crocker, D.E., Costa, D.P., 2017. Climate mediates the success of migration strategies
in a marine predator. Ecol. Lett. https://doi.org/10.1111/ele.12871

Abrahms, B., Scales, K.L., Hazen, E.L., Bograd, S.J., Schick, R.S., Robinson, P.W., Costa,
D.P., 2018. Mesoscale activity facilitates energy gain in a top predator. Proc. Natl.
Acad. Sci. B 285. https://doi.org/10.1098/rspb.2018.1101

Adachi, T., Takahashi, A., Costa, D.P., Robinson, P.W., Hückstädt, L.A., Peterson, S.H.,
Holser, R.R., Beltran, R.S., Keates, T.R., Naito, Y., 2021. Forced into an ecological
corner: Round-the-clock deep foraging on small prey by elephant seals. Sci. Adv. 7, 21–
25. https://doi.org/10.1126/sciadv.abg3628

Alewijnse, S., Stowasser, G., Saunders, R., Belcher, A., Crimmen, O., Cooper, N., Trueman,
C., 2021. Otolith-derived field metabolic rates of myctophids (Family Myctophidae)
from the Scotia Sea (Southern Ocean). Mar. Ecol. Prog. Ser. 675, 113–131.
https://doi.org/10.3354/meps13827

Atwood, E., Duffy-Anderson, J.T., Horne, J.K., Ladd, C., 2010. Influence of mesoscale
eddies on ichthyoplankton assemblages in the Gulf of Alaska. Fish. Oceanogr. 19, 493–
507. https://doi.org/10.1111/j.1365-2419.2010.00559.x

Bailleul, F., Cotté, C., Guinet, C., 2010. Mesoscale eddies as foraging area of a deep-diving
predator, the southern elephant seal. Mar. Ecol. Prog. Ser. 408, 251–264.

https://doi.org/10.3354/meps08560

Bakun, A., 2006. Fronts and eddies as key structures in the habitat of marine fish larvae: opportunity, adaptive response, and competitive advantage. Sci. Mar. 70S2, 105–122.

Barlow, D.R., Klinck, H., Ponirakis, D., Garvey, C., Torres, L.G., 2021. Temporal and spatial lags between wind , coastal upwelling , and blue whale occurrence. Sci. Rep. 1–10. https://doi.org/10.1038/s41598-021-86403-y

Beltran, R.S., Kendall-Bar, J.M., Pirotta, E., Adachi, T., Naito, Y., Takahashi, A., Cremers, J., Robinson, P.W., Crocker, D.E., Costa, D.P., 2021. Lightscapes of fear: how mesopredators balance starvation and predation in the open ocean. Sci. Adv. 1–9. https://doi.org/10.1126/sciadv.abd9818

Benoit-Bird, K.J., Battaile, B.C., Nordstrom, C.A., Trites, A.W., 2013. Foraging behavior of northern fur seals closely matches the hierarchical patch scales of prey. Mar. Ecol. Prog. Ser. 479, 283–302. https://doi.org/10.3354/meps10209

Biuw, M., McConnell, B., Bradshaw, C.J.A., Burton, H., Fedak, M., 2003. Blubber and buoyancy : monitoring the body condition of free-ranging seals using simple dive characteristics. J. Exp. Biol. 3405–3423. https://doi.org/10.1242/jeb.00583

Boehme, L., Lovell, P., Biuw, M., Roquet, F., Nicholson, J., Thorpe, S.E., Meredith, M.P., Fedak, M., 2009. Technical note: Animal-borne CTD-Satellite Relay Data Loggers for real-time oceanographic data collection. Ocean Sci. 5, 685–695. https://doi.org/10.5194/os-5-685-2009

Bograd, S.J., Block, B.A., Costa, D.P., Godley, B.J., 2010. Biologging technologies: New tools for conservation. Introduction. Endanger. Species Res. 10, 1–7.

https://doi.org/10.3354/esr00269

Bost, C.A., Cotté, C., Bailleul, F., Cherel, Y., Charrassin, J.B., Guinet, C., Ainley, D.G.,
Weimerskirch, H., 2009. The importance of oceanographic fronts to marine birds and
mammals of the southern oceans. J. Mar. Syst. 78, 363–376.
https://doi.org/10.1016/j.jmarsys.2008.11.022

Boyd, P.W., Law, C.S., Wong, C.S., Nojiri, Y., Tsuda, A., Levasseur, M., Takeda, S., Rivkin,
R., Harrison, P.J., Strzepak, R., Gower, J., McKay, R.M., Abraham, E.R., Arychuk, M.,
Barwell-Clarke, J., Crawford, W.R., Crawford, D., Hale, M., Harada, K., Johnson, K.S.,
Kiyosawa, H., Kudo, I., Marchetti, A., Miller, W., Needoba, J., Nishioka, J., Ogawa, H.,
Page, J., Robert, M., Saito, H., Sastri, A., Sherry, N., Soutar, T., Sutherland, N.E., Taira,
Y., Whitney, F., Wong, S.K.E., Yoshimura, T., 2004. The decline and fate of an iron-
induced subarctic phytoplankton bloom. Nature 428, 549–553.
https://doi.org/10.1029/2001jb001129

Boyd, S.H., Wiebe, P.H., Backus, R.H., Craddock, J.E., Daher, M.A., 1986. Biomass of the
micronekton in Gulf Stream ring 82-B and environs: changes with time. Deep Sea Res.
Part A, Oceanogr. Res. Pap. 33, 1885–1905. https://doi.org/10.1016/0198-
0149(86)90084-1

Bradshaw, C.J.A., Hindell, M.A., Sumner, M.D., Michael, K.J., 2004. Loyalty pays: Potential
life history consequences of fidelity to marine foraging regions by southern elephant
seals. Anim. Behav. 68, 1349–1360. https://doi.org/10.1016/j.anbehav.2003.12.013

Braun, C.D., Gaube, P., Sinclair-Taylor, T.H., Skomal, G.B., Thorrold, S.R., 2019. Mesoscale
eddies release pelagic sharks from thermal constraints to foraging in the ocean twilight
zone. Proc. Natl. Acad. Sci. 201903067. https://doi.org/10.1073/pnas.1903067116

Caiger, P.E., Lefebve, L.S., Llopiz, J.K., 2021. Growth and reproduction in mesopelagic
    fishes: A literature synthesis. ICES J. Mar. Sci. https://doi.org/10.1093/icesjms/fsaa247

Campagna, C., Piola, A.R., Rosa Marin, M., Lewis, M., Fernández, T., 2006. Southern
    elephant seal trajectories, fronts and eddies in the Brazil/Malvinas Confluence. Deep.
    Res. Part I Oceanogr. Res. Pap. 53, 1907–1924.
    https://doi.org/10.1016/j.dsr.2006.08.015

Chambault, P., Baudena, A., Bjorndal, K.A., Santos, M.A.R., Bolten, A.B., Vandeperre, F.,
    2019. Swirling in the ocean: Immature loggerhead turtles seasonally target old
    anticyclonic eddies at the fringe of the North Atlantic gyre. Prog. Oceanogr. 175, 345–
    358. https://doi.org/10.1016/j.pocean.2019.05.005

Chelton, D.B., Schlax, M.G., Samelson, R.M., 2011. Global observations of nonlinear
    mesoscale eddies. Prog. Oceanogr. 91, 167–216.
    https://doi.org/10.1016/j.pocean.2011.01.002

Cheng, Y.H., Ho, C.R., Zheng, Q., Kuo, N.J., 2014. Statistical characteristics of mesoscale
    eddies in the North Pacific derived from satellite altimetry. Remote Sens. 6, 5164–5183.
    https://doi.org/10.3390/rs6065164

Contreras-Catala, F., Sánchez-Velasco, L., Lavín, M.F., Godínez, V.M., 2012. Three-
    dimensional distribution of larval fish assemblages in an anticyclonic eddy in a semi-
    enclosed sea (Gulf of California). J. Plankton Res. 34, 548–562.
    https://doi.org/10.1093/plankt/fbs024

Costa, D.P., Boeuf, B.J.L., Huntley, A.C., Ortiz, C.L., 1986. The energetics of lactation in the
    Northern elephant seal, Mirounga angustirostris. J. Zool. 209, 21–33.

https://doi.org/10.1111/j.1469-7998.1986.tb03563.x

Costa, D.P., Breed, G. a., Robinson, P.W., 2012. New insights into pelagic migrations: Implications for ecology and conservation. Annu. Rev. Ecol. Evol. Syst. 43, 73–96. https://doi.org/10.1146/annurev-ecolsys-102710-145045

Cotté, C., D'Ovidio, F., Dragon, A.C., Guinet, C., Lévy, M., 2015. Flexible preference of southern elephant seals for distinct mesoscale features within the Antarctic Circumpolar Current. Prog. Oceanogr. 131, 46–58. https://doi.org/10.1016/j.pocean.2014.11.011

Cotté, C., Park, Y.H., Guinet, C., Bost, C.A., 2007. Movements of foraging king penguins through marine mesoscale eddies. Proc. R. Soc. B Biol. Sci. 274, 2385–2391. https://doi.org/10.1098/rspb.2007.0775

Crawford, W.R., Brickley, P.J., Peterson, T.D., Thomas, A.C., 2005. Impact of Haida Eddies on chlorophyll distribution in the Eastern Gulf of Alaska. Deep. Res. Part II Top. Stud. Oceanogr. 52, 975–989. https://doi.org/10.1016/j.dsr2.2005.02.011

Crawford, W.R., Brickley, P.J., Thomas, A.C., 2007. Mesoscale eddies dominate surface phytoplankton in northern Gulf of Alaska. Prog. Oceanogr. 75, 287–303. https://doi.org/10.1016/j.pocean.2007.08.016

Crocker, D.E., Le Boeuf, B.J., Costa, D.P., 1997. Drift diving in female northern elephant seals: Implications for food processing. Can. J. Zool. 75, 27–39. https://doi.org/10.1016/j.dnarep.2015.02.007

Cummins, P.F., Freeland, H.J., 2007. Variability of the North Pacific Current and its bifurcation. Prog. Oceanogr. 75, 253–265. https://doi.org/10.1016/j.pocean.2007.08.006

Cummins, P.F., Lagerloef, G.S.E., 2004. Wind-driven interannual variability over the

northeast Pacific Ocean. Deep. Res. Part I Oceanogr. Res. Pap. 51, 2105–2121. https://doi.org/10.1029/2001JC001131

D'Ovidio, F., De Monte, S., Penna, A. Della, Cotté, C., Guinet, C., 2013. Ecological implications of eddy retention in the open ocean: A Lagrangian approach. J. Phys. A Math. Theor. 46. https://doi.org/10.1088/1751-8113/46/25/254023

d'Ovidio, F., Fernández, V., Hernández-García, E., López, C., 2004. Mixing structures in the Mediterranean Sea from finite-size Lyapunov exponents. Geophys. Res. Lett. 31, 1–4. https://doi.org/10.1029/2004GL020328

Daudén-Bengoa, G., Jiménez-Rosenberg, S.P.A., Compaire, J.C., del Pilar Echeverri-García, L., Pérez-Brunius, P., Herzka, S.Z., 2020. Larval fish assemblages of myctophids in the deep water region of the southern Gulf of Mexico linked to oceanographic conditions. Deep. Res. Part I Oceanogr. Res. Pap. 155. https://doi.org/10.1016/j.dsr.2019.103181

Della Penna, A., De Monte, S., Kestenare, E., Guinet, C., d'Ovidio, F., 2016. Quasi-planktonic behavior of foraging top marine predators. Sci. Rep. 5, 18063. https://doi.org/10.1038/srep18063

Della Penna, A., Gaube, P., 2020. Mesoscale Eddies Structure Mesopelagic Communities. Front. Mar. Sci. 7, 1–9. https://doi.org/10.3389/fmars.2020.00454

Della Penna, A., Llort, J., Moreau, S., Patel, R., 2021. The impact of a Southern Ocean cyclonic eddy on mesopelagic micronekton. ESSOAr. https://doi.org/10.1002/essoar.10507935.1

Devine, B., Fennell, S., Themelis, D., Fisher, J.A.D., 2021. Influence of anticyclonic, warm-core eddies on mesopelagic fish assemblages in the Northwest Atlantic Ocean. Deep.

Res. Part I Oceanogr. Res. Pap. 173, 103555. https://doi.org/10.1016/j.dsr.2021.103555

Dragon, A.C., Monestiez, P., Bar-Hen, A., Guinet, C., 2010. Linking foraging behaviour to physical oceanographic structures: Southern elephant seals and mesoscale eddies east of Kerguelen Islands. Prog. Oceanogr. 87, 61–71. https://doi.org/10.1016/j.pocean.2010.09.025

Dufois, F., Hardman-Mountford, N.J., Greenwood, J., Richardson, A.J., Feng, M., Matear, R.J., 2016. Anticyclonic eddies are more productive than cyclonic eddies in subtropical gyres because of winter mixing. Sci. Adv. 2, 1–7. https://doi.org/10.1126/sciadv.1600282

Fasiolo, M., Nedellec, R., Goude, Y., Wood, S.N., 2020. Scalable Visualization Methods for Modern Generalized Additive Models. J. Comput. Graph. Stat. 29, 78–86. https://doi.org/10.1080/10618600.2019.1629942

Fennell, S., Rose, G., 2015. Oceanographic influences on Deep Scattering Layers across the North Atlantic. Deep. Res. Part I Oceanogr. Res. Pap. 105, 132–141. https://doi.org/10.1016/j.dsr.2015.09.002

Flierl, G., McGillicuddy, D.J., 2002. Mesoscale and submesoscale physical-biological interactions, in: Robinson, A., McCarthy, J., Rothschild, B. (Eds.), The Sea. pp. 113–185.

Franks, P.J.S., Wroblewski, J.S., Flierl, G.R., 1986. Prediction of phytoplankton growth in response to the frictional decay of a warm-core ring. J. Geophys. Res. 91, 7603–7610.

Gaube, P., Braun, C.D., Lawson, G.L., McGillicuddy, D.J., Penna, A. Della, Skomal, G.B., Fischer, C., Thorrold, S.R., 2018. Mesoscale eddies influence the movements of mature

female white sharks in the Gulf Stream and Sargasso Sea. Sci. Rep. 8, 7363.

https://doi.org/10.1038/s41598-018-25565-8

Gaube, P., Chelton, D.B., Strutton, P.G., Behrenfeld, M.J., 2013. Satellite observations of

chlorophyll, phytoplankton biomass, and Ekman pumping in nonlinear mesoscale

eddies. J. Geophys. Res. Ocean. 118, 6349–6370.

https://doi.org/10.1002/2013JC009027

Gaube, P., McGillicuddy, D.J., Chelton, D.B., Behrenfeld, M.J., Strutton, P.G., 2014.

Regional variations in the influence of mesoscale eddies on near-surface chlorophyll. J.

Geophys. Res. Ocean. 119, 8195–8220. https://doi.org/10.1002/2014JC010111

Gjøsæter, J., Kawaguchi, K., 1980. A Review of the World Resources of Mesopelagic Fish,

Fisheries. ed. Food and Agriculture Organization of the United Nations.

Godø, O.R., Samuelsen, A., Macaulay, G.J., Patel, R., Hjøllo, S.S., Horne, J., Kaartvedt, S.,

Johannessen, J.A., 2012. Mesoscale eddies are oases for higher trophic marine life.

PLoS One 7, 1–9. https://doi.org/10.1371/journal.pone.0030161

Goetsch, C., Conners, M.G., Budge, S.M., Mitani, Y., Walker, W.A., Bromaghin, J.F.,

Simmons, S.E., Reichmuth, C., Costa, D.P., 2018. Energy-rich mesopelagic fishes

revealed as a critical prey resource for a deep-diving predator using Quantitative Fatty

Acid Signature Analysis. Front. Mar. Sci. 5, 1–19.

https://doi.org/10.3389/fmars.2018.00430

Guinet, C., Dubroca, L., Lea, M.A., Goldsworthy, S., Cherel, Y., Duhamel, G., Bonadonna,

F., Donnay, J.P., 2001. Spatial distribution of foraging in female antarctic fur seals

Arctocephalus gazella in relation to oceanographic variables: A scale-dependent

approach using geographic information systems. Mar. Ecol. Prog. Ser. 219, 251–264. https://doi.org/10.3354/meps219251

Harcourt, R., Sequeira, A.M.M., Zhang, X., Roquet, F., Komatsu, K., Heupel, M., McMahon, C., Whoriskey, F., Meekan, M., Carroll, G., Brodie, S., Simpfendorfer, C., Hindell, M., Jonsen, I., Costa, D.P., Block, B., Muelbert, M., Woodward, B., Weise, M., Aarestrup, K., Biuw, M., Boehme, L., Bograd, S.J., Cazau, D., Charrassin, J.-B., Cooke, S.J., Cowley, P., de Bruyn, P.J.N., Jeanniard du Dot, T., Duarte, C., Eguíluz, V.M., Ferreira, L.C., Fernández-Gracia, J., Goetz, K., Goto, Y., Guinet, C., Hammill, M., Hays, G.C., Hazen, E.L., Hückstädt, L.A., Huveneers, C., Iverson, S., Jaaman, S.A., Kittiwattanawong, K., Kovacs, K.M., Lydersen, C., Moltmann, T., Naruoka, M., Phillips, L., Picard, B., Queiroz, N., Reverdin, G., Sato, K., Sims, D.W., Thorstad, E.B., Thums, M., Treasure, A.M., Trites, A.W., Williams, G.D., Yonehara, Y., Fedak, M.A., 2019. Animal-Borne Telemetry: An Integral Component of the Ocean Observing Toolkit. Front. Mar. Sci. 6. https://doi.org/10.3389/fmars.2019.00326

Haury, L.R., McGowan, J.A., Wiebe, P.H., 1978. Patterns and processes in the time-space scales of plankton distributions, in: Steele, J.H. (Ed.), Spatial Pattern in Plankton Communities. Plenum Press, New Y, pp. 277–328.

Holser, R.R., 2020. A Top Predator in Hot Water: Effects of a Marine Heatwave on Foraging and Reproduction in the Northern Elephant Seal. University of California, Santa Cruz.

Holte, J., Talley, L., 2009. A new algorithm for finding mixed layer depths with applications to Argo data and Subantarctic Mode Water formation. J. Atmos. Ocean. Technol. 26, 1920–1939. https://doi.org/10.1175/2009JTECHO543.1

Hussey, N.E., Kessel, S.T., Aarestrup, K., Cooke, S.J., Cowley, P.D., Fisk, A.T., Harcourt,

R.G., Holland, K.N., Iverson, S.J., Kocik, J.F., Flemming, J.E.M., Whoriskey, F.G., 2015. Aquatic animal telemetry: A panoramic window into the underwater world. Science (80-.). 348, 1255642. https://doi.org/10.1126/science.1255642

Irigoien, X., Klevjer, T.A., Røstad, A., Martinez, U., Boyra, G., Acuña, J.L., Bode, A., Echevarria, F., Gonzalez-Gordillo, J.I., Hernandez-Leon, S., Agusti, S., Aksnes, D.L., Duarte, C.M., Kaartvedt, S., 2014. Large mesopelagic fishes biomass and trophic efficiency in the open ocean. Nat. Commun. 5, 3271. https://doi.org/10.1038/ncomms4271

Johnson, W.K., Miller, L.A., Sutherland, N.E., Wong, C.S., 2005. Iron transport by mesoscale Haida eddies in the Gulf of Alaska. Deep. Res. Part II Top. Stud. Oceanogr. 52, 933–953. https://doi.org/10.1016/j.dsr2.2004.08.017

Jonsen, I.D., McMahon, C.R., Patterson, T.A., Auger-Méthé, M., Harcourt, R., Hindell, M.A., Bestley, S., 2019. Movement responses to environment: fast inference of variation among southern elephant seals with a mixed effects model. Ecology 100, 1–8. https://doi.org/10.1002/ecy.2566

Jonsen, I.D., Patterson, T.A., Costa, D.P., Doherty, P.D., Godley, B.J., Grecian, W.J., Guinet, C., Hoenner, X., Kienle, S.S., Robinson, P.W., Votier, S.C., Witt, M.J., Hindell, M.A., Harcourt, R.G., McMahon, C.R., 2020. A continuous-time state-space model for rapid quality-control of Argos locations from animal-borne tags. Mov. Ecol. 8. https://doi.org/10.1186/s40462-020-00217-7

Kienle, S.S., 2019. Intraspecific variation and behavioral flexibility in the foraging strategies of seals. University Of California Santa Cruz.

Koblick, D., 2021. Vectorized solar azimuth and elevation estimation [WWW Document].
MATLAB Cent. File Exch. URL
https://www.mathworks.com/matlabcentral/fileexchange/23051-vectorized-solar-
azimuth-and-elevation-estimation

Lam, V., Pauly, D., 2005. Mapping the global biomass of mesopelagic fishes. Sea around Us
Proj. Newsl. July/Augus, 4.

Lambardi, P., Lutjeharms, J.R.E., Mencacci, R., Hays, G.C., Luschi, P., 2008. Influence of
ocean currents on long-distance movement of leatherback sea turtles in the Southwest
Indian Ocean. Mar. Ecol. Prog. Ser. 353, 289–301. https://doi.org/10.3354/meps07118

Lander, M.E., Fadely, B.S., Gelatt, T.S., Sterling, J.T., Johnson, D.S., Pelland, N.A., 2020.
Mixing it up in Alaska: Habitat use of adult female Steller sea lions reveals a variety of
foraging strategies. Ecosphere 11, 2. https://doi.org/10.1002/ecs2.3021

Le Boeuf, B.J., Crocker, D.E., Costa, D.P., Blackwell, S.B., Webb, P.M., Houser, D.S., 2000.
Foraging ecology of northern elephant seals. Ecol. Monogr. 70, 353–382.
https://doi.org/10.1890/0012-9615(2000)070[0353:FEONES]2.0.CO;2

Legal, C., Klein, P., Treguier, A.M., Paillet, J., 2007. Diagnosis of the vertical motions in a
mesoscale stirring region. J. Phys. Oceanogr. 37, 1413–1424.
https://doi.org/10.1175/JPO3053.1

Mackas, D.L., Denman, K.L., Abbott, M.R., 1985. Plankton patchiness: biology in the
physical vernacular. Bull. Mar. Sci. 37, 653–674.

Mackas, D.L., Tsurumi, M., Galbraith, M.D., Yelland, D.R., 2005. Zooplankton distribution
and dynamics in a North Pacific Eddy of coastal origin: II. Mechanisms of eddy

colonization by and retention of offshore species. Deep. Res. Part II Top. Stud. Oceanogr. 52, 1011–1035. https://doi.org/10.1016/j.dsr2.2005.02.008

Martin, A., Boyd, P., Buesseler, K., Cetinic, I., Claustre, H., Giering, S., Henson, S., Irigoien, X., Kriest, I., Mémery, L., Robinson, C., Saba, G., Sanders, R., Siegel, D., Villa-Alfageme, M., Guidi, L., 2020. Study the twilight zone before it is too late. Nature 580, 26–28. https://doi.org/10.1038/d41586-020-00915-7

Martin, A.P., Richards, K.J., 2001. Mechanisms for vertical nutrient transport within a North Atlantic mesoscale eddy. Deep. Res. Part II Top. Stud. Oceanogr. 48, 757–773. https://doi.org/10.1016/S0967-0645(00)00096-5

Martin, J.H., Gordon, R.M., Fitzwater, S., Broenkow, W.W., 1989. VERTEX: phytoplankton/iron studies in the Gulf of Alaska. Deep Sea Res. Part A, Oceanogr. Res. Pap. 36, 649–680. https://doi.org/10.1016/0198-0149(89)90144-1

Massie, P.P., McIntyre, T., Ryan, P.G., Bester, M.N., Bornemann, H., Ansorge, I.J., 2016. The role of eddies in the diving behaviour of female southern elephant seals. Polar Biol. 39, 297–307. https://doi.org/10.1007/s00300-015-1782-0

Maxwell, S.M., Frank, J.J., Breed, G.A., Robinson, P.W., Simmons, S.E., Crocker, D.E., Gallo-Reynoso, J.P., Costa, D.P., 2012. Benthic foraging on seamounts: A specialized foraging behavior in a deep-diving pinniped. Mar. Mammal Sci. 28, 1–12. https://doi.org/10.1111/j.1748-7692.2011.00527.x

McDougall, T.J., Barker, P.M., 2011. Getting started with TEOS-10 and the Gibbs Seawater (GSW) Oceanographic Toolbox. SCOR/IAPSO WG127.

McGillicuddy, D.J., Robinson, A.R., 1997. Eddy-induced nutrient supply and new production

in the Sargasso Sea. Deep. Res. Part I Oceanogr. Res. Pap. 44, 1427–1450. https://doi.org/10.1016/S0967-0637(97)00024-1

McHuron, E.A., Hazen, E., Costa, D.P., 2018. Constrained by consistency? Repeatability of foraging behavior at multiple timescales for a generalist marine predator. Mar. Biol. 165, 1–13. https://doi.org/10.1007/s00227-018-3382-3

Muhling, B.A., Beckley, L.E., Olivar, M.P., 2007. Ichthyoplankton assemblage structure in two meso-scale Leeuwin Current eddies, eastern Indian Ocean. Deep. Res. Part II Top. Stud. Oceanogr. 54, 1113–1128. https://doi.org/10.1016/j.dsr2.2006.05.045

Naito, Y., Costa, D.P., Adachi, T., Robinson, P.W., Fowler, M., Takahashi, A., 2013. Unravelling the mysteries of a mesopelagic diet: A large apex predator specializes on small prey. Funct. Ecol. 27, 710–717. https://doi.org/10.1111/1365-2435.12083

Naito, Y., Costa, D.P., Adachi, T., Robinson, P.W., Peterson, S.H., Mitani, Y., Takahashi, A., 2017. Oxygen minimum zone: An important oceanographic habitat for deep-diving northern elephant seals , Mirounga angustirostris. Ecol. Evol. 1–12. https://doi.org/10.1002/ece3.3202

Nishimoto, M.M., Washburn, L., 2002. Patterns of coastal eddy circulation and abundance of pelagic juvenile fish in the Santa Barbara Channel, California, USA. Mar. Ecol. Prog. Ser. 241, 183–199. https://doi.org/10.3354/meps241183

Olson, D.B., 1986. Lateral exchange within Gulf Stream warm-core ring surface layers. Deep Sea Res. Part A, Oceanogr. Res. Pap. 33, 1691–1704. https://doi.org/10.1016/0198-0149(86)90074-9

Palacios, D.M., Bograd, S.J., Foley, D.G., Schwing, F.B., 2006. Oceanographic

characteristics of biological hot spots in the North Pacific: A remote sensing

perspective. Deep. Res. Part II Top. Stud. Oceanogr. 53, 250–269.

https://doi.org/10.1016/j.dsr2.2006.03.004

Paradis, E., Schliep, K., 2019. ape 5.0: an environment for modern phylogenetics and

evolutionary analyses in R. Bioinformatics 35, 526–528.

https://doi.org/10.1093/bioinformatics/bty633

Pelland, N.A., Sterling, J.T., Lea, M.A., Bond, N.A., Ream, R.R., Lee, C.M., Eriksen, C.C.,

2014. Fortuitous encounters between Seagliders and adult female northern fur seals

(Callorhinus ursinus) off the Washington (USA) coast: Upper ocean variability and

links to top predator behavior. PLoS One 9.

https://doi.org/10.1371/journal.pone.0101268

Petersen, M.R., Williams, S.J., Maltrud, M.E., Hecht, M.W., Hamann, B., 2013. A three-

dimensional eddy census of a high-resolution global ocean simulation. J. Geophys. Res.

Ocean. 118, 1759–1774. https://doi.org/10.1002/jgrc.20155

Peterson, T.D., Whitney, F.A., Harrison, P.J., 2005. Macronutrient dynamics in an

anticyclonic mesoscale eddy in the Gulf of Alaska. Deep. Res. Part II Top. Stud.

Oceanogr. 52, 909–932. https://doi.org/10.1016/j.dsr2.2005.02.004

Polovina, J., Uchida, I., Balazs, G., Howell, E.A., Parker, D., Dutton, P., 2006. The Kuroshio

Extension Bifurcation Region: A pelagic hotspot for juvenile loggerhead sea turtles.

Deep. Res. Part II Top. Stud. Oceanogr. 53, 326–339.

https://doi.org/10.1016/j.dsr2.2006.01.006

Proud, R., Cox, M.J., Brierley, A.S., 2017. Biogeography of the global ocean's mesopelagic

zone. Curr. Biol. 27, 113–119. https://doi.org/10.1016/j.cub.2016.11.003

R Core Team, 2022. R: A language and environment for statistical computing.

Ream, R.R., Sterling, J.T., Loughlin, T.R., 2005. Oceanographic features related to northern
fur seal migratory movements. Deep. Res. Part II Top. Stud. Oceanogr. 52, 823–843.
https://doi.org/10.1016/j.dsr2.2004.12.021

Robinson, P.W., Costa, D.P., Crocker, D.E., Gallo-Reynoso, J.P., Champagne, C.D., Fowler,
M.A., Goetsch, C., Goetz, K.T., Hassrick, J.L., Hückstädt, L.A., Kuhn, C.E., Maresh,
J.L., Maxwell, S.M., McDonald, B.I., Peterson, S.H., Simmons, S.E., Teutschel, N.M.,
Villegas-Amtmann, S., Yoda, K., 2012. Foraging behavior and success of a mesopelagic
predator in the northeast Pacific Ocean: insights from a data-rich species, the northern
elephant seal. PLoS One 7. https://doi.org/10.1371/journal.pone.0036728

Robinson, P.W., Simmons, S.E., Crocker, D.E., Costa, D.P., 2010. Measurements of foraging
success in a highly pelagic marine predator, the northern elephant seal. J. Anim. Ecol.
79, 1146–1156. https://doi.org/10.1111/j.1365-2656.2010.01735.x

Roden, G.I., 1991. Subarctic-subtropical transition zone of the North Pacific: Large-scale
aspects and mesoscale structure. NOAA Tech. Rep. NMFS 105, 1–38.

Samuelsen, A., Hjøllo, S.S., Johannessen, J.A., Patel, R., 2012. Particle aggregation at the
edges of anticyclonic eddies and implications for distribution of biomass. Ocean Sci. 8,
389–400. https://doi.org/10.5194/os-8-389-2012

Santora, J.A., Field, J.C., Schroeder, I.D., Sakuma, K.M., Wells, B.K., Sydeman, W.J., 2012.
Spatial ecology of krill, micronekton and top predators in the central California Current:
Implications for defining ecologically important areas. Prog. Oceanogr. 106, 154–174.

https://doi.org/10.1016/j.pocean.2012.08.005

Scales, K.L., Hazen, E.L., Jacox, M.G., Castruccio, F., Maxwell, S.M., Lewison, R.L., Bograd, S.J., 2018. Fisheries bycatch risk to marine megafauna is intensified in Lagrangian coherent structures. Proc. Natl. Acad. Sci. 201801270. https://doi.org/10.1073/pnas.1801270115

Scales, K.L., Miller, P.I., Hawkes, L.A., Ingram, S.N., Sims, D.W., Votier, S.C., 2014. On the front line: Frontal zones as priority at-sea conservation areas for mobile marine vertebrates. J. Appl. Ecol. 51, 1575–1583. https://doi.org/10.1111/1365-2664.12330

Schmid, M.S., Cowen, R.K., Robinson, K., Luo, J.Y., Briseño-Avena, C., Sponaugle, S., 2020. Prey and predator overlap at the edge of a mesoscale eddy: fine-scale, in-situ distributions to inform our understanding of oceanographic processes. Sci. Rep. 10, 1–16. https://doi.org/10.1038/s41598-020-57879-x

Simmons, S.E., Crocker, D.E., Kudela, R.M., Costa, D.P., 2007. Linking foraging behaviour of the northern elephant seal with oceanography and bathymetry at mesoscales. Mar. Ecol. Prog. Ser. 346, 265–275. https://doi.org/10.3354/meps07014

Simmons, S.E., Tremblay, Y., Costa, D.P., 2009. Pinnipeds as ocean-temperature samplers: calibrations, validations, and data quality. Limnol. Oceanogr. Methods 7, 648–656. https://doi.org/10.4319/lom.2009.7.648

Smith, W.H.F., Sandwell, D.T., 1997. Global seafloor topography from satellite altimetry and ship depth soundings. Science (80-.). 277, 1957–1962.

Steele, J.H., 1978. Spatial pattern in plankton communities, NATO Conference Series, Marine Sciences IV. Plenum Press, New York, NY.

Stegmann, P.M., Schwing, F., 2007. Demographics of mesoscale eddies in the California
Current. Geophys. Res. Lett. 34, 2–5. https://doi.org/10.1029/2007GL029504

Sydeman, W.J., Thompson, S.A., Field, J.C., Peterson, W.T., Tanasichuk, R.W., Freeland,
H.J., Bograd, S.J., Rykaczewski, R.R., 2011. Does positioning of the North Pacific
Current affect downstream ecosystem productivity? Geophys. Res. Lett. 38, 1–6.
https://doi.org/10.1029/2011GL047212

Visser, F., Hartman, K.L., Pierce, G.J., Valavanis, V.D., Huisman, J., 2011. Timing of
migratory baleen whales at the Azores in relation to the North Atlantic spring bloom.
Mar. Ecol. Prog. Ser. 440, 267–279. https://doi.org/10.3354/meps09349

Webb, P.M., Crocker, D.E., Blackwell, S.B., Costa, D.P., Le Boeuf, B.J., 1998. Effects of
buoyancy on the diving behavior of northern elephant seals. J. Exp. Biol. 201, 2349–
2358. https://doi.org/10.1242/jeb.00952

Wood, S.N., 2017. Generalized Additive Models: An Introduction with R, 2nd ed. Chapman
and Hall/CRC, Boca Raton. https://doi.org/10.1201/9781315370279

Woodson, C.B., Litvin, S.Y., 2015. Ocean fronts drive marine fishery production and
biogeochemical cycling. Proc. Natl. Acad. Sci. 112, 1710–1715.
https://doi.org/10.1073/pnas.1417143112

Woodworth, P.A., Schorr, G.S., Baird, R.W., Webster, D.L., Mcsweeney, D.J., Hanson,
M.B., Andrews, R.D., Polovina, J.J., 2012. Eddies as offshore foraging grounds for
melon-headed whales (Peponocephala electra). Mar. Mammal Sci. 28, 638–647.
https://doi.org/10.1111/j.1748-7692.2011.00509.x

Xiu, P., Palacz, A.P., Chai, F., Roy, *E.G.*, Wells, M.L., 2011. Iron flux induced by Haida

eddies in the Gulf of Alaska. Geophys. Res. Lett. 38, 1–5. https://doi.org/10.1029/2011GL047946

Yoshino, K., Takahashi, A., Adachi, T., Costa, D.P., Robinson, P.W., Peterson, S.H., Hückstädt, L.A., Holser, R.R., Naito, Y., 2020. Acceleration-triggered animal-borne videos show a dominance of fish in the diet of female northern elephant seals. J. Exp. Biol. jeb.212936. https://doi.org/10.1242/jeb.212936

Yuan, X., Talley, L.D., 1996. The subarctic frontal zone in the North Pacific: Characteristics of frontal structure from climatological data and synoptic surveys. J. Geophys. Res. 101, 16491–16508.

Zainuddin, M., Saitoh, K., Saitoh, S.I., 2008. Albacore (Thunnus alalunga) fishing ground in relation to oceanographic conditions in the western North Pacific Ocean using remotely sensed satellite data. Fish. Oceanogr. 17, 61–73. https://doi.org/10.1111/j.1365-2419.2008.00461.x

Zhang, W.Z., Xue, H., Chai, F., Ni, Q., 2015. Dynamical processes within an anticyclonic eddy revealed from Argo floats. Geophys. Res. Lett. 42, 2342–2350. https://doi.org/10.1002/2015GL063120
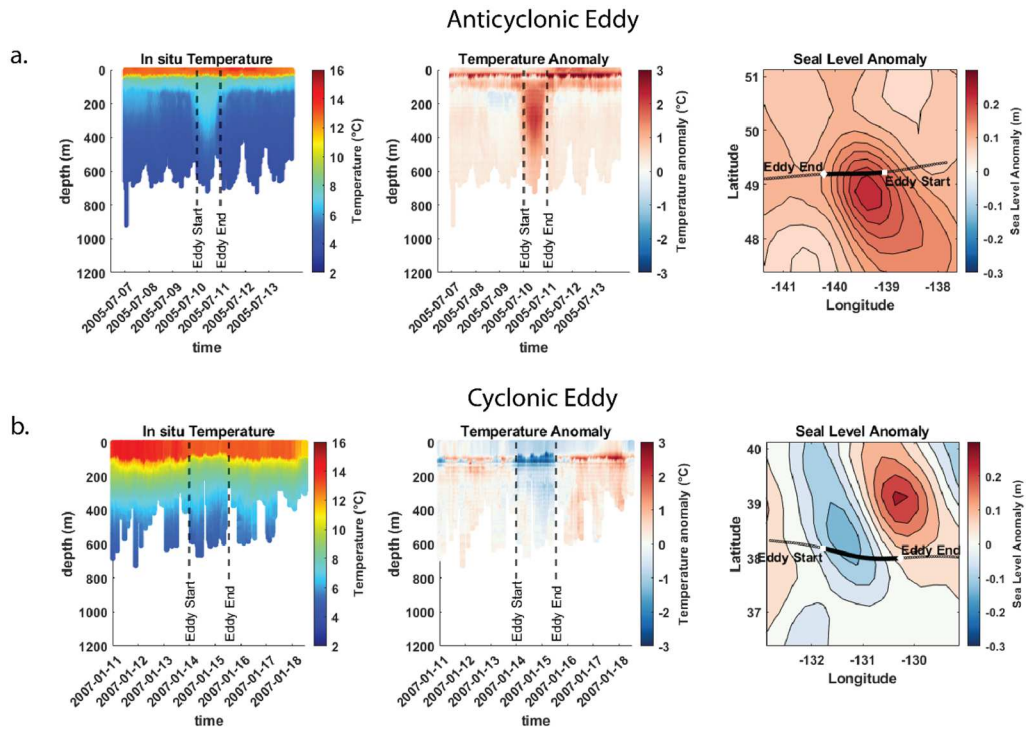
Figure 1.1. Elephant seals profiling eddies, showing *in situ* temperature measurements on the left, temperature anomaly in the center, and remotely sensed seal level anomaly with seal's track overlaid on the right, for (a) an anticyclonic eddy in Gulf of Alaska and (b) a cyclonic eddy in the California Current.
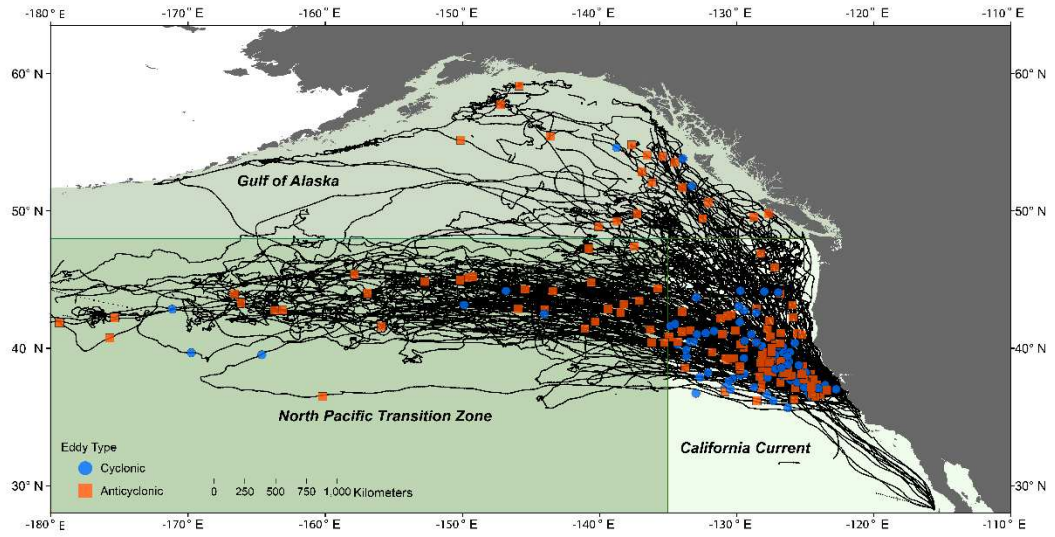
Figure 1.2. Map showing elephant seal tracks (lines) and the locations of eddy encounters (blue circles and orange squares).

Table 1.1. Covariates included in mixed effects models testing the response variables transit rate, movement persistence, and diving behavior (12-hour averaged).

[1] See Mesoscale Eddy Trajectory Atlas Product Handbook for detailed information. https://www.aviso.altimetry.fr/fileadmin/documents/data/tools/hdbk_eddytrajectory_META2.0_DT.pdf Note that dataset releases may differ in reported units.

Covariate Name	Covariate Description	Units
Season	Levels: Post-breeding foraging trip, Post-molt foraging trip	Categorical
DayinTrip	Days since seal left shore	Days
EddyCategory	Levels: Not in an eddy, In a cyclonic eddy, In an anticyclonic eddy	Categorical
FSLE_max	Maximum Finite-sized Lyapunov Exponent within ~25 km radius, 2 days	$Days^{-1}$
SST_sd	Standard deviation of *in situ* SST across 12 hr period	Degrees Celsius
MLD_mean	Mean *in situ* mixed layer depth across 12 hr period	Meters
Lat,Lon	Latitude and longitude of seal's location	Decimal degrees
TOPPID	Unique ID for seal track	Categorical
EddyAge[1]	Days since eddy first detected in META	Days
EddyAmplitude[1]	Height difference between maximum sea level of eddy and the sea level of eddy perimeter	Centimeters
EddyRadius[1]	Radius of circle enclosing contour of maximum rotational speed	Kilometers
EddySpeed[1]	Average speed at radius defined above	Centimeters/Second
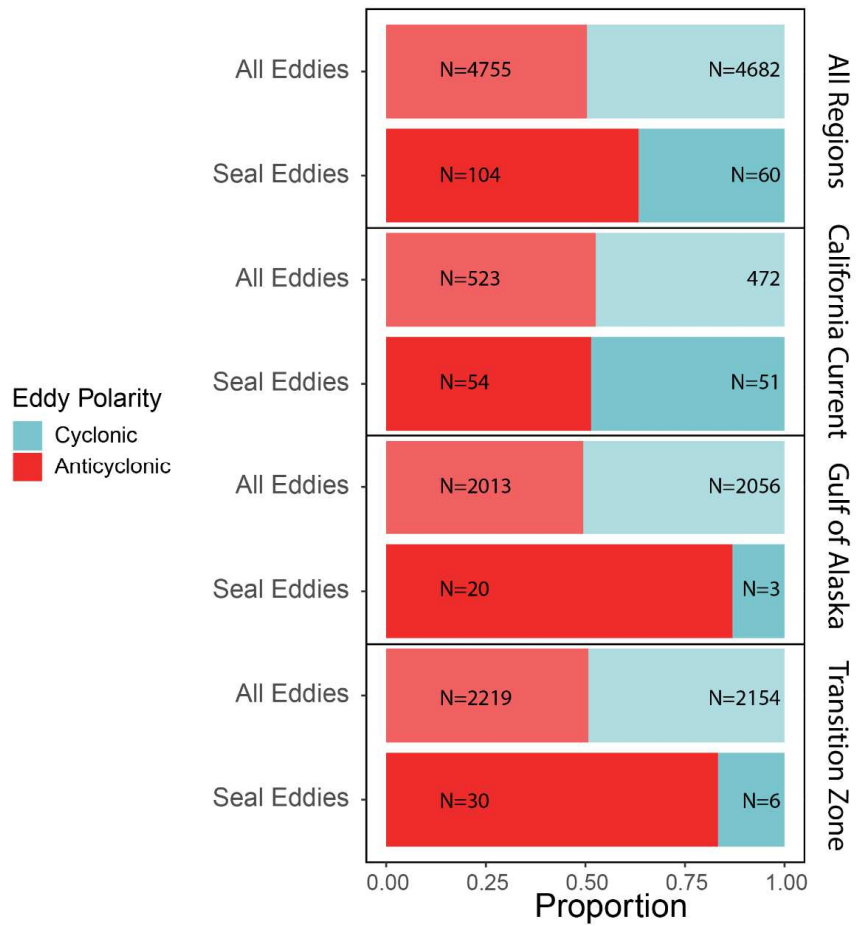
Figure 1.3. Proportion of cyclonic and anticyclonic eddies by region for total eddies in study area and eddies encountered by seals. Numbers refer to number of individual eddies.
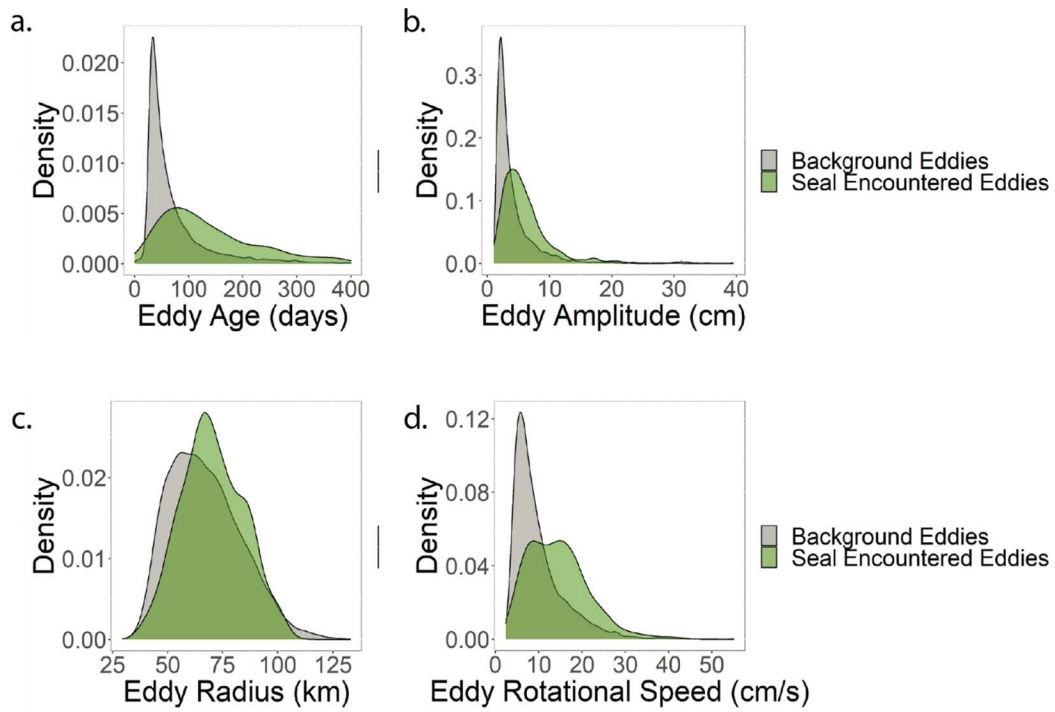
Figure 1.4. Density of eddy properties of all mesoscale eddies in study area and those encountered by seals indicates seal-encountered eddies were on average older (a), larger (b, c), and faster (d).
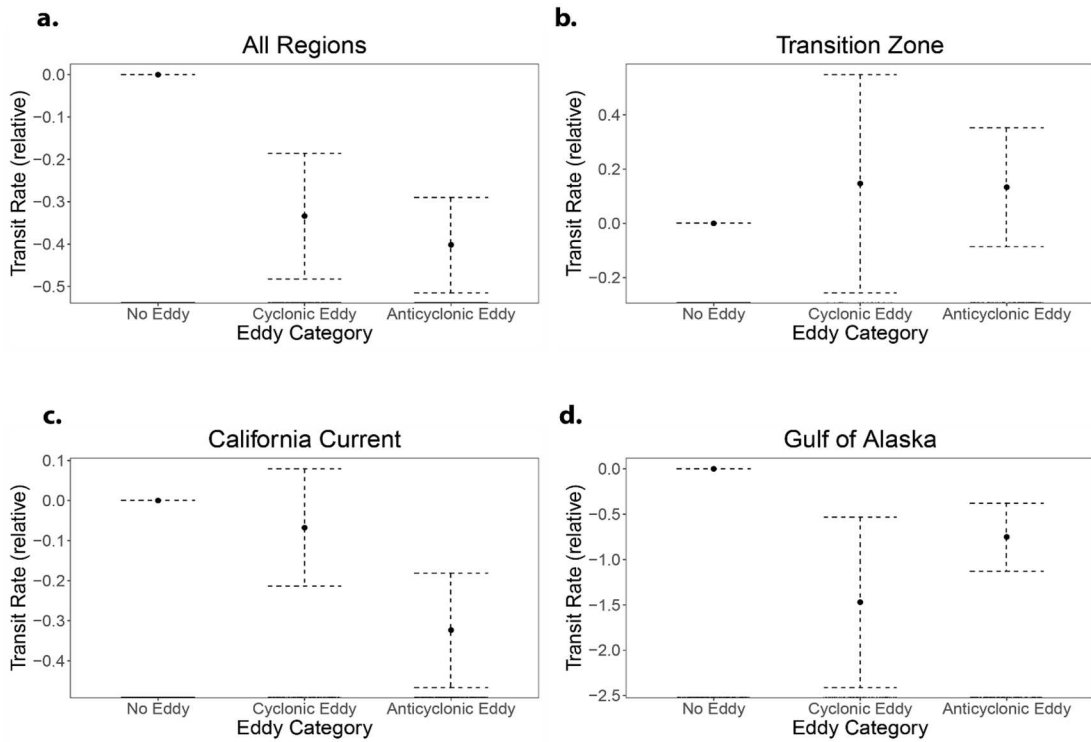
Figure 1.5. Boxplots of GAMM output illustrating the effect of eddy encounters on horizontal transit rate. Vertical axes show transit rate relative to outside of eddies (*i.e.* transit rate outside of eddies are shown as 0 on the y axis such that increases in transit rate are positive and decreases are negative values). Error bars represent the 95% confidence interval. See Table S1 for sample sizes of eddies in each subregion.

Table 1.2. Summary of GAMMs testing the influence of eddies on elephant seal transit rate. Models were run for the whole dataset and for subregions individually. R^2 values for the full model are reported, R^2 for a model containing only the categorical factor "Eddy Category", the reduced R^2 for the full model rerun with Eddy Category removed, and the R^2 deviance calculated as the difference between the full model and the reduced model without Eddy Category.

Response Variable	Full Model	R^2 full model	R^2 Eddy Category	R^2 reduced	R^2 deviance
Transit Rate All Regions	Season+s(DayinTrip)+EddyCategory +s(FSLE_max)+s(SST_sd) +s(MLD_mean)+te(Lat,Lon)	0.343	0.066	0.323	0.019
Transit Rate California Current	Season+s(DayinTrip)+EddyCategory +s(FSLE_max)+s(SST_sd) +s(MLD_mean)+te(Lat,Lon)	0.370	0.015	0.347	0.023
Transit Rate Transition Zone	Season+s(DayinTrip)+EddyCategory +s(FSLE_max)+s(SST_sd) +s(MLD_mean)+te(Lat,Lon)	0.158	0.005	0.162	-0.004
Transit Rate Gulf of Alaska	Season+s(DayinTrip)+EddyCategory +s(FSLE_max)+s(SST_sd) +s(MLD_mean)+te(Lat,Lon)	0.382	0.371	0.456	-0.074
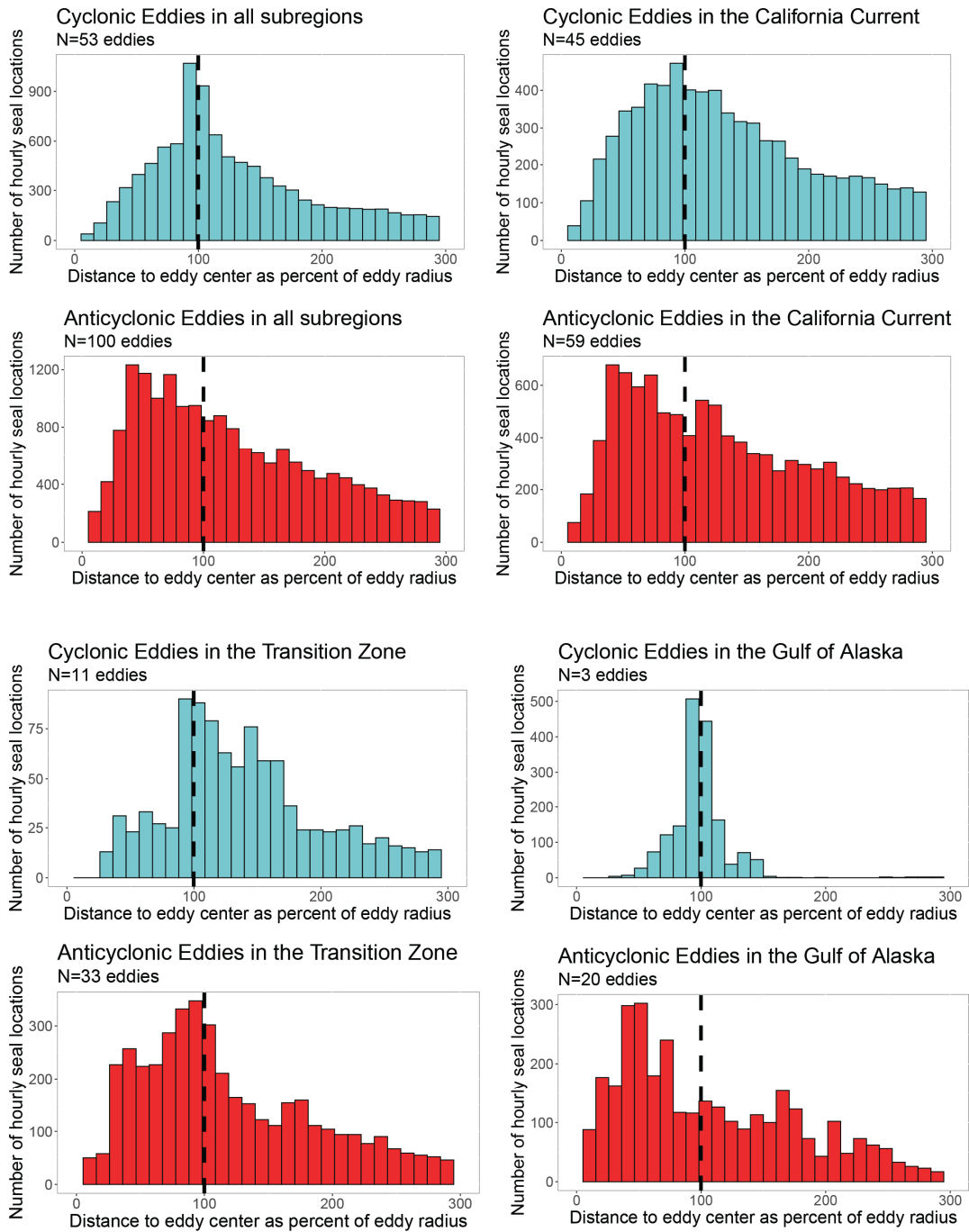
Figure 1.6. Histograms of hourly seal locations by distance from eddy center split by eddy polarity and subregions. Vertical dashed line indicates eddy edge (100% of eddy radius) such that locations to the left of the line are inside the eddy and locations to the right are outside of the eddy. Note some individual eddies traveled to different subregions between seal encounters, resulting in sample size mismatch to the total number of eddies.
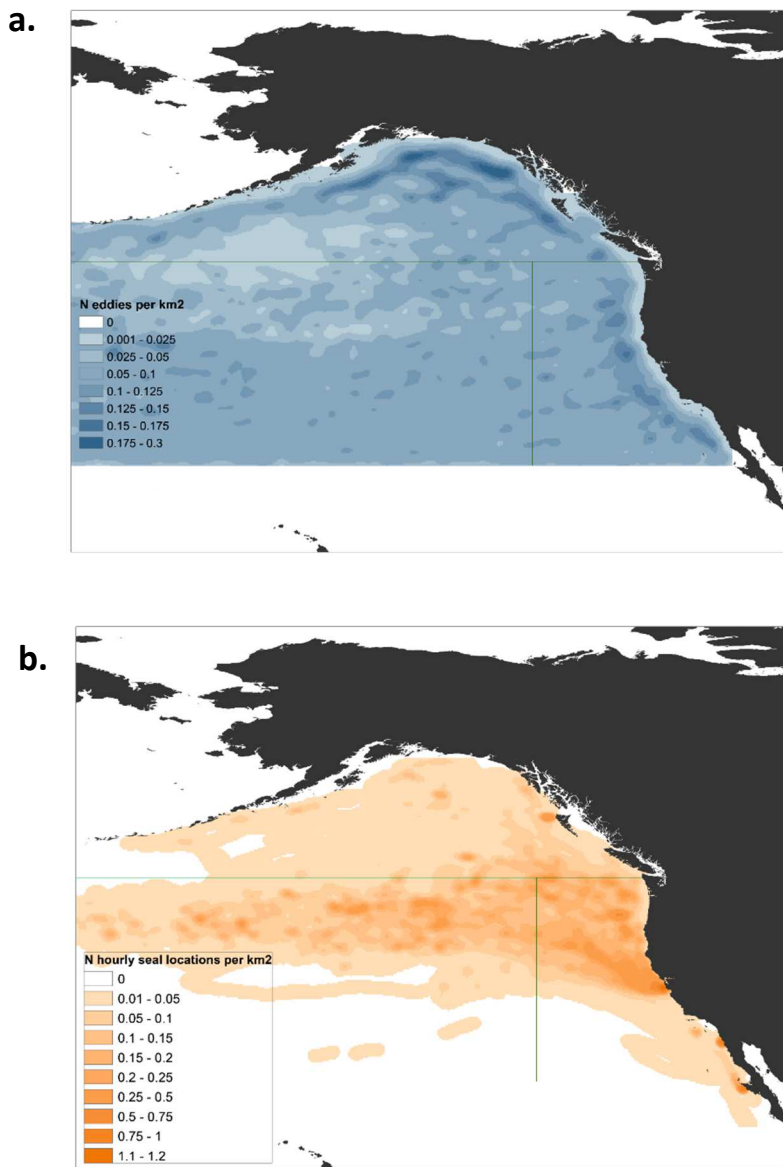
Figure 1.S1. Kernel density of (A) all eddies and (B) hourly seal locations in the study area illustrating areas of likely seal-eddy encounters. Lines represent the regional subdivisions used in this study (Gulf of Alaska, Transition Zone, and California Current.
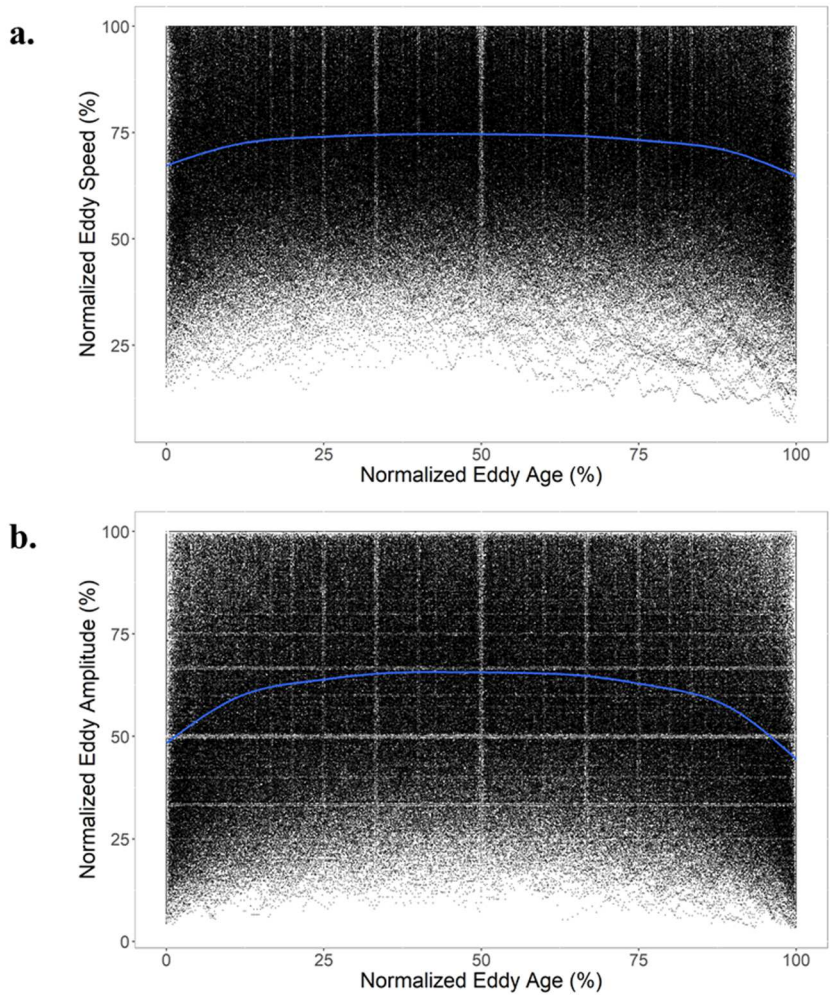
Figure 1.S2. Normalized a) amplitude and b) rotational speed over normalized eddy age for all eddies in the study region indicates approximate trends in timing of eddy intensification and decay phases. A loess smoother is added to aid visual interpretation.

Table 1.S1. Summary of eddy encounters by seals across subregions.

Subregion	Eddy Polarity	Number of unique eddies	Days spent in eddies	% of time in subregion spent in eddies
California Current	Cyclonic	50	168	2.6
California Current	Anticyclonic	54	219	3.3
Gulf of Alaska	Cyclonic	3	71	3.1
Gulf of Alaska	Anticyclonic	18	121	5.2
North Pacific Transition Zone	Cyclonic	6	17	0.2
North Pacific Transition Zone	Anticyclonic	31	138	1.8

Table 1.S2. Summary of GAMMs testing the influence of eddies on elephant seal transit rate. Models were run for the whole dataset and for subregions individually. R^2 values for the full model are reported, R^2 for a model containing only one individual covariate, the reduced R^2 for the full model rerun with that covariate removed, removed, and the R^2 deviance calculated as the difference between the full model and the reduced model. All models additionally contained individual seal as a random effect.

Response Variable	Explanatory Variable	R^2 full model	R^2 single variable	R^2 reduced	R^2 deviance
Transit Rate All Regions	Season+s(DayinTrip)+EddyCategory+s(FSLE_mean) +s(SST_sd)+s(MLD_mean)+te(Lat,Lon)				
	Season	0.343	0.128	0.312	0.030
	DayinTrip	0.343	0.243	0.233	0.109
	EddyCategory	0.343	0.066	0.323	0.019
	FSLE_mean	0.343	0.000	0.341	0.002
	SST_sd	0.343	0.000	0.340	0.002
	MLD_mean	0.343	0.000	0.343	0.000
	Lat/Lon	0.343	0.150	0.317	0.026
Transit Rate California Current	Season+s(DayinTrip)+EddyCategory+s(FSLE_mean) +s(SST_sd)+s(MLD_mean)+te(Lat,Lon)				
	Season	0.370	0.095	0.309	0.061
	DayinTrip	0.370	0.181	0.241	0.129
	EddyCategory	0.370	0.015	0.347	0.023
	FSLE_mean	0.370	0.000	0.370	0.000
	SST_sd	0.370	0.001	0.370	0.000
	MLD_mean	0.370	0.001	0.364	0.006
	Lat/Lon	0.370	0.140	0.271	0.099
Transit Rate Transition Zone	Season+s(DayinTrip)+EddyCategory+s(FSLE_mean) +s(SST_sd)+s(MLD_mean)+te(Lat,Lon)				
	Season	0.158	0.116	0.156	0.002
	DayinTrip	0.158	0.199	0.119	0.039
	EddyCategory	0.158	0.005	0.162	-0.004
	FSLE_mean	0.158	0.010	0.158	0.000
	SST_sd	0.158	0.000	0.159	-0.001

		0.158	0.018	0.147	0.011
	MLD_mean	0.158	0.018	0.147	0.011
	Lat/Lon	0.158	0.096	0.234	-0.076
Transit Rate Gulf of Alaska	Season+s(DayinTrip)+EddyCategory+s(FSLE_mean) +s(SST_sd)+s(MLD_mean)+te(Lat,Lon)				
	Season	0.382	0.025	0.472	-0.090
	DayinTrip	0.382	0.354	0.271	0.111
	EddyCategory	0.382	0.371	0.456	-0.074
	FSLE_mean	0.382	0.000	0.357	0.025
	SST_sd	0.382	0.000	0.389	-0.007
	MLD_mean	0.382	0.014	0.419	-0.037
	Lat/Lon	0.382	0.444	0.386	-0.003

a.

b.

93
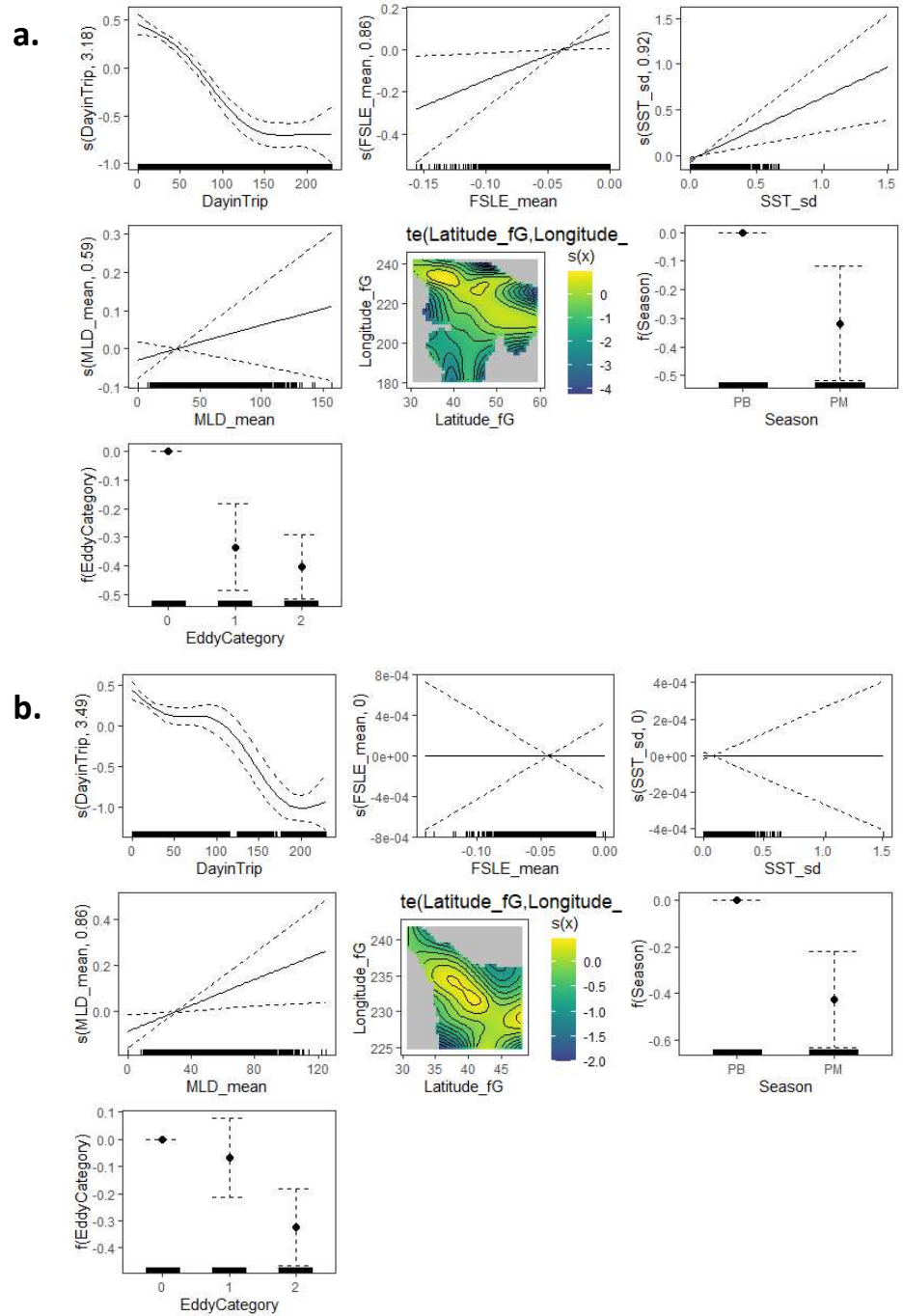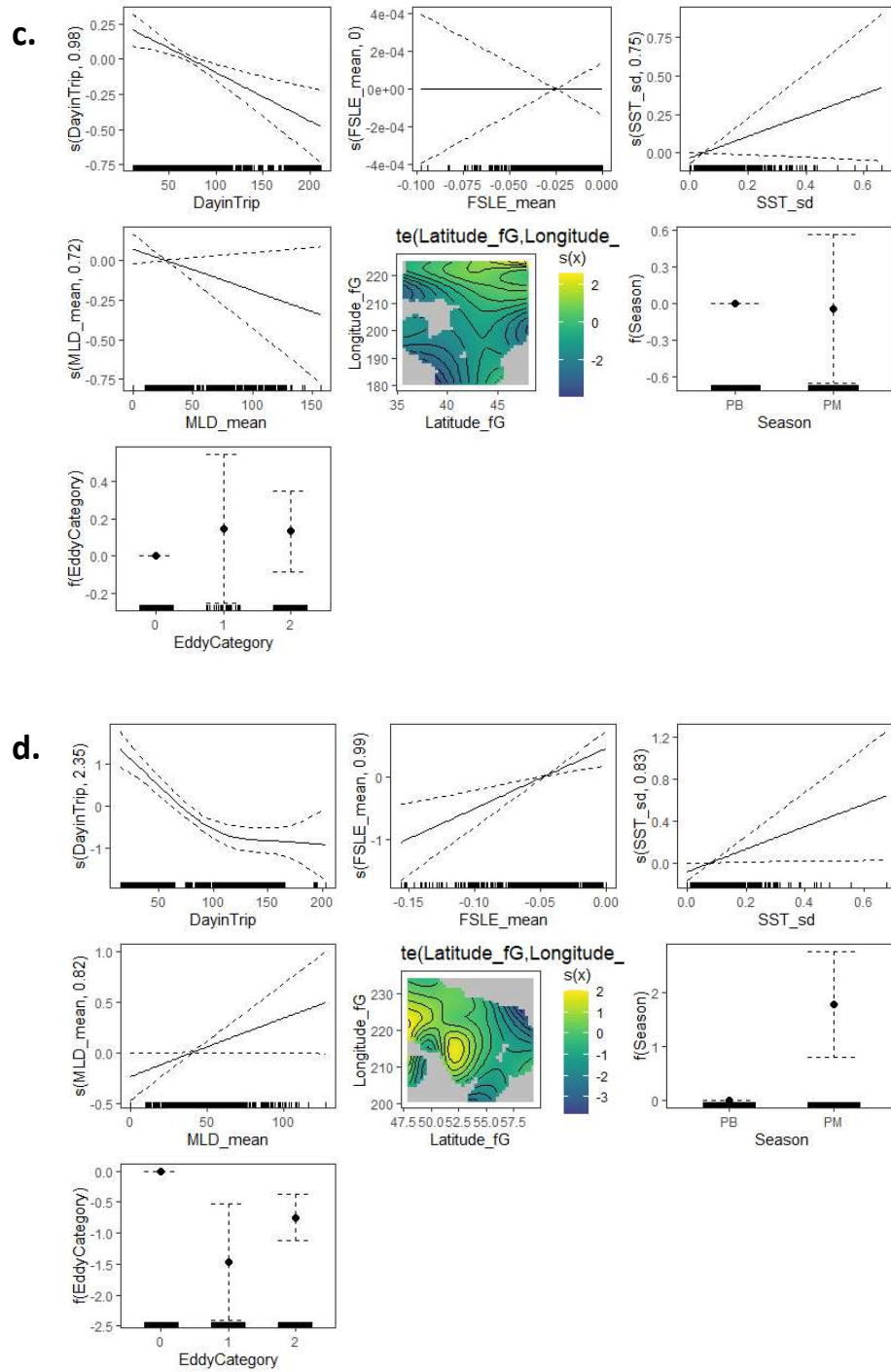
Figure 1.S3. Visual output of GAMM testing the influence of eddies on elephant seal transit rate in (a) all regions, (b) the California Current, (c) Transition Zone, (d) Gulf of Alaska. Eddy Category 0 is outside of eddies, 1 is cyclonic eddies, and 2 is anticyclonic eddies.

Table 1.S3. Summary of GAMMs testing the influence of eddies on elephant seal movement persistence. Models were run for the whole dataset and for subregions individually. R^2 values for the full model are reported, R^2 for a model containing only one individual covariate, the reduced R^2 for the full model rerun with that covariate removed, removed, and the R^2 deviance calculated as the difference between the full model and the reduced model. All models additionally contained individual seal as a random effect.

Response Variable	Explanatory Variable	R^2 full model	R^2 single variable	R^2 reduced	R^2 deviance
Movement Persistence All Regions	Season+s(DayinTrip)+EddyCategory+s(FSLE_mean) +s(SST_sd)+s(MLD_mean)+te(Lat,Lon)				
	Season	0.396	0.124	0.392	0.005
	DayinTrip	0.396	0.151	0.449	-0.052
	EddyCategory	0.396	0.097	0.382	0.015
	FSLE_mean	0.396	0.023	0.397	0.000
	SST_sd	0.396	0.006	0.396	0.001
	MLD_mean	0.396	0.000	0.391	0.005
	Lat/Lon	0.396	0.389	0.206	0.190
Movement Persistence California Current	Season+s(DayinTrip)+EddyCategory+s(FSLE_mean) +s(SST_sd)+s(MLD_mean)+te(Lat,Lon)				
	Season	0.452	0.089	0.432	0.020
	DayinTrip	0.452	0.238	0.388	0.064
	EddyCategory	0.452	0.105	0.421	0.031
	FSLE_mean	0.452	0.000	0.452	0.000
	SST_sd	0.452	0.003	0.455	-0.003
	MLD_mean	0.452	0.000	0.450	0.003
	Lat/Lon	0.452	0.284	0.301	0.152
Movement Persistence Transition Zone	Season+s(DayinTrip)+EddyCategory+s(FSLE_mean) +s(SST_sd)+s(MLD_mean)+te(Lat,Lon)				

	Season	0.112	0.150	NA	NA
	DayinTrip	0.112	0.000	0.112	0.000
	EddyCategory	0.112	0.027	0.109	0.004
	FSLE_mean	0.112	0.068	0.124	-0.012
	SST_sd	0.112	0.025	0.111	0.002
	MLD_mean	0.112	0.000	0.120	-0.007
	Lat/Lon	0.112	0.071	0.146	-0.033
Movement Persistence Gulf of Alaska	Season+s(DayinTrip)+EddyCategory+s(FSLE_mean) +s(SST_sd)+s(MLD_mean)+te(Lat,Lon)				
	Season	0.388	0.044	0.239	0.148
	DayinTrip	0.388	0.029	0.706	-0.318
	EddyCategory	0.388	0.377	0.382	0.005
	FSLE_mean	0.388	0.184	0.388	0.000
	SST_sd	0.388	0.000	0.391	-0.003
	MLD_mean	0.388	0.022	0.351	0.037
	Lat/Lon	0.388	0.727	0.555	-0.167

a.
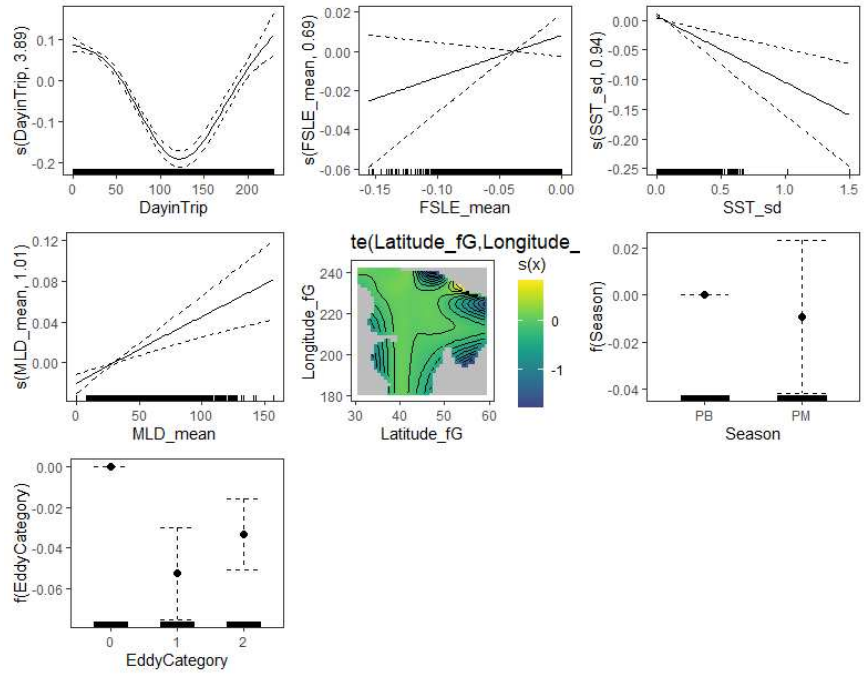
b.
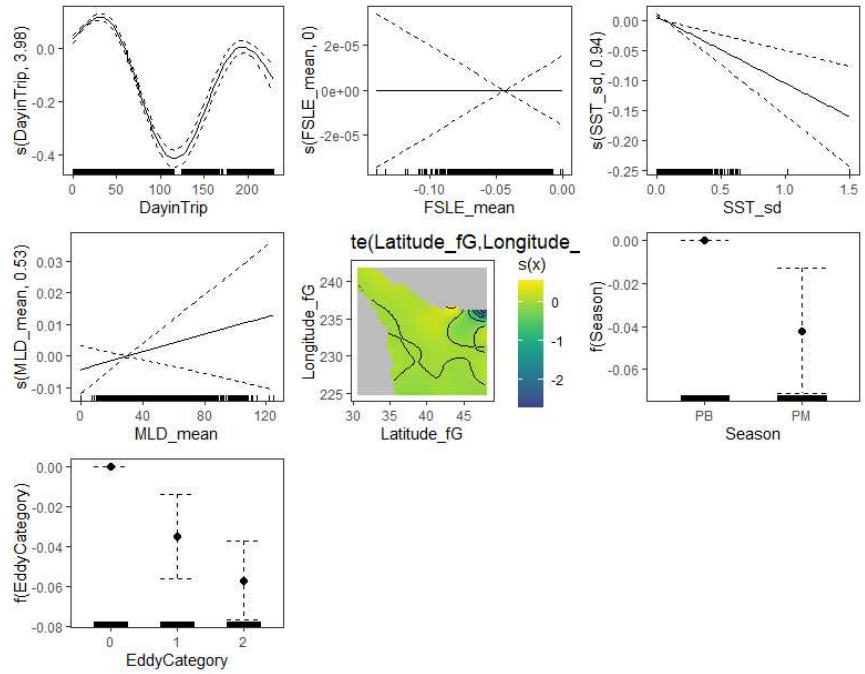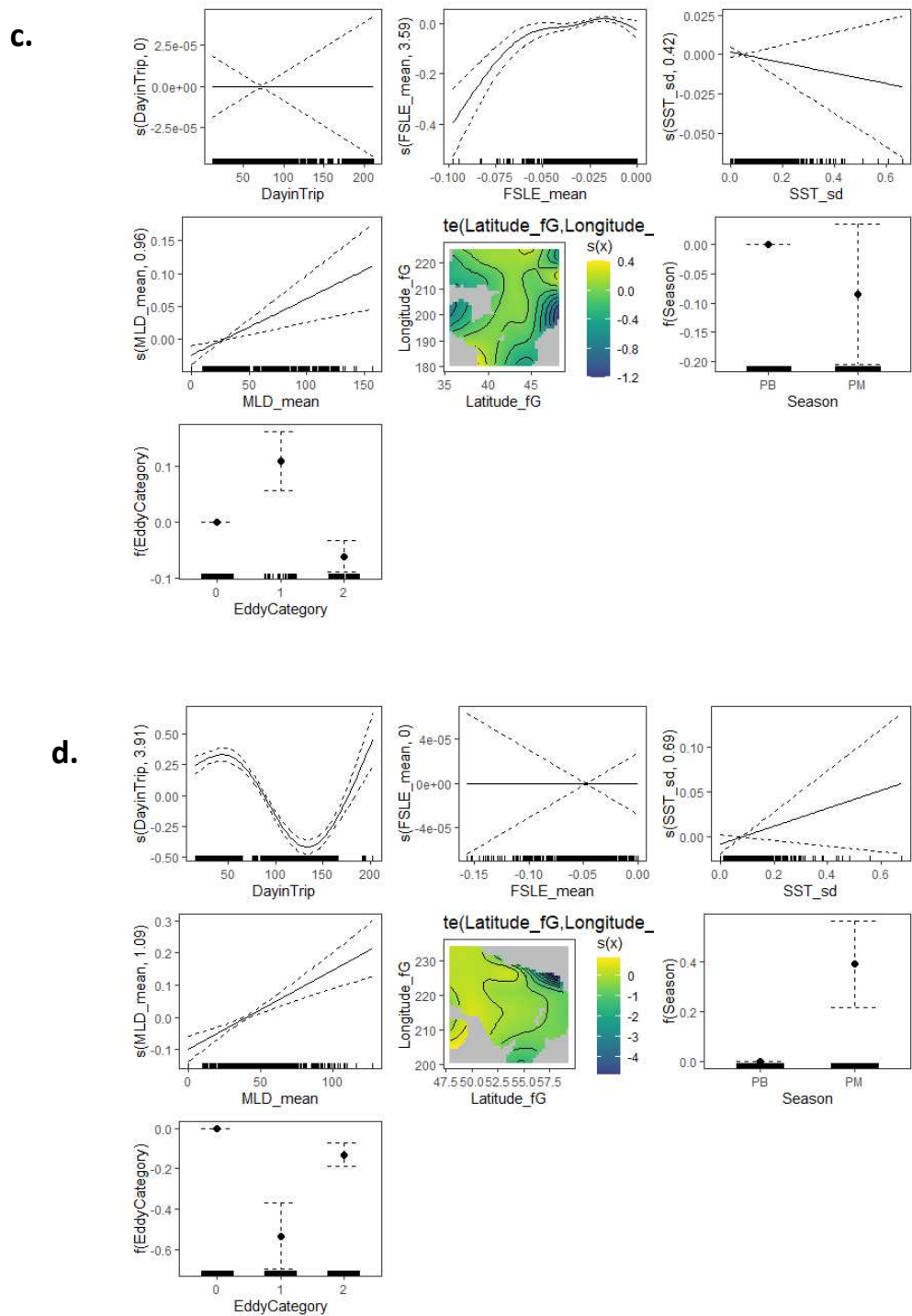
Figure 1.S4. Visual output of GAMM testing the influence of eddies on elephant seal movement persistence in (a) all regions, (b) the California Current, (c) Transition Zone, (d) Gulf of Alaska. Eddy Category 0 is outside of eddies, 1 is cyclonic eddies, and 2 is anticyclonic eddies.

Table 1.S4. Significant Moran's I values for GAMMs showing some degree of positive spatial autocorrelation. All models additionally contained individual seal as a random effect.

Dataset	Model Formula	Moran's I
Transit Rate All Regions	Season+s(DayinTrip)+EddyCategory+s(FSLE_mean)+s(SST_sd)+s(MLD_mean)+te(Lat,Lon)	0.245103
Transit Rate California Current	Season+s(DayinTrip)+EddyCategory+s(FSLE_mean)+s(SST_sd)+s(MLD_mean)+te(Lat,Lon)	0.229588
Transit Rate Transition Zone	Season+s(DayinTrip)+EddyCategory+s(FSLE_mean)+s(SST_sd)+s(MLD_mean)+te(Lat,Lon)	0.307903
Transit Rate Gulf of Alaska	Season+s(DayinTrip)+EddyCategory+s(FSLE_mean)+s(SST_sd)+s(MLD_mean)+te(Lat,Lon)	0.33139
Movement Persistence All Regions	Season+s(DayinTrip)+EddyCategory+s(FSLE_mean)+s(SST_sd)+s(MLD_mean)+te(Lat,Lon)	0.330379
Movement Persistence California Current	Season+s(DayinTrip)+EddyCategory+s(FSLE_mean)+s(SST_sd)+s(MLD_mean)+te(Lat,Lon)	0.372888
Movement Persistence Transition Zone	Season+s(DayinTrip)+EddyCategory+s(FSLE_mean)+s(SST_sd)+s(MLD_mean)+te(Lat,Lon)	0.29148
Movement Persistence Gulf of Alaska	Season+s(DayinTrip)+EddyCategory+s(FSLE_mean)+s(SST_sd)+s(MLD_mean)+te(Lat,Lon)	0.464418

Table 1.S5. Mean ± standard deviation of daily averaged diving behavior within cyclonic and anticyclonic eddies, separated between day and night as elephant seals exhibit diel behavioral shifts.

Behavior	Cyclonic eddies, daytime	Cyclonic eddies, nighttime	Anticyclonic eddies, daytime	Anticyclonic eddies, nighttime
Dive Depth (m)	557 ± 137	508 ± 141	580 ± 97	476 ± 106
Bottom Time (sec)	800 ± 330	606 ± 245	803 ± 306	659 ± 264
Number of Wiggles	16 ± 78	11 ± 4	16 ± 6	13 ± 5
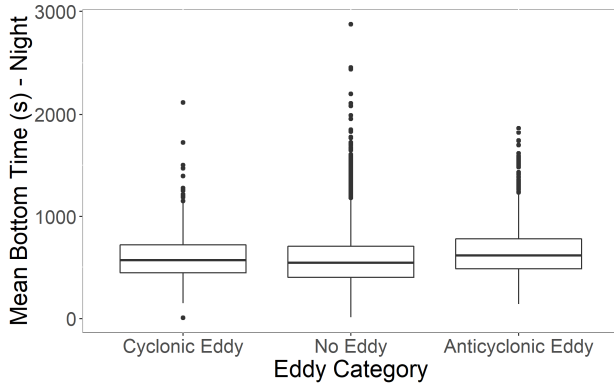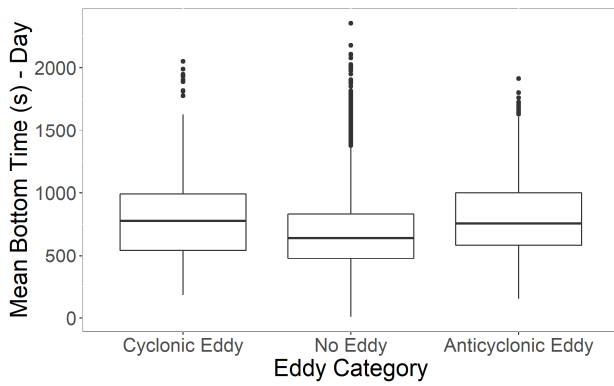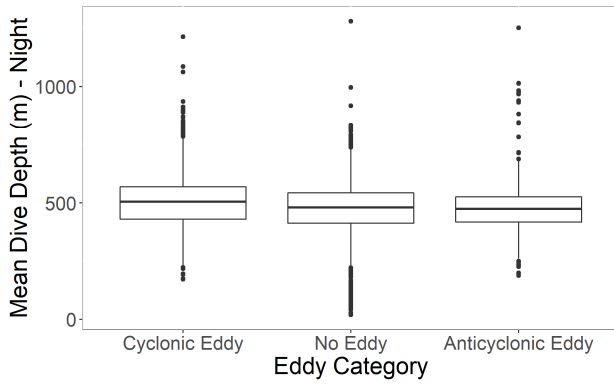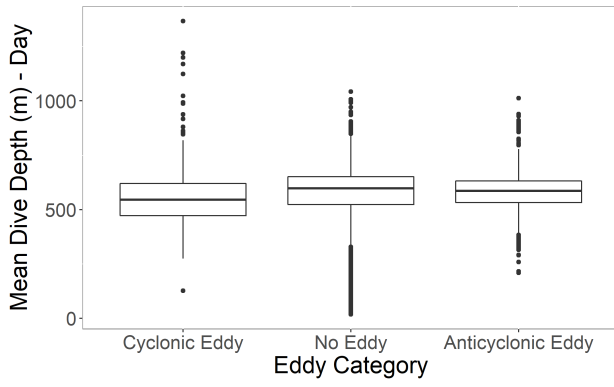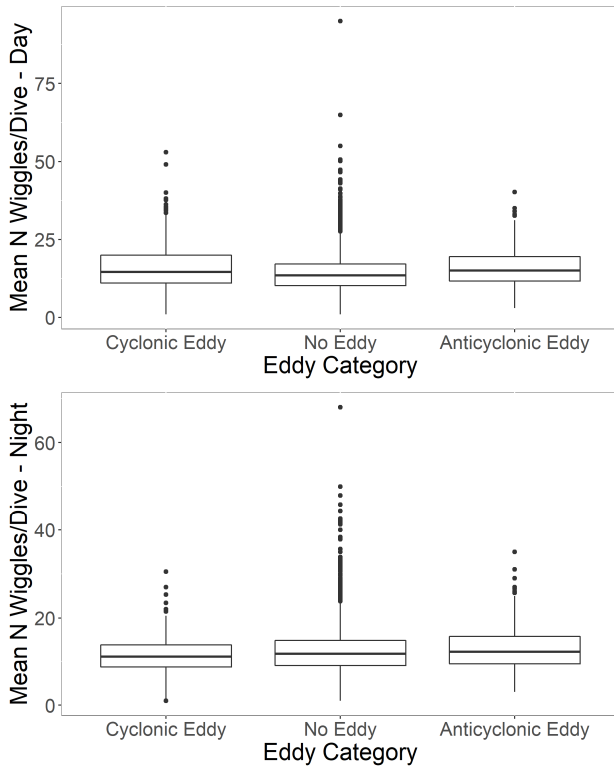
Figure 1.S5. Boxplots of mean daily diving behavior in association with an eddy or outside of eddies. As these data are not independent (notably repeated behavior from the same seal), see Table S5 for statistical analysis of significant changes in diving behavior when a seal encountered an eddy.

Table 1.S6. Proportion of eddy encounters that elicited significantly different diving behavior compared to behavior before/after the eddy encounter determined by p<0.05 of two-sample t-test.

Behavior	Eddy Type	Behavioral Change	Proportion of Encounters
Dive Depth Day	Anticyclonic	Increase	0.34
Dive Depth Day	Anticyclonic	Decrease	0.24
Dive Depth Day	Cyclonic	Increase	0.27
Dive Depth Day	Cyclonic	Decrease	0.32
Dive Depth Night	Anticyclonic	Increase	0.33
Dive Depth Night	Anticyclonic	Decrease	0.29
Dive Depth Night	Cyclonic	Increase	0.25
Dive Depth Night	Cyclonic	Decrease	0.29
Bottom Time Day	Anticyclonic	Increase	0.21
Bottom Time Day	Anticyclonic	Decrease	0.20
Bottom Time Day	Cyclonic	Increase	0.19
Bottom Time Day	Cyclonic	Decrease	0.17
Bottom Time Night	Anticyclonic	Increase	0.24
Bottom Time Night	Anticyclonic	Decrease	0.20
Bottom Time Night	Cyclonic	Increase	0.19
Bottom Time Night	Cyclonic	Decrease	0.23
Wiggles Day	Anticyclonic	Increase	0.24
Wiggles Day	Anticyclonic	Decrease	0.14
Wiggles Day	Cyclonic	Increase	0.20
Wiggles Day	Cyclonic	Decrease	0.19
Wiggles Night	Anticyclonic	Increase	0.20
Wiggles Night	Anticyclonic	Decrease	0.18
Wiggles Night	Cyclonic	Increase	0.19
Wiggles Night	Cyclonic	Decrease	0.20

Table 1.S7. Model outputs testing the influence of eddy properties on transit rate within eddies. All models additionally contained individual seal as a random effect. NAs indicate models that did not converge.

Response	Model	R2.full.model	R2.deviance
Transit Rate In Anticyclonic Eddies in All Regions			
	s(DayinTrip)+te(Lat,Lon)	0.176	0.000
	s(DayinTrip)+te(Lat,Lon)+s(EddyAge)	0.176	0.000
	s(DayinTrip)+te(Lat,Lon)+s(EddyRadius)	0.206	0.030
	s(DayinTrip)+te(Lat,Lon)+s(EddyAmplitude)	0.179	0.003
	s(DayinTrip)+te(Lat,Lon)+s(EddySpeed)	0.176	0.000
	s(DayinTrip)+te(Lat,Lon)+s(EddyAgePercent)	0.191	0.015
Transit Rate In Cyclonic Eddies in All Regions			
	s(DayinTrip)+te(Lat,Lon)	0.302	0.000
	s(DayinTrip)+te(Lat,Lon)+s(EddyAge)	0.302	0.000
	s(DayinTrip)+te(Lat,Lon)+s(EddyRadius)	0.302	0.000
	s(DayinTrip)+te(Lat,Lon)+s(EddyAmplitude)	0.317	0.014
	s(DayinTrip)+te(Lat,Lon)+s(EddySpeed)	0.303	0.001
	s(DayinTrip)+te(Lat,Lon)+s(EddyAgePercent)	0.302	0.000
Transit Rate In Anticyclonic Eddies in California Current			
	s(DayinTrip)	0.037	0.000
	s(DayinTrip)+s(EddyAge)	0.035	-0.001
	s(DayinTrip)+s(EddyRadius)	0.042	0.005
	s(DayinTrip)+s(EddyAmplitude)	0.037	0.000
	s(DayinTrip)+s(EddySpeed)	0.037	0.000
	s(DayinTrip)+s(EddyAgePercent)	0.059	0.022
Transit Rate In Cyclonic Eddies in California Current			
	s(DayinTrip)	0.115	0.000
	s(DayinTrip)+s(EddyAge)	0.117	0.002
	s(DayinTrip)+s(EddyRadius)	0.116	0.001
	s(DayinTrip)+s(EddyAmplitude)	0.134	0.019
	s(DayinTrip)+s(EddySpeed)	0.115	0.000
	s(DayinTrip)+s(EddyAgePercent)	0.115	0.000
Transit Rate In Anticyclonic Eddies in Gulf of Alaska			
	s(DayinTrip)	0.061	0.000
	s(DayinTrip)+s(EddyAge)	0.061	0.000
	s(DayinTrip)+s(EddyRadius)	0.121	0.060
	s(DayinTrip)+s(EddyAmplitude)	0.061	0.000
	s(DayinTrip)+s(EddySpeed)	0.061	0.000
	s(DayinTrip)+s(EddyAgePercent)	0.080	0.019

	Transit Rate In Anticyclonic Eddies in Transition Zone		
	s(DayinTrip)	0.064	0.000
	s(DayinTrip)+s(EddyAge)	0.064	0.000
	s(DayinTrip)+s(EddyRadius)	0.082	0.018
	s(DayinTrip)+s(EddyAmplitude)	0.064	0.000
	s(DayinTrip)+s(EddySpeed)	0.064	0.000
	s(DayinTrip)+s(EddyAgePercent)	0.064	0.000

Table 1.S8. Model outputs testing the influence of eddy properties on movement persistence within eddies. All models additionally contained individual seal as a random effect. NAs indicate models that did not converge.

Response	Model	R2.full.model	R2.deviance
Movement Persistence In Anticyclonic Eddies in All Regions			
	s(DayinTrip)+te(Lat,Lon)	0.192	0.000
	s(DayinTrip)+te(Lat,Lon)+s(EddyAge)	NA	NA
	s(DayinTrip)+te(Lat,Lon)+s(EddyRadius)	NA	NA
	s(DayinTrip)+te(Lat,Lon)+s(EddyAmplitude)	NA	NA
	s(DayinTrip)+te(Lat,Lon)+s(EddySpeed)	NA	NA
	s(DayinTrip)+te(Lat,Lon)+s(EddyAgePercent)	NA	NA
Movement Persistence In Cyclonic Eddies in All Regions			
	s(DayinTrip)+te(Lat,Lon)	0.442	0.000
	s(DayinTrip)+te(Lat,Lon)+s(EddyAge)	0.442	0.000
	s(DayinTrip)+te(Lat,Lon)+s(EddyRadius)	0.442	0.000
	s(DayinTrip)+te(Lat,Lon)+s(EddyAmplitude)	0.442	0.000
	s(DayinTrip)+te(Lat,Lon)+s(EddySpeed)	0.441	-0.002
	s(DayinTrip)+te(Lat,Lon)+s(EddyAgePercent)	0.442	0.000
Movement Persistence In Anticyclonic Eddies in California Current			
	s(DayinTrip)	0.000	0.000
	s(DayinTrip)+s(EddyAge)	0.000	0.000
	s(DayinTrip)+s(EddyRadius)	0.000	0.000
	s(DayinTrip)+s(EddyAmplitude)	0.000	0.000
	s(DayinTrip)+s(EddySpeed)	0.012	0.011
	s(DayinTrip)+s(EddyAgePercent)	0.000	0.000
Movement Persistence In Cyclonic Eddies in California Current			
	s(DayinTrip)	0.074	0.000
	s(DayinTrip)+s(EddyAge)	0.074	0.000
	s(DayinTrip)+s(EddyRadius)	0.074	0.000
	s(DayinTrip)+s(EddyAmplitude)	0.074	0.000
	s(DayinTrip)+s(EddySpeed)	0.074	0.000

	s(DayinTrip)+s(EddyAgePercent)	NA	NA
Movement Persistence In Anticyclonic Eddies in Gulf of Alaska			
	s(DayinTrip)	NA	NA
	s(DayinTrip)+s(EddyAge)	0.000	NA
	s(DayinTrip)+s(EddyRadius)	0.000	NA
	s(DayinTrip)+s(EddyAmplitude)	NA	NA
	s(DayinTrip)+s(EddySpeed)	0.000	NA
	s(DayinTrip)+s(EddyAgePercent)	0.000	NA
Movement Persistence In Anticyclonic Eddies in Transition Zone			
	s(DayinTrip)	0.000	0.000
	s(DayinTrip)+s(EddyAge)	NA	NA
	s(DayinTrip)+s(EddyRadius)	0.018	0.018
	s(DayinTrip)+s(EddyAmplitude)	0.000	0.000
	s(DayinTrip)+s(EddySpeed)	0.000	0.000
	s(DayinTrip)+s(EddyAgePercent)	0.000	0.000

Table 1.S9. Model outputs testing the influence of eddy type on diving behavior within eddies showed no strong effect of polarity. All models additionally contained individual seal as a random effect. NAs indicate models that did not converge.

Response	Model	R2.full.model	R2.deviance
Wiggles Night In Eddy All Regions			
	Season+s(DayinTrip)+te(Lat,Lon)	0.107	0.000
	Season+s(DayinTrip)+te(Lat,Lon)+EddyType	0.095	-0.012
Wiggles Night In Eddy California Current			
	Season+s(DayinTrip)+te(Lat,Lon)	0.027	0.000
	Season+s(DayinTrip)+te(Lat,Lon)+EddyType	0.000	-0.028
Wiggles Night In Eddy Transition Zone			
	Season+s(DayinTrip)+te(Lat,Lon)	NA	NA
	Season+s(DayinTrip)+te(Lat,Lon)+EddyType	NA	NA
Wiggles Night In Eddy Gulf of Alaska			
	Season+s(DayinTrip)+te(Lat,Lon)	NA	NA
	Season+s(DayinTrip)+te(Lat,Lon)+EddyType	NA	NA
Wiggles Day In Eddy All Regions			
	Season+s(DayinTrip)+te(Lat,Lon)	0.297	0.000
	Season+s(DayinTrip)+te(Lat,Lon)+EddyType	0.294	-0.003
Wiggles Day In Eddy California Current			
	Season+s(DayinTrip)+te(Lat,Lon)	0.312	0.000
	Season+s(DayinTrip)+te(Lat,Lon)+EddyType	0.305	-0.007
Wiggles Day In Eddy Transition Zone			

	Season+s(DayinTrip)+te(Lat,Lon)	0.601	0.000
	Season+s(DayinTrip)+te(Lat,Lon)+EddyType	0.585	-0.016
Wiggles Day In Eddy Gulf of Alaska			
	Season+s(DayinTrip)+te(Lat,Lon)	NA	NA
	Season+s(DayinTrip)+te(Lat,Lon)+EddyType	NA	NA
BottomTime Night In Eddy All Regions			
	Season+s(DayinTrip)+te(Lat,Lon)	0.355	0.000
	Season+s(DayinTrip)+te(Lat,Lon)+EddyType	0.350	-0.005
BottomTime Night In Eddy California Current			
	Season+s(DayinTrip)+te(Lat,Lon)	NA	NA
	Season+s(DayinTrip)+te(Lat,Lon)+EddyType	0.295	NA
BottomTime Night In Eddy Transition Zone			
	Season+s(DayinTrip)+te(Lat,Lon)	NA	NA
	Season+s(DayinTrip)+te(Lat,Lon)+EddyType	NA	NA
BottomTime Night In Eddy Gulf of Alaska			
	Season+s(DayinTrip)+te(Lat,Lon)	NA	NA
	Season+s(DayinTrip)+te(Lat,Lon)+EddyType	NA	NA
BottomTime Day In Eddy All Regions			
	Season+s(DayinTrip)+te(Lat,Lon)	0.313	0.000
	Season+s(DayinTrip)+te(Lat,Lon)+EddyType	0.307	-0.005
BottomTime Day In Eddy California Current			
	Season+s(DayinTrip)+te(Lat,Lon)	0.402	0.000
	Season+s(DayinTrip)+te(Lat,Lon)+EddyType	0.401	-0.001
BottomTime Day In Eddy Transition Zone			
	Season+s(DayinTrip)+te(Lat,Lon)	0.510	0.000
	Season+s(DayinTrip)+te(Lat,Lon)+EddyType	0.521	0.011
BottomTime Day In Eddy Gulf of Alaska			
	Season+s(DayinTrip)+te(Lat,Lon)	0.619	0.000
	Season+s(DayinTrip)+te(Lat,Lon)+EddyType	0.531	-0.089
DiveDepth Night In Eddy All Regions			
	Season+s(DayinTrip)+te(Lat,Lon)	NA	NA
	Season+s(DayinTrip)+te(Lat,Lon)+EddyType	0.282	NA
DiveDepth Night In Eddy California Current			
	Season+s(DayinTrip)+te(Lat,Lon)	0.227	0.000
	Season+s(DayinTrip)+te(Lat,Lon)+EddyType	0.234	0.007
DiveDepth Night In Eddy Transition Zone			
	Season+s(DayinTrip)+te(Lat,Lon)	NA	NA
	Season+s(DayinTrip)+te(Lat,Lon)+EddyType	NA	NA
DiveDepth Night In Eddy Gulf of Alaska			

	Season+s(DayinTrip)+te(Lat,Lon)	NA	NA
	Season+s(DayinTrip)+te(Lat,Lon)+EddyType	NA	NA

Table 1.S10. Models testing the influence of eddy properties (absolute age, relative age, radius, amplitude, and speed) on diving behavior within eddies. All models additionally contained individual seal as a random effect. NAs indicate models that did not converge.

Response	Model	R2.full.model	R2.deviance
Wiggles Night In Anticyclonic Eddies in All Regions			
	s(DayinTrip)+te(Lat,Lon)	0.112	0.000
	s(DayinTrip)+te(Lat,Lon)+s(EddyAge)	0.112	0.000
	s(DayinTrip)+te(Lat,Lon)+s(EddyRadius)	0.112	0.000
	s(DayinTrip)+te(Lat,Lon)+s(EddyAmplitude)	0.128	0.016
	s(DayinTrip)+te(Lat,Lon)+s(EddySpeed)	0.117	0.005
	s(DayinTrip)+te(Lat,Lon)+s(EddyAgePercent)	0.089	-0.023
Wiggles Night In Cyclonic Eddies in All Regions			
	s(DayinTrip)+te(Lat,Lon)	-0.056	0.000
	s(DayinTrip)+te(Lat,Lon)+s(EddyAge)	NA	NA
	s(DayinTrip)+te(Lat,Lon)+s(EddyRadius)	-0.056	0.000
	s(DayinTrip)+te(Lat,Lon)+s(EddyAmplitude)	-0.056	0.000
	s(DayinTrip)+te(Lat,Lon)+s(EddySpeed)	-0.056	0.000
	s(DayinTrip)+te(Lat,Lon)+s(EddyAgePercent)	-0.056	0.000
Wiggles Night In Anticyclonic Eddies in California Current			
	s(DayinTrip)	0.061	0.000
	s(DayinTrip)+s(EddyAge)	0.055	-0.006
	s(DayinTrip)+s(EddyRadius)	0.061	0.000
	s(DayinTrip)+s(EddyAmplitude)	0.061	0.000
	s(DayinTrip)+s(EddySpeed)	0.061	0.000
	s(DayinTrip)+s(EddyAgePercent)	0.056	-0.005
Wiggles Night In Cyclonic Eddies in California Current			
	s(DayinTrip)	0.000	0.000
	s(DayinTrip)+s(EddyAge)	0.034	0.034
	s(DayinTrip)+s(EddyRadius)	0.004	0.004
	s(DayinTrip)+s(EddyAmplitude)	0.000	0.000
	s(DayinTrip)+s(EddySpeed)	0.000	0.000
	s(DayinTrip)+s(EddyAgePercent)	0.000	0.000

Wiggles Night In Anticyclonic Eddies in Gulf of Alaska			
	s(DayinTrip)	0.000	0.000
	s(DayinTrip)+s(EddyAge)	0.000	0.000
	s(DayinTrip)+s(EddyRadius)	0.103	0.103
	s(DayinTrip)+s(EddyAmplitude)	0.043	0.043
	s(DayinTrip)+s(EddySpeed)	0.000	0.000
	s(DayinTrip)+s(EddyAgePercent)	0.000	0.000
Wiggles Night In Anticyclonic Eddies in Transition Zone			
	s(DayinTrip)	0.099	0.000
	s(DayinTrip)+s(EddyAge)	0.000	-0.099
	s(DayinTrip)+s(EddyRadius)	0.000	-0.099
	s(DayinTrip)+s(EddyAmplitude)	NA	NA
	s(DayinTrip)+s(EddySpeed)	0.000	-0.099
	s(DayinTrip)+s(EddyAgePercent)	0.099	0.000
Wiggles Day In Anticyclonic Eddies in All Regions			
	s(DayinTrip)+te(Lat,Lon)	0.382	0.000
	s(DayinTrip)+te(Lat,Lon)+s(EddyAge)	0.381	0.000
	s(DayinTrip)+te(Lat,Lon)+s(EddyRadius)	0.382	0.000
	s(DayinTrip)+te(Lat,Lon)+s(EddyAmplitude)	0.394	0.013
	s(DayinTrip)+te(Lat,Lon)+s(EddySpeed)	0.382	0.000
	s(DayinTrip)+te(Lat,Lon)+s(EddyAgePercent)	0.373	-0.008
Wiggles Day In Cyclonic Eddies in All Regions			
	s(DayinTrip)+te(Lat,Lon)	0.135	0.000
	s(DayinTrip)+te(Lat,Lon)+s(EddyAge)	0.142	0.007
	s(DayinTrip)+te(Lat,Lon)+s(EddyRadius)	0.135	0.001
	s(DayinTrip)+te(Lat,Lon)+s(EddyAmplitude)	0.137	0.002
	s(DayinTrip)+te(Lat,Lon)+s(EddySpeed)	0.135	0.001
	s(DayinTrip)+te(Lat,Lon)+s(EddyAgePercent)	0.097	-0.038
Wiggles Day In Anticyclonic Eddies in California Current			
	s(DayinTrip)	0.213	0.000
	s(DayinTrip)+s(EddyAge)	0.214	0.001
	s(DayinTrip)+s(EddyRadius)	0.213	0.000
	s(DayinTrip)+s(EddyAmplitude)	0.216	0.003
	s(DayinTrip)+s(EddySpeed)	0.218	0.005
	s(DayinTrip)+s(EddyAgePercent)	0.213	0.000
Wiggles Day In Cyclonic Eddies in California Current			
	s(DayinTrip)	0.100	0.000
	s(DayinTrip)+s(EddyAge)	0.077	-0.023
	s(DayinTrip)+s(EddyRadius)	0.100	0.000

	s(DayinTrip)+s(EddyAmplitude)	0.100	0.000
	s(DayinTrip)+s(EddySpeed)	0.100	0.000
	s(DayinTrip)+s(EddyAgePercent)	0.100	0.000
Wiggles Day In Anticyclonic Eddies in Gulf of Alaska			
	s(DayinTrip)	0.049	0.000
	s(DayinTrip)+s(EddyAge)	0.049	0.000
	s(DayinTrip)+s(EddyRadius)	0.186	0.136
	s(DayinTrip)+s(EddyAmplitude)	0.049	0.000
	s(DayinTrip)+s(EddySpeed)	0.049	0.000
	s(DayinTrip)+s(EddyAgePercent)	0.049	0.000
Wiggles Day In Anticyclonic Eddies in Transition Zone			
	s(DayinTrip)	0.054	0.000
	s(DayinTrip)+s(EddyAge)	0.054	0.000
	s(DayinTrip)+s(EddyRadius)	0.054	0.000
	s(DayinTrip)+s(EddyAmplitude)	0.198	0.143
	s(DayinTrip)+s(EddySpeed)	0.239	0.185
	s(DayinTrip)+s(EddyAgePercent)	0.054	0.000
BottomTime Night In Anticyclonic Eddies in All Regions			
	s(DayinTrip)+te(Lat,Lon)	NA	NA
	s(DayinTrip)+te(Lat,Lon)+s(EddyAge)	0.321	NA
	s(DayinTrip)+te(Lat,Lon)+s(EddyRadius)	0.321	NA
	s(DayinTrip)+te(Lat,Lon)+s(EddyAmplitude)	0.321	NA
	s(DayinTrip)+te(Lat,Lon)+s(EddySpeed)	0.321	NA
	s(DayinTrip)+te(Lat,Lon)+s(EddyAgePercent)	0.323	NA
BottomTime Night In Cyclonic Eddies in All Regions			
	s(DayinTrip)+te(Lat,Lon)	NA	NA
	s(DayinTrip)+te(Lat,Lon)+s(EddyAge)	NA	NA
	s(DayinTrip)+te(Lat,Lon)+s(EddyRadius)	0.422	NA
	s(DayinTrip)+te(Lat,Lon)+s(EddyAmplitude)	0.376	NA
	s(DayinTrip)+te(Lat,Lon)+s(EddySpeed)	0.360	NA
	s(DayinTrip)+te(Lat,Lon)+s(EddyAgePercent)	NA	NA
BottomTime Night In Anticyclonic Eddies in California Current			
	s(DayinTrip)	0.265	0.000
	s(DayinTrip)+s(EddyAge)	0.261	-0.005
	s(DayinTrip)+s(EddyRadius)	0.265	0.000
	s(DayinTrip)+s(EddyAmplitude)	0.259	-0.006
	s(DayinTrip)+s(EddySpeed)	0.254	-0.012
	s(DayinTrip)+s(EddyAgePercent)	0.265	0.000
BottomTime Night In Cyclonic Eddies in California Current			

	s(DayinTrip)	0.339	0.000
	s(DayinTrip)+s(EddyAge)	0.370	0.031
	s(DayinTrip)+s(EddyRadius)	0.355	0.016
	s(DayinTrip)+s(EddyAmplitude)	0.349	0.010
	s(DayinTrip)+s(EddySpeed)	0.313	-0.026
	s(DayinTrip)+s(EddyAgePercent)	0.339	0.000
BottomTime Night In Anticyclonic Eddies in Gulf of Alaska			
	s(DayinTrip)	0.000	0.000
	s(DayinTrip)+s(EddyAge)	0.048	0.048
	s(DayinTrip)+s(EddyRadius)	0.000	0.000
	s(DayinTrip)+s(EddyAmplitude)	0.000	0.000
	s(DayinTrip)+s(EddySpeed)	0.000	0.000
	s(DayinTrip)+s(EddyAgePercent)	0.000	0.000
BottomTime Night In Anticyclonic Eddies in Transition Zone			
	s(DayinTrip)	0.274	0.000
	s(DayinTrip)+s(EddyAge)	NA	NA
	s(DayinTrip)+s(EddyRadius)	NA	NA
	s(DayinTrip)+s(EddyAmplitude)	NA	NA
	s(DayinTrip)+s(EddySpeed)	NA	NA
	s(DayinTrip)+s(EddyAgePercent)	0.274	0.000
BottomTime Day In Anticyclonic Eddies in All Regions			
	s(DayinTrip)+te(Lat,Lon)	0.298	0.000
	s(DayinTrip)+te(Lat,Lon)+s(EddyAge)	0.298	0.000
	s(DayinTrip)+te(Lat,Lon)+s(EddyRadius)	0.298	0.000
	s(DayinTrip)+te(Lat,Lon)+s(EddyAmplitude)	0.340	0.042
	s(DayinTrip)+te(Lat,Lon)+s(EddySpeed)	0.298	0.000
	s(DayinTrip)+te(Lat,Lon)+s(EddyAgePercent)	0.262	-0.036
BottomTime Day In Cyclonic Eddies in All Regions			
	s(DayinTrip)+te(Lat,Lon)	0.231	0.000
	s(DayinTrip)+te(Lat,Lon)+s(EddyAge)	0.252	0.021
	s(DayinTrip)+te(Lat,Lon)+s(EddyRadius)	0.455	0.224
	s(DayinTrip)+te(Lat,Lon)+s(EddyAmplitude)	0.232	0.000
	s(DayinTrip)+te(Lat,Lon)+s(EddySpeed)	NA	NA
	s(DayinTrip)+te(Lat,Lon)+s(EddyAgePercent)	0.445	0.213
BottomTime Day In Anticyclonic Eddies in California Current			
	s(DayinTrip)	0.295	0.000
	s(DayinTrip)+s(EddyAge)	0.295	0.000
	s(DayinTrip)+s(EddyRadius)	0.295	0.000
	s(DayinTrip)+s(EddyAmplitude)	0.295	0.000

	s(DayinTrip)+s(EddySpeed)	0.295	0.000
	s(DayinTrip)+s(EddyAgePercent)	0.342	0.047
BottomTime Day In Cyclonic Eddies in California Current			
	s(DayinTrip)	0.172	0.000
	s(DayinTrip)+s(EddyAge)	0.172	0.000
	s(DayinTrip)+s(EddyRadius)	0.172	0.000
	s(DayinTrip)+s(EddyAmplitude)	0.172	0.000
	s(DayinTrip)+s(EddySpeed)	0.172	0.000
	s(DayinTrip)+s(EddyAgePercent)	0.172	0.000
BottomTime Day In Anticyclonic Eddies in Gulf of Alaska			
	s(DayinTrip)	0.000	0.000
	s(DayinTrip)+s(EddyAge)	0.000	0.000
	s(DayinTrip)+s(EddyRadius)	0.028	0.028
	s(DayinTrip)+s(EddyAmplitude)	0.236	0.236
	s(DayinTrip)+s(EddySpeed)	0.208	0.208
	s(DayinTrip)+s(EddyAgePercent)	0.000	0.000
BottomTime Day In Anticyclonic Eddies in Transition Zone			
	s(DayinTrip)	0.489	0.000
	s(DayinTrip)+s(EddyAge)	0.489	0.000
	s(DayinTrip)+s(EddyRadius)	0.489	0.000
	s(DayinTrip)+s(EddyAmplitude)	0.489	0.000
	s(DayinTrip)+s(EddySpeed)	0.489	0.000
	s(DayinTrip)+s(EddyAgePercent)	0.489	0.000
Dive Depth Night In Anticyclonic Eddies in All Regions			
	s(DayinTrip)+te(Lat,Lon)	NA	NA
	s(DayinTrip)+te(Lat,Lon)+s(EddyAge)	NA	NA
	s(DayinTrip)+te(Lat,Lon)+s(EddyRadius)	NA	NA
	s(DayinTrip)+te(Lat,Lon)+s(EddyAmplitude)	NA	NA
	s(DayinTrip)+te(Lat,Lon)+s(EddySpeed)	NA	NA
	s(DayinTrip)+te(Lat,Lon)+s(EddyAgePercent)	NA	NA
DiveDepth Night In Cyclonic Eddies in All Regions			
	s(DayinTrip)+te(Lat,Lon)	0.301	0.000
	s(DayinTrip)+te(Lat,Lon)+s(EddyAge)	0.301	0.000
	s(DayinTrip)+te(Lat,Lon)+s(EddyRadius)	0.301	0.000
	s(DayinTrip)+te(Lat,Lon)+s(EddyAmplitude)	0.318	0.016
	s(DayinTrip)+te(Lat,Lon)+s(EddySpeed)	0.301	0.000
	s(DayinTrip)+te(Lat,Lon)+s(EddyAgePercent)	0.301	0.000
DiveDepth Night In Anticyclonic Eddies in California Current			
	s(DayinTrip)	0.000	0.000

	s(DayinTrip)+s(EddyAge)	0.043	0.043
	s(DayinTrip)+s(EddyRadius)	0.068	0.068
	s(DayinTrip)+s(EddyAmplitude)	0.000	0.000
	s(DayinTrip)+s(EddySpeed)	0.000	0.000
	s(DayinTrip)+s(EddyAgePercent)	0.000	0.000
DiveDepth Night In Cyclonic Eddies in California Current			
	s(DayinTrip)	0.000	0.000
	s(DayinTrip)+s(EddyAge)	0.064	0.064
	s(DayinTrip)+s(EddyRadius)	0.000	0.000
	s(DayinTrip)+s(EddyAmplitude)	0.000	0.000
	s(DayinTrip)+s(EddySpeed)	0.000	0.000
	s(DayinTrip)+s(EddyAgePercent)	0.000	0.000
DiveDepth Night In Anticyclonic Eddies in Gulf of Alaska			
	s(DayinTrip)	0.847	0.000
	s(DayinTrip)+s(EddyAge)	0.847	0.000
	s(DayinTrip)+s(EddyRadius)	0.847	0.000
	s(DayinTrip)+s(EddyAmplitude)	0.907	0.060
	s(DayinTrip)+s(EddySpeed)	0.896	0.049
	s(DayinTrip)+s(EddyAgePercent)	0.957	0.110
DiveDepth Night In Anticyclonic Eddies in Transition Zone			
	s(DayinTrip)	0.000	0.000
	s(DayinTrip)+s(EddyAge)	0.000	0.000
	s(DayinTrip)+s(EddyRadius)	0.000	0.000
	s(DayinTrip)+s(EddyAmplitude)	0.000	0.000
	s(DayinTrip)+s(EddySpeed)	0.000	0.000
	s(DayinTrip)+s(EddyAgePercent)	0.000	0.000
Dive Depth Day In Anticyclonic Eddies in All Regions			
	s(DayinTrip)+te(Lat,Lon)	0.193	0.000
	s(DayinTrip)+te(Lat,Lon)+s(EddyAge)	0.197	0.004
	s(DayinTrip)+te(Lat,Lon)+s(EddyRadius)	0.193	0.000
	s(DayinTrip)+te(Lat,Lon)+s(EddyAmplitude)	0.193	0.000
	s(DayinTrip)+te(Lat,Lon)+s(EddySpeed)	0.193	0.000
	s(DayinTrip)+te(Lat,Lon)+s(EddyAgePercent)	0.217	0.024
DiveDepth Day In Cyclonic Eddies in All Regions			
	s(DayinTrip)+te(Lat,Lon)	0.504	0.000
	s(DayinTrip)+te(Lat,Lon)+s(EddyAge)	0.500	-0.004
	s(DayinTrip)+te(Lat,Lon)+s(EddyRadius)	0.504	0.000
	s(DayinTrip)+te(Lat,Lon)+s(EddyAmplitude)	0.507	0.003
	s(DayinTrip)+te(Lat,Lon)+s(EddySpeed)	0.504	0.001

	s(DayinTrip)+te(Lat,Lon)+s(EddyAgePercent)	0.499	-0.005
DiveDepth Day In Anticyclonic Eddies in California Current			
	s(DayinTrip)	0.493	0.000
	s(DayinTrip)+s(EddyAge)	0.499	0.006
	s(DayinTrip)+s(EddyRadius)	0.493	0.000
	s(DayinTrip)+s(EddyAmplitude)	NA	NA
	s(DayinTrip)+s(EddySpeed)	0.493	0.000
	s(DayinTrip)+s(EddyAgePercent)	0.513	0.019
DiveDepth Day In Cyclonic Eddies in California Current			
	s(DayinTrip)	0.580	0.000
	s(DayinTrip)+s(EddyAge)	0.600	0.019
	s(DayinTrip)+s(EddyRadius)	0.580	0.000
	s(DayinTrip)+s(EddyAmplitude)	0.580	0.000
	s(DayinTrip)+s(EddySpeed)	0.469	-0.111
	s(DayinTrip)+s(EddyAgePercent)	0.582	0.002
DiveDepth Day In Anticyclonic Eddies in Gulf of Alaska			
	s(DayinTrip)	0.000	0.000
	s(DayinTrip)+s(EddyAge)	0.000	0.000
	s(DayinTrip)+s(EddyRadius)	0.000	0.000
	s(DayinTrip)+s(EddyAmplitude)	0.000	0.000
	s(DayinTrip)+s(EddySpeed)	0.000	0.000
	s(DayinTrip)+s(EddyAgePercent)	0.028	0.028
DiveDepth In Anticyclonic Eddies in Transition Zone			
	s(DayinTrip)	0.147	0.000
	s(DayinTrip)+s(EddyAge)	0.147	0.000
	s(DayinTrip)+s(EddyRadius)	0.147	0.000
	s(DayinTrip)+s(EddyAmplitude)	0.147	0.000
	s(DayinTrip)+s(EddySpeed)	0.147	0.000
	s(DayinTrip)+s(EddyAgePercent)	0.159	0.011

Chapter 2: A Comparative Study Across Two Ocean Basins: How Does Oceanography Drive Northern and Southern Elephant Seal Behavior?

Theresa R. Keates, Ian D. Jonsen, Fabien Roquet, Rachel R. Holser, Luis A. Hückstädt, Clive R. McMahon, Mark A. Hindell, Christophe Guinet, Daniel P. Costa

2.1 Abstract

Northern and southern elephant seals are closely related, yet operate in two very different ocean basins, the northeast Pacific and the Southern Ocean. Electronic tags that collect temperature and salinity data were deployed on adult females of both species. We used *in situ* oceanographic data alongside seal behavioral data to compare movement patterns relative to ocean conditions between these two species. Trip lengths and durations were similar for both species and showed no significant differences in movement and diving behavior. We used mixed effects models to test the relationship between seal transit rate, a proxy for foraging behavior, and dive depth relative to temperature, salinity, and mixed layer depth. Data were both measured *in situ* by the instruments carried by the seals and from a data assimilating oceanographic model. The *in situ* data influenced the seals' dive depth, while the seals' transit rate was better explained by modeled representation of the broader spatiotemporal context. Horizontal variability in temperature and salinity had a greater effect on transit rate during the post-molt trip than the post-breeding trip in both species. At the same time, both species showed faster, more directed movement during the post-breeding trip. The patterns of the biannual foraging trips were

consistent between northern and southern elephant seals despite their foraging trips happening in slightly offset seasons in their respective hemispheres. While behavioral differences in foraging trips are likely partly driven by internal pressures related to regaining body condition in a limited time before breeding or molting, there is an environmental component to this strategy shift. Despite the different temperature and light conditions, both species range in areas of elevated primary productivity during their respective post-breeding trips relative to their post-molt trips. The weaker response to oceanographic variability during the post-breeding season may be associated with a more homogenous distribution of resources during highly productive periods. By the post-molt trip, the prey field may have become patchier as this resource pulse becomes advected and diffused through mesoscale processes. Our data support the conclusion that adult female northern and southern elephant seals employ similar strategies to support their extreme feeding and fasting lifestyle in two seasonally variable ocean basins.

2.2 Introduction

Understanding how oceanographic processes drive the distribution of biological resources is central to predicting the effects of climate change on organisms across trophic levels. Tracking marine megafauna can investigate such pelagic ecological processes (Hückstädt and Reisinger, 2022). No marine predators have been tracked while simultaneously collecting *in situ* oceanographic data more extensively than elephant seals (*Mirounga* sp.). Elephant seal biologging studies have provided unparalleled insight into seals' interactions with their oceanographic environment at

and have contributed to ocean observation from physics to ecosystems (Harcourt et al., 2019; McMahon et al., 2021; Roquet et al., 2013, 2009).

Closely related northern elephant seals (*Mirounga angustirostris,* NES) in the North Pacific and southern elephant seals (*Mirounga leonina*, SES) in the Southern Ocean exhibit very similar life histories in two distant ocean basins (Hindell, 2018; Hindell et al., 2016; Le Boeuf et al., 2000; Robinson et al., 2012). The two species diverged relatively recently, between 0.61 and 3.96 million years ago (Higdon et al., 2007), although their ocean basin of origin is a subject of debate (Boessenecker and Churchill, 2016; Fulton and Strobeck, 2010). In this study, we leverage their close resemblance in life history, physiology, and diet to compare the influence of oceanography on their at-sea behavior. Despite long-term research programs on both species, direct comparisons of morphology, behavior, and life history of NES and SES are few (Beltran et al., 2022 but see Schick et al., 2013 for a study using data from both species to model body condition). SES are on average larger than NES (Beltran et al., 2022; Le Boeuf and Laws, 1994; Schick et al., 2013), though this difference is far less pronounced in females than males (Hindell, 2018). Foraging trip durations appear similar when comparing data from different studies. There has been only one comparison based on a small sample size between NES in California and SES in Patagonia which found longer trips in NES (Beltran et al., 2022; Campagna et al., 1998; Robinson et al., 2012).

Adult female NES and SES undergo two foraging trips a year between on-land fasting periods to breed and to molt. They spend two to three months at sea after

breeding (between November and January in SES; between February and April in NES) and about 8 months after molting (between March and October in SES; between June and January in NES) (Hindell and Burton, 1988; Le Boeuf and Laws, 1994). They predominately spend this time in the open ocean (Bailleul et al., 2010a; Hindell et al., 2021, 1991; Kienle et al., 2022; Le Boeuf et al., 2000; Robinson et al., 2012) diving continuously and heavily utilizing the mesopelagic zone (McMahon et al., 2019; Naito et al., 2017; Robinson et al., 2012). The diet of female seals is dominated by diel vertical migrators, mainly mesopelagic fishes, especially myctophids, and some squid (Bailleul et al., 2010a; Banks et al., 2014; Bradshaw et al., 2003; Cherel et al., 2008; Ducatez et al., 2008; Goetsch et al., 2018; Guinet et al., 2014; Naito et al., 2013; Yoshino et al., 2020). Mirroring this, pelagically foraging seals exhibit diel changes in diving depth, in which dives are deeper during the day and shallower at night (Le Boeuf et al., 2000; McIntyre et al., 2010; McMahon et al., 2019; Naito et al., 2017; Robinson et al., 2012). Spatial variation in the diet has been documented for SES (Banks et al., 2014; Newland et al., 2009) and NES (Goetsch, 2018; McHuron et al., 2019; Peterson et al., 2015). In one of the few studies directly comparing the two species, foraging location predicted lipid acquisition in both NES and SES (Schick et al., 2013), suggesting a strong influence of environment on foraging success.

The distribution of prey can be driven by physical oceanographic processes that operate at different temporal and spatial scales and is a critical determinant of predator movements. The patchy distribution of prey driven by physical and

biological processes is critical to understanding pelagic ecosystems (Benoit-Bird et al., 2013). Like many pelagic predators, foraging elephant seals may preferentially use different water masses (Biuw et al., 2007), affiliate with basin-scale features such as fronts (Bost et al., 2009; Cotté et al., 2015; Gordine et al., 2019; Simmons et al., 2007), or benefit from meso- or submesoscale features such as eddies and filaments (Abrahms et al., 2018; Bailleul et al., 2010b; Campagna et al., 2006; Cotté et al., 2015; Dragon et al., 2010; Green et al., 2020; Massie et al., 2016, Keates et al., 2022) While previous studies have investigated oceanographic influences on behavior in NES and SES separately, this is the first study to use tracking data from species to directly compare them between ocean basins with different physical conditions and seasonal patterns.

2.3 Methods

2.3.1 Instrument Deployment

Adult female elephant seals were equipped with Conductivity Temperature Depth Satellite Relay Data Loggers (CTD-SRDLs, Sea Mammal Research Unit, U.K.) at four colonies: NES at Año Nuevo State Park (37.11°N, -122.33°W, n=23) and San Nicolas Island (33.26°N, -119.48°W, n=8), and SES at Iles Kerguelen (-49.25°S, 69.17°E, n=92), and Macquarie Island (-54.35°S, 159.17°E, n=10). All NES handling protocols were authorized by the University of California Santa Cruz Institutional Animal Care and Use Committee. All SES work was approved and executed under University of Tasmania Animal Ethics Committee guidelines (A12141, A14523), and by Macquarie University Ethics Committee ARA2014_057 (Australia) and Comité d'éthique Anses/ENVA/UPEC (no. APAFiS: 21375) and Authorisation de Projet

utilisant des Animaux à des Fins Scientifiques N° 2019070612143224 et le Comité

pour l'Environnement Polaire (France).

Only complete tracking records containing the entirety of an offshore foraging trip

were retained for further analysis.

2.3.2 *In situ* Oceanographic Data Processing

The CTD-SRDLs collect pressure readings at 0.25 Hz. During the deepest dive in

every 6-hour period, pressure, temperature, and salinity readings are recorded at a

frequency of 1 Hz during the upcast (Boehme et al., 2009). A summary of the

temperature and salinity data are transmitted via the Argos satellite system; when

instruments are recovered, the full resolution dataset can be accessed. For detailed

data collection and transmission protocols, see (Boehme et al., 2009) and

(Photopoulou et al., 2015).

The post-processing of seal-derived temperature and salinity data are detailed in

(Roquet et al., 2014, 2011; Siegelman et al., 2019a). In summary, temperature and

salinity data are corrected for thermal mass-induced errors commonly affecting

conductivity cells (Mensah et al., 2018; Siegelman et al., 2019a). They are further

adjusted by comparing to independent CTD or Argo data or by cross-comparison to

other tag-collected data (Roquet et al., 2014, 2011). The resulting data set is quality

controlled using validation methods detailed in (Roquet et al., 2014). The resulting

accuracies are estimated as ±0.02°C for temperature (±0.04°C for reconstructed

profiles from transmitted data) and ±0.03 g kg^{-1} for salinity (Siegelman et al., 2019a).

These data are archived in the MEOP database (https://www.meop.net/) (Roquet et

119

al., 2014, 2013; Treasure et al., 2017). All code used to process the CTD data are publicly available on GitHub (https://github.com/fabien-roquet/MEOP_process). Temperature and salinity measurements were interpolated to 1 m and converted to absolute salinity (hereafter S) and conservative temperature (hereafter T) using the Gibbs Seawater (GSW) Oceanographic Toolbox in Matlab (McDougall and Barker, 2011). Sea surface temperature (SST) was calculated for each profile as the mean T within the upper 10 m of the water column. Temperature at the bottom of the dive was calculated as the mean of the temperature measurements over deepest 5 m of the dive. The mixed layer depth (MLD) was determined using the density algorithm presented in (Holte and Talley, 2009). Standard deviations in these physical parameters were used as indicators of horizontal variability. Outliers in *in situ* T, S, and MLD data (defined as >5*sd from the mean) were removed to avoid extreme values driving trends in the models. T, S, and MLD were scaled to each ocean basin to facilitate comparison between the North Pacific and the Southern Ocean.

2.3.3 Seal Behavioral Data Processing

All seals were tracked using the Argos system (https://www.argos-system.org/). Erroneous locations on land were first filtered out by cross-referencing to bathymetry data (dataset ID usgsCeSS111 from NOAA CoastWatch ERDDAP) within 0.01° of the seal's interpolated location. Argos location estimates were further refined using the foieGras package in R (Jonsen et al., 2020, 2019; Jonsen and Patterson, 2020) version 0.7-7.9276, which uses a continuous time state-space model incorporating location error estimates to filter the tracking data. Locations were interpolated to one-

hour intervals and assigned to each temperature-salinity profile based on time. Any interpolated locations with a standard error $\geq$ 30 km were omitted. Only complete foraging trips were retained for further analyses, *i.e.* the tag collected data until the seal returned to shore. Distances seals travelled were calculated using the geodist package version 0.0.7 in R (Padgham and Sumner, 2021).

The relationship between diving behavior and inferred foraging success is complex. Jouma'a et al. (2016) found more prey capture events in dives with shorter bottom times, as predicted in (Thompson and Fedak, 2001)'s models. In constrast, Thums et al. (2013) documented longer dive durations and bottom time in lower-quality food patches, which aligns with the marginal value theorem (Charnov, 1976). Further, diving parameters, especially bottom time and duration, vary with body condition (Jouma'a et al., 2016; Thums et al., 2013). This makes them challenging behavioral proxies as body changes drastically during extended foraging trips. We used transit rate as our foraging proxy as there are no other comparable proxies for both species. Horizontal surface transit rate, which performs well as a simple proxy for elephant seal foraging behavior (Robinson et al., 2010), was calculated over 12-hour intervals from the interpolated tracks. Movement persistence was derived from the foieGras state-space model for each 12-hour interval. This behavioral metric ranges from 0, indicating low persistence and frequent changes in direction and/or speed, to 1, indicating high persistence and infrequent changes in direction and/or speed (Jonsen et al., 2019). We consider dive depth relative to physical water column properties in this study as has been done independently for both species previously.

We considered elephant seal behavior at three different resolutions, 12 hours, 3 days, and 7 days, to investigate the spatiotemporal scale of environment-behavior relationships. We calculated the mean seal transit rate for each time window and assigned a centralized latitude and longitude as the average of all interpolated locations generated during that time frame. We summarized diving behavior by taking the mean and standard deviation of maximum depth. Dives made during the day and dives made at night were kept separate due to known diel patterns in elephant seal diving behavior. To focus on putative foraging dives, we removed dives identified as drift dives using the slimmingDive package designed for transmitted dive data from CTD-SRDLs (Arce et al., 2019). Passively drifting during a dive, a characteristic behavior of elephant seals, is hypothesized to be food processing and/or rest behavior (Biuw et al., 2003; Crocker et al., 1997). Benthic foraging is a minor foraging strategy for female elephant seals (Bailleul et al., 2010a; Hindell et al., 2021; Kienle et al., 2022; Le Boeuf et al., 2000; Robinson et al., 2012; Simmons et al., 2010). To focus on pelagic behavior, we excluded, portions of tracks on the Kerguelen Plateau, Antarctic shelf, and coastal northeast Pacific from behavioral analyses (see Subregions section for definitions).

2.3.4 Modeled Oceanographic Data

For each dive, including those without *in situ* T and S data, the closest available modeled potential temperature, salinity, and MLD were derived from the monthly 0.25° resolution CMEMS Global Ocean Ensemble Physics Reanalysis from Copernicus (dataset ID GLOBAL_REANALYSIS_PHY_001_031,

https://doi.org/10.48670/moi-00024). This model is data assimilative, meaning that major oceanographic features encountered by seals should also be in the model. For both *in situ* and modeled data, we considered SST (defined as the mean of the upper 10 m of the water column for *in situ* data and the surface value from the model), surface salinity (defined in the same way as SST), T and S at 100 m, T and S at 200 m, T and S at 600 m, and MLD. We calculated a metric of variability in these parameters based on modeled data in the vicinity of seals. We did this by calculating the standard deviation of the modeled data within a 0.75° radius of a seal's location, an area approximating the distance a seal may travel in a day.

We first extracted modeled data within a spatial radius of a seal location to determine the likelihood of seal profiles capturing horizontal variability in T, S, and MLD similar to the spatial variability in the model. This would not be the case if seals were interacting with features in a preferential way, such as staying on one side of a front rather than crossing it. For this analysis, the radius in which we extracted modeled data was determined using the average transit rate of the seal to estimate a distance traveled over the 3-day time window. We divided this distance by two and extracted modeled data from within this radius, using the approximation of 100 km ≈ 1 degree. We chose a 3-day window for this analysis because only 2 profiles were collected in 12 hours. This is too few to calculate a meaningful standard deviation. The typical distance seals travel in three days is an appropriate spatial scale (~100-300 km) to document mesoscale features potentially influencing seal behavior. We then randomly subsampled the modeled data within the spatial window to match the

resolution of seal data (12 profiles were collected over 3 days) and did this 10,000 times. We calculated the proportion of 3-day seal data windows for which the 95% confidence interval of the 10,000 bootstrapped estimates of T, S, and MLD standard deviation encompassed the value calculated using all available modeled data from the spatial window. We additionally compared the midpoint of the 95% confidence interval of bootstrapped values to the values from all available modeled data using a major axis Type II regression using the package "lmodel2" in R.

Due to the low sampling frequency of *in situ* data, we calculated variability in T, S, and MLD based on *in situ* data only for 3- and 7-day windows. We used a static 0.75° window rather than a variable spatial radius based on the seal's transit rate. This prevented the seals' transit rate from biasing our variability metric. For example, a faster transit rate would give us more space over which standard deviation in T, S, and MLD are calculated, generating a greater variance. This could lead to a meaningless result in which slower transit rate is associated with a lower modeled standard deviation in T, S, and MLD.

All analyses in R were carried out in version 4.1.3 (R Core Team, 2022).

2.3.5 Subregional Divisions

We divided the northeast Pacific into six subregions. The North Pacific Transition Zone lies between approximately 34-39°N and is bordered by two frontal zones to the north and south. The Subarctic Frontal Zone (SAFZ) lies to the to the north (40-43°N) and is a weak density front as temperature and salinity both decrease northward with little seasonal variability (Dinniman and Rienecker, 1999; Kazmin and Rienecker,

124

1996; Roden, 1991, 1980). The Subtropical Frontal Zone (STFZ) lies at the south of the Transition Zone (31-34° N) and shows more seasonal variability; the temperature front can fully disappear in the summer (White et al., 1978). Few elephant seals are found in this region. These frontal zones usually do not vary more than 150-200 km interannually from their climatological means (Roden, 1991). As models falling within 2° latitude of observations is a good agreement (Dinniman and Rienecker, 1999) and in the absence of robust *in situ* identifiers of these broad frontal zones, we used these latitudinal definitions. These zonal delineations are disrupted when the North Pacific Current nears the continent and bifurcates (Roden, 1991). Here, we divided seal locations between the California Current and the Gulf of Alaska at 48°N. While there is no clear western delineation of the California Current (Cummins and Freeland, 2007), we chose a 500 km width based on the schematic in (Roden, 1991). We defined seal locations in the California Current and Gulf of Alaska as "coastal" if a seal's position was less than 100 km from the coastline and the bathymetry was shallower than 1000 m.

We designated nine subregions within the range of southern elephant seals in the Southern Ocean. The dominant current, the Antarctic Circumpolar Current (ACC), contains several large fronts: the Subarctic Front (SAF), the Polar Front (PF), and the Southern Antarctic Circumpolar Front (SACCF) (Orsi et al., 1995). The temperature and salinity characteristics of these circumpolar fronts change across subregions (Sokolov and Rintoul, 2009); therefore, we used mean positions in this study rather than definitions based on T and S measurements. We used a shapefile of Southern

Ocean fronts based on data in (Orsi et al., 1995) and determined seal locations within 100 km (as in (Banks et al., 2014)) using the packages sf version 1.0-7 (Pebesma, 2018) and geosphere version 1.5-10 (Hijmans, 2019) in R. Between these fronts lie four zones: the Subantarctic Zone (north of SAF), the Polar Frontal Zone (between SAF and PF), the Antarctic Zone (between PF and SACCF), and the Southern Zone (between SACCF and the ACC's southern boundary) (Talley et al., 2011). Additionally, we identified seal locations as on the Kerguelen Plateau as bathymetry shallower than 2000m and between 56-45.5°S and 61-83°E as in (Allegue et al., 2022). We classified seal locations as on the Antarctic shelf where bathymetry was shallower than 2000 m south of 60°S (Allegue et al., 2022; Hindell et al., 2021).

2.3.6 Statistical Analyses

Behavioral ranges for both species were first compared to establish whether NES and SES are likely capable of similar behaviors, despite their differences in environment. For dive depth, a repeated, non-independent behavior, we tested the influence of a "Species" term in linear mixed models using lmer() in the package lme4 with individual seal as a random effect and "Season" (which of the two foraging trips a seal was on, post-breeding or post-molt) as an additional categorical term.

To evaluate relationships between seal behavior and oceanography, we ran generalized additive models (gam) using the mgcv package version 1.8-39 in R (Wood, 2011). Individual seal was included as a random effect in all models. A tensor smooth on latitude and longitude was added to deal with spatial autocorrelation inherent to tracking data. Covariates tested included internal drivers to seal behavior

(Season, Day in Trip) and oceanographic variables (Table 2.1). Models with transit

rate as the response variable were run with a Tweedie log-link distribution. Dive

depth models used a Gamma log-link family. We removed dives identified as likely

drift dives to focus on likely foraging in our dive behavior models.

2.4 Results

Our final dataset of complete tracks contained 129 seals: 21 NES from Año Nuevo

State Park, 7 NES from San Nicolas Island, 91 SES from Iles Kerguelen, and 10 SES

from Macquarie Island (Table 2.1, Fig. 2.2.1). Cumulatively, these seals travelled

1,192,399 km and collected 23,603 days of data. We received 687,172 dive records

and 80,843 *in situ* temperature-salinity profiles.

2.4.1 Seal Behavior

NES and SES underwent foraging trips of similar duration both PB (NES mean ±

sd 74 ± 11 days, n=7, SES 79 ± 9 days, n=35) and PM (NES 221 ± 29 days, n=21,

SES 237 ± 32 days, n=66). Mean distances travelled by each species were within one

standard deviation of each other, though with considerable interindividual variation in

both species, especially in SES during the PM season: NES PB 5,278 ± 1,631 km,

SES PB 4,324 ± 1,225 km; NES PM 12,008 ± 1,662 km, SES PM 11,393 ± 4,109 km

(Table 2.2). The ranges in dive depth were similar in both species (Table 2.2,

ANOVA linear model versus reduced model p=0.38 daytime and p=0.68 nighttime

dive depth).

Of all intrinsic values tested, both species' at-sea behavior was most strongly

influenced by the day into the trip (Table 2.3). For both species and across both

seasons, transit rate was slowest in the middle of the trip (Fig. 2.2, Table 2.3). The "Colony" factor added no explanatory power to the model, so was not included in any further models. This aligns with previous work in NES (Kienle, 2019; Robinson et al., 2012) showing indiscernible differences in behavior between colonies. The average transit rate was higher during the PB trip by 9% and movement persistence was higher by 14%. However, season only added a small amount of explanatory power to the model. Species did not add explanatory power to the model.

Dive depth was also strongly influenced by the day into the trip (Table 2.4), with seals diving deeper as the trip progressed, then shoaling dives approaching the very end of the trip (Fig. 2.2.3). Season did not add explanatory power to the model; species added a minimal amount of explanatory power (0.0001 R^2 deviance, no difference in deviance explained) (Table 2.4).

2.4.2 Oceanographic Conditions Encountered

Seal-collected data showed a saltier Southern Ocean and a warmer northeast Pacific, with overlap in T and S measured in each ocean basin (Table 2.5). To compare ocean basins, we normalized T, S, and MLD. The relative ranges of T, S, and MLD encountered measured *in situ* were similar (Fig. 2.4). However, SES encountered multiple peaks in salinity at 200 m that were not encountered by NES (Fig. 2.4f). Typical temperatures at 200 m measured by NES had a wider distribution, though SES documented more extreme outliers. Closer to the surface (100 m and shallower), where more dramatic seasonal fluctuations occur than at 200 m depth and below, temperature and salinity ranges were similar in NES and SES. However,

greater extremes in surface salinity were seen in SES. The PB trip showed colder SST and deeper MLDs on average than the PM trip in the northeast Pacific. In contrast, the Southern Ocean data showed the opposite seasonal trend (Fig. 2.5). Surface salinity in the Southern Ocean was extremely similar between PB and PM in SES (Fig. 2.5d); in NES, a wider range of surface salinities were encountered PM than PB (Fig. 2.5c).

The large-scale frontal zones were more strongly characterized by elevated subsurface horizontal variability in T and S in the Southern Ocean than in the northeast Pacific. To evaluate this, we used modeled data to avoid possible biases in seal-collected data resulting from seals preferentially staying on one side of a front. The standard deviation (sd) in modeled SST was higher in frontal regions than non-frontal in both ocean basins (t-test $p<1e-10$ in SES, $p<0.005$ in NES). Surface salinity variability was not different between frontal and non-frontal regions in either basin (SES $p=0.81$, NES $p=0.55$). Modeled T at 100m sd higher in fronts in SES ($p<1e-10$), not NES ($p=0.65$). Modeled S at 100m sd almost significantly higher in fronts in SES ($p=0.066$), not different in NES ($p=0.50$). T at 200m sd higher in fronts in SES ($p<1e-10$), almost significant in NES ($p=0.053$, though opposite, sd was higher in non-frontal regions). S at 200m sd modeled higher in frontal zones in SES ($p<1e-9$) but opposite in NES ($p=0.015$). Variability in MLD was higher in frontal zones in SES ($p<1e-7$) but opposite in NES ($p=0.0016$).

2.4.3 Behavior Relative to Oceanography

Species adds very little to oceanography-informed models

Trends between species were compared using models testing a behavioral response to an oceanographic covariate with a "Species" term to a model without a "Species" term. The deviance explained and R^2 of the models were compared. The "Species" term added $0.0001 \pm 0.00024\%$ deviance explained and an increase in R^2 of 0.0001 ± 0.00029 for transit rate models (Table 2.6). 0.000052 ± 0.00013 % deviance explained and -0.000038 ± 0.000050 R^2 for dive depth models (Table 2.7).

Modeled data explain transit rate better, in situ data explain diving behavior better

Transit rate models had greater explanatory power at 3-day timescales than 12 hours; explanatory power at 7-day timescales were similar to those at 3-day timescales. Therefore, we used a 3-day transit rate in subsequent models to resolve interactions with oceanographic features at mesoscales. Transit rate models had the greatest increases in explanatory power with the addition of T, S, and MLD variability based on modeled data. These explanatory power improvements from modeled variability were greater than those from absolute modeled T, S, and MLD. Transit rate was poorly explained by *in situ* T, S, and MLD data except for transit rate PB in NES, for which both absolute values and variance increased explanatory power of the models (Table 2.8).

Dive depth was best explained at the 12-hour scale. It was most influenced by *in situ* temperature, salinity, and MLD (relative to modeled data or horizontal variability in these physical parameters). It was not well explained by modeled data (Table 2.9).

Depth at night in PB NES was an exception: *in situ* measurements did not explain

dive depth at night but did during the day.

Importance of oceanography differs across seasons and ocean basins

The increase in transit rate explanatory power due to the addition of oceanographic

variables was greater during the PM trip than PB (Table 2.8). The influence of

oceanography on transit rate was greater in SES than NES models. This was

evidenced by the relative increase in R^2 and deviance explained after adding a

oceanographic covariates to the transit rate models. This difference was more

pronounced in the PM trip than the PB trip (Table 2.8).

The seasonal difference between dive depth models was more variable: NES

daytime dive depths showed similar increases in explanatory power due to

oceanography in either season. NES nighttime dive depth showed a greater effect of

oceanography PM than PB. In SES dive depth, both day and night, had a greater

association with oceanography PB than PM (Table 2.9). Overall, SES dive depth was

more influenced by oceanography than NES dive depth during the PB trip and NES

dive depth more than SES dive depth during the PM trip (Table 2.9).

Temperature effects on dive depth

Higher SST was associated with deeper dives in NES during the PM trip (Fig. 2.6).

There was only a weak relationship with subsurface temperatures. However, we saw a

similar result to the SST relationship with the difference in temperature between the

surface and 200 m: a higher temperature difference, indicative of stronger

stratification, was associated with deeper dives in NES PM (Fig. 2.7). The

relationship was weaker with MLD (Fig. 2.8). While SES temperature influence on dive depth larger PB than PM (Table 2.9), we did not see a similar relationship between temperature and dive depth in SES as in NES for either season (Fig. 2.6-8).

The most common temperatures at the bottom of dives, presumably where foraging is occurring, spanned a similar range of approximately 4° C, with temperatures for NES warmer (90% of dives encountered temperatures between 3.6° C and 7.7° C at the bottom) and mostly non-overlapping with those SES were diving to (90% between 0.3° C and 4.0° C at the bottom, Fig. 2.9). Differences between daytime and nighttime were minimal (Fig. 2.9). Dive depths to reach these temperatures were insignificantly different (see "Seal Behavior").

Effect of Fronts
The frontal effect on transit rate was extremely weak in both species (Table 2.8). Subregion added some explanatory power to transit rate models, slightly more than the categorical effect "Front," in SES but not NES (Table 2.8).

How well do in situ data replicate variability documented in modeled data?
We used a bootstrap analysis to determine how likely random *in situ* profiles are to capture the horizontal variance in T, S, and MLD resolved by the modeled data. The 95% confidence interval of the bootstrapped standard deviations in modeled T, S, and MLD encompassed the standard deviation calculated from all modeled data 59.6 ± 3.2% of the time for T and S between the surface and 100m and for MLD. For T and S at 200 m, the bootstrapped confidence interval included the estimate based on all available modeled data for 16.8 ± 6.9% of locations (Table 2.10).

The model II regressions showed close relationships between horizontal variability calculated from bootstrapped data and those calculated from all available model data: the mean slope was 0.91 and R^2 was 0.996 (Table 2.11). The relationship was slightly nonlinear, as bootstrapped values started to slightly underestimate the variability at high values (Fig. 2.10). These observations held between the surface and 100 m for T and S, but were much weaker at 200 m.

2.5 Discussion

This is the first study to directly compare the at-sea behavior of NES and SES relative to oceanographic parameters. Our results demonstrate that despite inhabiting very different environments, the relationship between NES and SES behavior and oceanographic conditions they encountered are extremely similar, as are their seasonal patterns despite the offset timing of their respective PB and PM trips.

2.5.1 Why oceanographic influence may be stronger in SES
In general, the relative influence of oceanographic parameters on transit rate was higher in SES than in NES. More T-S structure, especially in salinity, in the Southern Ocean is likely responsible for the more significant role oceanography plays in SES movement. T and S data collected by both species encompassed similar ranges. Still, SES spent considerable time in a broader range of salinities. Relative to the North Pacific, the Southern Ocean has several well-defined water masses, with deep and bottom water formation occurring at the Antarctic shelf (Talley et al., 2011). By contrast, as the low-density end member of global circulation, the North Pacific is relatively fresh with weak thermohaline circulation and no deep or bottom water

formation (Talley et al., 2011). Instead, North Pacific deep water masses are formed through internal mixing and upwelling of Antarctic waters, without contact with the atmosphere, and are weakly distinguishable (Emery, 2001; Talley et al., 2011). This is why we observed lower salinity in the NES data. At the same time, SES encountered a wider range of distinct salinity conditions compared to NES, likely due to the more clearly differentiated water masses in the Southern Ocean. SES have been observed to change behavior between water masses (Field et al., 2001), preferentially using Circumpolar Deep Water and avoiding Antarctic Intermediate Water (Biuw et al., 2007, 2003; Hindell et al., 2017). NES encounter mainly Pacific Subarctic Upper Water and Pacific Subarctic Intermediate Water (Holser et al., 2022). The foraging behavior relative to water masses is understudied in NES but is likely weak. SES encounter much more physically distinct water masses and show weak behavioral differences, likely using the boundaries between water masses rather than water masses per se (Gordine et al., 2019).

Frontal boundaries between water properties punctuate pelagic homogeneity, often supporting elevated primary productivity and increased densities of organisms from primary consumers to higher predators (Olson et al., 1994; Olson, 2002). Biologging studies have demonstrated the use of fronts by megafauna such as basking sharks (Miller et al., 2015), northern fur seals (Nordstrom et al., 2013), albacore tuna (Snyder et al., 2017; Zainuddin et al., 2008), and southern elephant seals (Bost et al., 2009; Cotté et al., 2015; Gordine et al., 2019). Higher fisheries yield at fronts is further evidence of increased prey density for higher predators (Woodson and Litvin,

2015). Largescale frontal zones are more strongly defined by physical water column variability in the Southern Ocean. The modeled data in the Southern Ocean showed elevated horizontal variability in T, S, and MLD which generally did not occur in northeast Pacific. The Southern Ocean fronts are also more positionally sTable 2.; they are broadly constrained by bathymetry and consistently associated with SSH streamlines (Belkin and Gordon, 1996; Orsi et al., 1995; Sokolov and Rintoul, 2009). This makes them more reliable habitat features than the frontal zones in the northeast Pacific that occupy large latitudinal ranges. SES use these major fronts (Bost et al., 2009; Gordine et al., 2019), especially at higher latitudes (Gordine et al., 2019). Still, for SES, frontal zones did very little to explain behavior in our study, suggesting there is no universal effect of being in a front such that every front encountered would affect behavior similarly. As the subregional classifications added slightly more explanatory power than the binary "Front" term, certain fronts may affect behavior more than others. Additionally, the regions between fronts are often very dynamic and eddy dominated; this is especially the case for the Polar Frontal Zone which lies between the SAF and the PF (Orsi et al., 1995; Talley et al., 2011). Both NES (Abrahms et al., 2018; Keates et al., 2022) and SES (Bailleul et al., 2010b; Campagna et al., 2006; Cotté et al., 2015; Dragon et al., 2010; Green et al., 2020; Massie et al., 2016) use elevated mesoscale activity such as eddies. While fronts help SES forage efficiently, the regions between them may also offer benefits through smaller scale processes. Such mesoscale processes may reduce the relative magnitude of the frontal influence on behavior in our dataset.

There is no clear analog for Southern Ocean fronts in the North Pacific, marking one major difference in the habitat of SES relative to NES. The northeast Pacific lacks strong boundary currents and has relatively smooth topography, removing some significant features that can constraint fronts (Roden, 1991). The primary current within NES's range is the North Pacific Current, which does not have analogous sTable 2.fronts to the ACC. Instead, our major frontal designation relied on the Subarctic Frontal Zone (SAFZ). The SAFZ occupies a relatively sizeable latitudinal range (approximately 3° latitude) and tends to have weak density gradients as a result of opposing density effects of decreasing temperature alongside decreasing salinity south to north (Dinniman and Rienecker, 1999; Kazmin and Rienecker, 1996; Roden, 1991, 1980). Previous work showed that NES use the gyre-gyre boundary (Robinson et al., 2012; Simmons et al., 2010), including the SAFZ. While NES in this study spent considerable time in this region, we did not observe a behavioral difference associated with the SAFZ.

The large scale of Southern Ocean fronts, their distinct defining physical characteristics, and relative stability may allow them to accumulate or attract prey species better than the more poorly defined, dynamic frontal zones in the northeast Pacific. Despite this, neither NES nor SES behavior was strongly influenced by being within a frontal region at the scales we considered. Seal behavior in both ocean basins showed a stronger relationship to smaller-scale oceanographic variability than these large-scale frontal designations. This could represent responses to meso- or submesoscale features such as eddies, smaller fronts, and filaments. The greater

strength of this relationship in the Southern Ocean likely reflects the availability of these smaller-scale hydrographic features. For example, eddies are more abundant in the Southern Ocean than in the northeast Pacific (Chelton et al., 2011; Roden, 1991). Both northern and southern elephant seals responded more strongly to mesoscale features, suggesting that physical and/or biological processes at this spatial scale influence their mesopelagic prey field.

2.5.2 Scales of seal decision-making

Using a combination of *in situ* and modeled data allowed us to explore the spatial and temporal scales that influenced behavior. Dive depth was better explained by physical conditions encountered by the seal on that day. This was best demonstrated with the *in situ* data than the modeled data. This is because the modeled T, S, and MLD data were averaged over larger spatial scales than would be experienced by a seal during each dive. Dive depth was not influenced by horizontal variability in SES and only very weakly in a few NES exceptions with no apparent relationship.

Transit rate is relevant over broader spatiotemporal scales than dive depth. The spatial scale of transit rate was thus more appropriate to compare to the more averaged modeled output of the of the seals' environment. The behavioral responses of elephant seals were stronger to modeled horizontal variances in physical parameters (T, S, and MLD) than variances calculated from *in situ* data. The stronger relationship of seal transit rate to modeled variance in water properties than those calculated using *in situ* data poses a challenge in using *in situ* data to determine a relationship to mesoscale features. *In situ* data may capture small-scale nuances in T

and S that are not large or long-lived enough to influence seal behavior. Based on our bootstrap analysis, 4 random profiles per day are only just over 50% likely to capture the "true" variability that can be resolved at 0.25° resolution. Therefore, discrepancies between seal-documented T-S profiles and actual horizontal variability are equally likely to be chance rather or biased sampling due to seals' behavioral responses to mesoscale features. However, while our bootstrap analysis demonstrated that numerical disagreement between variance estimates can be common with random sampling, the relationship between bootstrapped and "true" values was very close. Therefore, trends in horizontal variability should be reasonably well estimated by 4 random profiles per day. Still, *in situ* estimates of variability explained less variability in seal behavior than the model-based value. This could be because *in situ* data are resolving small-scale variability that modeled data are not, but that is at too small of a scale to matter to seals. The modeled data better explained seal transit rate than the *in situ* data, indicating that relatively sTable 2.and long-lived (at least one month, the temporal resolution of the model) features influence seals' search for food. The higher predictive power of modeled data could be due to their behavioral responses to mesoscale features. Seals may be biasing their sampling, by, for example, remaining on one side of a small front rather than crossing it. Based on the bootstrap analysis, random sampling at 4 profiles per day is more likely to underestimate variability in areas of high physical heterogeneity, which was associated with elevated foraging behavior. Some studies have deployed oceanographic tags programmed to sample at

higher frequencies (*e.g.* Siegelman et al., 2019b). Future data of this kind may help us further investigate this question.

2.5.3 Seasonal variability in oceanographic influence on behavior

The environment had a stronger influence on horizontal movement during the PM trip compared to the PB trip. Both species exhibited on average more searching behavior during this trip (slower transit, lower movement persistence). The stronger influence of horizontal variability in physical water properties suggests more exploitation of oceanographic heterogeneity during the PM trip. A stronger response to mesoscale features PM has been seen in other studies in SES (Cotté et al., 2015) and NES (Keates et al., in review). Drivers of this pattern could include seasonal changes to the environment and internal pressures that differ between the two foraging trips.

As the timing within a trip dominated behavioral models in both species, the internal pressure to gain enough resources in time to return to the colony for the breeding or molting season is a significant behavioral influence. Having just lost about 35%-40% of their body mass due to lactating and fasting on shore (Arnbom et al., 1997; Carlini et al., 1997; Costa et al., 1986), elephant seals may experience greater time constraints on the shorter PB trip to partially recover their body condition. Jaw accelerometry in NES PB has shown near-constant foraging, and further demonstrated that this is necessary to achieve positive energy balance (Adachi et al., 2021). Guinet et al. (2014) documented a fairly consistent rate of prey capture

in PB using accelerometry in SES. However, neither study collected accelerometry data during the PM trip for comparison. In NES, the number of wiggles (vertical excursions at the bottom phase of dives inferred to indicate prey pursuit) tend to be more homogeneously distributed in space and time during the PB trip than PM (Holser, 2020). At the same time, more drift dives are performed PM which are used for rest and/or food processing and the distribution of drift dives in space and time is more heterogeneous during the PM trip than PB (Holser, 2020). Both lines of evidence suggest foraging is patchier during the PM trip than the PB trip. The uniformity of foraging behavior PB may mean seals are less selective in prey choice, which would explain the more variable diet observed in NES PB than PM (Goetsch, 2018). In both species, the longer PM trip may allow seals to seek out and exploit profiTable 2.patches that they do not have time to or the ability to travel far enough to during the short PB trip, or the prey field may be more patchily distributed that time of year.

This latter explanation is suggested by Cotté et al. (2015), which tracked SES relative to post-phytoplankton bloom waters from the Kerguelen colony. The authors posit that high productivity from a seasonal bloom supported a relatively homogenously distributed prey field during the seals' PB trip which subsequently became more patchily distributed as those highly productive waters where advected and modified by (sub)mesoscale circulation. Such conditions were then encountered by seals during their PM trip. The seasonal trip timings of NES and SES are not equivalent (SES PB trip is in late austral spring/early summer, NES PB trip is during

the boreal winter/early spring). However, the timing of seasonal blooms within the seals' ranges is analogous between the North Pacific and the Southern Ocean relative to the seals' biannual foraging trips. In the Southern Ocean, where light limitation is the dominant factor controlling phytoplankton division, phytoplankton concentrations are high in the spring-summer, peaking in December-January, which coincides with SES' PB trip (Arrigo et al., 2008; Arteaga et al., 2020). Most major phytoplankton blooms in the Southern Ocean occur at the continental margin and ice edge, where melting ice generates a sTable 2.shallow mixed layer (<40m) that supports accumulation of phytoplankton biomass (Smetacek and Nicol, 2005). Nonetheless, the deeper offshore waters with deeper MLDs where seals pelagically forage often support higher cumulative phytoplankton biomass throughout the water column than the blooms at the ice edge and continental margin (Smetacek and Nicol, 2005). After peaking in summer, primary productivity declines and is spatially heterogeneous as blooms and their consumers become mixed with less productive waters during SES' PM trip (Arrigo et al., 2008; Cotté et al., 2015; O'Toole et al., 2015). The elapsed time may allow the energy to translate from the base of the food web to higher trophic levels. In the northeast Pacific, more of the NES' range also contains elevated primary productivity during the PB trip in the boreal winter, than the PM trip in the boreal summer (Ayers and Lozier, 2010). While significant summer blooms in the northeast Pacific occur in the coastal Gulf of Alaska and the Bering Sea (Zhang et al., 2021), a greater area of the NES range supports elevated phytoplankton concentrations due to the positioning of the Transition Zone Chlorophyll Front

(TZCF). The TZCF is a major feature in NES's range with a dramatic seasonal shift: it lies at the gyre-gyre boundary in the summertime near 40-45° N and migrates over 1,000 km south in the wintertime to 30-35° N (Bograd et al., 2004; Polovina et al., 2017, 2001). Qualitative observations showed that female NES associate with the TZCF in the summer, when the front coincides with the gyre-gyre boundary, but not in the winter when the front migrates south (Robinson et al., 2012). During their PM trip, far less of the NES's range contains high chlorophyll concentrations and the influence of chlorophyll prior to seal presence on behavior was higher: seals likely gain foraging benefits from elevated primary productivity that had been present previously, allowing time for a phytoplankton bloom's energy to be relevant to a top predator (Chapter 3).

Whether internal drivers or environment play a larger role in strategic differences during the PM trip, the result may be advantageous, as energy gain rate and mass gain rate are higher PM NES (Holser, 2020). Limited data (N < 26) on SES suggest the opposite may be true (Bradshaw et al., 2004); the logistical challenges of post-trip tag recovery and animal weighing are much higher in the remote SES colonies. Consequently, we cannot compare these mass gain trends between species with confidence. However, observing the difference in environmental influence on behavior between foraging trips in two very different oceans suggests that the internal drivers of at-sea behavior exert a strong influence in both species. Both ocean basins may also support similar seasonal patterns in prey distribution despite the two trips not occurring in analogous seasons in both hemispheres, with, most strikingly,

opposite inter-trip patterns in SST and MLD, though similar trends in seasonal

primary productivity pulses. These differences in stratification and primary

productivity patterns by time of year constitute a major difference in the cyclical

dynamics of the seals' respective environments and illustrate a surprising consistency

in strategy between NES and SES foraging trip timing in their seasonally variable

ocean basins.

The seasonal differences in environmental effects on diving behavior were more

variable. As dive depth was also better explained by *in situ* data than transit rate was,

diving decisions may be based on immediate surroundings, which can be made even

if seal is constrained by time during a short trip to maximize energy gains, reducing

the seasonal differences in dive depth. This may also be a reason for some transit rate

sensitivity to *in situ* conditions in NES PB, an exception to the general pattern we saw

of *in situ* data poorly describing transit rate: the time constraint within the PB trip

may result in seals making decisions based on finer-scale conditions.

2.5.4 Dive depth and water temperature

Depth of diving has been related to water temperature extensively in the literature

and is a topic of specific interest in a warming ocean. We observed deeper diving in

warmer water (surface and at 100 m) in NES PM, but we did not see this pattern

emerge in SES as previous studies have (Biuw et al., 2007; Guinet et al., 2014;

McIntyre et al., 2011) (but see also (Field et al., 2001) who saw little relationship

between behavior and thermal structure in SES from Macquarie Island). In NES,

foraging behavior positively associated with colder SST (Crocker et al., 2006; Simmons et al., 2007), but these studies did not specifically investigate dive depth.

Waters encountered by NES during their PM trip tend to be warmer and more stratified than during their PB trip; the opposite is true in SES. Further, the northeast Pacific has on average shallower MLDs than the Southern Ocean during their respective seasons of elevated water column stratification. Stronger stratification may drive deeper diving in seals as shallow mixed layers, while keeping phytoplankton close to light, can limit primary productivity due to a lack of nutrient recirculation from deeper water. This creates a clearer water column which drives diel vertical migrating organisms into deeper water to reduce predation risk by visual predators (Benoit-Bird and Moline, 2021; Catul et al., 2011; Irigoien et al., 2014; Ohman and Romagnan, 2016). This may occur in the northeast Pacific, as NES dive depths are deeper when SST is high and when the difference between SST and temperature at 200 m is higher, two proxies for stronger stratification. The same effect was observed when MLDs were shallow, though to a lesser degree. However, in the Southern Ocean, the season with shallower MLDs and warmer SST (PB instead of PM) is when phytoplankton concentrations are highest: the summer. Based on our observations in the context of seasonal patterns in productivity in both oceans, the shallower mixed layers during the PB season in the Southern Ocean, unlike the even shallower PM MLDs in the northeast Pacific, do not generally inhibit primary productivity. The lack of dive depth effect of SST may be due to the water column not being optically more transparent. We considered daytime and nighttime diving

separately based on solar elevation. This allowed us to control for differences in day length between the two habitats in case light level directly impacted the vertical distribution of prey due to predator avoidance behavior (rather than the level of primary productivity).

Temperatures at the bottom of dives, where foraging is likely occurring, spanned similar ranges of approximately 3° C, but with NES dives reaching warmer temperatures than SES with little overlap. There was no significant difference in NES and SES dive depths. Therefore, their primary prey reside in different thermal niches. How the species composition of NES and SES diets compare is an important area of future research to compare the mesopelagic ecosystem between these two ocean basins.

2.6 Conclusion

Two closely related species, the northern and southern elephant seal, show remarkably behavioral patterns despite operating in very different oceans. As deep-water predators, average physical conditions in which their prey operate are not too dissimilar. Still, there are noTable 2.differences in temperature, salinity, light, mixing, and meso- to basin-scale features between the northeast Pacific and the Southern Ocean. Despite contrasting trends in temperature and mixing between the post-molt and post-breeding trips between the Southern Ocean and northeast Pacific, both trips' timing relative to seasonal productivity peaks were roughly aligned. We conclude that both species employ similar strategies in two very different oceans. This suggests that

their mesopelagic prey responds to similar oceanographic processes and seasonal

resource pulses.

2.7 References

Abrahms, B., Scales, K.L., Hazen, E.L., Bograd, S.J., Schick, R.S., Robinson, P.W.,

Costa, D.P., 2018. Mesoscale activity facilitates energy gain in a top predator.

Proc. Natl. Acad. Sci. B 285. doi:10.1098/rspb.2018.1101

Adachi, T., Takahashi, A., Costa, D.P., Robinson, P.W., Hückstädt, L.A., Peterson,

S.H., Holser, R.R., Beltran, R.S., Keates, T.R., Naito, Y., 2021. Forced into an

ecological corner: Round-the-clock deep foraging on small prey by elephant

seals. Sci. Adv. 7, 21–25. doi:10.1126/sciadv.abg3628

Allegue, H., Guinet, C., Patrick, S.C., Hindell, M.A., McMahon, C.R., Réale, D.,

2022. Sex, body size, and boldness shape the seasonal foraging habitat selection

in southern elephant seals. Ecol. Evol. 1–16. doi:10.1002/ece3.8457

Arce, F., Bestley, S., Hindell, M.A., McMahon, C.R., Wotherspoon, S., 2019. A

quantitative, hierarchical approach for detecting drift dives and tracking

buoyancy changes in southern elephant seals. Sci. Rep. 9, 8936.

doi:10.1038/s41598-019-44970-1

Arnbom, T., Fedak, M.A., Boyd, I.L., 1997. Factors affecting maternal expenditure in

southern elephant seals during lactation. Ecology 78, 471–483.

doi:10.1890/0012-9658(1997)078[0471:FAMEIS]2.0.CO;2

Arrigo, K.R., van Dijken, G.L., Bushinsky, S., 2008. Primary production in the

Southern Ocean, 1997-2006. J. Geophys. Res. Ocean. 113, 1997–2006. doi:10.1029/2007JC004551

Arteaga, L.A., Boss, E., Behrenfeld, M.J., Westberry, T.K., Sarmiento, J.L., 2020. Seasonal modulation of phytoplankton biomass in the Southern Ocean. Nat. Commun. 11. doi:10.1038/s41467-020-19157-2

Ayers, J.M., Lozier, M.S., 2010. Physical controls on the seasonal migration of the North Pacific transition zone chlorophyll front. J. Geophys. Res. Ocean. 115, 1–11. doi:10.1029/2009JC005596

Bailleul, F., Authier, M., Ducatez, S., Roquet, F., Charrassin, J.B., Cherel, Y., Guinet, C., 2010a. Looking at the unseen: Combining animal bio-logging and stable isotopes to reveal a shift in the ecological niche of a deep diving predator. Ecography (Cop.). 33, 709–719. doi:10.1111/j.1600-0587.2009.06034.x

Bailleul, F., Cotté, C., Guinet, C., 2010b. Mesoscale eddies as foraging area of a deep-diving predator, the southern elephant seal. Mar. Ecol. Prog. Ser. 408, 251–264. doi:10.3354/meps08560

Banks, J., Lea, M.A., Wall, S., McMahon, C.R., Hindell, M.A., 2014. Combining bio-logging and fatty acid signature analysis indicates spatio-temporal variation in the diet of the southern elephant seal, Mirounga leonina. J. Exp. Mar. Bio. Ecol. 450, 79–90. doi:10.1016/j.jembe.2013.10.024

Belkin, I.M., Gordon, A.L., 1996. Southern Ocean fronts from the Greenwich

meridian to Tasmania. J. Geophys. Res. Ocean. 101, 3675–3696. doi:10.1029/95JC02750

Beltran, R.S., Hindell, M.A., McMahon, C.R., 2022. The elephant seal: linking phenotypic variation with behavior and fitness in a sexually dimorphic phocid, in: Costa, D.P., Mchuron, E.A. (Eds.), Ethology and Behavioral Ecology of Phocids. Springer, pp. 401–440. doi:10.1007/978-3-030-88923-4

Benoit-Bird, K.J., Battaile, B.C., Heppell, S.A., Hoover, B., Irons, D., Jones, N., Kuletz, K.J., Nordstrom, C.A., Paredes, R., Suryan, R.M., Waluk, C.M., Trites, A.W., 2013. Prey patch patterns predict habitat use by top marine predators with diverse foraging strategies. PLoS One 8. doi:10.1371/journal.pone.0053348

Benoit-Bird, K.J., Moline, M.A., 2021. Vertical migration timing illuminates the importance of visual and nonvisual predation pressure in the mesopelagic zone. Limnol. Oceanogr. 66, 3010–3019. doi:10.1002/lno.11855

Biuw, M., Boehme, L., Guinet, C., Hindell, M., Costa, D., Charrassin, J.-B., Roquet, F., Bailleul, F., Meredith, M., Thorpe, S., Tremblay, Y., McDonald, B., Park, Y.-H., Rintoul, S.R., Bindoff, N., Goebel, M., Crocker, D., Lovell, P., Nicholson, J., Monks, F., Fedak, M.A., 2007. Variations in behavior and condition of a Southern Ocean top predator in relation to *in situ* oceanographic conditions. Proc. Natl. Acad. Sci. U. S. A. 104, 13705–10. doi:10.1073/pnas.0701121104

Biuw, M., McConnell, B., Bradshaw, C.J.A., Burton, H., Fedak, M., 2003. Blubber and buoyancy : monitoring the body condition of free-ranging seals using simple

dive characteristics. J. Exp. Biol. 3405–3423. doi:10.1242/jeb.00583

Boehme, L., Lovell, P., Biuw, M., Roquet, F., Nicholson, J., Thorpe, S.E., Meredith, M.P., Fedak, M., 2009. Technical note: Animal-borne CTD-Satellite Relay Data Loggers for real-time oceanographic data collection. Ocean Sci. 5, 685–695. doi:10.5194/os-5-685-2009

Boessenecker, R.W., Churchill, M., 2016. The origin of elephant seals: implications of a fragmentary late Pliocene seal (Phocidae: Miroungini) from New Zealand. New Zeal. J. Geol. Geophys. 59, 544–550. doi:10.1080/00288306.2016.1199437

Bograd, S.J., Foley, D.G., Schwing, F.B., Wilson, C., Laurs, R.M., Polovina, J.J., Howell, E.A., Brainard, R.E., 2004. On the seasonal and interannual migrations of the transition zone chlorophyll front. Geophys. Res. Lett. 31, 1–5. doi:10.1029/2004GL020637

Bost, C.A., Cotté, C., Bailleul, F., Cherel, Y., Charrassin, J.B., Guinet, C., Ainley, D.G., Weimerskirch, H., 2009. The importance of oceanographic fronts to marine birds and mammals of the southern oceans. J. Mar. Syst. 78, 363–376. doi:10.1016/j.jmarsys.2008.11.022

Bradshaw, C.J.A., Hindell, M.A., Best, N.J., Phillips, K.L., Wilson, G., Nichols, P.D., 2003. You are what you eat: describing the foraging ecology of southern elephant seals (Mirounga leonina) using blubber fatty acids. Proc. R. Soc. B Biol. Sci. 207, 1283–1292. doi:10.1098/rspb.2003.2371

Bradshaw, C.J.A., Hindell, M.A., Sumner, M.D., Michael, K.J., 2004. Loyalty pays: Potential life history consequences of fidelity to marine foraging regions by southern elephant seals. Anim. Behav. 68, 1349–1360. doi:10.1016/j.anbehav.2003.12.013

Campagna, C., Piola, A.R., Rosa Marin, M., Lewis, M., Fernández, T., 2006. Southern elephant seal trajectories, fronts and eddies in the Brazil/Malvinas Confluence. Deep. Res. Part I Oceanogr. Res. Pap. 53, 1907–1924. doi:10.1016/j.dsr.2006.08.015

Campagna, C., Quintana, F., Le Boeuf, B.J., Blackwell, S.B., Crocker, D.E., 1998. Diving behaviour and foraging location of female southern elephant seals from Patagonia. Aquat. Mamm. doi:10.1111/j.1469-7998.1995.tb01784.x

Carlini, A.R., Daneri, G.A., Marquez, M.E.I., Soave, G.E., Poljak, S., 1997. Mass transfer from mothers to pups and mass recovery by mothers during the post-breeding foraging period in southern elephant seals (Mirounga leonina) at King George Island. Polar Biol. 18, 305–310. doi:10.1007/s003000050192

Catul, V., Gauns, M., Karuppasamy, P.K., 2011. A review on mesopelagic fishes belonging to family Myctophidae. Rev. Fish Biol. Fish. 21, 339–354. doi:10.1007/s11160-010-9176-4

Charnov, E.L., 1976. Optimal foraging theory: the marginal value theorem. Theor. Popul. Biol. 9, 129–136. doi:10.1016/0040-5809(76)90040-X

Chelton, D.B., Gaube, P., Schlax, M.G., Early, J.J., Samelson, R.M., 2011. The influence of nonlinear mesoscale eddies on near-surface oceanic chlorophyll. Science (80-.). 334, 328–332. doi:10.1126/science.1208897

Cherel, Y., Ducatez, S., Fontaine, C., Richard, P., Guinet, C., 2008. Stable isotopes reveal the trophic position and mesopelagic fish diet of female southern elephant seals breeding on the Kerguelen Islands. Mar. Ecol. Prog. Ser. 370, 239–247. doi:10.3354/meps07673

Costa, D.P., Boeuf, B.J.L., Huntley, A.C., Ortiz, C.L., 1986. The energetics of lactation in the Northern elephant seal, Mirounga angustirostris. J. Zool. 209, 21–33. doi:10.1111/j.1469-7998.1986.tb03563.x

Cotté, C., D'Ovidio, F., Dragon, A.C., Guinet, C., Lévy, M., 2015. Flexible preference of southern elephant seals for distinct mesoscale features within the Antarctic Circumpolar Current. Prog. Oceanogr. 131, 46–58. doi:10.1016/j.pocean.2014.11.011

Crocker, D.E., Costa, D.P., Le Boeuf, B.J., Webb, P.M., Houser, D.S., 2006. Impact of El Niño on the foraging behavior of female northern elephant seals. Mar. Ecol. Prog. Ser. 309, 1–10. doi:10.3354/meps309001

Crocker, D.E., Le Boeuf, B.J., Costa, D.P., 1997. Drift diving in female northern elephant seals: Implications for food processing. Can. J. Zool. 75, 27–39. doi:10.1016/j.dnarep.2015.02.007

Cummins, P.F., Freeland, H.J., 2007. Variability of the North Pacific Current and its

    bifurcation. Prog. Oceanogr. 75, 253–265. doi:10.1016/j.pocean.2007.08.006

Dinniman, M.S., Rienecker, M.M., 1999. Frontogenesis in the North Pacific Oceanic

    Frontal Zones—A Numerical Simulation. J. Phys. Oceanogr. 29, 537–559.

    doi:10.1175/1520-0485(1999)029<0537:fitnpo>2.0.co;2

Dragon, A.C., Monestiez, P., Bar-Hen, A., Guinet, C., 2010. Linking foraging

    behaviour to physical oceanographic structures: Southern elephant seals and

    mesoscale eddies east of Kerguelen Islands. Prog. Oceanogr. 87, 61–71.

    doi:10.1016/j.pocean.2010.09.025

Ducatez, S., Dalloyau, S., Richard, P., Guinet, C., Cherel, Y., 2008. Stable isotopes

    document winter trophic ecology and maternal investment of adult female

    southern elephant seals (Mirounga leonina) breeding at the Kerguelen Islands.

    Mar. Biol. 155, 413–420. doi:10.1007/s00227-008-1039-3

Emery, W.J., 2001. Water Types And Water Masses, in: Steele, J.H., Turekian, K.K.,

    Thorpe, S.A. (Eds.), Encyclopedia of Ocean Sciences. Acaemic Press, pp. 3179–

    3187. doi:10.1006/rwos.2001.0108

Field, I., Hindell, M.A., Slip, D., Michael, K., 2001. Foraging strategies of southern

    elephant seals (Mirounga leonina) in relation to frontal zones and water masses.

    Antarct. Sci. 13, 371–379. doi:10.1017/S0954102001000529

Fulton, T.L., Strobeck, C., 2010. Multiple fossil calibrations, nuclear loci and

mitochondrial genomes provide new insight into biogeography and divergence timing for true seals (Phocidae, Pinnipedia). J. Biogeogr. 37, 814–829. doi:10.1111/j.1365-2699.2010.02271.x

Goetsch, C., 2018. Illuminating the Twilight Zone: Diet and Foraging Strategies of a Deep-Sea Predator, the Northern Elephant Seal. University of California, Santa Cruz.

Goetsch, C., Conners, M.G., Budge, S.M., Mitani, Y., Walker, W.A., Bromaghin, J.F., Simmons, S.E., Reichmuth, C., Costa, D.P., 2018. Energy-rich mesopelagic fishes revealed as a critical prey resource for a deep-diving predator using Quantitative Fatty Acid Signature Analysis. Front. Mar. Sci. 5, 1–19. doi:10.3389/fmars.2018.00430

Gordine, S.A., Fedak, M.A., Boehme, L., 2019. The importance of Southern Ocean frontal systems for the improvement of body condition in southern elephant seals. Aquat. Conserv. Mar. Freshw. Ecosyst. 29, 283–304. doi:10.1002/aqc.3183

Green, D.B., Bestley, S., Trebilco, R., Corney, S.P., Lehodey, P., McMahon, C.R., Guinet, C., Hindell, M.A., 2020. Modelled mid-trophic pelagic prey fields improve understanding of marine predator foraging behaviour. Ecography (Cop.). 43, 1–13. doi:10.1111/ecog.04939

Guinet, C., Vacquie-Garcia, J., Picard, B., Bessigneul, G., Lebras, Y., Dragon, A.C., Viviant, M., Arnould, J.P.Y., Bailleul, F., 2014. Southern elephant seal foraging

success in relation to temperature and light conditions: Insight into prey
distribution. Mar. Ecol. Prog. Ser. 499, 285–301. doi:10.3354/meps10660

Harcourt, R., Sequeira, A.M.M., Zhang, X., Roquet, F., Komatsu, K., Heupel, M.,
McMahon, C., Whoriskey, F., Meekan, M., Carroll, G., Brodie, S.,
Simpfendorfer, C., Hindell, M., Jonsen, I., Costa, D.P., Block, B., Muelbert, M.,
Woodward, B., Weise, M., Aarestrup, K., Biuw, M., Boehme, L., Bograd, S.J.,
Cazau, D., Charrassin, J.-B., Cooke, S.J., Cowley, P., de Bruyn, P.J.N.,
Jeanniard du Dot, T., Duarte, C., Eguíluz, V.M., Ferreira, L.C., Fernández-
Gracia, J., Goetz, K., Goto, Y., Guinet, C., Hammill, M., Hays, G.C., Hazen,
E.L., Hückstädt, L.A., Huveneers, C., Iverson, S., Jaaman, S.A.,
Kittiwattanawong, K., Kovacs, K.M., Lydersen, C., Moltmann, T., Naruoka, M.,
Phillips, L., Picard, B., Queiroz, N., Reverdin, G., Sato, K., Sims, D.W.,
Thorstad, E.B., Thums, M., Treasure, A.M., Trites, A.W., Williams, G.D.,
Yonehara, Y., Fedak, M.A., 2019. Animal-Borne Telemetry: An Integral
Component of the Ocean Observing Toolkit. Front. Mar. Sci. 6.
doi:10.3389/fmars.2019.00326

Higdon, J.W., Bininda-Emonds, O.R.P., Beck, R.M.D., Ferguson, S.H., 2007.
Phylogeny and divergence of the pinnipeds (Carnivora: Mammalia) assessed
using a multigene dataset. BMC Evol. Biol. 7. doi:10.1186/1471-2148-7-216

Hijmans, R.J., 2019. geosphere: Spherical Trigonometry.

Hindell, M.A., 2018. Elephant Seals: Mirounga angustirostris and M. leonina, in:

Encyclopedia of Marine Mammals. pp. 303–307. doi:10.1016/b978-0-12-804327-1.00115-1

Hindell, M.A., Burton, H.R., 1988. Seasonal Haul-Out Patterns of the Southern Elephant Seal (Mirounga leonina L.), at Macquarie Island. J. Mammal. 69, 81–88.

Hindell, M.A., Burton, H.R., Slip, D.J., 1991. Foraging areas of southern elephant seals, mirounga leonina, as inferred from water temperature data. Mar. Freshw. Res. 42, 115–128. doi:10.1071/MF9910115

Hindell, M.A., McMahon, C.R., Bester, M.N., Boehme, L., Costa, D., Fedak, M.A., Guinet, C., Herraiz-Borreguero, L., Harcourt, R.G., Huckstadt, L., Kovacs, K.M., Lydersen, C., McIntyre, T., Muelbert, M., Patterson, T., Roquet, F., Williams, G., Charrassin, J.B., 2016. Circumpolar habitat use in the southern elephant seal: Implications for foraging success and population trajectories. Ecosphere 7, 1–27. doi:10.1002/ecs2.1213

Hindell, M.A., McMahon, C.R., Jonsen, I., Harcourt, R., Arce, F., Guinet, C., 2021. Inter- and intrasex habitat partitioning in the highly dimorphic southern elephant seal. Ecol. Evol. 1–14. doi:10.1002/ece3.7147

Hindell, M.A., Sumner, M., Bestley, S., Wotherspoon, S., Harcourt, R.G., Lea, M.A., Alderman, R., McMahon, C.R., 2017. Decadal changes in habitat characteristics influence population trajectories of southern elephant seals. Glob. Chang. Biol. 23, 5136–5150. doi:10.1111/gcb.13776

Holser, R.R., 2020. A Top Predator in Hot Water: Effects of a Marine Heatwave on Foraging and Reproduction in the Northern Elephant Seal. University of California, Santa Cruz.

Holser, R.R., Keates, T.R., Costa, D.P., Edwards, C.A., 2022. Extent and Magnitude of Subsurface Anomalies During the Northeast Pacific Blob as Measured by Animal-Borne Sensors. J. Geophys. Res. Ocean. 127. doi:10.1029/2021JC018356

Holte, J., Talley, L., 2009. A new algorithm for finding mixed layer depths with applications to Argo data and Subantarctic Mode Water formation. J. Atmos. Ocean. Technol. 26, 1920–1939. doi:10.1175/2009JTECHO543.1

Hückstädt, L.A., Reisinger, R.R., 2022. Habitat Utilization and Behavior of Phocid Seals in Relation to Oceanography, in: Costa, D.P., Mchuron, E.A. (Eds.), Ethology and Behavioral Ecology of Phocids. Springer International Publishing, pp. 127–178. doi:10.1007/978-3-030-88923-4

Irigoien, X., Klevjer, T.A., Røstad, A., Martinez, U., Boyra, G., Acuña, J.L., Bode, A., Echevarria, F., Gonzalez-Gordillo, J.I., Hernandez-Leon, S., Agusti, S., Aksnes, D.L., Duarte, C.M., Kaartvedt, S., 2014. Large mesopelagic fishes biomass and trophic efficiency in the open ocean. Nat. Commun. 5, 3271. doi:10.1038/ncomms4271

Jonsen, I.D., McMahon, C.R., Patterson, T.A., Auger-Méthé, M., Harcourt, R., Hindell, M.A., Bestley, S., 2019. Movement responses to environment: fast

inference of variation among southern elephant seals with a mixed effects model. Ecology 100, 1–8. doi:10.1002/ecy.2566

Jonsen, I.D., Patterson, T.A., 2020. foieGras: fit latent variable movement models to animal tracking data for location quality control and behavioural inference. Zenodo. doi:10.5281/zenodo.3899972

Jonsen, I.D., Patterson, T.A., Costa, D.P., Doherty, P.D., Godley, B.J., Grecian, W.J., Guinet, C., Hoenner, X., Kienle, S.S., Robinson, P.W., Votier, S.C., Witt, M.J., Hindell, M.A., Harcourt, R.G., McMahon, C.R., 2020. A continuous-time state-space model for rapid quality-control of Argos locations from animal-borne tags. Mov. Ecol. 8. doi:10.1186/s40462-020-00217-7

Jouma'a, J., Le Bras, Y., Richard, G., Vacquié-Garcia, J., Picard, B., El Ksabi, N., Guinet, C., 2016. Adjustment of diving behaviour with prey encounters and body condition in a deep diving predator: The Southern Elephant Seal. Funct. Ecol. 30, 636–648. doi:10.1111/1365-2435.12514

Kazmin, A.S., Rienecker, M.M., 1996. Variability and frontogenesis in the large-scale oceanic frontal zones. J. Geophys. Res. C Ocean. 101, 907–921. doi:10.1029/95JC02992

Keates, T.R., Hazen, E.L., Holser, R.R., Fiechter, J., Bograd, S.J., Robinson, P.W., Gallo-reynoso, J.P., Costa, D.P., 2022. Foraging behavior of a mesopelagic predator, the northern elephant seal, in northeastern Pacific eddies. Deep. Res. Part I 189, 103866. doi:10.1016/j.dsr.2022.103866

Kienle, S.S., 2019. Intraspecific variation and behavioral flexibility in the foraging

   strategies of seals. University Of California Santa Cruz.

Kienle, S.S., Friedlaender, A.S., Crocker, D.E., Mehta, R.S., Costa, D.P., 2022.

   Trade-offs between foraging reward and mortality risk drive sex-specific

   foraging strategies in sexually dimorphic northern elephant seals. R. Soc. Open

   Sci. 9. doi:10.1098/rsos.210522

Le Boeuf, B.J., Crocker, D.E., Costa, D.P., Blackwell, S.B., Webb, P.M., Houser,

   D.S., 2000. Foraging ecology of northern elephant seals. Ecol. Monogr. 70, 353–

   382. doi:10.1890/0012-9615(2000)070[0353:FEONES]2.0.CO;2

Le Boeuf, B.J., Laws, R.M. (Eds.), 1994. Elephant seals: population ecology,

   behavior, and physiology. . University of California Press, Berkeley.

Massie, P.P., McIntyre, T., Ryan, P.G., Bester, M.N., Bornemann, H., Ansorge, I.J.,

   2016. The role of eddies in the diving behaviour of female southern elephant

   seals. Polar Biol. 39, 297–307. doi:10.1007/s00300-015-1782-0

McDougall, T.J., Barker, P.M., 2011. Getting started with TEOS-10 and the Gibbs

   Seawater (GSW) Oceanographic Toolbox. SCOR/IAPSO WG127.

McHuron, E.A., Holser, R.R., Costa, D.P., 2019. What's in a whisker? Disentangling

   ecological and physiological isotopic signals. Rapid Commun. Mass Spectrom.

   33, 57–66. doi:10.1002/rcm.8312

McIntyre, T., Ansorge, I.J., Bornemann, H., Plötz, J., Tosh, C.A., Bester, M.N., 2011.

Elephant seal dive behaviour is influenced by ocean temperature: Implications for climate change impacts on an ocean predator. Mar. Ecol. Prog. Ser. 441, 257–272. doi:10.3354/meps09383

McIntyre, T., de Bruyn, P.J.N., Ansorge, I.J., Bester, M.N., Bornemann, H., Plötz, J., Tosh, C.A., 2010. A lifetime at depth: Vertical distribution of southern elephant seals in the water column. Polar Biol. 33, 1037–1048. doi:10.1007/s00300-010-0782-3

McMahon, C.R., Hindell, M.A., Charrassin, J.-B., Corney, S., Guinet, C., Harcourt, R., Jonsen, I., Trebilco, R., Williams, G., Bestley, S., 2019. Finding mesopelagic prey in a changing Southern Ocean. Sci. Rep. 9, 1–11. doi:10.1038/s41598-019-55152-4

McMahon, C.R., Roquet, F., Baudel, S., Belbeoch, M., Bestley, S., Blight, C., Boehme, L., Carse, F., Costa, D.P., Fedak, M.A., Guinet, C., Harcourt, R., Heslop, E., Hindell, M.A., Hoenner, X., Holland, K., Holland, M., Jaine, F.R.A., du Dot, T., Jonsen, I., Keates, T.R., Kovacs, K.M., Labrousse, S., Lovell, P., Lydersen, C., March, D., Mazloff, M., McKinzie, M.K., Muelbert, M.M.C., O'Brien, K., Phillips, L., Portela, E., Pye, J., Rintoul, S., Sato, K., Sequeira, A.M.M., Simmons, S.E., Tsontos, V.M., Turpin, V., van Wijk, E., Vo, D., Wege, M., Whoriskey, F.G., Wilson, K., Woodward, B., 2021. Animal Borne Ocean Sensors – AniBOS – An Essential Component of the Global Ocean Observing System. Front. Mar. Sci. 8, 1625. doi:10.3389/fmars.2021.751840

Mensah, V., Roquet, F., Siegelman-Charbit, L., Picard, B., Pauthenet, E., Guinet, C., 2018. A correction for the thermal mass-induced errors of CTD tags mounted on marine mammals. J. Atmos. Ocean. Technol. 35, 1237–1252. doi:10.1175/JTECH-D-17-0141.1

Miller, P.I., Scales, K.L., Ingram, S.N., Southall, E.J., Sims, D.W., 2015. Basking sharks and oceanographic fronts: Quantifying associations in the north-east Atlantic. Funct. Ecol. 29, 1099–1109. doi:10.1111/1365-2435.12423

Naito, Y., Costa, D.P., Adachi, T., Robinson, P.W., Fowler, M., Takahashi, A., 2013. Unravelling the mysteries of a mesopelagic diet: A large apex predator specializes on small prey. Funct. Ecol. 27, 710–717. doi:10.1111/1365-2435.12083

Naito, Y., Costa, D.P., Adachi, T., Robinson, P.W., Peterson, S.H., Mitani, Y., Takahashi, A., 2017. Oxygen minimum zone: An important oceanographic habitat for deep-diving northern elephant seals , Mirounga angustirostris. Ecol. Evol. 1–12. doi:10.1002/ece3.3202

Newland, C., Field, I.C., Nichols, P.D., Bradshaw, C.J.A., Hindell, M.A., 2009. Blubber fatty acid profiles indicate dietary resource partitioning between adult and juvenile southern elephant seals. Mar. Ecol. Prog. Ser. 384, 303–312. doi:10.3354/meps08010

Nordstrom, C.A., Battaile, B.C., Cotté, C., Trites, A.W., 2013. Foraging habitats of lactating northern fur seals are structured by thermocline depths and

submesoscale fronts in the eastern Bering Sea. Deep. Res. Part II Top. Stud. Oceanogr. 88–89, 78–96. doi:10.1016/j.dsr2.2012.07.010

O'Toole, M.D., Lea, M.-A., Guinet, C., Schick, R., Hindell, M. a., 2015. Foraging strategy switch of a top marine predator according to seasonal resource differences. Front. Mar. Sci. 2, 1–10. doi:10.3389/fmars.2015.00021

Ohman, M.D., Romagnan, J.B., 2016. Nonlinear effects of body size and optical attenuation on Diel Vertical Migration by zooplankton. Limnol. Oceanogr. 61, 765–770. doi:10.1002/lno.10251

Olson, D., Hitchcock, G., Mariano, A., Ashjian, C., Peng, G., Nero, R., Podesta, G., 1994. Life on the Edge: Marine Life and Fronts. Oceanography 7, 52–60. doi:10.5670/oceanog.1994.03

Olson, D.B., 2002. Biophysical dynamics of ocean fronts, in: Robinson, A., McCarthy, J., Rothschild, B. (Eds.), The Sea. pp. 187–218.

Orsi, A.H., Whitworth, T., Nowlin, W.D., 1995. On the meridional extent and fronts of the Antarctic Circumpolar Current. Deep. Res. Part I 42, 641–673. doi:10.1016/0967-0637(95)00021-W

Padgham, M., Sumner, M.D., 2021. geodist: Fast, dependency-free geodesic distance calculations.

Pebesma, E., 2018. Simple features for R: Standardized support for spatial vector data. R J. 10, 439–446. doi:10.32614/rj-2018-009

Peterson, S.H., Ackerman, J.T., Costa, D.P., 2015. Marine foraging ecology

   influences mercury bioaccumulation in deep-diving northern elephant seals.

   Proc. R. Soc. B Biol. Sci. 282, 1–9. doi:10.1098/rspb.2015.0710

Photopoulou, T., Fedak, M.A., Matthiopoulos, J., Mcconnell, B., Lovell, P., 2015.

   The generalized data management and collection protocol for Conductivity-

   Temperature-Depth Satellite Relay Data Loggers. Anim. Biotelemetry.

   doi:10.1186/s40317-015-0053-8

Polovina, J.J., Howell, E., Kobayashi, D.R., Seki, M.P., 2001. The transition zone

   chlorophyll front, a dynamic global feature defining migration and forage habitat

   for marine resources. Prog. Oceanogr. 49, 469–483. doi:10.1016/S0079-

   6611(01)00036-2

Polovina, J.J., Howell, E.A., Kobayashi, D.R., Seki, M.P., 2017. The Transition Zone

   Chlorophyll Front updated: Advances from a decade of research. Prog.

   Oceanogr. 150, 79–85. doi:10.1016/j.pocean.2015.01.006

R Core Team, 2022. R: A language and environment for statistical computing.

Robinson, P.W., Costa, D.P., Crocker, D.E., Gallo-Reynoso, J.P., Champagne, C.D.,

   Fowler, M.A., Goetsch, C., Goetz, K.T., Hassrick, J.L., Hückstädt, L.A., Kuhn,

   C.E., Maresh, J.L., Maxwell, S.M., McDonald, B.I., Peterson, S.H., Simmons,

   S.E., Teutschel, N.M., Villegas-Amtmann, S., Yoda, K., 2012. Foraging

   behavior and success of a mesopelagic predator in the northeast Pacific Ocean:

   insights from a data-rich species, the northern elephant seal. PLoS One 7.

doi:10.1371/journal.pone.0036728

Robinson, P.W., Simmons, S.E., Crocker, D.E., Costa, D.P., 2010. Measurements of
foraging success in a highly pelagic marine predator, the northern elephant seal.
J. Anim. Ecol. 79, 1146–1156. doi:10.1111/j.1365-2656.2010.01735.x

Roden, G.I., 1991. Subarctic-subtropical transition zone of the North Pacific: Large-
scale aspects and mesoscale structure. NOAA Tech. Rep. NMFS 105, 1–38.

Roden, G.I., 1980. On the variability of surface temperature fronts in the western
Pacific as detected by satellite. J. Geophys. Res. 85, 2704–2710.
doi:10.1029/JC085iC05p02704

Roquet, F., Charrassin, J.B., Marchand, S., Boehme, L., Fedak, M., Reverdin, G.,
Guinet, C., 2011. Delayed-mode calibration of hydrographic data obtained from
animal-borne satellite relay data loggers. J. Atmos. Ocean. Technol. 28, 787–
801. doi:10.1175/2010JTECHO801.1

Roquet, F., Park, Y.H., Guinet, C., Bailleul, F., Charrassin, J.B., 2009. Observations
of the Fawn Trough Current over the Kerguelen Plateau from instrumented
elephant seals. J. Mar. Syst. 78, 377–393. doi:10.1016/j.jmarsys.2008.11.017

Roquet, F., Williams, G., Hindell, M.A., Harcourt, R., Mcmahon, C., Guinet, C.,
Charrassin, J., Reverdin, G., Boehme, L., Lovell, P., Fedak, M., 2014. A
Southern Indian Ocean database of hydrographic profiles obtained with
instrumented elephant seals. Sci. Data. doi:10.1038/sdata.2014.28

Roquet, F., Wunsch, C., Forget, G., Heimbach, P., Guinet, C., Reverdin, G.,
Charrassin, J.B., Bailleul, F., Costa, D.P., Huckstadt, L.A., Goetz, K.T., Kovacs,
K.M., Lydersen, C., Biuw, M., Nøst, O.A., Bornemann, H., Ploetz, J., Bester,
M.N., McIntyre, T., Muelbert, M.C., Hindell, M.A., McMahon, C.R., Williams,
G., Harcourt, R., Field, I.C., Chafik, L., Nicholls, K.W., Boehme, L., Fedak,
M.A., 2013. Estimates of the Southern Ocean general circulation improved by
animal-borne instruments. Geophys. Res. Lett. 40, 6176–6180.
doi:10.1002/2013GL058304

Schick, R.S., New, L.F., Thomas, L., Costa, D.P., Hindell, M.A., Mcmahon, C.R.,
Robinson, P.W., Simmons, S.E., Thums, M., Harwood, J., Clark, J.S., 2013.
Estimating resource acquisition and at-sea body condition of a marine predator.
J. Anim. Ecol. 82, 1300–1315. doi:10.1111/1365-2656.12102

Siegelman, L., Roquet, F., Mensah, V., Rivière, P., Pauthenet, E., Picard, B., Guinet,
C., 2019a. Correction and accuracy of high- and low-resolution CTD data from
animal-borne instruments. J. Atmos. Ocean. Technol. 36, 745–760.
doi:10.1175/JTECH-D-18-0170.1

Siegelman, L., Toole, M.O., Flexas, M., Rivière, P., Klein, P., 2019b. Submesoscale
ocean fronts act as biological hotspot for southern elephant seal. Sci. Rep. 9, 1–
13. doi:10.1038/s41598-019-42117-w

Simmons, S.E., Crocker, D.E., Hassrick, J.L., Kuhn, C.E., Robinson, P.W., Tremblay,
Y., Costa, D.P., 2010. Climate-scale hydrographic features related to foraging

success in a capital breeder, the northern elephant seal Mirounga angustirostris. Endanger. Species Res. 10, 233–243. doi:10.3354/esr00254

Simmons, S.E., Crocker, D.E., Kudela, R.M., Costa, D.P., 2007. Linking foraging behaviour of the northern elephant seal with oceanography and bathymetry at mesoscales. Mar. Ecol. Prog. Ser. 346, 265–275. doi:10.3354/meps07014

Smetacek, V., Nicol, S., 2005. Polar ocean ecosystems in a changing world. Nature 437, 362–368.

Snyder, S., Franks, P.J.S., Talley, L.D., Xu, Y., Kohin, S., 2017. Crossing the line: Tunas actively exploit submesoscale fronts to enhance foraging success. Limnol. Oceanogr. Lett. doi:10.1002/lol2.10049

Sokolov, S., Rintoul, S.R., 2009. Circumpolar structure and distribution of the antarctic circumpolar current fronts: 1. Mean circumpolar paths. J. Geophys. Res. Ocean. 114, 1–19. doi:10.1029/2008JC005108

Talley, L.D., Pickard, G.L., Emery, W.J., Swift, J.H., 2011. Descriptive Physical Oceanography: An Introduction, 6th ed.

Thompson, D., Fedak, M.A., 2001. How long should a dive last? A simple model of foraging decisions by breath-hold divers in a patchy environment. Anim. Behav. 61, 287–296. doi:10.1006/anbe.2000.1539

Thums, M., Bradshaw, C.J.A., Sumner, M.D., Horsburgh, J.M., Hindell, M.A., 2013. Depletion of deep marine food patches forces divers to give up early. J. Anim.

Ecol. 82, 72–83. doi:10.1111/j.1365-2656.2012.02021.x

Treasure, A., Roquet, F., Ansorge, I., Bester, M., Boehme, L., Bornemann, H., Charrassin, J.-B., Chevallier, D., Costa, D., Fedak, M., Guinet, C., Hammill, M., Harcourt, R., Hindell, M., Kovacs, K., Lea, M.-A., Lovell, P., Lowther, A., Lydersen, C., McIntyre, T., McMahon, C., Muelbert, M., Nicholls, K., Picard, B., Reverdin, G., Trites, A., Williams, G., de Bruyn, P.J.N., 2017. Marine Mammals Exploring the Oceans Pole to Pole: A Review of the MEOP Consortium. Oceanography 30, 132–138. doi:10.5670/oceanog.2017.234

White, W.B., Hasunuma, K., Solomon, H., 1978. Large-scale seasonal and secular variability of the subtropical front in the western North Pacific from 1954 to 1974. J. Geophys. Res. 83, 4531–4544. doi:10.1029/jc083ic09p04531

Wood, S.N., 2011. Fast stable restricted maximum likelihood and marginal likelihood estimation of semiparametric generalized linear models. J. R. Stat. Soc. Ser. B Stat. Methodol. 73, 3–36. doi:10.1111/j.1467-9868.2010.00749.x

Woodson, C.B., Litvin, S.Y., 2015. Ocean fronts drive marine fishery production and biogeochemical cycling. Proc. Natl. Acad. Sci. 112, 1710–1715. doi:10.1073/pnas.1417143112

Yoshino, K., Takahashi, A., Adachi, T., Costa, D.P., Robinson, P.W., Peterson, S.H., Hückstädt, L.A., Holser, R.R., Naito, Y., 2020. Acceleration-triggered animal-borne videos show a dominance of fish in the diet of female northern elephant seals. J. Exp. Biol. jeb.212936. doi:10.1242/jeb.212936

Zainuddin, M., Saitoh, K., Saitoh, S.I., 2008. Albacore (Thunnus alalunga) fishing

ground in relation to oceanographic conditions in the western North Pacific

Ocean using remotely sensed satellite data. Fish. Oceanogr. 17, 61–73.

doi:10.1111/j.1365-2419.2008.00461.x

Zhang, H.R., Wang, Y., Xiu, P., Chai, F., 2021. Modeling the seasonal variability of

phytoplankton in the subarctic northeast Pacific Ocean. Mar. Ecol. Prog. Ser.

680, 33–50. doi:10.3354/meps13914

Table 2.1. Covariates used in generalized additive mixed effects models. Temperature, salinity, and mixed layer depth were determined using *in situ* data from seal-borne instruments and additionally extracted from CMEMS Global Ocean Ensemble Physics Reanalysis from Copernicus (dataset ID GLOBAL_REANALYSIS_PHY_001_031, https://doi.org/10.48670/moi-00024).

Covariate Name	Units	Description
Season	Categorical	Which foraging trip a seal is on: post-breeding (PB) or post-molt (PM)
DayinTripPercent	%	Day in trip divided by the length of the trip, expressed as %
te(Latitude,Longitude)	Decimal Degrees	Tensor smooth on seals' geographical locations
SealID	Categorical	Unique identifier for seal trip
Colony	Categorical	Name of the location of tag deployment
SST	°C	Mean temperature in upper 10 m of water column
T_at_100m	°C	Temperature at 100 m from values interpolated to 1 m
T_at_200m	°C	Temperature at 200 m from values interpolated to 1 m
Surface_S	g/kg	Mean salinity in upper 10 m of water column
S_at_100m	g/kg	Salinity at 100 m from values interpolated to 1 m
S_at_200m	g/kg	Salinity at 200 m from values interpolated to 1 m
MLD	Meters	Mixed layer depth determined from density
SST_sd	°C	Standard deviation of sea surface temperature within spatiotemporal radius described in text
T_at_100m_sd	°C	Standard deviation of temperature at 100 m depth within spatiotemporal radius described in text
T_at_200m_sd	°C	Standard deviation of temperature at 200 m depth within spatiotemporal radius described in text
Surface_S_sd	g/kg	Standard deviation of sea surface salinity within spatiotemporal radius described in text
S_at_100m_sd	g/kg	Standard deviation of salinity at 100 m depth within spatiotemporal radius described in text
S_at_200m_sd	g/kg	Standard deviation of salinity at 200 m depth within spatiotemporal radius described in text
MLD_sd	Meters	Standard deviation of mixed layer depth within spatiotemporal radius described in text
Subregion	Categorical	Subregional designation of seals' location, detailed in "Subregions" section of Methods

Front	Categorical	Two-level categorical of whether "Subregion" is a frontal zone
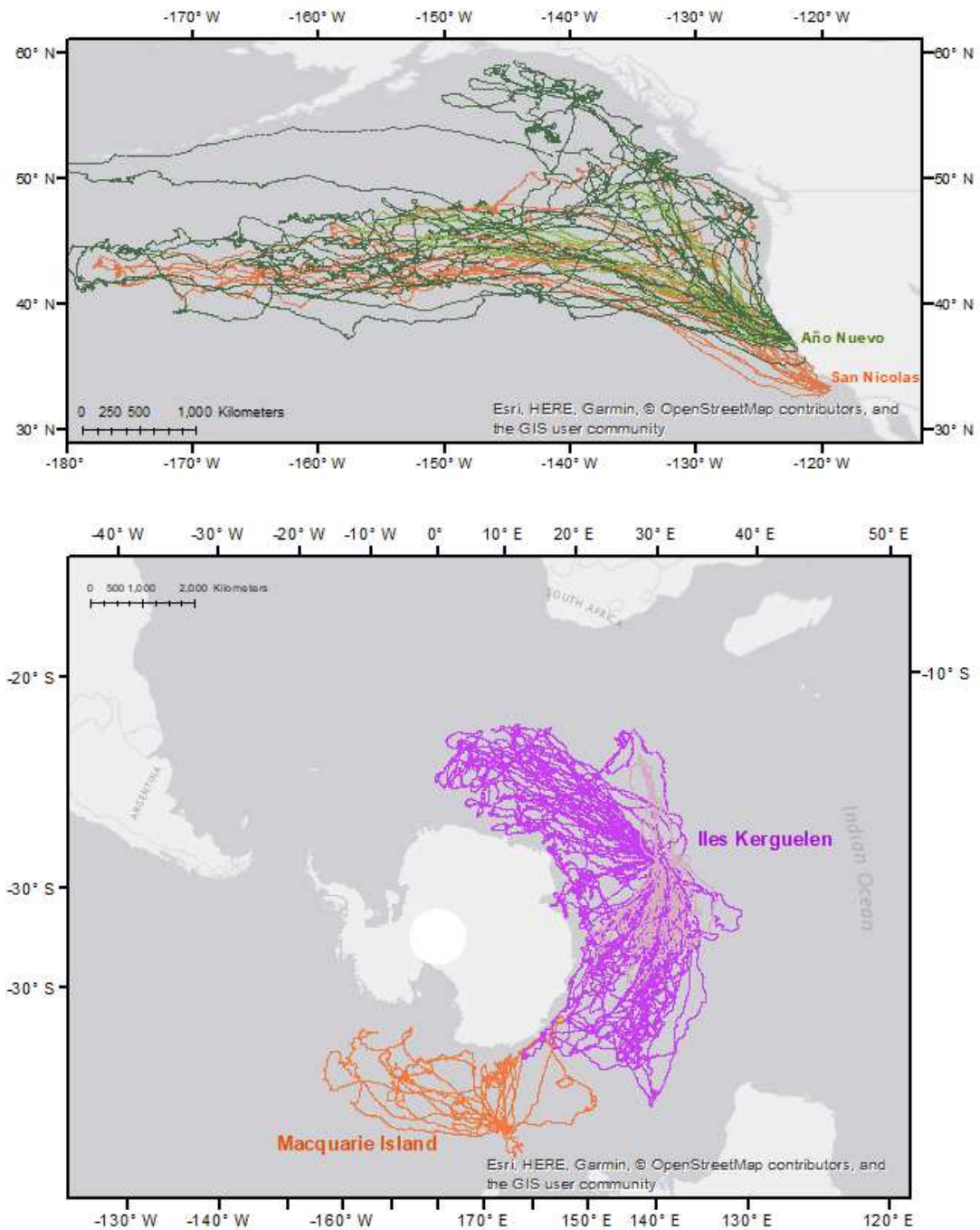
Figure 2.1. Map of NES (above) and SES tracks (below). Light colors are post-breeding (PB) trips, dark colors are post-molt (PM) trips. Seals from San Nicolas and Macquarie Islands were only tracked PM.

Table 2.2. Summary of elephant seal offshore foraging trips and diving behavior used in this study.

Colony	Season	N	Mean Trip Duration (days)	SD Trip Duration (days)	Mean Distance Travelled (km)	SD Distance Travelled (km)	Mean Max Distance from Colony (km)	SD Max Distance from Colony (km)	Latitude Range (°)	Longitude Range (°)	Mean Max Dive Depth (m)	SD Max Dive Depth (m)	Diel Dive Depth Difference (m)
Año Nuevo	PB	7	74	11	5278	1631	2252	579	14.61	35.10	514	36	81
Año Nuevo	PM	14	219	35	12228	1898	3575	955	22.62	61.95	436	53	102
San Nicolas	PM	7	226	4	11567	1029	3961	1195	18.32	58.31	478	28	119
Iles Kerguelen	PB	35	79	9	4324	1225	1418	615	14.30	34.20	458	90	116
Iles Kerguelen	PM	56	236	34	11806	4316	2954	1061	22.66	74.68	447	58	125
Macquarie Island	PM	10	246	17	9081	1057	2295	875	18.76	63.80	435	30	187

Table 2.3. The explanatory power contributed by intrinsic variables to transit rate. The full model contained all variables; subsequent models dropped one variable at a time. Deviance in R^2 and deviance explained are that of the reduced model subtracted from that of the full model. Day in the trip, normalized to trip length, contributed the most explanatory power. Species (NES or SES) added very little to the model.

Variable Dropped	Model R^2	Model Deviance Explained	Difference in R^2	Difference in deviance explained
Full Model	*0.4024*	*0.3740*	*NA*	*NA*
Species	0.4024	0.3740	0.0000	0.0000

Season	0.4023	0.3740	0.0001	0.0000
DayinTripPercent	0.2974	0.2735	0.1050	0.1006
te(Lat,Lon)	0.3630	0.3338	0.0394	0.0402
Colony	0.4024	0.3740	0.0000	0.0000
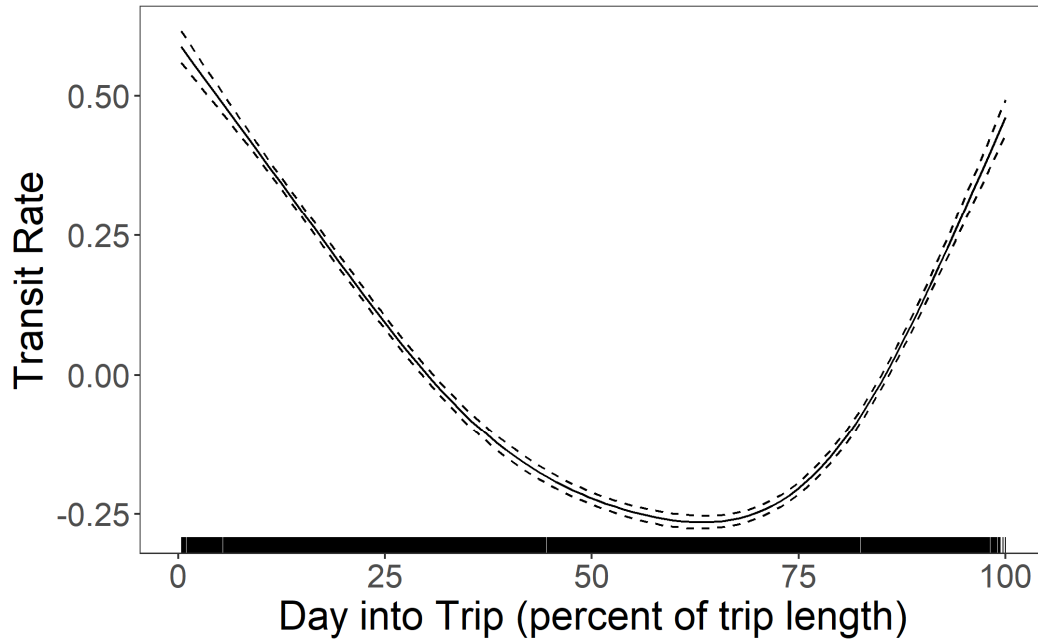
Figure 2.2. Smoother plot of trip timing influencing transit rate, in which transit rate is lowest near the middle of the trip.

Table 2.4. The explanatory power contributed by intrinsic variables to dive depth. The full model contained all variables; subsequent models dropped one variable at a time. Deviance in R^2 and deviance explained are that of the reduced model subtracted from that of the full model. As expected with diel patterns in dive depth, whether a dive occurred during the day or at night contributed the most explanatory power to the model. Species (NES or SES) added very little to the model.

Variable Dropped	Model R²	Model Deviance Explained	Difference in R²	Difference in deviance explained
Full Model	*0.5294*	*0.5160*	*NA*	*NA*
Species	0.5293	0.5160	0.0001	0.0000
Season	0.5294	0.5160	0.0000	0.0000
DayinTripPercent	0.4581	0.4441	0.0713	0.0719
te(Latitude,Longitude)	0.4883	0.4801	0.0411	0.0359
DayorNight	0.2898	0.2831	0.2396	0.2329
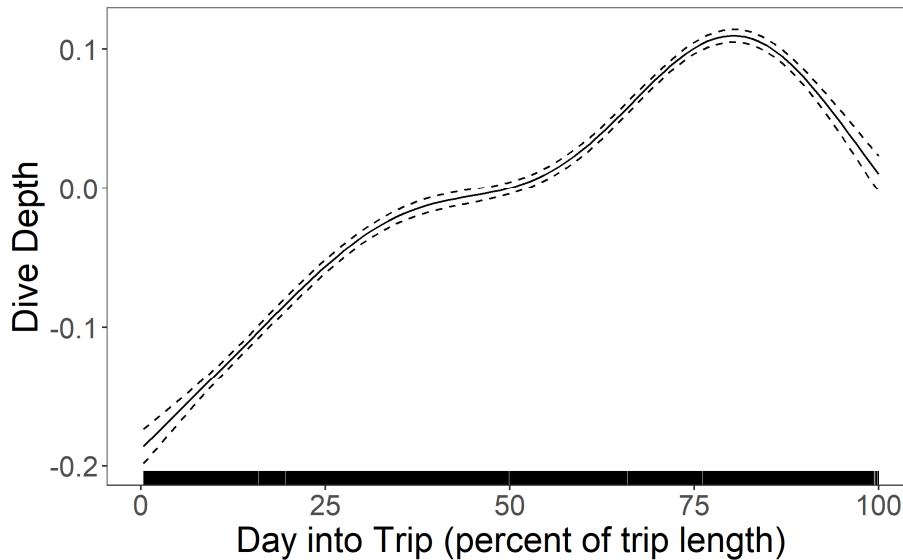
Figure 2.3. Smoother showing influence of timing within trip on dive depth (see Table 2.4).

Table 2.5. Summary of temperature, salinity, mixed layer depths, and bathymetric depth encountered by seals. Minima and maxima are 1st and 99th percentile, respectively.

Colony	Season	N	SST Min (°C)	SST Max (°C)	SST Range (°C)	Temperature Min (°C)	Temperature Max (°C)	Temperature Range (°C)	Salinity Min (g/kg)	Salinity Max (g/kg)	Salinity Range (g/kg)	Mean MLD (m)	SD MLD (m)	Mean Bathymetric Depth (m)
Año Nuevo	PB	7	6.32	14.91	1.79	3.19	15.06	11.88	32.32	34.64	2.33	53.9	8.6	3794
Año Nuevo	PM	14	5.29	22.46	2.62	2.84	22.57	19.73	31.49	34.69	3.20	34.3	8.1	4229
San Nicolas	PM	7	11.56	21.98	3.28	3.23	22.17	18.94	31.64	34.60	2.97	32.1	9.3	4379
Iles Kerguelen	PB	35	-1.71	11.52	-1.72	-1.75	11.76	13.51	33.63	35.18	1.56	61.5	17.8	2979
Iles Kerguelen	PM	56	-1.93	11.42	-0.20	-2.00	11.86	13.85	32.86	35.21	2.34	98.5	19.2	3483
Macquarie Island	PM	10	-1.97	8.69	7.12	-2.00	9.02	11.02	32.77	34.96	2.20	83.5	38.3	3540
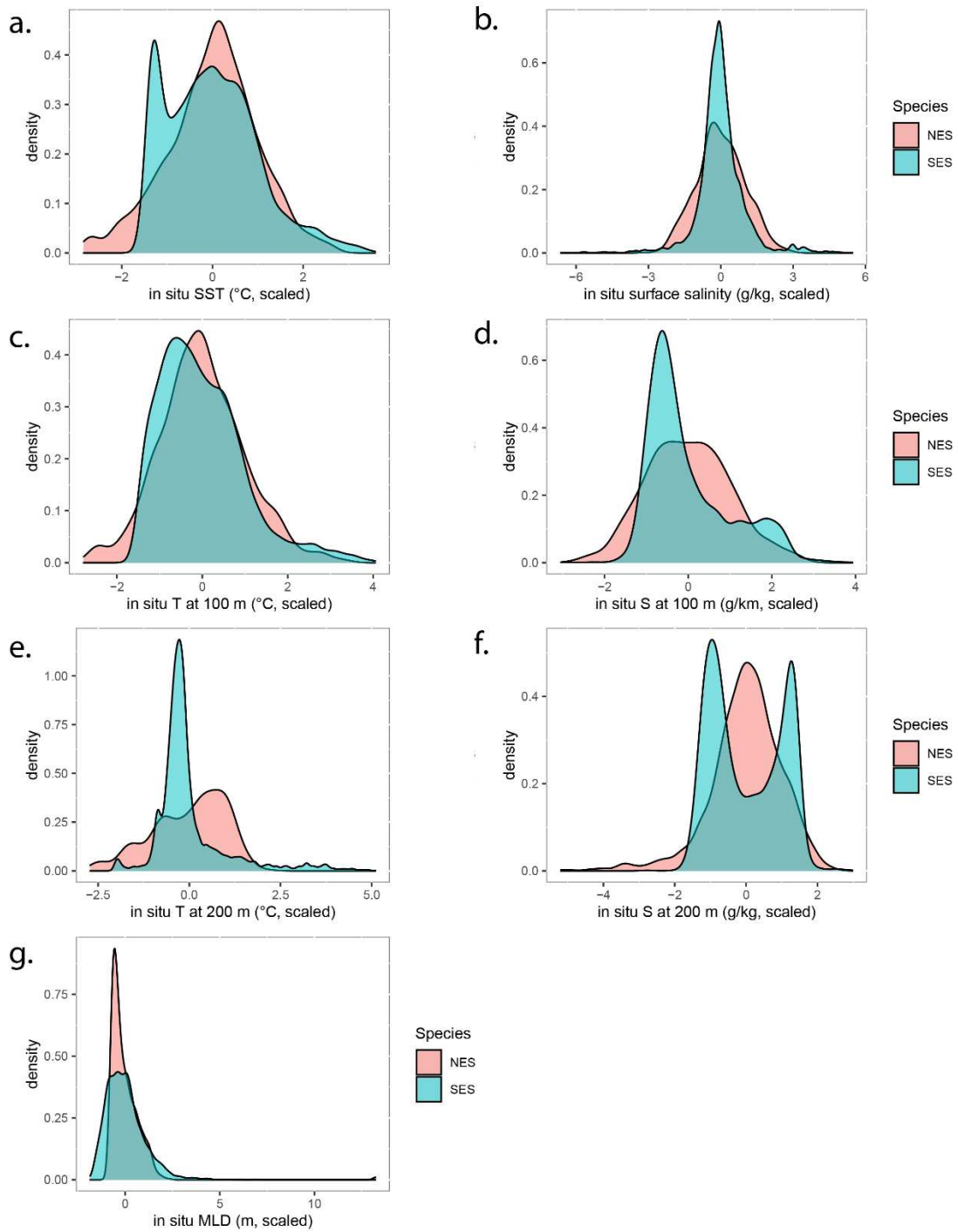
Figure 2.4. Density plots comparing scaled temperature and salinity at the surface, 100 m, and 200 m, and mixed layer depth measured *in situ* by instruments carried by NES and SES.
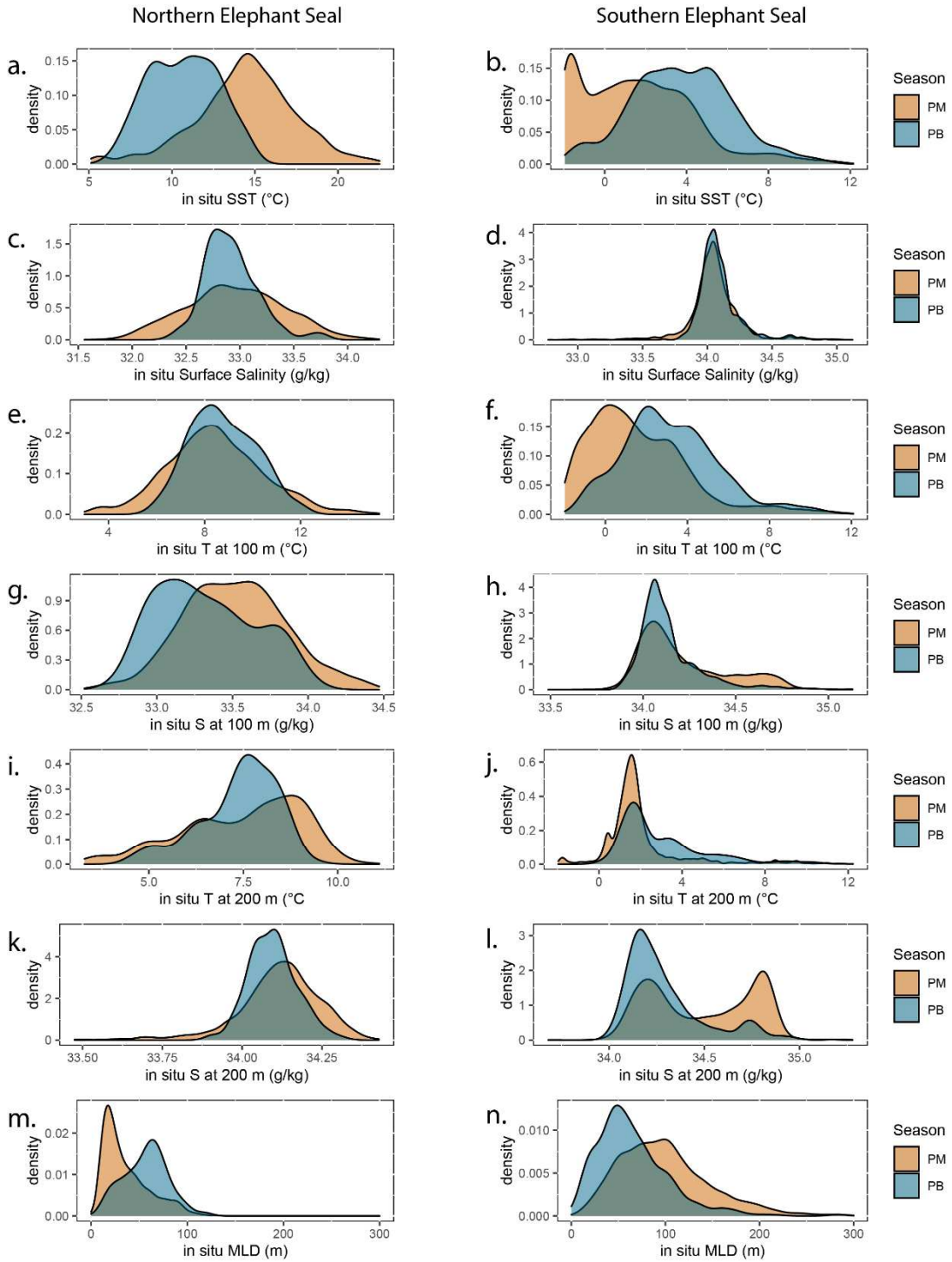
Figure 2.5. Density plots contrast seasonal distributions in oceanographic parameters measured by NES (left) and SES (right).

Table 2.6. "Species" term added no or < 1% explanatory power to models testing oceanographic influences on transit rate. T, S, and MLD were scaled to ocean basin. Blue indicates *in situ* covariates; green shows modeled data. Dark green is horizontal standard deviation of modeled data within 0.75° of mean seal location. Base model formula was gam(TransitRate ~ s(DayinTripPercent, k=6) + Season + te(Latitude,Longitude) + s(SealID,bs="re")

Oceanographic Covariate In Model	R² with "Species"	R² without "Species"	Difference in R² due to "Species"	% change in R²	Deviance Explained with "Species"	Deviance Explained without "Species"	Difference in Deviance Explained	% change in Deviance Explained
SST *in situ*	0.368	0.367	0.0003	0.0924	0.339	0.338	0.0003	0.0862
T at 100m *in situ*	0.367	0.367	0.0004	0.0961	0.338	0.338	0.0003	0.0798
T at 200m *in situ*	0.367	0.366	0.0005	0.1323	0.338	0.338	0.0004	0.1048
Surface S *in situ*	0.368	0.368	0.0003	0.0884	0.339	0.339	0.0003	0.0786
S at 100m *in situ*	0.367	0.367	0.0004	0.0965	0.338	0.338	0.0003	0.0865
S at 200m *in situ*	0.367	0.366	0.0003	0.0927	0.338	0.338	0.0003	0.0936
MLD (log) *in situ*	0.369	0.368	0.0004	0.1141	0.339	0.339	0.0003	0.1029
MLD (log) modeled	0.426	0.426	0.0000	-0.0016	0.393	0.393	0.0000	-0.0004
SST modeled	0.426	0.426	0.0000	-0.005	0.393	0.393	0.0000	-0.0018
T at 100m modeled	0.425	0.425	0.0000	0.0025	0.392	0.392	0.0000	0.0008

T at 200m modeled	0.424	0.424	0.0000	-0.0053	0.391	0.391	0.0000	-0.0025
Surface S modeled	0.428	0.428	0.0000	-0.0042	0.395	0.395	0.0000	0.0001
S at 100m modeled	0.426	0.426	0.0000	-0.005	0.393	0.393	0.0000	-0.0014
S at 200m modeled	0.428	0.428	0.0000	0.0013	0.395	0.395	0.0000	0.0058
SST sd modeled	0.426	0.426	0.0000	-0.0061	0.393	0.393	0.0000	-0.0028
T at 100m sd Modeled	0.426	0.426	0.0000	-0.0053	0.393	0.393	0.0000	-0.0022
T at 200m sd Modeled	0.425	0.425	0.0000	-0.0055	0.392	0.392	0.0000	-0.0026
Surface S sd modeled	0.424	0.425	-0.0008	-0.1793	0.391	0.392	-0.0007	-0.1897
S at 100m sd Modeled	0.426	0.426	0.0000	-0.0009	0.394	0.394	0.0000	0.0013
S at 200m sd Modeled	0.426	0.426	0.0000	-0.0054	0.393	0.393	0.0000	-0.0017
MLD sd modeled	0.425	0.425	0.0000	-0.0035	0.392	0.392	0.0000	-0.0026
Front	0.403	0.402	0.0007	0.1684	0.375	0.374	0.0004	0.1081

Table 2.7. "Species" term added no or >1% explanatory power to models testing oceanographic influences on dive depth. T, S, and MLD were scaled to ocean basin. Blue indicates *in situ* covariates; green shows modeled data. Dark green is horizontal standard deviation of modeled data within 0.75° of mean seal location. Base model formula was gam(DiveDepth ~ s(DayinTripPercent, k=6) + Season + DayorNight + te(Latitude,Longitude) + s(SealID,bs="re")

Oceanographic Covariate In Model	R² with "Species"	R² without "Species"	Difference in R² due to "Species"	% change in R²	Deviance Explained with "Species"	Deviance Explained without "Species"	Difference in Deviance Explained	% change in Deviance Explained
SST *in situ*	0.537	0.537	-0.0001	-0.0117	0.526	0.526	0.0000	-0.0009
T at 100m *in situ*	0.536	0.536	-0.0001	-0.0102	0.523	0.523	0.0000	-0.0010
T at 200m *in situ*	0.535	0.535	-0.0001	-0.0125	0.522	0.522	0.0000	-0.0010
Surface Salinity *in situ*	0.538	0.538	-0.0001	-0.0138	0.525	0.525	0.0000	-0.0010
S at 100m *in situ*	0.536	0.536	-0.0001	-0.0160	0.523	0.523	0.0000	-0.0007
S at 200m *in situ*	0.534	0.534	-0.0001	-0.0164	0.522	0.522	0.0000	-0.0004
MLD (log) *in situ*	0.535	0.535	-0.0001	-0.0129	0.523	0.523	0.0000	-0.0002
MLD (log) modeled	0.524	0.524	0.0000	0.0067	0.510	0.510	0.0003	0.0652
SST modeled	0.527	0.527	0.0000	-0.0058	0.515	0.515	0.0000	-0.0031
T at 100m modeled	0.527	0.527	-0.0001	-0.0193	0.514	0.513	0.0004	0.0843
T at 200m modeled	0.525	0.525	0.0000	-0.0045	0.512	0.512	0.0000	-0.0030
Surface S modeled	0.523	0.524	0.0000	-0.0023	0.511	0.511	0.0000	-0.0037
S at 100m modeled	0.522	0.522	0.0000	-0.0019	0.509	0.509	0.0000	-0.0031
S at 200m modeled	0.522	0.522	0.0000	-0.0021	0.508	0.508	0.0004	0.0819

	Model R^2	R^2 reduced model	Difference in R^2	% change in R^2	Model Deviance Explained	Deviance Explained Reduced Model	Difference in Deviance Explained	% change in Deviance Explained
SST sd modeled	0.521	0.521	0.0000	-0.0012	0.508	0.508	0.0000	-0.0033
T at 100m sd Modeled	0.521	0.521	0.0000	-0.0065	0.508	0.508	0.0000	-0.0018
T at 200m sd Modeled	0.521	0.521	0.0000	-0.0018	0.508	0.508	0.0000	-0.0027
Surface S sd modeled	0.521	0.521	0.0000	-0.0012	0.508	0.508	0.0000	-0.0031
S at 100m sd Modeled	0.522	0.522	0.0000	-0.0018	0.509	0.509	0.0000	-0.0032
S at 200m sd Modeled	0.521	0.521	0.0000	-0.0017	0.508	0.508	0.0000	-0.0030
MLD sd modeled	0.521	0.521	0.0000	-0.0050	0.508	0.508	0.0000	-0.0010

Table 2.8. Explanatory power contributed by oceanographic covariates to seal transit rate at a 3-day timescale. T, S, and MLD were scaled to ocean basin. Blue indicates *in situ* covariates; green shows modeled data. Dark colors are horizontal standard deviation of measurements; these were calculated using all data from 3 days for *in situ* data and within 0.75° of mean seal location for modeled data. Base model formula was gam(TransitRate ~ s(DayinTripPercent, k=6) + te(Latitude, Longitude) + s(SealID,bs="re").

Species	Season	Covariate Added	Model R^2	R^2 reduced model	Difference in R^2	% change in R^2	Model Deviance Explained	Deviance Explained Reduced Model	Difference in Deviance Explained	% change in Deviance Explained
NES	PB	SST *in situ*	0.803	0.720	0.084	10.39	0.815	0.738	0.078	9.54
NES	PB	T at 100m *in situ*	0.795	0.720	0.075	9.45	0.815	0.738	0.077	9.43
NES	PB	T at 200m *in situ*	0.804	0.720	0.084	10.45	0.821	0.738	0.083	10.1
NES	PB	Surface S *in situ*	0.832	0.720	0.112	13.51	0.841	0.738	0.104	12.31

NES	PB	S at 100m *in situ*	0.794	0.720	0.074	9.31	0.806	0.738	0.068	8.42
NES	PB	S at 200m *in situ*	0.816	0.720	0.096	11.76	0.827	0.738	0.090	10.85
NES	PB	MLD *in situ*	0.804	0.720	0.084	10.44	0.818	0.738	0.080	9.8
NES	PB	SST modeled	0.720	0.720	0.000	0.06	0.741	0.738	0.003	0.43
NES	PB	T at 100m modeled	0.715	0.720	-0.005	-0.67	0.737	0.738	-0.001	-0.07
NES	PB	T at 200m modeled	0.722	0.720	0.002	0.23	0.740	0.738	0.003	0.38
NES	PB	Surface S modeled	0.718	0.720	-0.002	-0.27	0.740	0.738	0.003	0.38
NES	PB	S at 100m modeled	0.722	0.720	0.002	0.23	0.737	0.738	0.000	-0.03
NES	PB	S at 200m modeled	0.725	0.720	0.005	0.66	0.743	0.738	0.005	0.69
NES	PB	MLD modeled	0.727	0.720	0.008	1.04	0.745	0.738	0.007	0.99
NES	PB	SST sd *In situ*	0.807	0.720	0.088	10.83	0.821	0.738	0.084	10.18
NES	PB	T at 100m sd *In situ*	0.789	0.720	0.069	8.78	0.805	0.738	0.067	8.37
NES	PB	T at 200m sd *In situ*	0.817	0.720	0.097	11.92	0.835	0.738	0.098	11.67
NES	PB	Surface S sd *in situ*	0.811	0.720	0.091	11.24	0.826	0.738	0.088	10.66
NES	PB	S at 100m sd *in situ*	0.820	0.720	0.100	12.22	0.834	0.738	0.096	11.54
NES	PB	S at 200m sd *in situ*	0.806	0.720	0.086	10.71	0.816	0.738	0.079	9.62
NES	PB	MLD sd *in situ*	0.791	0.720	0.071	8.95	0.803	0.738	0.066	8.18
NES	PB	SST sd *In situ*	0.715	0.720	-0.005	-0.68	0.731	0.738	-0.006	-0.86
NES	PB	SST sd	0.713	0.720	-0.006	-0.9	0.729	0.738	-0.009	-1.21

		Modeled								
NES	PB	T at 100m sd Modeled	0.719	0.720	-0.001	-0.18	0.739	0.738	0.001	0.12
NES	PB	T at 200m sd Modeled	0.718	0.720	-0.002	-0.29	0.733	0.738	-0.005	-0.68
NES	PB	Surface S sd Modeled	0.715	0.720	-0.005	-0.66	0.741	0.738	0.003	0.41
NES	PB	S at 100m sd Modeled	0.717	0.720	-0.003	-0.4	0.731	0.738	-0.007	-0.94
NES	PB	S at 200m sd Modeled	0.754	0.720	0.034	4.53	0.773	0.738	0.036	4.61
NES	PB	Front	0.718	0.720	-0.002	-0.24	0.739	0.738	0.002	0.24
NES	PB	Subregion	0.712	0.720	-0.008	-1.17	0.734	0.738	-0.004	-0.49
NES	PM	SST *in situ*	0.518	0.562	-0.044	-8.52	0.497	0.542	-0.045	-9
NES	PM	T at 100m *in situ*	0.519	0.562	-0.043	-8.19	0.499	0.542	-0.043	-8.6
NES	PM	T at 200m *in situ*	0.523	0.562	-0.039	-7.4	0.503	0.542	-0.039	-7.79
NES	PM	Surface S *in situ*	0.523	0.562	-0.039	-7.45	0.503	0.542	-0.039	-7.69
NES	PM	S at 100m *in situ*	0.536	0.562	-0.026	-4.78	0.519	0.542	-0.023	-4.51
NES	PM	S at 200m *in situ*	0.524	0.562	-0.038	-7.17	0.505	0.542	-0.037	-7.37
NES	PM	MLD *in situ*	0.514	0.562	-0.048	-9.3	0.496	0.542	-0.046	-9.25
NES	PM	SST modeled	0.565	0.562	0.003	0.6	0.546	0.542	0.004	0.73
NES	PM	T at 100m modeled	0.563	0.562	0.001	0.25	0.548	0.542	0.005	0.99
NES	PM	T at 200m modeled	0.568	0.562	0.006	1.05	0.553	0.542	0.011	1.9
NES	PM	Surface S modeled	0.576	0.562	0.014	2.48	0.559	0.542	0.017	3.03
NES	PM	S at 100m modeled	0.573	0.562	0.011	1.9	0.559	0.542	0.017	3.05

NES	PM	S at 200m modeled	0.572	0.562	0.010	1.78	0.556	0.542	0.013	2.41
NES	PM	MLD modeled	0.574	0.562	0.013	2.22	0.559	0.542	0.017	3.05
NES	PM	SST sd *In situ*	0.521	0.562	-0.040	-7.76	0.500	0.542	-0.042	-8.43
NES	PM	T at 100m sd *In situ*	0.524	0.562	-0.038	-7.15	0.505	0.542	-0.037	-7.39
NES	PM	T at 200m sd *In situ*	0.524	0.562	-0.038	-7.18	0.504	0.542	-0.039	-7.66
NES	PM	Surface S sd *in situ*	0.520	0.562	-0.042	-7.99	0.500	0.542	-0.042	-8.38
NES	PM	S at 100m sd *in situ*	0.525	0.562	-0.037	-7.01	0.504	0.542	-0.038	-7.46
NES	PM	S at 200m sd *in situ*	0.522	0.562	-0.039	-7.54	0.503	0.542	-0.039	-7.68
NES	PM	MLD sd *in situ*	0.511	0.562	-0.050	-9.84	0.494	0.542	-0.048	-9.68
NES	PM	SST sd Modeled	0.570	0.562	0.009	1.52	0.553	0.542	0.011	2.04
NES	PM	T at 100m sd Modeled	0.571	0.562	0.009	1.58	0.555	0.542	0.013	2.33
NES	PM	T at 200m sd Modeled	0.575	0.562	0.014	2.37	0.559	0.542	0.017	3
NES	PM	Surface S sd Modeled	0.570	0.562	0.009	1.51	0.553	0.542	0.011	1.96
NES	PM	S at 100m sd Modeled	0.570	0.562	0.008	1.47	0.553	0.542	0.011	1.92
NES	PM	S at 200m sd Modeled	0.577	0.562	0.015	2.6	0.565	0.542	0.023	4.02
NES	PM	MLD sd modeled	0.571	0.562	0.009	1.55	0.553	0.542	0.011	1.99
NES	PM	Front	0.566	0.562	0.004	0.7	0.546	0.542	0.004	0.8
NES	PM	Subregion	0.565	0.562	0.003	0.58	0.547	0.542	0.005	0.89
SES	PB	SST *in situ*	0.488	0.516	-0.028	-5.68	0.474	0.496	-0.023	-4.76
SES	PB	T at 100m	0.483	0.516	-0.033	-6.8	0.470	0.496	-0.027	-5.64

		in situ								
SES	PB	T at 200m *in situ*	0.485	0.516	-0.030	-6.23	0.472	0.496	-0.025	-5.19
SES	PB	Surface S *in situ*	0.479	0.516	-0.036	-7.59	0.466	0.496	-0.030	-6.39
SES	PB	S at 100m *in situ*	0.486	0.516	-0.029	-6.01	0.471	0.496	-0.025	-5.36
SES	PB	S at 200m *in situ*	0.486	0.516	-0.030	-6.11	0.469	0.496	-0.027	-5.74
SES	PB	MLD *in situ*	0.481	0.516	-0.035	-7.28	0.467	0.496	-0.029	-6.22
SES	PB	SST modeled	0.519	0.516	0.003	0.54	0.499	0.496	0.003	0.6
SES	PB	T at 100m modeled	0.521	0.516	0.006	1.11	0.500	0.496	0.004	0.87
SES	PB	T at 200m modeled	0.523	0.516	0.007	1.36	0.500	0.496	0.004	0.8
SES	PB	Surface S modeled	0.519	0.516	0.004	0.67	0.498	0.496	0.002	0.39
SES	PB	S at 100m modeled	0.520	0.516	0.005	0.9	0.499	0.496	0.003	0.6
SES	PB	S at 200m modeled	0.520	0.516	0.004	0.78	0.499	0.496	0.003	0.64
SES	PB	MLD modeled	0.520	0.516	0.004	0.81	0.501	0.496	0.005	0.96
SES	PB	SST sd *In situ*	0.485	0.516	-0.031	-6.34	0.470	0.496	-0.026	-5.58
SES	PB	T at 100m sd *In situ*	0.484	0.516	-0.032	-6.63	0.470	0.496	-0.027	-5.63
SES	PB	T at 200m sd *In situ*	0.483	0.516	-0.033	-6.75	0.469	0.496	-0.027	-5.66
SES	PB	Surface S sd *in situ*	0.484	0.516	-0.032	-6.6	0.469	0.496	-0.027	-5.72
SES	PB	S at 100m sd *in situ*	0.485	0.516	-0.031	-6.36	0.470	0.496	-0.026	-5.53
SES	PB	S at 200m sd *in situ*	0.485	0.516	-0.031	-6.31	0.471	0.496	-0.025	-5.35

SES	PB	MLD sd *in situ*	0.491	0.516	-0.025	-4.98	0.479	0.496	-0.018	-3.66
SES	PB	SST sd Modeled	0.520	0.516	0.004	0.79	0.499	0.496	0.003	0.67
SES	PB	T at 100m sd Modeled	0.521	0.516	0.005	0.99	0.500	0.496	0.004	0.87
SES	PB	T at 200m sd Modeled	0.525	0.516	0.009	1.69	0.504	0.496	0.008	1.51
SES	PB	Surface S sd Modeled	0.525	0.516	0.010	1.86	0.505	0.496	0.009	1.68
SES	PB	S at 100m sd Modeled	0.526	0.516	0.010	1.91	0.503	0.496	0.007	1.47
SES	PB	S at 200m sd Modeled	0.526	0.516	0.010	1.98	0.505	0.496	0.009	1.83
SES	PB	MLD sd modeled	0.519	0.516	0.004	0.71	0.498	0.496	0.002	0.4
SES	PB	Front	0.519	0.516	0.004	0.68	0.500	0.496	0.004	0.85
SES	PB	Subregion	0.520	0.516	0.005	0.88	0.506	0.496	0.010	1.96
SES	PM	SST *in situ*	0.459	0.480	-0.021	-4.65	0.447	0.467	-0.019	-4.32
SES	PM	T at 100m *in situ*	0.457	0.480	-0.023	-5.13	0.445	0.467	-0.022	-4.94
SES	PM	T at 200m *in situ*	0.456	0.480	-0.024	-5.26	0.444	0.467	-0.023	-5.11
SES	PM	Surface S *in situ*	0.459	0.480	-0.021	-4.53	0.446	0.467	-0.020	-4.56
SES	PM	S at 100m *in situ*	0.457	0.480	-0.023	-5.05	0.445	0.467	-0.022	-5.02
SES	PM	S at 200m *in situ*	0.458	0.480	-0.022	-4.76	0.446	0.467	-0.021	-4.69
SES	PM	MLD *in situ*	0.457	0.480	-0.023	-4.95	0.444	0.467	-0.023	-5.11
SES	PM	SST modeled	0.501	0.480	0.021	4.12	0.482	0.467	0.015	3.06
SES	PM	T at 100m modeled	0.500	0.480	0.020	3.93	0.480	0.467	0.013	2.66
SES	PM	T at 200m	0.500	0.480	0.020	3.92	0.480	0.467	0.013	2.68

		modeled								
SES	PM	Surface S modeled	0.506	0.480	0.026	5.05	0.484	0.467	0.017	3.54
SES	PM	S at 100m modeled	0.505	0.480	0.025	4.97	0.485	0.467	0.018	3.71
SES	PM	S at 200m modeled	0.512	0.480	0.032	6.2	0.490	0.467	0.023	4.75
SES	PM	MLD modeled	0.503	0.480	0.023	4.5	0.483	0.467	0.016	3.33
SES	PM	SST sd *In situ*	0.459	0.480	-0.021	-4.65	0.447	0.467	-0.020	-4.55
SES	PM	T at 100m sd *In situ*	0.457	0.480	-0.023	-5.04	0.444	0.467	-0.023	-5.19
SES	PM	T at 200m sd *In situ*	0.456	0.480	-0.024	-5.35	0.443	0.467	-0.024	-5.38
SES	PM	Surface S sd *in situ*	0.459	0.480	-0.021	-4.54	0.446	0.467	-0.021	-4.72
SES	PM	S at 100m sd *in situ*	0.456	0.480	-0.024	-5.24	0.443	0.467	-0.024	-5.32
SES	PM	S at 200m sd *in situ*	0.457	0.480	-0.023	-5.07	0.444	0.467	-0.023	-5.06
SES	PM	MLD sd *in situ*	0.462	0.480	-0.019	-4.01	0.448	0.467	-0.019	-4.32
SES	PM	SST sd Modeled	0.503	0.480	0.023	4.5	0.484	0.467	0.017	3.45
SES	PM	T at 100m sd Modeled	0.503	0.480	0.023	4.53	0.483	0.467	0.017	3.44
SES	PM	T at 200m sd Modeled	0.501	0.480	0.021	4.18	0.481	0.467	0.014	2.91
SES	PM	Surface S sd Modeled	0.504	0.480	0.024	4.81	0.483	0.467	0.017	3.44
SES	PM	S at 100m sd Modeled	0.503	0.480	0.023	4.5	0.484	0.467	0.017	3.47
SES	PM	S at 200m sd Modeled	0.501	0.480	0.021	4.1	0.481	0.467	0.014	2.9
SES	PM	MLD sd modeled	0.502	0.480	0.022	4.32	0.482	0.467	0.015	3.15

SES	PM	Front	0.480	0.480	0.000	-0.05	0.467	0.467	0.001	0.11
SES	PM	Subregion	0.485	0.480	0.005	0.95	0.471	0.467	0.004	0.85

Table 2.9. Explanatory power contributed by oceanographic covariates to seal dive depth at a 12-hour timescale. T, S, and MLD were scaled to ocean basin. Blue indicates *in situ* covariates; green shows modeled data. Dark green is horizontal standard deviation of measurements within 0.75° of mean seal location for modeled data. Note a standard deviation was not calculated from *in situ* data due to the low number of profiles collected in 12 hours. Base model formula was gam(DiveDepth ~ s(DayinTripPercent, k=6) + te(Latitude, Longitude) + s(SealID,bs="re").

Species	Season	Day or Night	Covariate Added	Model R^2	R^2 reduced model	Difference in R^2	% change in R^2	Model Deviance Explained	Deviance Explained Reduced Model	Difference in Deviance Explained	% change in Deviance Explained
NES	PB	Day	SST *in situ*	0.561	0.542	0.019	3.32	0.610	0.578	0.033	5.32
NES	PB	Day	T at 100m *in situ*	0.565	0.542	0.022	3.93	0.622	0.578	0.044	7.07
NES	PB	Day	T at 200m *in situ*	0.554	0.542	0.012	2.12	0.607	0.578	0.029	4.82
NES	PB	Day	Surface S *in situ*	0.585	0.542	0.043	7.32	0.652	0.578	0.074	11.36
NES	PB	Day	S at 100m *in situ*	0.568	0.542	0.025	4.45	0.623	0.578	0.045	7.18
NES	PB	Day	S at 200m *in situ*	0.560	0.542	0.017	3.07	0.612	0.578	0.034	5.52
NES	PB	Day	MLD (log)	0.581	0.542	0.038	6.58	0.632	0.578	0.054	8.55

			in situ								
NES	PB	Day	SST modeled	0.548	0.542	0.006	1.06	0.588	0.578	0.010	1.69
NES	PB	Day	T at 100m modeled	0.565	0.542	0.023	4.01	0.602	0.578	0.024	4.03
NES	PB	Day	T at 200m modeled	0.551	0.542	0.009	1.59	0.590	0.578	0.012	2.1
NES	PB	Day	Surface S modeled	0.541	0.542	-0.002	-0.31	0.578	0.578	0.000	0
NES	PB	Day	S at 100m modeled	0.546	0.542	0.004	0.71	0.583	0.578	0.005	0.91
NES	PB	Day	S at 200m modeled	0.556	0.542	0.013	2.4	0.594	0.578	0.016	2.69
NES	PB	Day	MLD modeled	0.565	0.542	0.023	4.04	0.593	0.578	0.015	2.56
NES	PB	Day	SST sd modeled	0.546	0.542	0.004	0.64	0.583	0.578	0.006	0.95
NES	PB	Day	T at 100m sd Modeled	0.544	0.542	0.002	0.3	0.582	0.578	0.004	0.74
NES	PB	Day	T at 200m sd Modeled	0.540	0.542	-0.002	-0.39	0.578	0.578	0.000	-0.01
NES	PB	Day	S at 100m sd Modeled	0.554	0.542	0.012	2.13	0.593	0.578	0.015	2.51
NES	PB	Day	S at 200m sd Modeled	0.541	0.542	-0.001	-0.21	0.579	0.578	0.001	0.18
NES	PB	Day	MLD sd Modeled	0.549	0.542	0.007	1.22	0.590	0.578	0.012	2.1
NES	PB	Day	Surface S sd modeled	0.542	0.542	-0.001	-0.15	0.580	0.578	0.002	0.38
NES	PB	Night	SST *in situ*	0.326	0.479	-0.153	-47.1	0.401	0.541	-0.140	-34.94
NES	PB	Night	T at 100m *in situ*	0.284	0.479	-0.195	-68.46	0.348	0.541	-0.193	-55.4

NES	PB	Night	T at 200m *in situ*	0.306	0.479	-0.173	-56.39	0.369	0.541	-0.172	-46.69
NES	PB	Night	Surface S *in situ*	0.303	0.479	-0.177	-58.31	0.363	0.541	-0.177	-48.86
NES	PB	Night	S at 100m *in situ*	0.272	0.479	-0.207	-76.03	0.334	0.541	-0.207	-61.9
NES	PB	Night	S at 200m *in situ*	0.325	0.479	-0.155	-47.62	0.373	0.541	-0.168	-45
NES	PB	Night	MLD (log) *in situ*	0.287	0.479	-0.192	-67.02	0.344	0.541	-0.197	-57.18
NES	PB	Night	SST modeled	0.492	0.479	0.013	2.55	0.555	0.541	0.014	2.51
NES	PB	Night	T at 100m modeled	0.496	0.479	0.017	3.44	0.545	0.541	0.005	0.89
NES	PB	Night	T at 200m modeled	0.503	0.479	0.024	4.69	0.542	0.541	0.002	0.35
NES	PB	Night	Surface S modeled	0.479	0.479	-0.001	-0.14	0.530	0.541	-0.010	-1.94
NES	PB	Night	S at 100m modeled	0.481	0.479	0.002	0.36	0.549	0.541	0.008	1.54
NES	PB	Night	S at 200m modeled	0.472	0.479	-0.007	-1.5	0.530	0.541	-0.011	-2.08
NES	PB	Night	MLD modeled	0.478	0.479	-0.002	-0.33	0.518	0.541	-0.022	-4.27
NES	PB	Night	SST sd modeled	0.491	0.479	0.012	2.41	0.555	0.541	0.015	2.61
NES	PB	Night	T at 100m sd Modeled	0.478	0.479	-0.001	-0.26	0.542	0.541	0.001	0.18
NES	PB	Night	T at 200m sd Modeled	0.478	0.479	-0.002	-0.34	0.541	0.541	0.001	0.12
NES	PB	Night	S at 100m sd Modeled	0.513	0.479	0.034	6.6	0.576	0.541	0.035	6.14
NES	PB	Night	S at 200m sd	0.479	0.479	-0.001	-0.1	0.543	0.541	0.002	0.42

			Modeled								
NES	PB	Night	MLD sd Modeled	0.478	0.479	-0.002	-0.35	0.541	0.541	0.000	0.02
NES	PB	Night	Surface S sd modeled	0.486	0.479	0.007	1.38	0.557	0.541	0.017	2.99
NES	PM	Day	SST *in situ*	0.571	0.544	0.026	4.61	0.579	0.537	0.042	7.31
NES	PM	Day	T at 100m *in situ*	0.564	0.544	0.019	3.44	0.572	0.537	0.035	6.2
NES	PM	Day	T at 200m *in situ*	0.565	0.544	0.021	3.68	0.572	0.537	0.036	6.27
NES	PM	Day	Surface S *in situ*	0.562	0.544	0.018	3.21	0.568	0.537	0.032	5.56
NES	PM	Day	S at 100m *in situ*	0.565	0.544	0.021	3.63	0.571	0.537	0.034	6.01
NES	PM	Day	S at 200m *in situ*	0.564	0.544	0.020	3.45	0.571	0.537	0.035	6.07
NES	PM	Day	MLD (log) *in situ*	0.565	0.544	0.020	3.58	0.571	0.537	0.034	5.98
NES	PM	Day	SST modeled	0.544	0.544	0.000	0.01	0.537	0.537	0.001	0.1
NES	PM	Day	T at 100m modeled	0.548	0.544	0.003	0.62	0.541	0.537	0.005	0.92
NES	PM	Day	T at 200m modeled	0.547	0.544	0.003	0.5	0.542	0.537	0.005	0.97
NES	PM	Day	Surface Salinity modeled	0.542	0.544	-0.002	-0.41	0.534	0.537	-0.003	-0.53
NES	PM	Day	S at 100m modeled	0.542	0.544	-0.002	-0.41	0.535	0.537	-0.002	-0.35
NES	PM	Day	S at 200m modeled	0.546	0.544	0.002	0.27	0.537	0.537	0.000	0.04
NES	PM	Day	MLD(log) modeled	0.542	0.544	-0.003	-0.47	0.534	0.537	-0.003	-0.47
NES	PM	Day	SST sd modeled	0.540	0.544	-0.004	-0.79	0.532	0.537	-0.004	-0.8
NES	PM	Day	T at 100m sd Modeled	0.543	0.544	-0.001	-0.17	0.535	0.537	-0.001	-0.26

NES	PM	Day	T at 200m sd Modeled	0.541	0.544	-0.004	-0.64	0.532	0.537	-0.005	-0.89
NES	PM	Day	S at 100m sd Modeled	0.541	0.544	-0.004	-0.66	0.532	0.537	-0.005	-0.86
NES	PM	Day	S at 200m sd Modeled	0.542	0.544	-0.002	-0.41	0.533	0.537	-0.003	-0.59
NES	PM	Day	MLD sd Modeled	0.540	0.544	-0.004	-0.8	0.531	0.537	-0.005	-1.01
NES	PM	Day	Surface S sd modeled	0.540	0.544	-0.005	-0.83	0.532	0.537	-0.005	-0.93
NES	PM	Night	SST *in situ*	0.414	0.340	0.075	18.02	0.426	0.336	0.090	21.18
NES	PM	Night	T at 100m *in situ*	0.387	0.340	0.047	12.16	0.396	0.336	0.060	15.07
NES	PM	Night	T at 200m *in situ*	0.393	0.340	0.053	13.5	0.401	0.336	0.065	16.18
NES	PM	Night	Surface S *in situ*	0.381	0.340	0.042	10.96	0.388	0.336	0.052	13.43
NES	PM	Night	S at 100m *in situ*	0.378	0.340	0.039	10.2	0.386	0.336	0.050	12.87
NES	PM	Night	S at 200m *in situ*	0.384	0.340	0.044	11.46	0.390	0.336	0.054	13.87
NES	PM	Night	MLD (log) *in situ*	0.377	0.340	0.038	9.95	0.384	0.336	0.048	12.52
NES	PM	Night	SST modeled	0.373	0.340	0.033	8.88	0.368	0.336	0.032	8.76
NES	PM	Night	T at 100m modeled	0.349	0.340	0.010	2.77	0.346	0.336	0.010	2.98
NES	PM	Night	T at 200m modeled	0.347	0.340	0.007	2.07	0.343	0.336	0.007	1.93
NES	PM	Night	Surface S modeled	0.346	0.340	0.006	1.75	0.343	0.336	0.007	2
NES	PM	Night	S at 100m	0.345	0.340	0.005	1.41	0.341	0.336	0.005	1.46

			modeled								
NES	PM	Night	S at 200m modeled	0.341	0.340	0.001	0.39	0.337	0.336	0.001	0.3
NES	PM	Night	MLD modeled	0.343	0.340	0.003	0.98	0.340	0.336	0.004	1.14
NES	PM	Night	SST sd modeled	0.341	0.340	0.001	0.38	0.340	0.336	0.003	1
NES	PM	Night	T at 100m sd Modeled	0.347	0.340	0.008	2.23	0.344	0.336	0.008	2.25
NES	PM	Night	T at 200m sd Modeled	0.343	0.340	0.003	0.93	0.340	0.336	0.004	1.09
NES	PM	Night	S at 100m sd Modeled	0.345	0.340	0.005	1.43	0.341	0.336	0.005	1.41
NES	PM	Night	S at 200m sd Modeled	0.343	0.340	0.003	1	0.340	0.336	0.004	1.04
NES	PM	Night	MLD sd Modeled	0.344	0.340	0.004	1.2	0.341	0.336	0.005	1.33
NES	PM	Night	Surface S sd modeled	0.341	0.340	0.001	0.25	0.337	0.336	0.001	0.25
SES	PB	Day	SST in situ	0.611	0.562	0.048	7.9	0.593	0.537	0.056	9.46
SES	PB	Day	T at 100m in situ	0.610	0.562	0.047	7.76	0.591	0.537	0.054	9.21
SES	PB	Day	T at 200m in situ	0.612	0.562	0.049	8.06	0.596	0.537	0.059	9.91
SES	PB	Day	Surface S in situ	0.608	0.562	0.045	7.45	0.590	0.537	0.053	9
SES	PB	Day	S at 100m in situ	0.610	0.562	0.048	7.8	0.592	0.537	0.055	9.25
SES	PB	Day	S at 200m in situ	0.610	0.562	0.048	7.87	0.593	0.537	0.056	9.5
SES	PB	Day	MLD (log) in situ	0.616	0.562	0.053	8.66	0.595	0.537	0.059	9.84
SES	PB	Day	SST	0.579	0.562	0.016	2.82	0.552	0.537	0.015	2.7

			modeled								
SES	PB	Day	T at 100m modeled	0.568	0.562	0.005	0.95	0.543	0.537	0.006	1.13
SES	PB	Day	T at 200m modeled	0.563	0.562	0.001	0.17	0.538	0.537	0.001	0.25
SES	PB	Day	Surface S modeled	0.563	0.562	0.000	0.05	0.539	0.537	0.002	0.42
SES	PB	Day	S at 100m modeled	0.565	0.562	0.003	0.54	0.539	0.537	0.003	0.48
SES	PB	Day	S at 200m modeled	0.567	0.562	0.004	0.75	0.542	0.537	0.005	0.87
SES	PB	Day	MLD modeled	0.567	0.562	0.005	0.84	0.545	0.537	0.008	1.43
SES	PB	Day	SST sd modeled	0.560	0.562	-0.002	-0.41	0.535	0.537	-0.002	-0.34
SES	PB	Day	T at 100m sd Modeled	0.560	0.562	-0.003	-0.47	0.535	0.537	-0.002	-0.35
SES	PB	Day	T at 200m sd Modeled	0.560	0.562	-0.003	-0.44	0.535	0.537	-0.002	-0.32
SES	PB	Day	S at 100m sd Modeled	0.561	0.562	-0.002	-0.29	0.536	0.537	-0.001	-0.18
SES	PB	Day	S at 200m sd Modeled	0.560	0.562	-0.002	-0.37	0.536	0.537	-0.001	-0.21
SES	PB	Day	MLD sd Modeled	0.561	0.562	-0.002	-0.28	0.536	0.537	-0.001	-0.21
SES	PB	Day	Surface S sd modeled	0.561	0.562	-0.002	-0.26	0.536	0.537	-0.001	-0.14
SES	PB	Night	SST in situ	0.537	0.525	0.011	2.06	0.584	0.540	0.044	7.49
SES	PB	Night	T at 100m in situ	0.535	0.525	0.010	1.78	0.582	0.540	0.042	7.28
SES	PB	Night	T at 200m in situ	0.534	0.525	0.009	1.61	0.582	0.540	0.042	7.21

SES	PB	Night	Surface S *in situ*	0.537	0.525	0.011	2.1	0.583	0.540	0.043	7.44
SES	PB	Night	S at 100m *in situ*	0.535	0.525	0.010	1.86	0.582	0.540	0.043	7.3
SES	PB	Night	S at 200m *in situ*	0.534	0.525	0.009	1.64	0.582	0.540	0.042	7.21
SES	PB	Night	MLD (log) *in situ*	0.536	0.525	0.011	2.01	0.584	0.540	0.044	7.48
SES	PB	Night	SST modeled	0.528	0.525	0.003	0.47	0.543	0.540	0.003	0.63
SES	PB	Night	T at 100m modeled	0.522	0.525	-0.004	-0.68	0.537	0.540	-0.003	-0.48
SES	PB	Night	T at 200m modeled	0.517	0.525	-0.008	-1.61	0.532	0.540	-0.009	-1.59
SES	PB	Night	Surface S modeled	0.531	0.525	0.006	1.05	0.547	0.540	0.007	1.32
SES	PB	Night	S at 100m modeled	0.518	0.525	-0.008	-1.49	0.531	0.540	-0.009	-1.74
SES	PB	Night	S at 200m modeled	0.531	0.525	0.005	0.97	0.544	0.540	0.004	0.67
SES	PB	Night	MLD modeled	0.528	0.525	0.003	0.48	0.545	0.540	0.005	0.96
SES	PB	Night	SST sd modeled	0.527	0.525	0.002	0.31	0.542	0.540	0.002	0.39
SES	PB	Night	T at 100m sd Modeled	0.527	0.525	0.002	0.36	0.543	0.540	0.003	0.48
SES	PB	Night	T at 200m sd Modeled	0.529	0.525	0.003	0.65	0.544	0.540	0.004	0.76
SES	PB	Night	S at 100m sd Modeled	0.517	0.525	-0.008	-1.55	0.531	0.540	-0.009	-1.62
SES	PB	Night	S at 200m sd Modeled	0.526	0.525	0.001	0.19	0.543	0.540	0.003	0.57
SES	PB	Night	MLD sd	0.526	0.525	0.000	0.02	0.541	0.540	0.001	0.15

			Modeled								
SES	PB	Night	Surface S sd modeled	0.527	0.525	0.002	0.37	0.542	0.540	0.002	0.33
SES	PM	Day	SST *in situ*	0.467	0.447	0.020	4.27	0.460	0.440	0.020	4.43
SES	PM	Day	T at 100m *in situ*	0.467	0.447	0.020	4.28	0.460	0.440	0.020	4.39
SES	PM	Day	T at 200m *in situ*	0.466	0.447	0.019	4.11	0.459	0.440	0.019	4.17
SES	PM	Day	Surface S *in situ*	0.470	0.447	0.023	4.92	0.462	0.440	0.023	4.87
SES	PM	Day	S at 100m *in situ*	0.467	0.447	0.020	4.25	0.459	0.440	0.020	4.26
SES	PM	Day	S at 200m *in situ*	0.465	0.447	0.018	3.82	0.458	0.440	0.018	3.99
SES	PM	Day	MLD (log) *in situ*	0.464	0.447	0.017	3.72	0.458	0.440	0.019	4.06
SES	PM	Day	SST modeled	0.445	0.447	-0.002	-0.52	0.436	0.440	-0.004	-0.88
SES	PM	Day	T at 100m modeled	0.445	0.447	-0.002	-0.53	0.433	0.440	-0.006	-1.46
SES	PM	Day	T at 200m modeled	0.447	0.447	0.000	-0.09	0.434	0.440	-0.005	-1.19
SES	PM	Day	Surface Salinity modeled	0.434	0.447	-0.013	-3.03	0.425	0.440	-0.015	-3.5
SES	PM	Day	S at 100m modeled	0.443	0.447	-0.004	-0.97	0.433	0.440	-0.007	-1.53
SES	PM	Day	S at 200m modeled	0.442	0.447	-0.005	-1.09	0.433	0.440	-0.007	-1.54
SES	PM	Day	MLD (log) modeled	0.438	0.447	-0.009	-2.06	0.430	0.440	-0.010	-2.29
SES	PM	Day	SST sd modeled	0.434	0.447	-0.013	-3.08	0.425	0.440	-0.015	-3.52
SES	PM	Day	T at 100m sd Modeled	0.436	0.447	-0.012	-2.65	0.426	0.440	-0.014	-3.21
SES	PM	Day	T at 200m sd	0.436	0.447	-0.011	-2.47	0.427	0.440	-0.013	-2.96

195

			Modeled									
SES	PM	Day	S at 100m sd Modeled	0.436	0.447	-0.011	-2.52	0.428	0.440	-0.012	-2.75
SES	PM	Day	S at 200m sd Modeled	0.436	0.447	-0.011	-2.47	0.427	0.440	-0.013	-3.01
SES	PM	Day	MLD sd Modeled	0.434	0.447	-0.013	-2.94	0.425	0.440	-0.015	-3.42
SES	PM	Day	Surface S sd modeled	0.434	0.447	-0.014	-3.11	0.425	0.440	-0.015	-3.48
SES	PM	Night	SST *in situ*	0.416	0.412	0.004	0.99	0.427	0.422	0.004	1.04
SES	PM	Night	T at 100m *in situ*	0.410	0.412	-0.002	-0.5	0.422	0.422	0.000	-0.08
SES	PM	Night	T at 200m *in situ*	0.409	0.412	-0.003	-0.84	0.421	0.422	-0.002	-0.39
SES	PM	Night	Surface S *in situ*	0.419	0.412	0.007	1.59	0.432	0.422	0.009	2.17
SES	PM	Night	S at 100m *in situ*	0.409	0.412	-0.003	-0.65	0.421	0.422	-0.001	-0.25
SES	PM	Night	S at 200m *in situ*	0.407	0.412	-0.005	-1.33	0.420	0.422	-0.003	-0.6
SES	PM	Night	MLD (log) *in situ*	0.410	0.412	-0.002	-0.55	0.423	0.422	0.001	0.31
SES	PM	Night	SST modeled	0.404	0.412	-0.008	-1.97	0.413	0.422	-0.010	-2.34
SES	PM	Night	T at 100m modeled	0.400	0.412	-0.012	-2.87	0.412	0.422	-0.011	-2.56
SES	PM	Night	T at 200m modeled	0.408	0.412	-0.004	-1.03	0.420	0.422	-0.002	-0.46
SES	PM	Night	Surface S modeled	0.401	0.412	-0.011	-2.67	0.413	0.422	-0.010	-2.31
SES	PM	Night	S at 100m modeled	0.402	0.412	-0.010	-2.41	0.411	0.422	-0.011	-2.6

SES	PM	Night	S at 200m modeled	0.401	0.412	-0.011	-2.66	0.410	0.422	-0.012	-3.02
SES	PM	Night	MLD modeled	0.402	0.412	-0.010	-2.4	0.412	0.422	-0.010	-2.47
SES	PM	Night	SST sd modeled	0.397	0.412	-0.015	-3.78	0.406	0.422	-0.016	-3.92
SES	PM	Night	T at 100m sd Modeled	0.396	0.412	-0.016	-3.97	0.405	0.422	-0.017	-4.16
SES	PM	Night	T at 200m sd Modeled	0.396	0.412	-0.016	-3.91	0.406	0.422	-0.017	-4.1
SES	PM	Night	S at 100m sd Modeled	0.398	0.412	-0.014	-3.41	0.407	0.422	-0.015	-3.7
SES	PM	Night	S at 200m sd Modeled	0.396	0.412	-0.016	-3.99	0.406	0.422	-0.017	-4.07
SES	PM	Night	MLD sd Modeled	0.395	0.412	-0.017	-4.23	0.404	0.422	-0.018	-4.44
SES	PM	Night	Surface S sd modeled	0.397	0.412	-0.015	-3.84	0.406	0.422	-0.016	-3.99
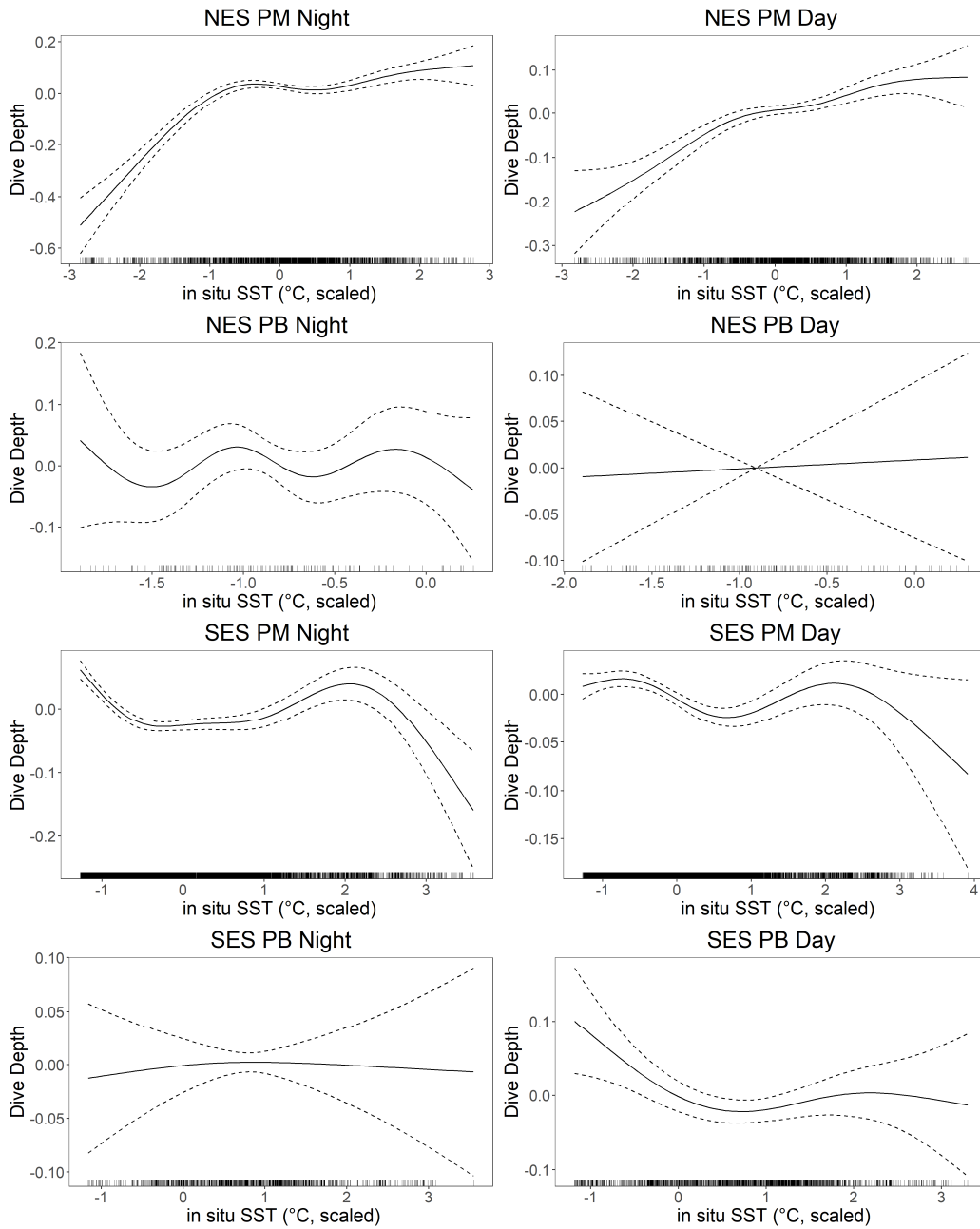
Figure 2.6. Smoother plots for the effect of SST on dive depth show strongest relationship NES PM, in which warmer SST is associated with deeper diving.
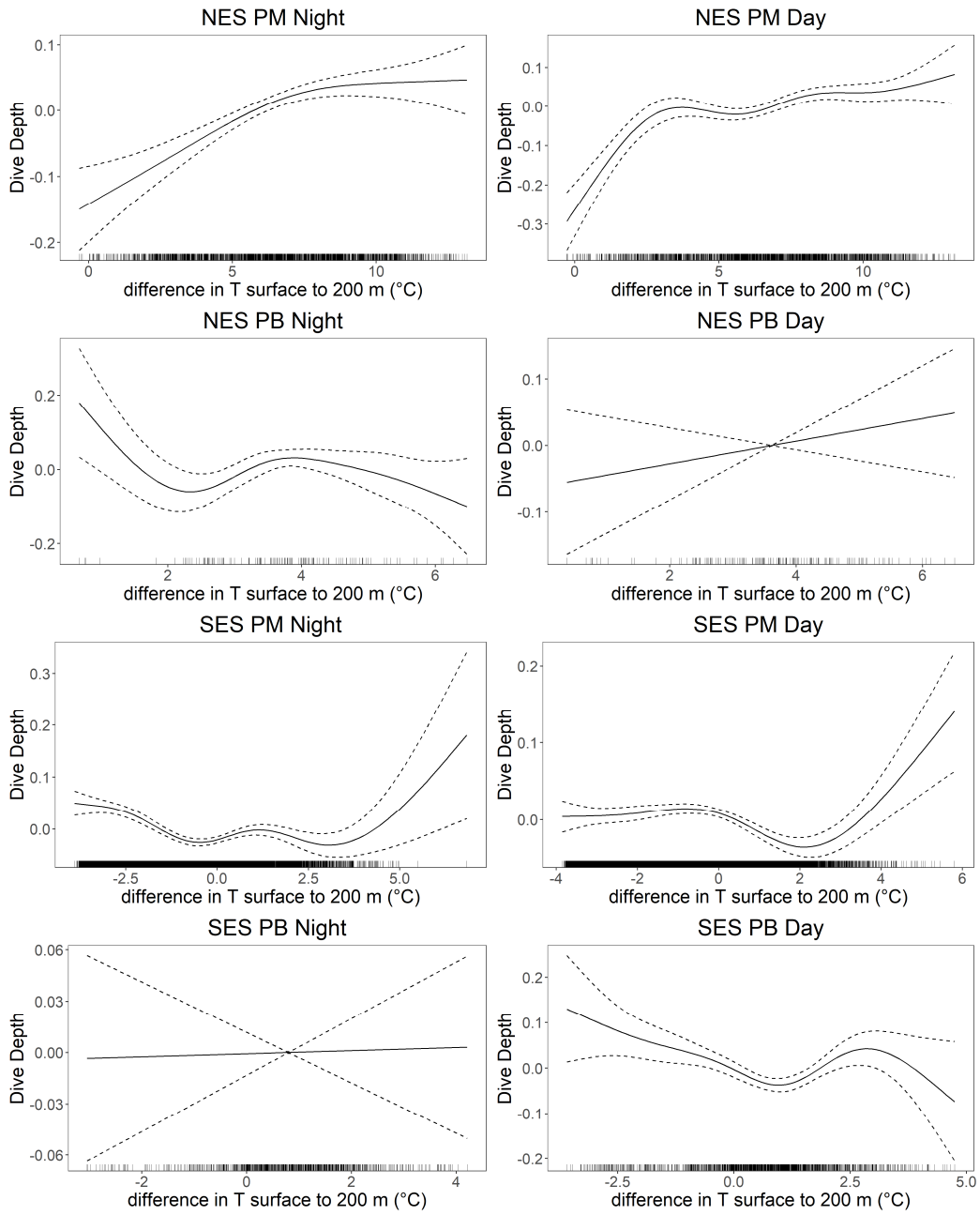
Figure 2.7. The strongest relationships between dive depth and the difference in temperature between the surface and 200 m, a proxy for stratification, matched those to SST: deeper diving in NES PM.
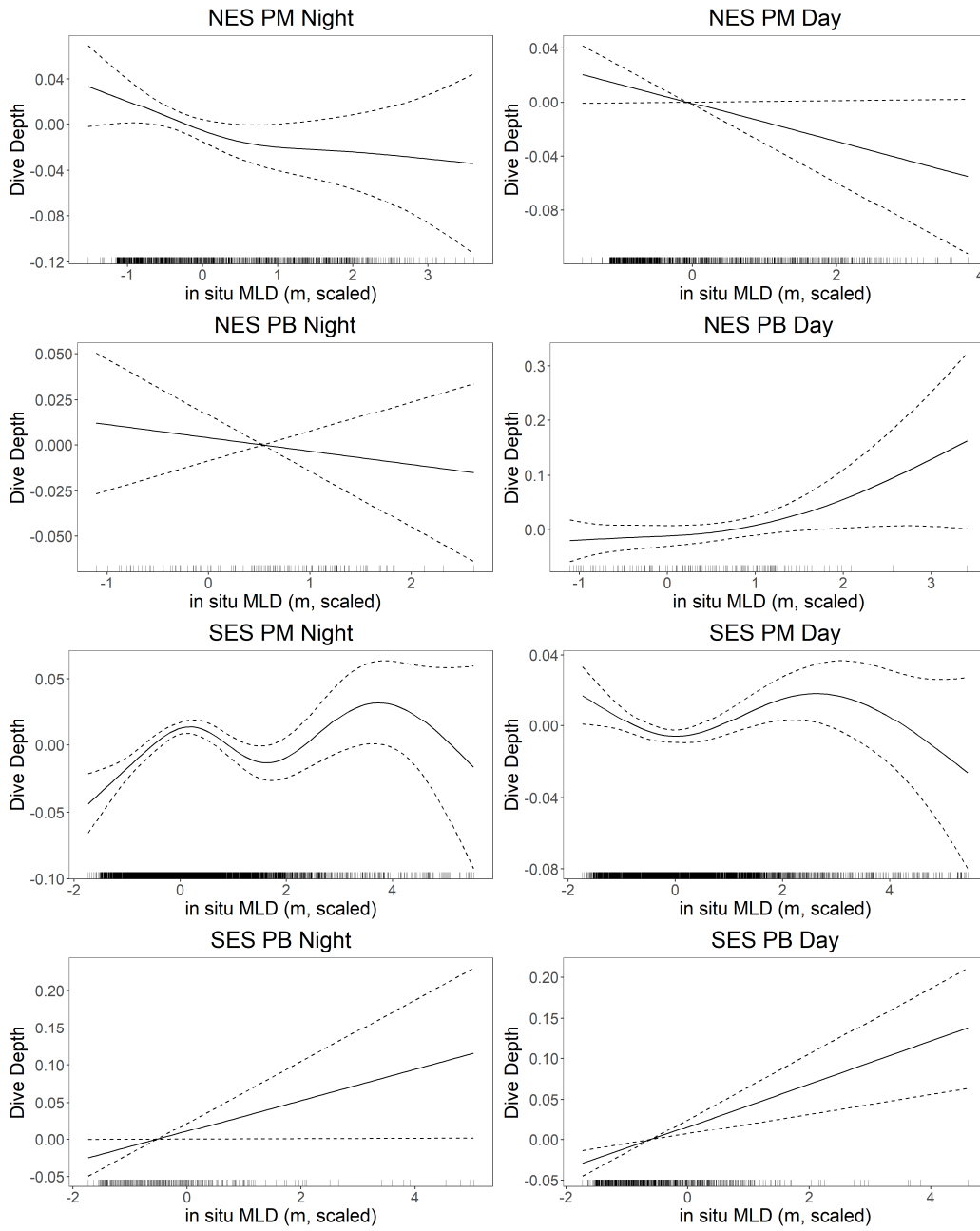
Figure 2.8. Relationships between dive depth and MLD were weaker and more variable compared to the temperature relationships.
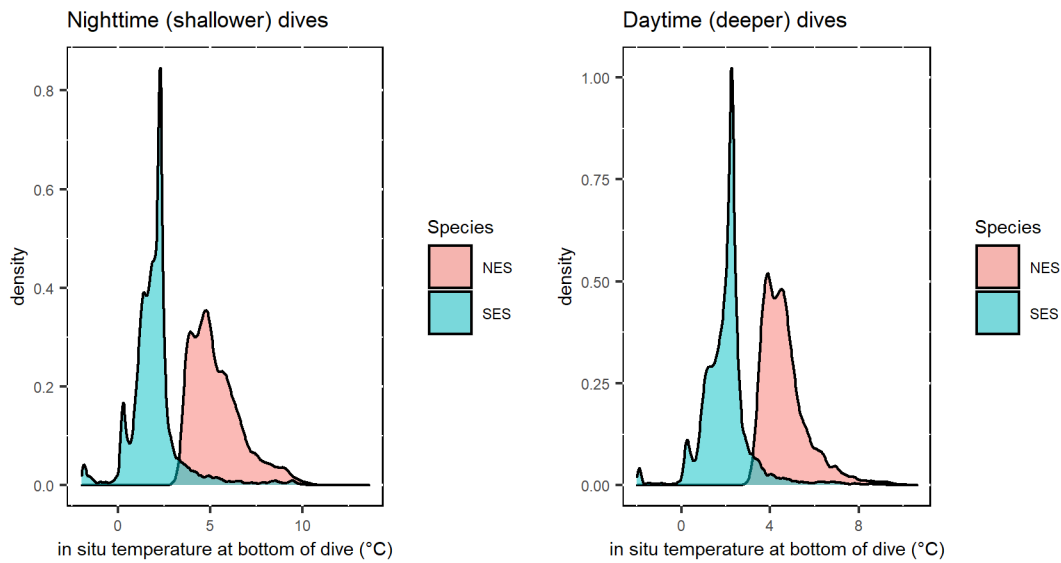
Figure 2.9. Temperatures at the bottom of dives were warmer in the northeast Pacific than the Southern Ocean but spanned a similar range (90% of dives within 3.7°C in SES and 4.1°C in NES), with minimal differences between daytime and nighttime dives.

Table 2.10. Percentage of 3-day data windows for which the standard deviation in an oceanographic variable using modeled data fell within the 95% confidence interval from 10,000 boostrapped standard deviations of the modeled subsampled to match the number of profiles a seal would collect during that time.

Variable	Species	Percent within 95% confidence interval
SST_sd	NES	62.03
SST_sd	SES	56.27
Surface S_sd	NES	62.54
Surface S_sd	SES	56.61
T at 100m_sd	NES	62.60
T at 100m_sd	SES	56.51
S at 100m_sd	NES	63.00
S at 100m_sd	SES	56.72
T at 200m_sd	NES	22.27
T at 200m_sd	SES	21.59
S at 200m_sd	NES	7.31
S at 200m_sd	SES	16.05
MLD_sd	NES	63.06
MLD_sd	SES	56.99
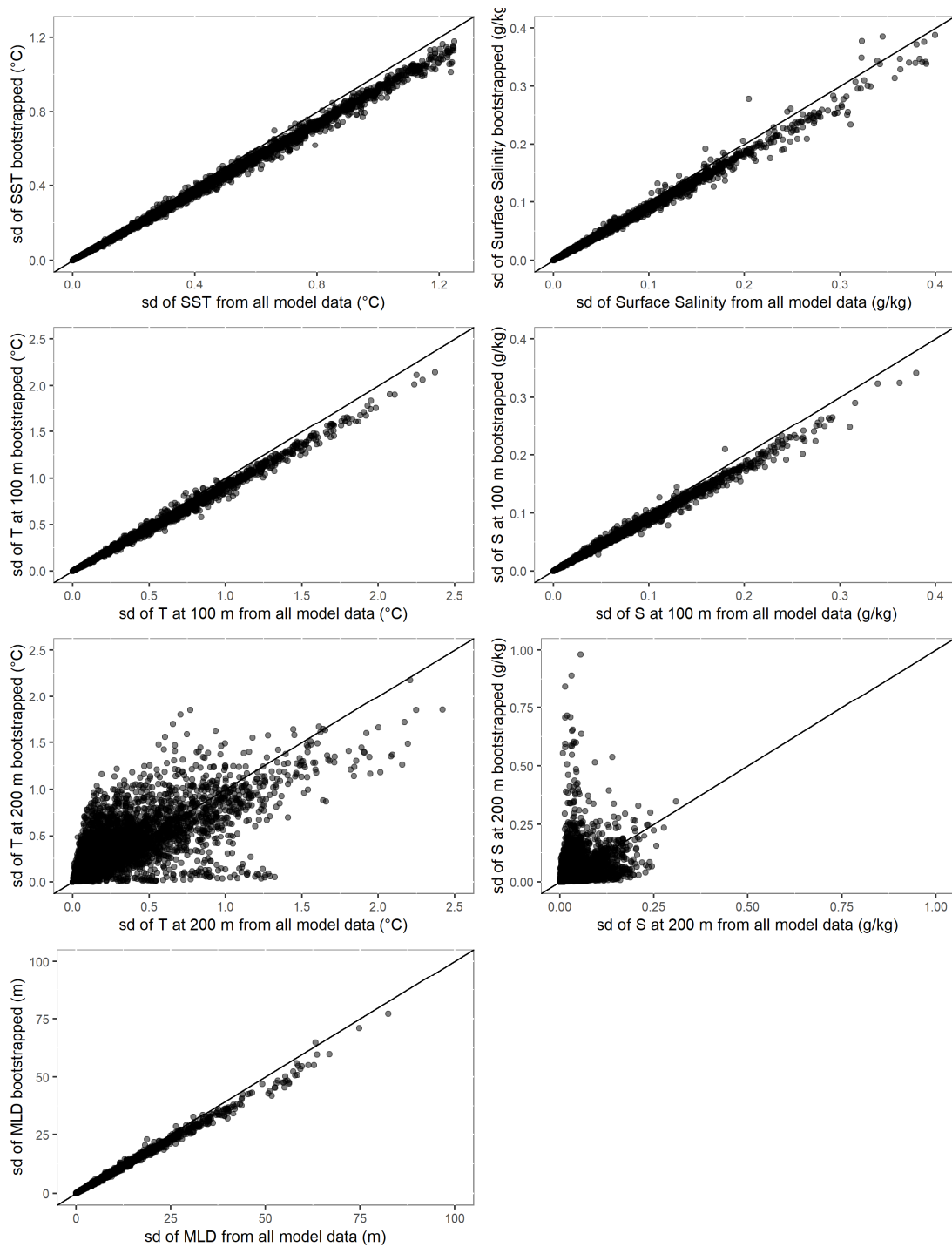
Figure 2.10. Scatter plots of standard deviation of T, S, and MLD from modeled data with calculated values based on all available modeled data with a spatiotemporal radius (x axis) and 10,000 random subsamples of the modeled data to match the

resolution of seal-collected profiles (4 per day) (y axis) with a 1:1 line. The spatiotemporal radii were 3 days and a spatial radius determined using the average transit rate of the seal. Bootstrapped standard deviations were closely related to standard deviations calculated from all available model data, except for data at 200 m. Slight underestimates in the bootstrapped data were evident at higher values. See Table 2.11 for model II regression results.

Table 2.11. Model II regression parameters for bootstrapped values. See figure x for scatter plots.

Variable	Slope	Intercept	R^2
SST_sd	0.911	0.0009	0.998
Surface S_sd	0.919	-0.0002	0.993
T at 100m_sd	0.907	0.0022	0.996
S at 100m_sd	0.901	0.0005	0.995
T at 200m_sd	0.917	0.0775	0.532
S at 200m_sd	5.786	-0.1809	0.058
MLD_sd	0.907	0.0820	0.996

Chapter 3: Spatiotemporal dynamics of chlorophyll's influence on northern elephant seal foraging behavior

Theresa R Keates, Rachel R Holser, Raphael M Kudela, Daniel P Costa

3.1 Abstract

With few exceptions, all life at sea ultimately depends on energy gained from the sun. There will always be some separation of the photosynthesizing plankton that harness this energy from the regions where upper trophic levels forage. We sought to quantify the scale over which this relationship operates. This was done by deploying electronic tags on adult female elephant seals that documented their behavior while concurrently measuring pressure, temperature, salinity, and chlorophyll fluorescence. Additionally, we incorporated remotely sensed ocean color data to consider a broader spatiotemporal context in our analyses. We found that seals did not change their behavior relative to *in situ* chlorophyll measurements. However, they exhibited slower transit rates, indicative of foraging behavior, in areas that had supported high remotely sensed chlorophyll concentrations two to four months prior. This time lag was less pronounced during the post-breeding trip. During the post-breeding trip, most of the seals' range exhibited higher chlorophyll concentrations compared to the post-molt trip. During the seals' post-molt trip, chlorophyll concentrations were lower, partly due to the seasonal northward migration of the Transition Zone Chlorophyll Front. Nevertheless, the effect of the elevated chlorophyll persisted over time and had a prolonged benefit. Our results suggest that it takes several months for

energy associated with primary production to translate up trophic levels to seal prey. Seals dove deeper when chlorophyll concentrations were low. This was likely due to their prey residing deeper to avoid visual predators in the clearer water column. The effect of phytoplankton concentrations on seal behavior is therefore multifaceted: there are physical influences (likely changes in light attenuation) and biological drivers (bottom-up energy transfer) that act on different timescales. Probing the relationship between elephant seal foraging behavior and chlorophyll concentrations has illustrated the importance of appropriate timescales and possible mechanisms that relate primary productivity to predator behavior.

3.2 Introduction

The spatiotemporal relationship between the base of the food web and higher trophic levels is a fundamental interest in marine ecology, especially in an ocean undergoing rapid change. Phytoplankton form the base of almost all marine food webs. Increases in primary production stimulate consumer biomass, consequently attracting higher predators. However, the linkage in time and space, especially in deep offshore environments such as the mesopelagic zone, remains understudied (St. John et al., 2016). Mesopelagic biomass is correlated with primary productivity at broad scales, demonstrating a coupling to primary productivity in the surface ocean (Davison et al., 2013; Irigoien et al., 2014; Proud et al., 2017). Determining the spatiotemporal scale of this relationship is challenging due to the difficulty of working in the mesopelagic ocean. However, new insights may be gained by tracking

the behavior of a mesopelagic predator while sampling its oceanographic environment.

Associations between primary productivity and consumers have been observed across various marine systems. Fisheries yields correlate to chlorophyll concentration (Friedland et al., 2012; Ware and Thomson, 2005). At broad scales, marine predators associate with regions of high primary productivity, including humpback whales (Trudelle et al., 2016), bluefin tuna (Walli et al., 2009), Cape gannets (Grémillet et al., 2008), Antarctic fur seals (Guinet et al., 2001; Lea and Dubroca, 2003), and southern elephant seals (Cotté et al., 2015). Beyond documenting distribution relative to oceanography, biologging has enabled the identification of behavioral states, enabling further inference of relevant ocean features to predator ecology. For example, foraging behavior has been correlated to primary productivity in several species. Southern elephant seals (*Mirounga leonina*) reduce their diving depth, decrease their path length, increase their diving frequency, and increase their bottom time in areas of higher productivity, all indicators of heightened foraging behavior (Dragon et al., 2010; Jaud et al., 2012; O'Toole et al., 2017). Blue and basking sharks shoal their dives in highly productive waters, suggesting that prey are more predictably distributed there (Queiroz et al., 2017). Associations between primary productivity and consumers vary by season (Cotté et al., 2015) and the spatial scale in question (Guinet et al., 2001), and often break down at higher trophic levels (Grémillet et al., 2008), possibly due to a time lag (Cotté et al., 2011). Such complexities in these bottom-up ecosystem processes warrant further investigation.

206

This study uses a high-resolution *in situ* chlorophyll fluorescence dataset derived from instruments carried by northern elephant seals (*Mirounga angustirostris*) to evaluate this mesopelagic predator's foraging behavior relative to primary productivity in the northeast Pacific. Chlorophyll concentration was used as a proxy for phytoplankton biomass. It is used to estimate primary productivity and is primarily measured remotely using ocean color calibrated to *in situ* measurements. While useful for providing global synoptic coverage, satellites are limited in resolution and cannot detect chlorophyll below an optical depth of the ocean's surface (Cullen 1982, Huisman et al. 2006, Kahru 2016). Using the seal-collected chlorophyll fluorescence data supplemented with remotely sensed ocean color data, we investigate whether chlorophyll affects the behavior of elephant seals. We expected increased foraging behavior in areas of elevated chlorophyll concentrations and that this relationship would be stronger with subsurface chlorophyll than surface chlorophyll. We predicted that there would be a time lag between elevated chlorophyll concentrations and the foraging behavior of elephant seals, a high trophic level organism.

3.3 Methods

3.3.1 CTDF Tag Description

We used two different models of conductivity-temperature-depth-fluorescence (CTDF) tag manufactured by the Sea Mammal Research Unit (SMRU, St. Andrews, Scotland). Both models have a CTD sensor head (Valeport Ltd, Totnes, U.K.) that contains a conductivity cell (resolution 0.002mS/cm, accuracy +/- 0.01mS/cm), thermistor (resolution 0.001°C, accuracy +/- 0.005°C), and pressure sensor

(resolution 0.05 dbar, accuracy 2 dbar +/- (0.3 + 0.053% * reading)/°K). The first tag design (N=6 deployments) has a customized Cyclops-7 fluorometer (Turner Designs, CA, USA) attached alongside the CTD sensor head. It weighed 680 grams with dimensions of 11.5 x 10 x 4 cm. This fluorometer's minimum chlorophyll detection limit was 0.03 μg L^{-1} and used an excitation wavelength of 465 nm and emission wavelength of 696 nm for chlorophyll detection. A newer instrument model (N=10 deployments) contained a fluorometer designed and manufactured by Valeport Ltd. This instrument was 7 x 10 x 6.5 cm and weighed 600 g. Its detection limit was 0.066 μg L^{-1} and its excitation and emission wavelengths were 470 nm and 696 nm, respectively.

The tags collect pressure readings at 0.25 Hz throughout the deployment. During the deepest dive in every 6-hour period, pressure, temperature, salinity, and fluorescence readings are recorded at a frequency of 1 Hz during the seal's ascent. For detailed data collection and transmission protocols, see (Boehme et al., 2009) and (Photopoulou et al., 2015). To conserve battery power, fluorescence is only measured between 180 m and the surface in the Cyclops fluorometer tags and 260 m and the surface in the Valeport fluorometer tags. The tag's software generates chlorophyll estimates from raw fluorescence values based on manufacturer calibrations using algae-derived chlorophyll-*a* solutions. A summary of the temperature, salinity, and chlorophyll fluorescence data are transmitted via the Argos satellite system (http://www.argos-system.org/); instrument recovery is required to receive the full resolution dataset (Boehme et al., 2009).

3.3.2 CTDF Fluorometer Calibrations

CTDF tags were immersed in a filtered seawater bath in a laboratory setting. Raw fluorescence readings were taken from a series of six to ten dilutions of a mixed phytoplankton culture ranging in chlorophyll concentrations from 0.005 to 22 μg L^{-1}. The mixed culture contained multiple algal genera of varying cell sizes typical of the northeastern Pacific, including *Pseudo-nitzschia*, *Chaetoceros*, *Alexandrium*, *Dunaliella*, *Synechococcus*, and *Isochrysis*. The raw fluorescence readings were plotted against extracted chlorophyll concentrations from each dilution. Extractions replicated the method of Welschmeyer (1994). We used a Turner Designs 10AU fluorometer that was cross-calibrated with HPLC pigment analysis of chlorophyll standards. These laboratory calibrations were supported by a field trial in an earlier study (Keates et al., 2020). The calibration curve generated for each CTDF tag in the lab was used to convert each tag's *in situ* fluorescence readings to chlorophyll concentrations.

3.3.3 CTDF Tag Deployment on Elephant Seals

CTDF tags were deployed on 19 adult female northern elephant seals in 2014, 2016, 2018, 2019, 2021, and 2022 at Año Nuevo State Park, California. Fourteen seals were instrumented during their post-breeding (PB) foraging trip spanning from about February to April. Five seals were instrumented for the post-molt (PM) trip (June to January). For instrument deployment and recovery, the seals were chemically immobilized using Tiletamine HCl/Zolazepam HCl following established protocols (Le Boeuf et al., 2000; Robinson et al., 2012). CTDF tags were attached to the head using Loctite® 5-minute epoxy. VHF transmitters (ATS, Isanti, MN, USA) were

similarly attached to the animal's dorsal side between the axilla and sternum and used to relocate the seals upon their return to shore. Location, diving, and oceanographic data summaries were transmitted via the Argos satellite system while the seals were at sea. Full-resolution data were archived on board the tags and downloaded upon instrument recovery. Epoxy patches left on the seal's fur after instrument recovery were shed during the annual molt. All animal handling was authorized by the University of California Santa Cruz Institutional Animal Care and Use Committee and conducted under National Marine Fisheries Service permit number 14636, 19108, and 23188.

3.3.4 CTDF Tag Data Processing

Full resolution CTDF data were downloaded after instrument recovery and were used for subsequent analyses. All seals were tracked using the Argos satellite array. Erroneous locations on land were first filtered out by cross-referencing to bathymetry data (as described above). Argos location estimates were further refined using the foieGras package in R (Jonsen et al., 2020, 2019; Jonsen and Patterson, 2020) version 0.7-7.9276, which uses a continuous time sate-space model incorporating location error estimates to filter the tracking data. Locations were interpolated to one-hour intervals and assigned to each temperature-salinity-fluorescence profile based on time. Locations with a standard error of greater than 30 km were omitted from further analyses.

For each CTDF cast, we converted fluorescence readings to estimated chlorophyll concentration using the laboratory-generated calibration curves for each tag. We

smoothed the fluorescence profiles using 8-meter depth intervals to reduce noise in the fluorescence signal while maintaining peaks following the methodology in Keates et al. (2020). We then calculated chlorophyll maxima from these smoothed profiles. We calculated "surface" chlorophyll concentrations as the weighted mean of the smoothed chlorophyll profiles within the approximated first optical depth using the method developed by Gordon and Clark (1980). As ocean color satellites sample the ocean surface to one optical depth (Morel and Berthon, 1989), this upper water column averaging improves the comparability of *in situ* chlorophyll quantification to satellite remote sensing. To determine an appropriate optical depth, we acquired diffuse attenuation coefficients at 490 nm (K_{490}) values for the sampling region for all elephant seal locations from the NOAA ERDDAP server (8-day composite, VIIRSN on Suomi-NPP, Level-3 SMI, NASA, 4km) using the rerdappXtracto (version 1.1.2) package in R (R Core Team, 2022). Concurrent K_{490} data for 74% of elephant seal cast locations were available within 0.2° and 8 days. For elephant seal casts missing K_{490} values, we linearly interpolated from that seal's closest position with an associated K_{490} value. We calculated the first optical depth for each elephant seal cast location as the inverse of the K_{490} value

We considered surface chlorophyll (the weighted mean of chlorophyll fluorescence across the first optical depth, determined using remotely sensed K490 data), maximum chlorophyll (the 90th percentile of the smoothed chlorophyll fluorescence measurements), and the integrated chlorophyll (integrated values across the upper 170 m, the common denominator of maximum depth of data collection, 180

m, with a small buffer as our laboratory tests demonstrated that the fluorometer often required 1-3 seconds to stabilize a reading). We used these metrics as explanatory variables in our models and evaluated the relationship between them. Fluorescence quenching was not observed in our data. This may have resulted from the "surface" chlorophyll being calculated at a weighted mean across the first optical depth, which may have reduced the dampening effect of high near-surface irradiance (Keates et al., 2020).

In situ temperature and salinity measurements were interpolated to 1 m. Absolute salinity and conservative temperature were calculated using the Gibbs Seawater Oceanographic Toolbox in Matlab (McDougall and Barker, 2011). For each temperature and salinity profile, the mixed layer depth (MLD) was determined using the density algorithm presented in (Holte and Talley, 2009). Sea surface temperature (SST) and surface salinity were determined as the mean *in situ* temperature and salinity measurements from the upper 10 m of the water column.

To address the possibility of a time lag between a phytoplankton bloom and the behavioral response of a predator, we used remotely sensed chlorophyll data. We downloaded VIIRSN R2018 Level-3 OCI algorithm chlorophyll-a products at 4 km resolution from NOAA's ERDDAP server using the package rerddapXtracto (version 1.1.2) in R as eight-day composites. We queried chlorophyll data within 0.1, 0.2, 0.3, 0.4, 0.5, 0.75, and 1.5° latitude and longitude of *in situ* casts. We did this for periods in which the 8-day composite included the time the *in situ* data were collected. We additionally also extracted data from the same location one, two, three, four, five, and

six months prior to the seals' presence. We used the average chlorophyll concentration and standard deviation within this spatial window as explanatory variables in our models.

3.3.5 Seal Behavioral Data

We derived daily transit rate (km/h or horizontal movement) from the tracking data processed with foieGras. This metric performs well as a simple proxy for northern elephant seal foraging behavior: a lower transit rate is related to higher foraging activity and higher transit rate to reduced foraging activity (Robinson et al., 2010). We calculated the daily mean transit rate as a response variable.

Due to known diel patterns in elephant seal diving behavior (Le Boeuf et al., 2000; Robinson et al., 2012), we separated diving behavior by day and night by determining the solar zenith angle for the time and putative location of each cast using the sun position package in Matlab (Reda and Andreas, 2004). We designated daytime as when solar zenith angle was less than 90°. Following a zero-offset correction to correct any drift in the depth sensor, maximum dive depth and the number of "wiggles" (small vertical inflections likely associated with prey pursuit (Robinson et al., 2010)) were determined for each dive using a custom-written toolbox in MATLAB. For statistical analyses, we calculated the mean maximum dive depth-and the mean number of wiggles per dive for each day.

3.3.6 Statistical Analyses

To evaluate relationships between seal behavioral metrics (transit rate, dive depth, and number of wiggles) and chlorophyll, we ran generalized additive mixed models

(GAMMs) using the gam() function in the mgcv package version 1.8-39 in R (Wood, 2011). Individual seal was included as a random effect in all models. Models included explanatory variables representing internal drivers to seal behavior (Season – post-breeding or post-molt, Day in Trip – days since leaving shore divided by the length of the foraging trip). A tensor smooth on latitude and longitude was included to account for geographic effects and to address spatial autocorrelation inherent to animal track data. Models with transit rate as the response variable were run with a Tweedie identity-link distribution family. Models of dive depth and wiggles used Gaussian and Gamma log-link families, respectively. We log-transformed chlorophyll concentrations and chlorophyll standard deviations due to skewed distributions with a smaller number of high values. To enable log calculations, we assigned values of 0 the value of the 1st quantile of the dataset. As a small number of extreme values in the standard deviations still strongly influenced the model results, we further the upper and lower 5% of the log-transformed values.

3.4 Results
3.4.1 Dataset Description

Laboratory calibrations adjusted manufacturer estimates of chlorophyll by -72.9 % to + 80.1 % (mean +21.8 ± 0.40 %) (Table 3. 1). Sixteen CTDF tag deployments successfully passed all QC, 11 deployments PB and 5 PM (Fig. 3.1). The seals spent 1,705 days at sea and collected 16,712 salinity, temperature, and chlorophyll fluorescence casts of at least 180 m depth.

The batteries in 4 CTDF tags were depleted upon the seals' return to shore. As the tag's sensors often become unreliable at low power levels (Keates et al., 2020), we visually quality controlled fluorescence data preceding battery depletion by examining deep water fluorescence readings (>170 m) throughout the record and visually identified unreliable data where readings began strongly deviating from near-zero values. These data were then removed along with a buffer of one week of data preceding these questionable readings.

3.4.2 Transit Rate

Surface chlorophyll, maximum chlorophyll, and integrated chlorophyll measured *in situ* added a small amount of explanatory power to the transit rate models for PB behavior but not PM behavior (Table 3. 2). During the PB trip, the greatest increase in explanatory power, using remotely sensed chlorophyll data, was associated with chlorophyll data between 0.1 and 0.3° of seal locations. This is comparable in scale to the distance a seal would travel in the daily timespan considered (mean distance traveled per 24 hours based on transit rate 66.7 km, with $1° \approx 100$ km). The explanatory power dropped using chlorophyll across wider spatial windows. The relationship between PB transit rate and *in situ* chlorophyll and concurrent remotely sensed chlorophyll were quite weak (i.e., showed large uncertainties) and nonlinear.

Time-lagged remotely sensed chlorophyll added considerable explanatory power to the PM transit rate models but not the PB models. During the PM trip, the increase in explanatory power compared to using concurrent remotely sensed chlorophyll data peaked between 2 and 4 months prior, falling off sharply after 5 months. Transit rate

during the PM trip tended to decrease, generally indicative of foraging behavior, in association with high remotely sensed chlorophyll concentrations during the preceding 2-4 months (Fig. 3.2). Chlorophyll at fine spatial scales (0.1-0.3°) added more explanatory power to the models than broad spatial scales for remotely sensed data, both concurrently sampled and with a time lag.

The spatial standard deviation in chlorophyll derived from remotely sensed data had a very small effect on transit rate during either season at any spatiotemporal scale tested (Table 3. 3).

3.4.3 Diving Behavior

In situ chlorophyll measurements did not increase the explanatory power of dive depth models in either the PB or PM season (Table 3. 4). Remotely sensed data, however, illuminate some behavioral trends: seals' nighttime dives were shallower in areas where chlorophyll concentrations were higher; this was true for daytime dives as well though the effect was weaker (Fig. 3.3). The influence of a time lag was more variable than with transit rate but similarly strongest between 2-4 months (Table 3. 4). The effect of chlorophyll on dive depth was strongest at 0.2° spatial windows around seal locations.

Daytime wiggles were only weakly influenced by any chlorophyll covariates (Table 3. 5). During the PM trip, the number of nighttime wiggles tended to be higher with higher remotely sensed chlorophyll, both concurrently sampled and with time lags (Fig. 3.4). *In situ* chlorophyll weakly increased the explanatory power of nighttime wiggles PM, but the relationships had high degrees of uncertainty. No

216

chlorophyll covariates increased explanatory power for PB nighttime wiggles (Table 3. 5).

3.5 Discussion
3.5.1 Overview

Assessing the relationship between a marine predator and its environment help investigate habitat use and infer the influence of ecological processes. However, such relationships operate at spatiotemporal scales that can be difficult to quantify, warranting caution when pairing predator behavior with oceanographic data. Animal-borne instruments measuring chlorophyll fluorescence (CTDF tags) have been deployed on southern elephant seals in the Southern Ocean (Blain et al., 2013; Guinet et al., 2013). Ours is the first dataset in the North Pacific (Keates et al., 2020) that enables incorporation of subsurface conditions at the scale encountered by the seals. Our results suggest that primary productivity encountered by northern elephant seal directly or indirectly has a small influence on their behavior. Chlorophyll concentrations and their relationship to seal behavior varied by season and had a higher effect prior to the seals' presence, highlighting the importance of spatiotemporal scale to ecological questions.

3.5.2 Temporal Lag

While elephant seals' prey, mainly myctophids (Goetsch et al., 2018), do not eat phytoplankton directly, they do consume primary consumers such as euphausiids (Catul et al., 2011), which do. Many mesozooplankton and myctophid species exhibit diel vertical migration behavior (Cohen and Forward, 2016), mirrored in the diel diving patterns of northern elephant seals. The passive sinking of biomass from the

217

euphotic zone into the deep ocean is extremely slow, but diel vertical migrators can

access elevated primary productivity near the surface and transport this energy into

the deeper ocean at accelerated timescales, thus playing an influential role in the

global carbon pump and linking the near-surface to deep ocean (Brierley, 2014;

Irigoien et al., 2014; Kelly et al., 2019). Regardless, there will be a delay between the

initiation of a phytoplankton bloom and its effects on subsurface biota, especially to

higher trophic levels (Lehodey et al., 2010). For example, a study in the California

Current found a 3-4 month time lag between a phytoplankton bloom and an increase

in euphausiid biomass, a low trophic level consumer (Croll et al., 2005). Other

predator studies in the northeast Pacific on northern fur seals (Nordstrom et al., 2013)

and northern elephant seals (Saijo et al., 2017) found no relationship between

behavior and chlorophyll. These studies suggest that a time lag is likely responsible

for the lack of association (*e.g.* Cotté et al. 2011).

Investigating the time lag between a phytoplankton bloom and elephant seals'

behavioral responses required the use of remotely sensed data. Unfortunately, this

prevented us from looking at subsurface chlorophyll across multiple timescales. A

time lag between surface chlorophyll concentrations explained seal behavior better

than surface chlorophyll concurrent to seal presence during the summer-fall trip (PM)

but not during the winter-spring trip (PB). Time lags between 2 and 4 months

increased the explanatory power of our behavioral models the most. Studies

quantifying the time lag between primary productivity and the presence of baleen

whales inferred a timescale between 1 and 4 months (Abrahms et al., 2019; Munger et

al., 2009; Prieto et al., 2017; Visser et al., 2011). This is similar to the euphausiid response in Croll et al. (2005) observed and what we observed with elephant seals occupying a higher trophic level. Southern elephant seals associate with advected water parcels up to 8 months after they contained the peak of a seasonal phytoplankton bloom (Cotté et al., 2015).

3.5.3 Seasonal Differences

We observed a weaker influence of chlorophyll during the PB trip than on the PM trip. Both northern and southern adult female elephant seals tend to show weaker responses to mesoscale oceanography during the PB trip than the PM trip (Cotté et al., 2015; Keates et al., 2022, Chapter 2). This may be due to internal life history pressures, such as the limited time to forage between onshore molting and breeding periods, and/or because the environment has different conditions between the PB and PM seasons.

A significant feature within the range of northern elephant seals which shows considerable seasonal variability is the Transition Zone Chlorophyll Front (TZCF) (Polovina et al., 2017, 2001). The nutrient content in the subpolar northeast Pacific is significantly higher than in the subtropical gyre, and the TZCF, operationally defined at the 0.2 mg m^{-3} chlorophyll-a isopleth, sits at the gyre-gyre boundary near 40-45° N in the summertime and migrates over 1,000 km south to 30-35° N in the wintertime (Bograd et al., 2004), likely due to seasonally heightened wind stress advecting the nutrient-rich water southward (Ayers and Lozier, 2010). Multiple pelagic predators associate with the TZCF, such as albacore and bluefin tuna (Polovina et al., 2001),

loggerhead and leatherback sea turtles (Polovina et al., 2006, 2004, 2001, 2000), blackfooted and Laysan albatross (Shaffer et al., 2005), and northern fur seals (Ream et al., 2005). The TZCF's significance to mesopelagic foraging elephant seals is not yet clear. Qualitatively, female northern elephant seals associate with the TZCF in the summer, when the front coincides with the gyre-gyre boundary, but not in the winter when the front migrates south (Robinson et al., 2012).

Time-lagged chlorophyll was far more influential to elephant seal behavior on the PM trip. During this season, the TZCF lies towards the north if its range roughly aligning with the gyre-gyre boundary (Fig. 3.5). This leaves a smaller area within the seals' range supporting elevated chlorophyll concentrations compared to the winter. Still, the recession of the TZCF to the north may leave behind an enhanced prey field in the south that persists for several months after chlorophyll concentrations have fallen. This is consistent with our observations of seals enhancing their foraging behavior during their PM trip in areas in which chlorophyll had been elevated several months prior. We did not observe this relationship to time-lagged chlorophyll during the PB trip in the winter. During this trip, the TZCF lies further south and most of the seals' range has high chlorophyll concentrations (Fig. 3.5); seals' behavior was more affected by real-time chlorophyll concentrations than past conditions.

Our current results show a very small effect of chlorophyll variability compared to absolute chlorophyll concentration on foraging behavior. Combined with qualitative observations of seals not tracking the southward movement of the TZCF (Robinson et al., 2012), this suggests that the TZCF as a productivity front likely has a negligible

influence on seal foraging. Seals may benefit from the high total productivity, rather than the boundary dynamics of productivity, including the aftermath of elevated primarily productivity in the season after the phytoplankton concentrations have fallen. The gyre-gyre boundary, which seals remain affiliated with throughout the year, may provide additional foraging benefits through physical mechanisms such as prey aggregation at fronts. Because the gyre-gyre boundary either overlaps with the TZCF or is within the high chlorophyll zone throughout the year, it is hard to disentangle the influence of chlorophyll from potential physical boundary effects associated with this basin-scale feature. Future studies using time-lagged physical parameters such as sea surface height may help tease apart such influences.

Differences in behavior between the two annual foraging trips can also be internally driven. The PB trip is shorter and seals must regain some of the energy lost during the lactation fast, when they can lose approximately 40% of their body mass (Costa et al., 1986; Crocker and Champagne, 2018). Seals traveled a shorter distance and at higher speeds during the PB trip, consistent with previous observations (Simmons et al., 2010). This compressed timeframe and geographic range may result in less time to spare to search for and exploit particularly rich, oceanographically created prey patches. It forces them to forage opportunistically on any prey items they encounter instead. Seals forage near-continuously during their short PB trip (Adachi et al., 2021). This foraging urgency could contribute to the lower behavioral response to chlorophyll we observed PB.

221

3.5.4 Diving Behavior

Elephant seal diel diving patterns are likely driven by the vertical migration of their prey (Le Boeuf et al., 2000; Robinson et al., 2012). Many elephant seal prey species such as myctophids move to shallower depths at night (Goetsch et al., 2018). This likely maximizes their foraging efficiency in the resource-abundant shallows while eluding visual predators under the cover of darkness (Benoit-Bird and Moline, 2021; Brierley, 2014; De Robertis, 2002; Iwasa, 1982; Lampert, 1989; Zaret and Suffern, 1976). Changes in seal diving relative to chlorophyll concentrations could be driven by a vertical shift in the distribution of seals' prey in response to changes in light level and/or due to trophic responses to energy injected into the base of the food web through enhanced primary productivity.

Light is a major cue in diel vertical migratory behavior, a relationship especially well documented in zooplankton (see review in Cohen and Forward, 2016). Myctophids may vertically track a preferred light level (*e.g.* Staby and Aksnes, 2011) and have experimentally shown an aversion to light (Gjøsæter, 1984). This behavior in myctophids may be driven by tracking their vertically migrating zooplankton prey and/or by predator avoidance (Catul et al., 2011; Irigoien et al., 2014). Elephant seals tended to dive more shallowly in association with higher remotely sensed chlorophyll concentrations during both PB and PM trips. Animals that are more conspicuous to predators, including larger organisms that are likely of higher foraging value to seals, tend to travel deeper under high light conditions (Benoit-Bird and Moline, 2021; Ohman and Romagnan, 2016). A high abundance of phytoplankton increases light

222

attenuation with depth, creating a darker environment in which vertically migrating organisms may feel less threatened. Therefore, high chlorophyll conditions could result in a shallower, more profiTable 3. prey field for elephant seals.

The behavioral pattern in this study aligns with previous studies finding that southern elephant seals dive deeper when light levels are high, especially during the day (Jaud et al., 2012), and deeper when chlorophyll concentrations are low, measured *in situ* with CTDF tags (Jaud et al., 2012) and using remotely sensed data (Dragon et al., 2010). We observed a stronger negative relationship between chlorophyll concentration and dive depth at nighttime than during the day. One might assume a stronger effect of light during the day. However, vertically migrating animals may be exposed to similar light levels in shallow water at night as they are at depth during the day (Benoit-Bird et al., 2009). Thus, ambient light levels may still drive predator avoidance behavior during the nighttime. We found no relationship between dive depth and *in situ* chlorophyll, which we would expect if light attenuation were the dominant mechanism altering the prey field. Instead, we observed the dive depth relationship relative to remotely sensed chlorophyll. Remotely sensed chlorophyll data may better represent the larger synoptic chlorophyll conditions than the more variable concentrations encountered during and between individual seal dives. We also observed this relationship with dive depth in relation to time-lagged chlorophyll, which often did not match the chlorophyll concentrations, and therefore light attenuation, the seals encountered in real time. This suggests that while light level is likely one indirect driver of seal behavior, there

may be another, likely ecological, mechanism at work in parallel. High surface primary productivity could drive myctophids to shallower, more risky depths to take advantage of rich foraging, balancing their mortality to foraging rate ratio (Gilliam and Fraser, 1987). Higher productivity may increase prey biomass, including at shallower depths, such that seals are able to perform less costly shallower dives to meet their energetic needs.

Dive depth can suggest where seals search for food; foraging success is more difficult to determine. However, the larger number of wiggles associated with high chlorophyll at night indicates more prey are pursued during these shallower nighttime dives. Deeper daytime dives tend to have few wiggles, making this a poor metric for daytime foraging behavior (Holser, 2020), which may explain the lack of relationship between chlorophyll and wiggles we observed during the day. These vertical excursions during the bottom phase of a dive imply the presence of prey but do not indicate foraging success. Change in drift rate can resolve changes in body condition on the order of a few days to a week (Biuw et al., 2003; Crocker et al., 1997; Robinson et al., 2010; Webb et al., 1998). While independent of time of day, this is likely too coarse a scale to resolve the effects of oceanography at mesoscales on the foraging success of northern elephant seals (*e.g.* Keates et al., 2022). The effects of chlorophyll on seal behavior in this study were strongest at mesoscales. Instead, jaw accelerometers can indicate prey capture (*e.g.* Naito et al., 2013), which offers promising future studies into trophic interactions at fine scales.

3.5.5 Complexity of Relationship

While we observed some behavioral trends, the relatively weak and often nonlinear relations between chlorophyll and seal behavior demonstrates that primary productivity is not a straightforward predictor of seal foraging. The time and spatial scales of observation modulate the nature of these relationships, as do intrinsic drivers of seal behavior such as the need to gain energy and return to shore. In our models, even the greatest influence of chlorophyll was far smaller than the explanatory power of internal factors such as the temporal context of the behavior within a foraging trip. This adds to previous evidence suggesting small-scale oceanography only slightly modulates behavior beyond such intrinsic drivers (Keates et al., 2022, Chapter 2).

The composition of phytoplankton communities can confound the relationship between chlorophyll concentration and ecosystem effects. Picophytoplankton generally dominate oligotrophic regions such as the subtropical northeast Pacific while larger cells such as diatoms thrive in high nutrient eutrophic environments, such as the upwelling-dominated California Current System (Agawin et al., 2000). Future work could utilize remotely sensed products that optically estimate phytoplankton community composition. Large phytoplankton generally transfer energy up trophic webs more efficiently than small phytoplankton (Jennings et al., 2002; Ryther, 1969). However, the energy transfer efficiency from primary producers to mesopelagic fishes in oligotrophic oceans has likely been underestimated, where it may be higher than traditionally assumed due to warm water temperatures increasing metabolic rate and clear water facilitating prey capture by visual predators (Irigoien et

al., 2014). These oligotrophic areas often have subsurface chlorophyll maxima (Huisman et al., 2006), meaning surface measurements of chlorophyll are unlikely to accurately represent primary productivity in these regions in the same way they can in eutrophic areas. We hypothesized that integrated water column chlorophyll would better predict seal behavior than surface chlorophyll. Instead, we found that no *in situ* chlorophyll measurements strongly affected seal diving behavior. We are unable to resolve subsurface chlorophyll prior to seal presence as we collected *in situ* data from seal-mounted instruments, so we are unable to further test this hypothesis with time-lagged data but expect there may be strong influences of subsurface chlorophyll prior to seal presence as time-lagged remotely sensed chlorophyll was so influential on seal behavior in this study.

3.5.6 Limitations of *in situ* data

Remotely sensed data overlapping in time with seal presence explained more variability in behavior than *in situ* data. The *in situ* measurements will likely resolve fine-scale structures that remotely sensed products cannot. Variability of chlorophyll at such small scales may not affect the ecology of a mesopelagic prey field and in turn, the behavior of a deep-water predator such as the elephant seal. A larger spatial and temporal context appears necessary to link the base of the food chain to the behavior of a top predator. These results suggest that the CTDF tags' main strength may lie in their collection of *in situ* data for oceanographic applications rather than explaining seal foraging behavior.

3.6 Conclusion

Except for in chemosynthetic environments, all marine organisms, including top predators, rely on energy derived from the sun by phytoplankton. However, if an energy pulse at the base of the food web benefits a top predator, this effect can be separated in space and time and may be challenging to observe using tracking data. Our observations of elephant seal behavior alongside the first *in situ* chlorophyll fluorescence dataset of its kind in the northeast Pacific suggest that phytoplankton concentrations throughout the euphotic zone encountered by seals in real time poorly predict foraging behavior in this species. The foraging behavior of lower trophic level predators and/or those foraging at shallower depths is likely to be more tightly coupled to chlorophyll. Elephant seals are more strongly influenced by phytoplankton that existed in a location during the preceding months, especially during the summer and fall seasons. Increased primary productivity may benefit seals through bottom-up enrichment of the food web and/or due to behavioral changes in their diel vertically migrating prey due to light level and/or food availability.

3.7 References

Abrahms, B., Hazen, E.L., Aikens, E.O., Savoca, M.S., Goldbogen, J.A., Bograd, S.J., 2019. Memory and resource tracking drive blue whale migrations. Proc. Natl. Acad. Sci. 1–6. doi:10.1073/pnas.1819031116

Adachi, T., Takahashi, A., Costa, D.P., Robinson, P.W., Hückstädt, L.A., Peterson, S.H., Holser, R.R., Beltran, R.S., Keates, T.R., Naito, Y., 2021. Forced into an ecological corner: Round-the-clock deep foraging on small prey by elephant seals. Sci. Adv. 7, 21–25. doi:10.1126/sciadv.abg3628

Agawin, N.S.R., Duarte, C.M., Agustí, S., 2000. Nutrient and temperature control of the contribution of picoplankton to phytoplankton biomass and production. Limnol. Oceanogr. 45, 591–600. doi:10.4319/lo.2000.45.3.0591

Ayers, J.M., Lozier, M.S., 2010. Physical controls on the seasonal migration of the North Pacific transition zone chlorophyll front. J. Geophys. Res. Ocean. 115, 1–11. doi:10.1029/2009JC005596

Benoit-Bird, K.J., Au, W.W.L., Wisdom, D.W., 2009. Nocturnal light and lunar cycle effects on diel migration of micronekton. Limnol. Oceanogr. 54, 1789–1800. doi:10.4319/lo.2009.54.5.1789

Benoit-Bird, K.J., Moline, M.A., 2021. Vertical migration timing illuminates the importance of visual and nonvisual predation pressure in the mesopelagic zone. Limnol. Oceanogr. 66, 3010–3019. doi:10.1002/lno.11855

Biuw, M., McConnell, B., Bradshaw, C.J.A., Burton, H., Fedak, M., 2003. Blubber and

buoyancy : monitoring the body condition of free-ranging seals using simple dive characteristics. J. Exp. Biol. 3405–3423. doi:10.1242/jeb.00583

Blain, S., Renaut, S., Xing, X., Claustre, H., Guinet, C., 2013. Instrumented elephant seals reveal the seasonality in chlorophyll and light-mixing regime in the iron-fertilized Southern Ocean. Geophys. Res. Lett. 40, 6368–6372. doi:10.1002/2013GL058065

Boehme, L., Lovell, P., Biuw, M., Roquet, F., Nicholson, J., Thorpe, S.E., Meredith, M.P., Fedak, M., 2009. Technical note: Animal-borne CTD-Satellite Relay Data Loggers for real-time oceanographic data collection. Ocean Sci. 5, 685–695. doi:10.5194/os-5-685-2009

Bograd, S.J., Foley, D.G., Schwing, F.B., Wilson, C., Laurs, R.M., Polovina, J.J., Howell, E.A., Brainard, R.E., 2004. On the seasonal and interannual migrations of the transition zone chlorophyll front. Geophys. Res. Lett. 31, 1–5. doi:10.1029/2004GL020637

Brierley, A.S., 2014. Diel vertical migration. Curr. Biol. 24, R1074–R1076. doi:10.1016/j.cub.2014.08.054

Catul, V., Gauns, M., Karuppasamy, P.K., 2011. A review on mesopelagic fishes belonging to family Myctophidae. Rev. Fish Biol. Fish. 21, 339–354. doi:10.1007/s11160-010-9176-4

Cohen, J.H., Forward, R.B.J., 2016. Zooplankton Diel Vertical Migration - A Review of Proximate Control. Oceanogr. Mar. Biol. An Annu. Rev. 47, 77–110. doi:10.1201/9781420094220-5

Costa, D.P., Boeuf, B.J.L., Huntley, A.C., Ortiz, C.L., 1986. The energetics of lactation in the Northern elephant seal, Mirounga angustirostris. J. Zool. 209, 21–33.

doi:10.1111/j.1469-7998.1986.tb03563.x

Cotté, C., D'Ovidio, F., Chaigneau, A., Levy, M., Taupier-Letage, I., Mate, B., Guinet, C., 2011. Scale-dependent interactions of Mediterranean whales with marine dynamics. Limnol. Oceanogr. 56, 219–232. doi:DOI 10.4319/lo.2011.56.1.0219

Cotté, C., D'Ovidio, F., Dragon, A.C., Guinet, C., Lévy, M., 2015. Flexible preference of southern elephant seals for distinct mesoscale features within the Antarctic Circumpolar Current. Prog. Oceanogr. 131, 46–58. doi:10.1016/j.pocean.2014.11.011

Crocker, D.E., Champagne, C.D., 2018. Pinniped Physiology, in: Encyclopedia of Marine Mammals. pp. 726–733. doi:10.1016/b978-0-12-804327-1.00198-9

Crocker, D.E., Le Boeuf, B.J., Costa, D.P., 1997. Drift diving in female northern elephant seals: Implications for food processing. Can. J. Zool. 75, 27–39. doi:10.1016/j.dnarep.2015.02.007

Croll, D.A., Marinovic, B., Benson, S., Chavez, F.P., Black, N., Ternullo, R., Tershy, B.R., 2005. From wind to whales: Trophic links in a coastal upwelling system. Mar. Ecol. Prog. Ser. 289, 117–130. doi:10.3354/meps289117

Cullen, J.J., 1982. The Deep Chlorophyll Maximum: Comparing Vertical Profiles of Chlorophyll *a*. Can. J. Fish. Aquat. Sci. 39, 791–803. doi:10.1139/f82-108

Davison, P.C., Checkley, D.M., Koslow, J.A., Barlow, J., 2013. Carbon export mediated by mesopelagic fishes in the northeast Pacific Ocean. Prog. Oceanogr. 116, 14–30. doi:10.1016/j.pocean.2013.05.013

De Robertis, A., 2002. Size-dependent visual predation risk and the timing of vertical migration: An optimization model. Limnol. Oceanogr. 47, 925–933.

doi:10.4319/lo.2002.47.4.0925

Dragon, A.C., Monestiez, P., Bar-Hen, A., Guinet, C., 2010. Linking foraging behaviour to physical oceanographic structures: Southern elephant seals and mesoscale eddies east of Kerguelen Islands. Prog. Oceanogr. 87, 61–71. doi:10.1016/j.pocean.2010.09.025

Friedland, K.D., Stock, C., Drinkwater, K.F., Link, J.S., Leaf, R.T., Burton, V., Rose, J.M., Pilskaln, C.H., Fogarty, M.J., 2012. Pathways between primary production and fisheries yields of Large Marine Ecosystems. PLoS One 7. doi:10.1371/journal.pone.0028945

Gilliam, J.F., Fraser, D.F., 1987. Habitat selection under predation hazard: Test of a model with foraging minnows. Ecology 68, 1856–1862. doi:10.2307/1939877

Gjøsæter, J., 1984. Mesopelagic fish, a large potential resource in the Arabian Sea. Deep Sea Res. Part A, Oceanogr. Res. Pap. 31, 1019–1035. doi:10.1016/0198-0149(84)90054-2

Goetsch, C., Conners, M.G., Budge, S.M., Mitani, Y., Walker, W.A., Bromaghin, J.F., Simmons, S.E., Reichmuth, C., Costa, D.P., 2018. Energy-rich mesopelagic fishes revealed as a critical prey resource for a deep-diving predator using Quantitative Fatty Acid Signature Analysis. Front. Mar. Sci. 5, 1–19. doi:10.3389/fmars.2018.00430

Gordon, H.R., Clark, D.K., 1980. Remote sensing optical properties of a stratified ocean: an improved interpretation. Appl. Opt. 19, 3428. doi:10.1364/AO.19.003428

Grémillet, D., Lewis, S., Drapeau, L., Van Der Lingen, C.D., Huggett, J.A., Coetzee, J.C., Verheye, H.M., Daunt, F., Wanless, S., Ryan, P.G., 2008. Spatial match-mismatch in the Benguela upwelling zone: Should we expect chlorophyll and sea-surface temperature to predict marine predator distributions? J. Appl. Ecol. 45, 610–621. doi:10.1111/j.1365-2664.2007.01447.x

Guinet, C., Dubroca, L., Lea, M.A., Goldsworthy, S., Cherel, Y., Duhamel, G., Bonadonna, F., Donnay, J.P., 2001. Spatial distribution of foraging in female antarctic fur seals Arctocephalus gazella in relation to oceanographic variables: A scale-dependent approach using geographic information systems. Mar. Ecol. Prog. Ser. 219, 251–264. doi:10.3354/meps219251

Guinet, C., Xing, X., Walker, E., Monestiez, P., Marchand, S., Picard, B., Jaud, T., Authier, M., Dragon, A.C., Diamond, E., Antoine, D., Lovell, P., Blain, S., Claustre, H., Mammal, S., 2013. Calibration procedures and first dataset of Southern Ocean chlorophyll a profiles collected by elephant seals equipped with a newly developed CTD-fluorescence tags. Earth Syst. Sci. Data 5, 15–29. doi:10.5194/essd-5-15-2013

Holser, R.R., 2020. A Top Predator in Hot Water: Effects of a Marine Heatwave on Foraging and Reproduction in the Northern Elephant Seal. University of California, Santa Cruz.

Holte, J., Talley, L., 2009. A new algorithm for finding mixed layer depths with applications to Argo data and Subantarctic Mode Water formation. J. Atmos. Ocean. Technol. 26, 1920–1939. doi:10.1175/2009JTECHO543.1

Huisman, J., Pham Thi, N.N., Karl, D.M., Sommeijer, B., 2006. Reduced mixing generates oscillations and chaos in the oceanic deep chlorophyll maximum. Nature 439, 322–325. doi:10.1038/nature04245

Irigoien, X., Klevjer, T.A., Røstad, A., Martinez, U., Boyra, G., Acuña, J.L., Bode, A., Echevarria, F., Gonzalez-Gordillo, J.I., Hernandez-Leon, S., Agusti, S., Aksnes, D.L., Duarte, C.M., Kaartvedt, S., 2014. Large mesopelagic fishes biomass and trophic efficiency in the open ocean. Nat. Commun. 5, 3271. doi:10.1038/ncomms4271

Iwasa, Y., 1982. Vertical Migration of Zooplankton : A Game Between Predator and Prey. Am. Nat. 120, 171–180.

Jaud, T., Dragon, A.-C., Garcia, J.V., Guinet, C., 2012. Relationship between chlorophyll a concentration, light attenuation and diving depth of the southern elephant seal Mirounga leonina. PLoS One 7, e47444. doi:10.1371/journal.pone.0047444

Jennings, S., Warr, K.J., Mackinson, S., 2002. Use of size-based production and stable isotope analyses to predict trophic transfer efficiencies and predator-prey body mass ratios in food webs. Mar. Ecol. Prog. Ser. 240, 11–20. doi:10.3354/meps240011

Jonsen, I.D., McMahon, C.R., Patterson, T.A., Auger-Méthé, M., Harcourt, R., Hindell, M.A., Bestley, S., 2019. Movement responses to environment: fast inference of variation among southern elephant seals with a mixed effects model. Ecology 100, 1–8. doi:10.1002/ecy.2566

Jonsen, I.D., Patterson, T.A., 2020. foieGras: fit latent variable movement models to animal tracking data for location quality control and behavioural inference. Zenodo. doi:10.5281/zenodo.3899972

Jonsen, I.D., Patterson, T.A., Costa, D.P., Doherty, P.D., Godley, B.J., Grecian, W.J., Guinet, C., Hoenner, X., Kienle, S.S., Robinson, P.W., Votier, S.C., Witt, M.J., Hindell, M.A., Harcourt, R.G., McMahon, C.R., 2020. A continuous-time state-space model for rapid quality-control of Argos locations from animal-borne tags. Mov. Ecol. 8. doi:10.1186/s40462-020-00217-7

Kahru, M., 2016. Ocean productivity from space: Commentary. Global Biogeochem. Cycles 28–30. doi:10.1002/2016GB005582

Keates, T.R., Hazen, E.L., Holser, R.R., Fiechter, J., Bograd, S.J., Robinson, P.W., Gallo-reynoso, J.P., Costa, D.P., 2022. Foraging behavior of a mesopelagic predator, the northern elephant seal, in northeastern Pacific eddies. Deep. Res. Part I 189, 103866. doi:10.1016/j.dsr.2022.103866

Keates, T.R., Kudela, R.M., Holser, R.R., Hückstädt, L.A., Simmons, S.E., Costa, D.P., 2020. Chlorophyll fluorescence as measured *in situ* by animal-borne instruments in the northeastern Pacific Ocean. J. Mar. Syst. 203. doi:10.1016/j.jmarsys.2019.103265

Kelly, T.B., Davison, P.C., Goericke, R., Landry, M.R., Ohman, M.D., Stukel, M.R., 2019. The importance of mesozooplankton diel vertical migration for sustaining a mesopelagic food web. Front. Mar. Sci. 6, 1–18. doi:10.3389/fmars.2019.00508

Lampert, W., 1989. The Adaptive Significance of Diel Vertical Migration of Zooplankton. Funct. Ecol. 3, 21–27.

Le Boeuf, B.J., Crocker, D.E., Costa, D.P., Blackwell, S.B., Webb, P.M., Houser, D.S., 2000. Foraging ecology of northern elephant seals. Ecol. Monogr. 70, 353–382. doi:10.1890/0012-9615(2000)070[0353:FEONES]2.0.CO;2

Lea, M.A., Dubroca, L., 2003. Fine-scale linkages between the diving behaviour of Antarctic fur seals and oceanographic features in the southern Indian Ocean. ICES J. Mar. Sci. J. du … 60, 990–1002. doi:10.1016/S1054

Lehodey, P., Murtugudde, R., Senina, I., 2010. Bridging the gap from ocean models to population dynamics of large marine predators: A model of mid-trophic functional groups. Prog. Oceanogr. 84, 69–84. doi:10.1016/j.pocean.2009.09.008

McDougall, T.J., Barker, P.M., 2011. Getting started with TEOS-10 and the Gibbs Seawater

(GSW) Oceanographic Toolbox. SCOR/IAPSO WG127.

Morel, A., Berthon, J.-F., 1989. Surface pigments, algal biomass profiles, and potential
production of the euphotic layer: Relationships reinvestigated in view of remote-sensing
applications. Limnol. Oceanogr. 34, 1545–1562.

Munger, L.M., Camacho, D., Havron, A., Campbell, G., Calambokidis, J., Douglas, A.,
Hildebrand, J., 2009. Baleen whale distribution relative to surface temperature and
zooplankton abundance of Southern California, 2004-20.

Naito, Y., Costa, D.P., Adachi, T., Robinson, P.W., Fowler, M., Takahashi, A., 2013.
Unravelling the mysteries of a mesopelagic diet: A large apex predator specializes on
small prey. Funct. Ecol. 27, 710–717. doi:10.1111/1365-2435.12083

Nordstrom, C.A., Battaile, B.C., Cotté, C., Trites, A.W., 2013. Foraging habitats of lactating
northern fur seals are structured by thermocline depths and submesoscale fronts in the
eastern Bering Sea. Deep. Res. Part II Top. Stud. Oceanogr. 88–89, 78–96.
doi:10.1016/j.dsr2.2012.07.010

O'Toole, M., Guinet, C., Lea, M., Hindell, M.A., 2017. Marine predators and phytoplankton :
how elephant seals use the recurrent Kerguelen plume. Mar. Ecol. Prog. Ser. 581, 215–
227.

Ohman, M.D., Romagnan, J.B., 2016. Nonlinear effects of body size and optical attenuation
on Diel Vertical Migration by zooplankton. Limnol. Oceanogr. 61, 765–770.
doi:10.1002/lno.10251

Photopoulou, T., Fedak, M.A., Matthiopoulos, J., Mcconnell, B., Lovell, P., 2015. The
generalized data management and collection protocol for Conductivity-Temperature-

Depth Satellite Relay Data Loggers. Anim. Biotelemetry. doi:10.1186/s40317-015-0053-8

Polovina, J., Uchida, I., Balazs, G., Howell, E.A., Parker, D., Dutton, P., 2006. The Kuroshio Extension Bifurcation Region: A pelagic hotspot for juvenile loggerhead sea turtles. Deep. Res. Part II Top. Stud. Oceanogr. 53, 326–339. doi:10.1016/j.dsr2.2006.01.006

Polovina, J.J., G.H.Balazs, E.A.Howell, D.M.Parker, M.P.Seki, P.H.Dutton, 2004. Forage and migration habitat of loggerhead (Caretta caretta) and olive ridley (Lepidochelys olivacea) sea turtles in the central North Pacific Ocean. Fish. Oceanogr. 13, 36–51.

Polovina, J.J., Howell, E., Kobayashi, D.R., Seki, M.P., 2001. The transition zone chlorophyll front, a dynamic global feature defining migration and forage habitat for marine resources. Prog. Oceanogr. 49, 469–483. doi:10.1016/S0079-6611(01)00036-2

Polovina, J.J., Howell, E.A., Kobayashi, D.R., Seki, M.P., 2017. The Transition Zone Chlorophyll Front updated: Advances from a decade of research. Prog. Oceanogr. 150, 79–85. doi:10.1016/j.pocean.2015.01.006

Polovina, J.J., Kobayashi, D.R., Parker, D.M., Seki, M.P., Balazs, G.H., 2000. Turtles on the edge: movement of loggerhead turtles (Caretta caretta) along oceanic fronts, spanning longline fishing grounds in the central North Pacific, 1997-1998. Fish. Oceanogr. 9, 71–82.

Prieto, R., Tobeña, M., Silva, M.A., 2017. Habitat preferences of baleen whales in a mid-latitude habitat. Deep. Res. Part II Top. Stud. Oceanogr. 141, 155–167. doi:10.1016/j.dsr2.2016.07.015

Proud, R., Cox, M.J., Brierley, A.S., 2017. Biogeography of the global ocean's mesopelagic

zone. Curr. Biol. 27, 113–119. doi:10.1016/j.cub.2016.11.003

Queiroz, N., Vila-Pouca, C., Couto, A., Southall, E.J., Mucientes, G., Humphries, N.E., Sims, D.W., 2017. Convergent foraging tactics of marine predators with different feeding strategies across heterogeneous ocean environments. Front. Mar. Sci. 4, 1–15. doi:10.3389/fmars.2017.00239

R Core Team, 2022. R: A language and environment for statistical computing.

Ream, R.R., Sterling, J.T., Loughlin, T.R., 2005. Oceanographic features related to northern fur seal migratory movements. Deep. Res. Part II Top. Stud. Oceanogr. 52, 823–843. doi:10.1016/j.dsr2.2004.12.021

Reda, I., Andreas, A., 2004. Solar position algorithm for solar radiation applications. Sol. Energy 76, 577–589. doi:10.1016/j.solener.2003.12.003

Robinson, P.W., Costa, D.P., Crocker, D.E., Gallo-Reynoso, J.P., Champagne, C.D., Fowler, M.A., Goetsch, C., Goetz, K.T., Hassrick, J.L., Hückstädt, L.A., Kuhn, C.E., Maresh, J.L., Maxwell, S.M., McDonald, B.I., Peterson, S.H., Simmons, S.E., Teutschel, N.M., Villegas-Amtmann, S., Yoda, K., 2012. Foraging behavior and success of a mesopelagic predator in the northeast Pacific Ocean: insights from a data-rich species, the northern elephant seal. PLoS One 7. doi:10.1371/journal.pone.0036728

Robinson, P.W., Simmons, S.E., Crocker, D.E., Costa, D.P., 2010. Measurements of foraging success in a highly pelagic marine predator, the northern elephant seal. J. Anim. Ecol. 79, 1146–1156. doi:10.1111/j.1365-2656.2010.01735.x

Ryther, J.H., 1969. Photosynthesis and fish production in the sea. Science (80-.). 166, 72.

Saijo, D., Mitani, Y., Abe, T., Sasaki, H., Goetsch, C., Costa, D.P., Miyashita, K., 2017.

Linking mesopelagic prey abundance and distribution to the foraging behavior of a deep-diving predator, the northern elephant seal. Deep. Res. Part II 140, 163–170. doi:10.1016/j.dsr2.2016.11.007

Shaffer, S.A., Tremblay, Y., Awkerman, J.A., Henry, R.W., Teo, S.L.H., Anderson, D.J., Croll, D.A., Block, B.A., Costa, D.P., 2005. Comparison of light- and SST-based geolocation with satellite telemetry in free-ranging albatrosses. Mar. Biol. 147, 833–843. doi:10.1007/s00227-005-1631-8

Simmons, S.E., Crocker, D.E., Hassrick, J.L., Kuhn, C.E., Robinson, P.W., Tremblay, Y., Costa, D.P., 2010. Climate-scale hydrographic features related to foraging success in a capital breeder, the northern elephant seal Mirounga angustirostris. Endanger. Species Res. 10, 233–243. doi:10.3354/esr00254

St. John, M.A., Borja, A., Chust, G., Heath, M., Grigorov, I., Mariani, P., Martin, A.P., Santos, R.S., 2016. A dark hole in our understanding of marine ecosystems and their services: Perspectives from the mesopelagic community. Front. Mar. Sci. 3, 1–6. doi:10.3389/fmars.2016.00031

Staby, A., Aksnes, D.L., 2011. Follow the light-diurnal and seasonal variations in vertical distribution of the mesopelagic fish Maurolicus muelleri. Mar. Ecol. Prog. Ser. 422, 265–273. doi:10.3354/meps08938

Trudelle, L., Cerchio, S., Zerbini, N., Geyer, Y., Mayer, F., Jung, J., Hervé, M.R., Adam, O., 2016. Influence of environmental parameters on movements and habitat utilization of humpback whales in the Madagascar breeding ground. R. Soc. Open Sci. 3.

Visser, F., Hartman, K.L., Pierce, G.J., Valavanis, V.D., Huisman, J., 2011. Timing of

migratory baleen whales at the Azores in relation to the North Atlantic spring bloom. Mar. Ecol. Prog. Ser. 440, 267–279. doi:10.3354/meps09349

Walli, A., Teo, S.L.H., Boustany, A., Farwell, C.J., Williams, T., Dewar, H., Prince, E., Block, B.A., 2009. Seasonal movements, aggregations and diving behavior of Atlantic bluefin tuna (Thunnus thynnus) revealed with archival tags. PLoS One 4. doi:10.1371/journal.pone.0006151

Ware, D.M., Thomson, R.E., 2005. Bottom-up ecosystem trophic dynamics determine fish production in the Northeast Pacific. Science (80-.). 308, 1280–1284. doi:10.1126/science.1109049

Webb, P.M., Crocker, D.E., Blackwell, S.B., Costa, D.P., Le Boeuf, B.J., 1998. Effects of buoyancy on the diving behavior of northern elephant seals. J. Exp. Biol. 201, 2349–2358. doi:10.1242/jeb.00952

Welschmeyer, N.A., 1994. Fluorometric analysis of chlorophyll a in the presence of chlorophyll b and pheopigments. Limnol. Oceanogr. 39, 1985–1992. doi:10.4319/lo.1994.39.8.1985

Wood, S.N., 2011. Fast stable restricted maximum likelihood and marginal likelihood estimation of semiparametric generalized linear models. J. R. Stat. Soc. Ser. B Stat. Methodol. 73, 3–36. doi:10.1111/j.1467-9868.2010.00749.x

Zaret, T.M., Suffern, J.S., 1976. Vertical migration in zooplankton as a predator avoidance mechanism. Limnol. Oceanogr. 21, 804–813.
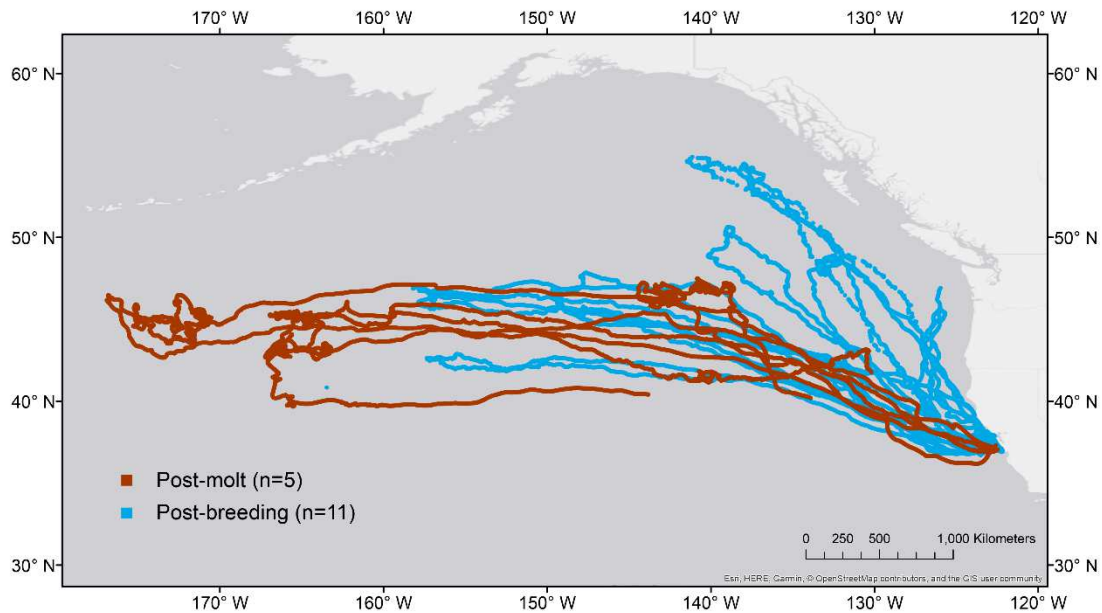
Figure 3.1. Map showing tracks of seals carrying CTDF tags between 2014 and 2022.

Table 3.1. Summary of successful CTDF tag deployments generating data used in this study.

TOPPID	Season	CTDF Serial Number	Fluorometer Model	Calibration equation
2014005	PB2014	12946	Cyclops	y = 1.6619x - 0.43831
2014036	PM2014	12995	Cyclops	y = 1.8099x - 0.86655
2014040	PM2014	12946	Cyclops	y = 1.6619x - 0.43831
2016008	PB2016	12946	Cyclops	y = 1.6619x - 0.43831
2018001	PB2018	14675	Valeport	y = 1.0459x + 0.1036
2018031	PM2018	14767	Valeport	y = 0.9589x - 0.2029
2018032	PM2018	12995	Cyclops	y = 1.8099x - 0.86655
2019006	PB2019	14959	Valeport	y = 1.1292x + 0.3025
2019008	PB2019	14950	Valeport	y = 1.6951x + 0.2116
2019028	PM2019	14415	Cyclops	y = 1.5444x - 0.1784
2021005	PB2021	15262	Valeport	y = 0.9022x - 0.0183
2021013	PB2021	15261	Valeport	y = 0.729x - 0.0366
2021014	PB2021	15258	Valeport	y = 0.993x - 0.0433
2021015	PB2021	15260	Valeport	y = 0.8173x - 0.0287
2022006	PB2022	15263	Valeport	y = 0.7435x + 0.029
2022013	PB2022	15260	Valeport	y = 0.8173x - 0.0287

Table 3.2. Change in explanatory power of GAMMs testing daily transit rate separated by season due to addition of chlorophyll covariates. Base model formula was gam(TransitRate ~ s(DayinTrip,k=6)+te(Latitude,Longitude)+s(SealID,bs="re"). All chlorophyll values were log-transformed. "RS" refers to remotely sensed data. Green shows values derived from *in situ* data. Blue shows remotely sensed data concurrent to seal presence. Yellow shows remotely sensed data prior to seal presence.

Season	Covariate	Model R²	R² reduced model	Difference in R²	% change in R²	Model Deviance Explained	Deviance Explained Reduced Model	Difference in Deviance Explained	% change in Deviance Explained
PB	ChlMax	0.54	0.53	0.0106	1.95	0.54	0.53	0.0109	2.02
PB	SurfaceChl	0.55	0.53	0.0167	3.04	0.54	0.53	0.0173	3.17
PB	IntegratedChl	0.54	0.53	0.0076	1.41	0.53	0.53	0.0073	1.36
PB	Chla_RS nolag	0.53	0.53	-0.0024	-0.45	0.53	0.53	0.0002	0.05
PB	Chla_RS 1monthlag	0.53	0.53	0.0003	0.06	0.53	0.53	0.0007	0.14
PB	Chla_RS 2monthlag	0.52	0.53	-0.0110	-2.12	0.52	0.53	-0.0025	-0.48
PB	Chla_RS 3monthlag	0.51	0.53	-0.0163	-3.17	0.53	0.53	0.0036	0.67
PB	Chla_RS 4monthlag	0.52	0.53	-0.0156	-3.03	0.51	0.53	-0.0158	-3.08
PB	Chla_RS 5monthlag	0.53	0.53	-0.0002	-0.03	0.53	0.53	0.0004	0.08
PB	Chla_RS 6monthlag	0.53	0.53	-0.0018	-0.34	0.52	0.53	-0.0053	-1.02
PB	Chla_RS nolag_10km	0.54	0.53	0.0083	1.55	0.54	0.53	0.0112	2.07
PB	Chla_RS nolag_20km	0.53	0.53	-0.0024	-0.45	0.53	0.53	0.0002	0.05
PB	Chla_RS nolag_30km	0.53	0.53	-0.0023	-0.43	0.53	0.53	0.0008	0.15
PB	Chla_RS nolag_40km	0.53	0.53	-0.0034	-0.64	0.53	0.53	-0.0012	-0.22
PB	Chla_RS	0.53	0.53	-0.0052	-0.98	0.52	0.53	-0.0029	-0.55

	nolag_50km							
PB	Chla_RS nolag_75km	0.53	0.53	-0.0048	-0.91	0.52	0.53	-0.0025	-0.47
PB	Chla_RS 1monthlag_10km	0.53	0.53	-0.0033	-0.63	0.53	0.53	-0.0020	-0.37
PB	Chla_RS 1monthlag_20km	0.53	0.53	0.0003	0.06	0.53	0.53	0.0007	0.14
PB	Chla_RS 1monthlag_30km	0.53	0.53	0.0040	0.75	0.53	0.53	0.0041	0.77
PB	Chla_RS 1monthlag_50km	0.53	0.53	0.0028	0.53	0.53	0.53	0.0031	0.59
PB	Chla_RS 1monthlag_75km	0.53	0.53	0.0035	0.66	0.53	0.53	0.0040	0.76
PB	Chla_RS 1monthlag_100km	0.54	0.53	0.0047	0.88	0.53	0.53	0.0049	0.91
PB	Chla_RS 1monthlag_150km	0.53	0.53	0.0032	0.61	0.53	0.53	0.0036	0.69
PB	Chla_RS 2monthlag_10km	0.50	0.53	-0.0302	-6.04	0.50	0.53	-0.0246	-4.89
PB	Chla_RS 2monthlag_20km	0.52	0.53	-0.0110	-2.12	0.52	0.53	-0.0025	-0.48
PB	Chla_RS 2monthlag_30km	0.53	0.53	0.0003	0.05	0.53	0.53	0.0075	1.40
PB	Chla_RS 2monthlag_50km	0.53	0.53	-0.0052	-0.98	0.52	0.53	-0.0029	-0.55
PB	Chla_RS 2monthlag_75km	0.55	0.53	0.0148	2.71	0.54	0.53	0.0166	3.06
PB	Chla_RS 2monthlag_100km	0.54	0.53	0.0116	2.14	0.54	0.53	0.0115	2.14
PB	Chla_RS 2monthlag_150km	0.54	0.53	0.0100	1.85	0.54	0.53	0.0109	2.03
PB	Chla_RS 3monthlag_20km	0.51	0.53	-0.0163	-3.17	0.53	0.53	0.0036	0.67
PB	Chla_RS 3monthlag_30km	0.51	0.53	-0.0168	-3.26	0.53	0.53	0.0051	0.95
PB	Chla_RS 3monthlag_50km	0.51	0.53	-0.0170	-3.31	0.52	0.53	-0.0025	-0.47
PB	Chla_RS 3monthlag_75km	0.51	0.53	-0.0183	-3.57	0.52	0.53	-0.0054	-1.03
PB	Chla_RS 3monthlag_100km	0.52	0.53	-0.0151	-2.92	0.52	0.53	-0.0053	-1.02
PB	Chla_RS 3monthlag_150km	0.52	0.53	-0.0079	-1.50	0.53	0.53	0.0011	0.20
PB	Chla_RS 4monthlag_10km	0.51	0.53	-0.0213	-4.17	0.51	0.53	-0.0189	-3.72
PB	Chla_RS 4monthlag_20km	0.52	0.53	-0.0156	-3.03	0.51	0.53	-0.0158	-3.08
PB	Chla_RS 4monthlag_30km	0.52	0.53	-0.0080	-1.54	0.52	0.53	-0.0098	-1.89
PB	Chla_RS 4monthlag_50km	0.52	0.53	-0.0145	-2.81	0.51	0.53	-0.0153	-2.98

PB	Chla_RS 4monthlag_75km	0.51	0.53	-0.0169	-3.29	0.51	0.53	-0.0200	-3.93
PB	Chla_RS 4monthlag_100km	0.52	0.53	-0.0133	-2.57	0.51	0.53	-0.0171	-3.35
PB	Chla_RS 4monthlag_150km	0.52	0.53	-0.0123	-2.38	0.51	0.53	-0.0197	-3.89
PM	ChlMax	0.66	0.67	-0.0021	-0.31	0.63	0.63	-0.0020	-0.32
PM	SurfaceChl	0.66	0.67	-0.0012	-0.18	0.63	0.63	-0.0013	-0.21
PM	IntegratedChl	0.67	0.67	0.0042	0.62	0.63	0.63	0.0032	0.51
PM	Chla_RS nolag	0.69	0.67	0.0208	3.02	0.65	0.63	0.0223	3.43
PM	Chla_RS 1monthlag	0.71	0.67	0.0489	6.84	0.66	0.63	0.0354	5.34
PM	Chla_RS 2monthlag	0.77	0.67	0.1002	13.08	0.73	0.63	0.1034	14.13
PM	Chla_RS 3monthlag	0.70	0.67	0.0379	5.39	0.68	0.63	0.0471	6.98
PM	Chla_RS 4monthlag	0.73	0.67	0.0647	8.86	0.71	0.63	0.0814	11.47
PM	Chla_RS 5monthlag	0.70	0.67	0.0329	4.71	0.66	0.63	0.0350	5.27
PM	Chla_RS 6monthlag	0.67	0.67	0.0070	1.04	0.64	0.63	0.0119	1.86
PM	Chla_RS nolag_10km	0.70	0.67	0.0318	4.55	0.66	0.63	0.0347	5.23
PM	Chla_RS nolag_20km	0.69	0.67	0.0208	3.02	0.65	0.63	0.0223	3.43
PM	Chla_RS nolag_30km	0.68	0.67	0.0138	2.03	0.64	0.63	0.0134	2.09
PM	Chla_RS nolag_40km	0.68	0.67	0.0121	1.79	0.64	0.63	0.0100	1.56
PM	Chla_RS nolag_50km	0.68	0.67	0.0159	2.33	0.64	0.63	0.0139	2.16
PM	Chla_RS nolag_75km	0.66	0.67	-0.0030	-0.45	0.62	0.63	-0.0043	-0.68
PM	Chla_RS 1monthlag_10km	0.74	0.67	0.0700	9.52	0.69	0.63	0.0584	8.51
PM	Chla_RS 1monthlag_20km	0.71	0.67	0.0489	6.84	0.66	0.63	0.0354	5.34
PM	Chla_RS 1monthlag_30km	0.69	0.67	0.0273	3.93	0.65	0.63	0.0168	2.61
PM	Chla_RS 1monthlag_50km	0.67	0.67	0.0025	0.38	0.62	0.63	-0.0066	-1.06
PM	Chla_RS 1monthlag_75km	0.67	0.67	-0.0005	-0.08	0.62	0.63	-0.0077	-1.23
PM	Chla_RS 1monthlag_100km	0.66	0.67	-0.0029	-0.44	0.62	0.63	-0.0085	-1.36
PM	Chla_RS 1monthlag_150km	0.67	0.67	0.0004	0.05	0.63	0.63	-0.0011	-0.18
PM	Chla_RS 2monthlag_10km	0.77	0.67	0.1081	13.96	0.74	0.63	0.1153	15.50

PM	Chla_RS 2monthlag_20km	0.77	0.67	0.1002	13.08	0.73	0.63	0.1034	14.13
PM	Chla_RS 2monthlag_30km	0.76	0.67	0.0938	12.35	0.72	0.63	0.0955	13.19
PM	Chla_RS 2monthlag_50km	0.68	0.67	0.0159	2.33	0.64	0.63	0.0139	2.16
PM	Chla_RS 2monthlag_75km	0.71	0.67	0.0461	6.47	0.68	0.63	0.0518	7.62
PM	Chla_RS 2monthlag_100km	0.70	0.67	0.0321	4.60	0.66	0.63	0.0358	5.39
PM	Chla_RS 2monthlag_150km	0.69	0.67	0.0221	3.21	0.65	0.63	0.0191	2.95
PM	Chla_RS 3monthlag_20km	0.70	0.67	0.0379	5.39	0.68	0.63	0.0471	6.98
PM	Chla_RS 3monthlag_30km	0.70	0.67	0.0296	4.26	0.66	0.63	0.0285	4.34
PM	Chla_RS 3monthlag_50km	0.69	0.67	0.0259	3.75	0.66	0.63	0.0275	4.20
PM	Chla_RS 3monthlag_75km	0.69	0.67	0.0286	4.12	0.66	0.63	0.0311	4.72
PM	Chla_RS 3monthlag_100km	0.69	0.67	0.0204	2.97	0.65	0.63	0.0237	3.64
PM	Chla_RS 3monthlag_150km	0.67	0.67	0.0061	0.91	0.64	0.63	0.0093	1.45
PM	Chla_RS 4monthlag_10km	0.73	0.67	0.0688	9.36	0.71	0.63	0.0860	12.04
PM	Chla_RS 4monthlag_20km	0.73	0.67	0.0647	8.86	0.71	0.63	0.0814	11.47
PM	Chla_RS 4monthlag_30km	0.73	0.67	0.0605	8.33	0.70	0.63	0.0697	9.98
PM	Chla_RS 4monthlag_50km	0.73	0.67	0.0634	8.69	0.70	0.63	0.0706	10.10
PM	Chla_RS 4monthlag_75km	0.71	0.67	0.0461	6.48	0.68	0.63	0.0505	7.43
PM	Chla_RS 4monthlag_100km	0.71	0.67	0.0413	5.85	0.67	0.63	0.0456	6.77
PM	Chla_RS 4monthlag_150km	0.69	0.67	0.0260	3.76	0.66	0.63	0.0277	4.22
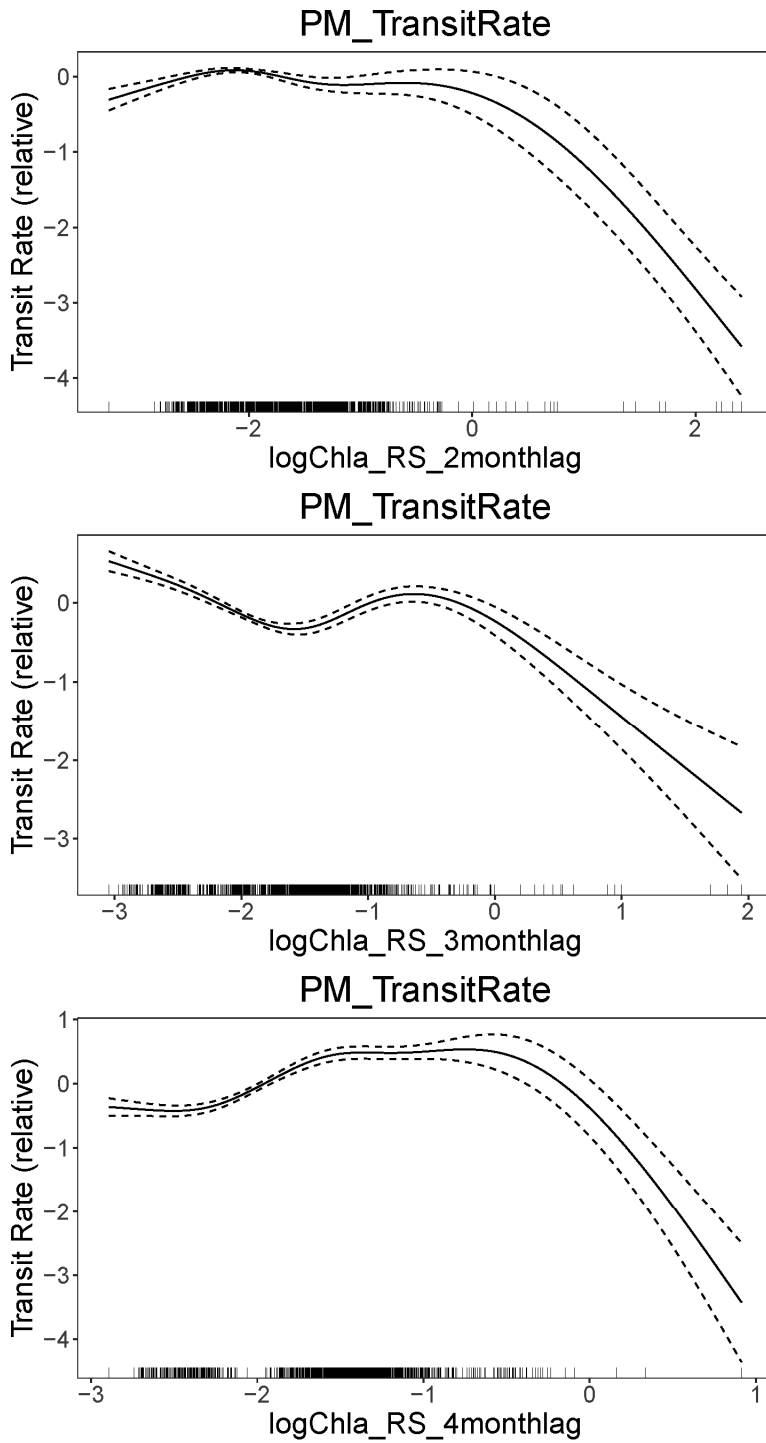
Figure 3.2. Smoother plots of transit rate during the PM trip in relation to time-lagged remotely sensed chlorophyll showed reduced transit rate associated with elevated chlorophyll concentrations.

Table 3.3. Change in explanatory power of GAMs testing daily transit rate separated by season due to addition of chlorophyll variability covariates. Base model formula was gam(TransitRate ~ s(DayinTrip,k=6)+te(Latitude,Longitude)+s(SealID,bs="re"). All chlorophyll values were log-transformed. "RS" refers to remotely sensed data. Blue shows remotely sensed data concurrent to seal presence. Yellow shows remotely sensed data prior to seal presence.

Season	Covariate	Model R^2	R^2 reduced model	Difference in R^2	% change in R^2	Model Deviance Explained	Deviance Explained Reduced Model	Difference in Deviance Explained	% change in Deviance Explained
PB	Chla_RS_nolag 10km_sd	0.71	0.71	0.0000	0.00	0.71	0.71	0.0010	0.13
PB	Chla_RS nolag_20km_sd	0.70	0.70	0.0006	0.09	0.70	0.70	0.0005	0.08
PB	Chla_RS nolag_30km_sd	0.69	0.69	-0.0001	-0.01	0.69	0.69	0.0000	0.00
PB	Chla_RS nolag_40km_sd	0.69	0.69	-0.0001	-0.01	0.69	0.69	0.0003	0.04
PB	Chla_RS nolag_50km_sd	0.69	0.69	0.0000	0.00	0.68	0.68	0.0000	0.00
PB	Chla_RS nolag_75km_sd	0.69	0.69	0.0002	0.03	0.68	0.68	0.0002	0.02
PB	Chla_RS 1monthlag_20km_sd	0.71	0.71	0.0010	0.14	0.71	0.71	0.0020	0.28
PB	Chla_RS 1monthlag_30km_sd	0.70	0.70	0.0000	0.00	0.70	0.70	0.0029	0.42
PB	Chla_RS 1monthlag_50km_sd	0.70	0.70	0.0008	0.12	0.69	0.69	0.0020	0.29
PB	Chla_RS 1monthlag_75km_sd	0.70	0.69	0.0014	0.20	0.69	0.69	0.0031	0.45
PB	Chla_RS 1monthlag_100km_sd	0.70	0.69	0.0034	0.48	0.69	0.68	0.0051	0.74

PB	Chla_RS 1monthlag_150km_sd	0.69	0.69	0.0059	0.85	0.69	0.68	0.0069	1.01
PB	Chla_RS 2monthlag_20km_sd	0.73	0.73	0.0049	0.67	0.75	0.74	0.0045	0.60
PB	Chla_RS 2monthlag_30km_sd	0.73	0.72	0.0065	0.89	0.74	0.73	0.0057	0.78
PB	Chla_RS 2monthlag_50km_sd	0.69	0.69	0.0000	0.00	0.68	0.68	0.0000	0.00
PB	Chla_RS 2monthlag_75km_sd	0.72	0.71	0.0096	1.32	0.72	0.72	0.0083	1.14
PB	Chla_RS 2monthlag_100km_sd	0.72	0.71	0.0155	2.14	0.72	0.71	0.0142	1.96
PB	Chla_RS 2monthlag_150km_sd	0.72	0.70	0.0161	2.24	0.71	0.70	0.0145	2.04
PB	Chla_RS 3monthlag_20km_sd	0.73	0.73	0.0049	0.66	0.72	0.72	0.0060	0.84
PB	Chla_RS 3monthlag_30km_sd	0.73	0.72	0.0041	0.57	0.72	0.71	0.0046	0.65
PB	Chla_RS 3monthlag_50km_sd	0.72	0.72	0.0050	0.69	0.71	0.71	0.0042	0.60
PB	Chla_RS 3monthlag_75km_sd	0.73	0.72	0.0075	1.03	0.72	0.71	0.0077	1.07
PB	Chla_RS 3monthlag_100km_sd	0.72	0.71	0.0077	1.07	0.71	0.71	0.0065	0.91
PB	Chla_RS 3monthlag_150km_sd	0.72	0.71	0.0100	1.40	0.71	0.70	0.0085	1.19
PB	Chla_RS 4monthlag_20km_sd	0.74	0.73	0.0084	1.14	0.75	0.74	0.0066	0.88
PB	Chla_RS 4monthlag_30km_sd	0.74	0.73	0.0125	1.69	0.74	0.73	0.0127	1.70
PB	Chla_RS 4monthlag_50km_sd	0.73	0.72	0.0086	1.17	0.73	0.73	0.0064	0.87
PB	Chla_RS 4monthlag_75km_sd	0.73	0.72	0.0107	1.46	0.73	0.72	0.0080	1.10
PB	Chla_RS 4monthlag_100km_sd	0.73	0.72	0.0135	1.85	0.73	0.72	0.0109	1.50
PB	Chla_RS 4monthlag_150km_sd	0.72	0.70	0.0151	2.10	0.71	0.70	0.0128	1.79
PM	Chla_RS nolag_10km_sd	0.71	0.71	0.0000	0.00	0.71	0.71	0.0010	0.13
PM	Chla_RS nolag_20km_sd	0.70	0.70	0.0006	0.09	0.70	0.70	0.0005	0.08
PM	Chla_RS nolag_30km_sd	0.69	0.69	-0.0001	-0.01	0.69	0.69	0.0000	0.00
PM	Chla_RS nolag_40km_sd	0.69	0.69	-0.0001	-0.01	0.69	0.69	0.0003	0.04
PM	Chla_RS nolag_50km_sd	0.69	0.69	0.0000	0.00	0.68	0.68	0.0000	0.00
PM	Chla_RS nolag_75km_sd	0.69	0.69	0.0002	0.03	0.68	0.68	0.0002	0.02
PM	Chla_RS 1monthlag_20km_sd	0.71	0.71	0.0010	0.14	0.71	0.71	0.0020	0.28

PM	Chla_RS 1monthlag_30km_sd	0.70	0.70	0.0000	0.00	0.70	0.70	0.0029	0.42
PM	Chla_RS 1monthlag_50km_sd	0.70	0.70	0.0008	0.12	0.69	0.69	0.0020	0.29
PM	Chla_RS 1monthlag_75km_sd	0.70	0.69	0.0014	0.20	0.69	0.69	0.0031	0.45
PM	Chla_RS 1monthlag_100km_sd	0.70	0.69	0.0034	0.48	0.69	0.68	0.0051	0.74
PM	Chla_RS 1monthlag_150km_sd	0.69	0.69	0.0059	0.85	0.69	0.68	0.0069	1.01
PM	Chla_RS 2monthlag_20km_sd	0.73	0.73	0.0049	0.67	0.75	0.74	0.0045	0.60
PM	Chla_RS 2monthlag_30km_sd	0.73	0.72	0.0065	0.89	0.74	0.73	0.0057	0.78
PM	Chla_RS 2monthlag_50km_sd	0.69	0.69	0.0000	0.00	0.68	0.68	0.0000	0.00
PM	Chla_RS 2monthlag_75km_sd	0.72	0.71	0.0096	1.32	0.72	0.72	0.0083	1.14
PM	Chla_RS 2monthlag_100km_sd	0.72	0.71	0.0155	2.14	0.72	0.71	0.0142	1.96
PM	Chla_RS 2monthlag_150km_sd	0.72	0.70	0.0161	2.24	0.71	0.70	0.0145	2.04
PM	Chla_RS 3monthlag_20km_sd	0.73	0.73	0.0049	0.66	0.72	0.72	0.0060	0.84
PM	Chla_RS 3monthlag_30km_sd	0.73	0.72	0.0041	0.57	0.72	0.71	0.0046	0.65
PM	Chla_RS 3monthlag_50km_sd	0.72	0.72	0.0050	0.69	0.71	0.71	0.0042	0.60
PM	Chla_RS 3monthlag_75km_sd	0.73	0.72	0.0075	1.03	0.72	0.71	0.0077	1.07
PM	Chla_RS 3monthlag_100km_sd	0.72	0.71	0.0077	1.07	0.71	0.71	0.0065	0.91
PM	Chla_RS 3monthlag_150km_sd	0.72	0.71	0.0100	1.40	0.71	0.70	0.0085	1.19
PM	Chla_RS 4monthlag_20km_sd	0.74	0.73	0.0084	1.14	0.75	0.74	0.0066	0.88
PM	Chla_RS 4monthlag_30km_sd	0.74	0.73	0.0125	1.69	0.74	0.73	0.0127	1.70
PM	Chla_RS 4monthlag_50km_sd	0.73	0.72	0.0086	1.17	0.73	0.73	0.0064	0.87
PM	Chla_RS 4monthlag_75km_sd	0.73	0.72	0.0107	1.46	0.73	0.72	0.0080	1.10
PM	Chla_RS 4monthlag_100km_sd	0.73	0.72	0.0135	1.85	0.73	0.72	0.0109	1.50
PM	Chla_RS 4monthlag_150km_sd	0.72	0.70	0.0151	2.10	0.71	0.70	0.0128	1.79

Table 3.4. Change in explanatory power of GAMMs testing daily mean dive depth separated by season and day and night due to addition of chlorophyll covariates. Base model formula was gam(TransitRate ~ s(DayinTrip,k=6)+te(Latitude,Longitude)+s(SealID,bs="re"). All chlorophyll values were log-transformed. "RS" refers to remotely sensed data. Green shows values derived from *in situ* data. Blue shows remotely sensed data concurrent to seal presence. Yellow shows remotely sensed data prior to seal presence.

Season	Day or Night	Covariate	Model R^2	R^2 reduced model	Difference in R^2	% change in R^2	Model Deviance Explained	Deviance Explained Reduced Model	Difference in Deviance Explained	% change in Deviance Explained
PB	Night	ChlMax	0.56	0.58	-0.0169	-2.99	0.57	0.59	-0.0148	-2.59
PB	Night	SurfaceChl	0.54	0.58	-0.0376	-6.92	0.55	0.59	-0.0354	-6.43
PB	Night	IntegratedChl	0.55	0.58	-0.0280	-5.05	0.56	0.59	-0.0270	-4.83
PB	Night	Chla_RS nolag	0.59	0.58	0.0118	1.99	0.60	0.59	0.0131	2.19
PB	Night	Chla_RS 1monthlag	0.63	0.58	0.0530	8.36	0.64	0.59	0.0538	8.41
PB	Night	Chla_RS 2monthlag	0.63	0.58	0.0513	8.12	0.64	0.59	0.0525	8.23
PB	Night	Chla_RS 3monthlag	0.64	0.58	0.0560	8.79	0.64	0.59	0.0590	9.15
PB	Night	Chla_RS 4monthlag	0.61	0.58	0.0300	4.91	0.62	0.59	0.0319	5.17
PB	Night	Chla_RS 5monthlag	0.61	0.58	0.0273	4.48	0.61	0.59	0.0284	4.63
PB	Night	Chla_RS 6monthlag	0.62	0.58	0.0393	6.34	0.63	0.59	0.0401	6.41
PB	Night	Chla_RS Nolag 10km	0.60	0.58	0.0168	2.81	0.60	0.59	0.0182	3.02
PB	Night	Chla_RS Nolag 20km	0.59	0.58	0.0118	1.99	0.60	0.59	0.0131	2.19
PB	Night	Chla_RS Nolag 30km	0.59	0.58	0.0110	1.86	0.60	0.59	0.0121	2.03

PB	Night	Chla_RS Nolag 40km	0.60	0.58	0.0180	3.01	0.60	0.59	0.0188	3.12
PB	Night	Chla_RS Nolag 50km	0.60	0.58	0.0238	3.94	0.61	0.59	0.0244	4.00
PB	Night	Chla_RS Nolag 75km	0.60	0.58	0.0182	3.04	0.60	0.59	0.0187	3.10
PB	Night	Chla_RS 1monthlag 10km	0.64	0.58	0.0567	8.89	0.64	0.59	0.0580	9.01
PB	Night	Chla_RS 1monthlag 20km	0.63	0.58	0.0530	8.36	0.64	0.59	0.0538	8.41
PB	Night	Chla_RS 1monthlag 30km	0.63	0.58	0.0540	8.50	0.64	0.59	0.0545	8.51
PB	Night	Chla_RS 1monthlag 50km	0.64	0.58	0.0590	9.22	0.64	0.59	0.0592	9.18
PB	Night	Chla_RS 1monthlag 75km	0.64	0.58	0.0573	8.97	0.64	0.59	0.0573	8.92
PB	Night	Chla_RS 1monthlag 100km	0.64	0.58	0.0582	9.10	0.64	0.59	0.0582	9.04
PB	Night	Chla_RS 1monthlag 150km	0.64	0.58	0.0581	9.09	0.64	0.59	0.0579	9.00
PB	Night	Chla_RS 2monthlag 10km	0.63	0.58	0.0516	8.15	0.64	0.59	0.0533	8.35
PB	Night	Chla_RS 2monthlag 20km	0.63	0.58	0.0513	8.12	0.64	0.59	0.0525	8.23
PB	Night	Chla_RS 2monthlag 30km	0.63	0.58	0.0491	7.79	0.64	0.59	0.0501	7.88
PB	Night	Chla_RS 2monthlag 50km	0.60	0.58	0.0238	3.94	0.61	0.59	0.0244	4.00
PB	Night	Chla_RS 2monthlag 75km	0.62	0.58	0.0426	6.83	0.63	0.59	0.0431	6.86
PB	Night	Chla_RS 2monthlag 100km	0.62	0.58	0.0429	6.87	0.63	0.59	0.0433	6.89
PB	Night	Chla_RS 2monthlag 150km	0.62	0.58	0.0406	6.53	0.63	0.59	0.0409	6.53
PB	Night	Chla_RS 3monthlag 20km	0.64	0.58	0.0560	8.79	0.64	0.59	0.0590	9.15
PB	Night	Chla_RS 3monthlag 30km	0.63	0.58	0.0498	7.89	0.64	0.59	0.0524	8.21

PB	Night	Chla_RS 3monthlag 50km	0.61	0.58	0.0276	4.54	0.61	0.59	0.0292	4.75
PB	Night	Chla_RS 3monthlag 75km	0.60	0.58	0.0196	3.26	0.61	0.59	0.0216	3.55
PB	Night	Chla_RS 3monthlag 100km	0.60	0.58	0.0184	3.07	0.61	0.59	0.0198	3.27
PB	Night	Chla_RS 3monthlag 150km	0.60	0.58	0.0219	3.64	0.61	0.59	0.0231	3.80
PB	Night	Chla_RS 4monthlag 10km	0.63	0.58	0.0460	7.34	0.63	0.59	0.0488	7.70
PB	Night	Chla_RS 4monthlag 20km	0.61	0.58	0.0300	4.91	0.62	0.59	0.0319	5.17
PB	Night	Chla_RS 4monthlag 30km	0.60	0.58	0.0230	3.81	0.61	0.59	0.0247	4.05
PB	Night	Chla_RS 4monthlag 50km	0.61	0.58	0.0244	4.02	0.61	0.59	0.0256	4.19
PB	Night	Chla_RS 4monthlag 75km	0.60	0.58	0.0223	3.69	0.61	0.59	0.0234	3.84
PB	Night	Chla_RS 4monthlag 100km	0.60	0.58	0.0222	3.68	0.61	0.59	0.0235	3.85
PB	Night	Chla_RS 4monthlag 150km	0.60	0.58	0.0186	3.09	0.60	0.59	0.0194	3.21
PB	Day	ChlMax	0.69	0.69	-0.0086	-1.26	0.69	0.70	-0.0072	-1.05
PB	Day	SurfaceChl	0.67	0.69	-0.0219	-3.25	0.68	0.70	-0.0200	-2.96
PB	Day	IntegratedChl	0.69	0.69	-0.0005	-0.07	0.70	0.70	0.0000	0.00
PB	Day	Chla_RS nolag	0.72	0.69	0.0217	3.03	0.72	0.70	0.0227	3.15
PB	Day	Chla_RS 1monthlag	0.73	0.69	0.0321	4.42	0.73	0.70	0.0328	4.50
PB	Day	Chla_RS 2monthlag	0.72	0.69	0.0302	4.17	0.73	0.70	0.0317	4.35
PB	Day	Chla_RS 3monthlag	0.72	0.69	0.0260	3.61	0.73	0.70	0.0284	3.91
PB	Day	Chla_RS 4monthlag	0.70	0.69	0.0083	1.18	0.71	0.70	0.0106	1.50
PB	Day	Chla_RS 5monthlag	0.69	0.69	-0.0047	-0.68	0.69	0.70	-0.0031	-0.45
PB	Day	Chla_RS 6monthlag	0.70	0.69	0.0057	0.82	0.70	0.70	0.0067	0.96
PB	Day	Chla_RS Nolag 10km	0.71	0.69	0.0144	2.03	0.71	0.70	0.0158	2.22
PB	Day	Chla_RS Nolag 20km	0.72	0.69	0.0217	3.03	0.72	0.70	0.0227	3.15

PB	Day	Chla_RS Nolag 30km	0.72	0.69	0.0276	3.83	0.73	0.70	0.0282	3.89
PB	Day	Chla_RS Nolag 40km	0.73	0.69	0.0315	4.34	0.73	0.70	0.0319	4.37
PB	Day	Chla_RS Nolag 50km	0.73	0.69	0.0344	4.72	0.73	0.70	0.0347	4.74
PB	Day	Chla_RS Nolag 75km	0.73	0.69	0.0349	4.79	0.73	0.70	0.0351	4.79
PB	Day	Chla_RS 1monthlag 10km	0.72	0.69	0.0293	4.05	0.73	0.70	0.0304	4.18
PB	Day	Chla_RS 1monthlag 20km	0.73	0.69	0.0321	4.42	0.73	0.70	0.0328	4.50
PB	Day	Chla_RS 1monthlag 30km	0.73	0.69	0.0333	4.58	0.73	0.70	0.0338	4.63
PB	Day	Chla_RS 1monthlag 50km	0.73	0.69	0.0374	5.12	0.73	0.70	0.0377	5.13
PB	Day	Chla_RS 1monthlag 75km	0.73	0.69	0.0374	5.12	0.73	0.70	0.0376	5.12
PB	Day	Chla_RS 1monthlag 100km	0.73	0.69	0.0329	4.52	0.73	0.70	0.0331	4.53
PB	Day	Chla_RS 1monthlag 150km	0.72	0.69	0.0272	3.77	0.72	0.70	0.0273	3.77
PB	Day	Chla_RS 2monthlag 10km	0.74	0.69	0.0420	5.70	0.74	0.70	0.0438	5.91
PB	Day	Chla_RS 2monthlag 20km	0.72	0.69	0.0302	4.17	0.73	0.70	0.0317	4.35
PB	Day	Chla_RS 2monthlag 30km	0.72	0.69	0.0309	4.27	0.73	0.70	0.0322	4.41
PB	Day	Chla_RS 2monthlag 50km	0.73	0.69	0.0344	4.72	0.73	0.70	0.0347	4.74
PB	Day	Chla_RS 2monthlag 75km	0.71	0.69	0.0147	2.07	0.71	0.70	0.0154	2.16
PB	Day	Chla_RS 2monthlag 100km	0.71	0.69	0.0148	2.08	0.71	0.70	0.0153	2.15
PB	Day	Chla_RS 2monthlag 150km	0.71	0.69	0.0149	2.10	0.71	0.70	0.0153	2.15
PB	Day	Chla_RS 3monthlag 20km	0.72	0.69	0.0260	3.61	0.73	0.70	0.0284	3.91

PB	Day	Chla_RS 3monthlag 30km	0.72	0.69	0.0265	3.68	0.73	0.70	0.0287	3.95
PB	Day	Chla_RS 3monthlag 50km	0.71	0.69	0.0209	2.93	0.72	0.70	0.0227	3.16
PB	Day	Chla_RS 3monthlag 75km	0.71	0.69	0.0164	2.31	0.72	0.70	0.0182	2.54
PB	Day	Chla_RS 3monthlag 100km	0.70	0.69	0.0081	1.16	0.71	0.70	0.0097	1.37
PB	Day	Chla_RS 3monthlag 150km	0.69	0.69	-0.0007	-0.10	0.70	0.70	0.0004	0.06
PB	Day	Chla_RS 4monthlag 10km	0.70	0.69	0.0067	0.96	0.71	0.70	0.0097	1.37
PB	Day	Chla_RS 4monthlag 20km	0.70	0.69	0.0083	1.18	0.71	0.70	0.0106	1.50
PB	Day	Chla_RS 4monthlag 30km	0.71	0.69	0.0148	2.09	0.71	0.70	0.0167	2.35
PB	Day	Chla_RS 4monthlag 50km	0.71	0.69	0.0156	2.20	0.71	0.70	0.0172	2.41
PB	Day	Chla_RS 4monthlag 75km	0.71	0.69	0.0159	2.24	0.71	0.70	0.0174	2.43
PB	Day	Chla_RS 4monthlag 100km	0.71	0.69	0.0160	2.26	0.71	0.70	0.0174	2.43
PB	Day	Chla_RS 4monthlag 150km	0.71	0.69	0.0128	1.82	0.71	0.70	0.0140	1.97
PM	Night	ChlMax	0.78	0.78	-0.0004	-0.05	0.78	0.78	-0.0002	-0.03
PM	Night	SurfaceChl	0.78	0.78	-0.0027	-0.35	0.78	0.78	-0.0024	-0.31
PM	Night	IntegratedChl	0.78	0.78	-0.0050	-0.65	0.78	0.78	-0.0049	-0.63
PM	Night	Chla_RS nolag	0.82	0.78	0.0374	4.55	0.82	0.78	0.0377	4.59
PM	Night	Chla_RS 1monthlag	0.83	0.78	0.0431	5.22	0.83	0.78	0.0436	5.27
PM	Night	Chla_RS 2monthlag	0.81	0.78	0.0293	3.60	0.81	0.78	0.0298	3.66
PM	Night	Chla_RS 3monthlag	0.84	0.78	0.0528	6.32	0.84	0.78	0.0530	6.33
PM	Night	Chla_RS 4monthlag	0.82	0.78	0.0368	4.49	0.82	0.78	0.0372	4.53
PM	Night	Chla_RS 5monthlag	0.77	0.78	-0.0148	-1.93	0.77	0.78	-0.0137	-1.77
PM	Night	Chla_RS 6monthlag	0.79	0.78	0.0110	1.38	0.80	0.78	0.0118	1.48
PM	Night	Chla_RS Nolag 10km	0.83	0.78	0.0437	5.29	0.83	0.78	0.0442	5.34

PM	Night	Chla_RS Nolag 20km	0.82	0.78	0.0374	4.55	0.82	0.78	0.0377	4.59
PM	Night	Chla_RS Nolag 30km	0.81	0.78	0.0295	3.63	0.81	0.78	0.0298	3.66
PM	Night	Chla_RS Nolag 40km	0.81	0.78	0.0273	3.38	0.81	0.78	0.0276	3.40
PM	Night	Chla_RS Nolag 50km	0.81	0.78	0.0279	3.44	0.81	0.78	0.0281	3.46
PM	Night	Chla_RS Nolag 75km	0.80	0.78	0.0202	2.52	0.80	0.78	0.0204	2.53
PM	Night	Chla_RS 1monthlag 10km	0.83	0.78	0.0466	5.62	0.83	0.78	0.0473	5.69
PM	Night	Chla_RS 1monthlag 20km	0.83	0.78	0.0431	5.22	0.83	0.78	0.0436	5.27
PM	Night	Chla_RS 1monthlag_30km	0.82	0.78	0.0326	3.99	0.82	0.78	0.0329	4.03
PM	Night	Chla_RS 1monthlag 50km	0.80	0.78	0.0221	2.75	0.81	0.78	0.0224	2.77
PM	Night	Chla_RS 1monthlag 75km	0.80	0.78	0.0179	2.24	0.80	0.78	0.0181	2.26
PM	Night	Chla_RS 1monthlag 100km	0.79	0.78	0.0120	1.52	0.80	0.78	0.0122	1.54
PM	Night	Chla_RS 1monthlag 150km	0.79	0.78	0.0054	0.68	0.79	0.78	0.0055	0.70
PM	Night	Chla_RS 2monthlag 10km	0.81	0.78	0.0271	3.35	0.81	0.78	0.0277	3.42
PM	Night	Chla_RS 2monthlag 20km	0.81	0.78	0.0293	3.60	0.81	0.78	0.0298	3.66
PM	Night	Chla_RS 2monthlag 30km	0.82	0.78	0.0339	4.15	0.82	0.78	0.0343	4.19
PM	Night	Chla_RS 2monthlag 50km	0.81	0.78	0.0279	3.44	0.81	0.78	0.0281	3.46
PM	Night	Chla_RS 2monthlag 75km	0.80	0.78	0.0215	2.68	0.81	0.78	0.0218	2.71
PM	Night	Chla_RS 2monthlag 100km	0.80	0.78	0.0176	2.20	0.80	0.78	0.0179	2.23
PM	Night	Chla_RS 2monthlag 150km	0.80	0.78	0.0162	2.02	0.80	0.78	0.0163	2.04
PM	Night	Chla_RS 3monthlag	0.84	0.78	0.0528	6.32	0.84	0.78	0.0530	6.33

		20km								
PM	Night	Chla_RS 3monthlag 30km	0.83	0.78	0.0471	5.68	0.83	0.78	0.0473	5.69
PM	Night	Chla_RS 3monthlag 50km	0.82	0.78	0.0367	4.48	0.82	0.78	0.0369	4.49
PM	Night	Chla_RS 3monthlag 75km	0.81	0.78	0.0287	3.54	0.81	0.78	0.0289	3.55
PM	Night	Chla_RS 3monthlag 100km	0.81	0.78	0.0253	3.13	0.81	0.78	0.0255	3.15
PM	Night	Chla_RS 3monthlag 150km	0.80	0.78	0.0204	2.54	0.80	0.78	0.0205	2.55
PM	Night	Chla_RS 4monthlag 10km	0.85	0.78	0.0694	8.15	0.85	0.78	0.0699	8.18
PM	Night	Chla_RS 4monthlag 20km	0.82	0.78	0.0368	4.49	0.82	0.78	0.0372	4.53
PM	Night	Chla_RS 4monthlag 30km	0.82	0.78	0.0339	4.15	0.82	0.78	0.0341	4.17
PM	Night	Chla_RS 4monthlag 50km	0.81	0.78	0.0253	3.13	0.81	0.78	0.0255	3.15
PM	Night	Chla_RS 4monthlag 75km	0.81	0.78	0.0253	3.13	0.81	0.78	0.0254	3.13
PM	Night	Chla_RS 4monthlag 100km	0.81	0.78	0.0265	3.27	0.81	0.78	0.0266	3.28
PM	Night	Chla_RS 4monthlag 150km	0.80	0.78	0.0143	1.80	0.80	0.78	0.0145	1.81
PM	Day	ChlMax	0.70	0.71	-0.0134	-1.92	0.70	0.71	-0.0130	-1.86
PM	Day	SurfaceChl	0.70	0.71	-0.0147	-2.11	0.70	0.71	-0.0143	-2.04
PM	Day	IntegratedChl	0.71	0.71	-0.0052	-0.73	0.71	0.71	-0.0051	-0.72
PM	Day	Chla_RS nolag	0.75	0.71	0.0357	4.77	0.75	0.71	0.0362	4.83
PM	Day	Chla_RS 1monthlag	0.74	0.71	0.0270	3.65	0.74	0.71	0.0278	3.75
PM	Day	Chla_RS 2monthlag	0.76	0.71	0.0501	6.56	0.76	0.71	0.0507	6.63
PM	Day	Chla_RS 3monthlag	0.75	0.71	0.0387	5.15	0.75	0.71	0.0391	5.19
PM	Day	Chla_RS 4monthlag	0.76	0.71	0.0449	5.92	0.76	0.71	0.0455	5.99
PM	Day	Chla_RS 5monthlag	0.73	0.71	0.0129	1.78	0.73	0.71	0.0142	1.95
PM	Day	Chla_RS 6monthlag	0.79	0.71	0.0804	10.13	0.79	0.71	0.0808	10.17
PM	Day	Chla_RS Nolag	0.75	0.71	0.0419	5.55	0.76	0.71	0.0426	5.63

		10km								
PM	Day	Chla_RS Nolag 20km	0.75	0.71	0.0357	4.77	0.75	0.71	0.0362	4.83
PM	Day	Chla_RS Nolag 30km	0.74	0.71	0.0242	3.28	0.74	0.71	0.0247	3.34
PM	Day	Chla_RS Nolag 40km	0.73	0.71	0.0221	3.01	0.74	0.71	0.0225	3.06
PM	Day	Chla_RS Nolag 50km	0.73	0.71	0.0125	1.72	0.73	0.71	0.0129	1.77
PM	Day	Chla_RS Nolag 75km	0.72	0.71	0.0063	0.87	0.72	0.71	0.0066	0.92
PM	Day	Chla_RS 1monthlag 10km	0.75	0.71	0.0346	4.63	0.75	0.71	0.0356	4.75
PM	Day	Chla_RS 1monthlag 20km	0.74	0.71	0.0270	3.65	0.74	0.71	0.0278	3.75
PM	Day	Chla_RS 1monthlag 30km	0.74	0.71	0.0279	3.77	0.74	0.71	0.0285	3.83
PM	Day	Chla_RS 1monthlag 50km	0.75	0.71	0.0360	4.81	0.75	0.71	0.0363	4.83
PM	Day	Chla_RS 1monthlag 75km	0.74	0.71	0.0227	3.09	0.74	0.71	0.0230	3.11
PM	Day	Chla_RS 1monthlag 100km	0.73	0.71	0.0168	2.31	0.73	0.71	0.0171	2.34
PM	Day	Chla_RS 1monthlag 150km	0.73	0.71	0.0129	1.78	0.73	0.71	0.0131	1.80
PM	Day	Chla_RS 2monthlag 10km	0.77	0.71	0.0581	7.54	0.77	0.71	0.0589	7.62
PM	Day	Chla_RS 2monthlag 20km	0.76	0.71	0.0501	6.56	0.76	0.71	0.0507	6.63
PM	Day	Chla_RS 2monthlag 30km	0.76	0.71	0.0432	5.72	0.76	0.71	0.0438	5.77
PM	Day	Chla_RS 2monthlag 50km	0.73	0.71	0.0125	1.72	0.73	0.71	0.0129	1.77
PM	Day	Chla_RS 2monthlag 75km	0.74	0.71	0.0276	3.73	0.74	0.71	0.0280	3.77
PM	Day	Chla_RS 2monthlag 100km	0.74	0.71	0.0308	4.14	0.75	0.71	0.0310	4.16
PM	Day	Chla_RS 2monthlag	0.74	0.71	0.0297	4.00	0.74	0.71	0.0298	4.01

		150km								
PM	Day	Chla_RS 3monthlag 20km	0.75	0.71	0.0387	5.15	0.75	0.71	0.0391	5.19
PM	Day	Chla_RS 3monthlag 30km	0.75	0.71	0.0327	4.38	0.75	0.71	0.0330	4.42
PM	Day	Chla_RS 3monthlag 50km	0.75	0.71	0.0328	4.40	0.75	0.71	0.0331	4.43
PM	Day	Chla_RS 3monthlag 75km	0.75	0.71	0.0327	4.39	0.75	0.71	0.0330	4.41
PM	Day	Chla_RS 3monthlag 100km	0.74	0.71	0.0265	3.59	0.74	0.71	0.0268	3.62
PM	Day	Chla_RS 3monthlag 150km	0.73	0.71	0.0194	2.65	0.73	0.71	0.0196	2.67
PM	Day	Chla_RS 4monthlag 10km	0.76	0.71	0.0435	5.75	0.76	0.71	0.0445	5.87
PM	Day	Chla_RS 4monthlag 20km	0.76	0.71	0.0449	5.92	0.76	0.71	0.0455	5.99
PM	Day	Chla_RS 4monthlag 30km	0.76	0.71	0.0460	6.06	0.76	0.71	0.0463	6.09
PM	Day	Chla_RS 4monthlag 50km	0.76	0.71	0.0472	6.21	0.76	0.71	0.0473	6.21
PM	Day	Chla_RS 4monthlag 75km	0.74	0.71	0.0294	3.97	0.74	0.71	0.0296	3.98
PM	Day	Chla_RS 4monthlag 100km	0.74	0.71	0.0236	3.20	0.74	0.71	0.0238	3.22
PM	Day	Chla_RS 4monthlag 150km	0.73	0.71	0.0166	2.28	0.73	0.71	0.0168	2.30
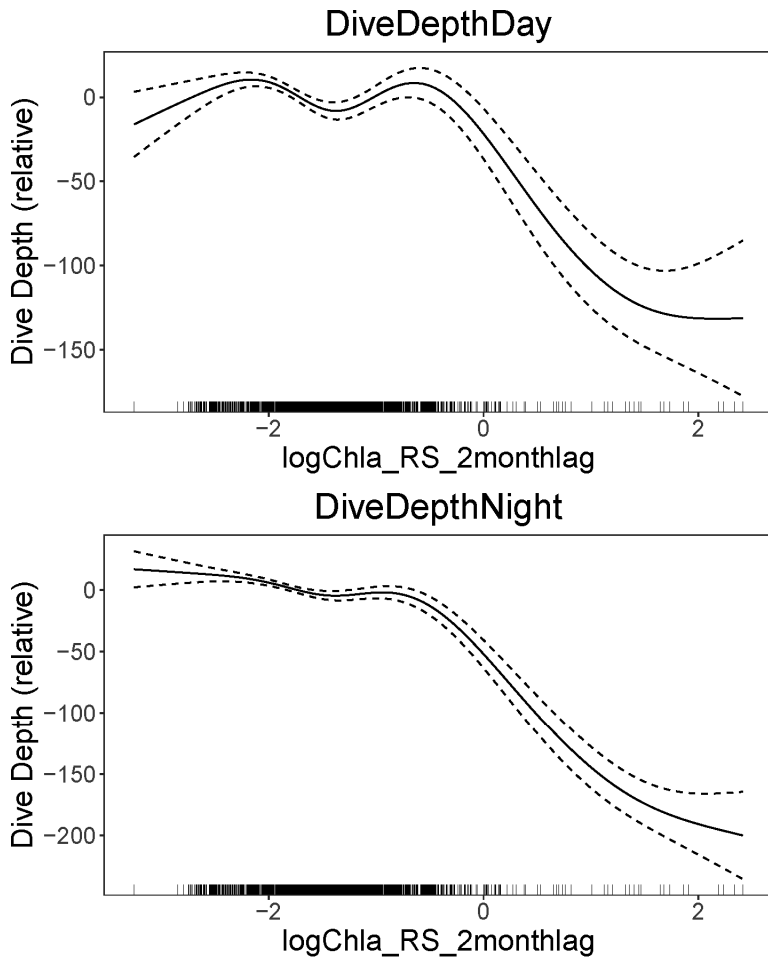
Figure 3.3. Smoother plots of mean daily dive depth showed shallower dives in relation to elevated chlorophyll concentrations.

Table 3.5. Change in explanatory power of GAMMs testing daily mean number of wiggles separated by season and day and night due to addition of chlorophyll covariates. Base model formula was gam(TransitRate ~ s(DayinTrip,k=6)+te(Latitude,Longitude)+s(SealID,bs="re"). All chlorophyll values were log-transformed. "RS" refers to remotely sensed data. Green shows values derived from *in situ* data. Blue shows remotely sensed data concurrent to seal presence. Yellow shows remotely sensed data prior to seal presence.

Season	Day or Night	Covariate	Model R^2	R^2 reduced model	Difference in R^2	% change in R^2	Model Deviance Explained	Deviance Explained Reduced Model	Difference in Deviance Explained	% change in Deviance Explained
PB	Night	ChlMax	0.56	0.54	0.0172	3.08	0.56	0.66	-0.0973	-17.23
PB	Night	SurfaceChl	0.52	0.54	-0.0248	-4.82	0.52	0.66	-0.1386	-26.50
PB	Night	IntegratedChl	0.52	0.54	-0.0239	-4.63	0.52	0.66	-0.1393	-26.67
PB	Night	Chla_RS nolag	0.59	0.54	0.0514	8.68	0.60	0.66	-0.0639	-10.70
PB	Night	Chla_RS 1monthlag	0.58	0.54	0.0359	6.22	0.58	0.66	-0.0792	-13.60
PB	Night	Chla_RS 2monthlag	0.62	0.54	0.0840	13.44	0.63	0.66	-0.0310	-4.91
PB	Night	Chla_RS 3monthlag	0.59	0.54	0.0482	8.18	0.60	0.66	-0.0646	-10.82
PB	Night	Chla_RS 4monthlag	0.60	0.54	0.0581	9.70	0.61	0.66	-0.0559	-9.22
PB	Night	Chla_RS 5monthlag	0.56	0.54	0.0169	3.03	0.56	0.66	-0.0975	-17.29
PB	Night	Chla_RS 6monthlag	0.56	0.54	0.0183	3.27	0.57	0.66	-0.0967	-17.11
PB	Night	Chla_RS Nolag 10km	0.59	0.54	0.0480	8.15	0.59	0.66	-0.0669	-11.24
PB	Night	Chla_RS Nolag 20km	0.59	0.54	0.0514	8.68	0.60	0.66	-0.0639	-10.70
PB	Night	Chla_RS Nolag 30km	0.59	0.54	0.0499	8.44	0.60	0.66	-0.0657	-11.02
PB	Night	Chla_RS Nolag 40km	0.59	0.54	0.0461	7.85	0.59	0.66	-0.0697	-11.76

PB	Night	Chla_RS Nolag 50km	0.58	0.54	0.0438	7.50	0.59	0.66	-0.0720	-12.21
PB	Night	Chla_RS Nolag 75km	0.57	0.54	0.0328	5.71	0.58	0.66	-0.0832	-14.37
PB	Night	Chla_RS 1monthlag 10km	0.58	0.54	0.0345	5.99	0.58	0.66	-0.0801	-13.76
PB	Night	Chla_RS 1monthlag 20km	0.58	0.54	0.0359	6.22	0.58	0.66	-0.0792	-13.60
PB	Night	Chla_RS 1monthlag 30km	0.59	0.54	0.0454	7.75	0.59	0.66	-0.0702	-11.86
PB	Night	Chla_RS 1monthlag 50km	0.61	0.54	0.0647	10.68	0.61	0.66	-0.0514	-8.43
PB	Night	Chla_RS 1monthlag 75km	0.60	0.54	0.0643	10.62	0.61	0.66	-0.0520	-8.53
PB	Night	Chla_RS 1monthlag 100km	0.62	0.54	0.0744	12.10	0.62	0.66	-0.0421	-6.79
PB	Night	Chla_RS 1monthlag 150km	0.62	0.54	0.0830	13.30	0.63	0.66	-0.0337	-5.37
PB	Night	Chla_RS 2monthlag 10km	0.63	0.54	0.0925	14.60	0.64	0.66	-0.0219	-3.42
PB	Night	Chla_RS 2monthlag 20km	0.62	0.54	0.0840	13.44	0.63	0.66	-0.0310	-4.91
PB	Night	Chla_RS 2monthlag 30km	0.62	0.54	0.0810	13.02	0.63	0.66	-0.0344	-5.49
PB	Night	Chla_RS 2monthlag 50km	0.58	0.54	0.0438	7.50	0.59	0.66	-0.0720	-12.21
PB	Night	Chla_RS 2monthlag 75km	0.61	0.54	0.0706	11.54	0.62	0.66	-0.0453	-7.34
PB	Night	Chla_RS 2monthlag 100km	0.61	0.54	0.0644	10.65	0.61	0.66	-0.0515	-8.43
PB	Night	Chla_RS 2monthlag 150km	0.60	0.54	0.0565	9.47	0.60	0.66	-0.0596	-9.89
PB	Night	Chla_RS 3monthlag 20km	0.59	0.54	0.0482	8.18	0.60	0.66	-0.0646	-10.82
PB	Night	Chla_RS 3monthlag 30km	0.57	0.54	0.0335	5.83	0.58	0.66	-0.0796	-13.67
PB	Night	Chla_RS 3monthlag 50km	0.56	0.54	0.0218	3.87	0.57	0.66	-0.0917	-16.08

PB	Night	Chla_RS 3monthlag 75km	0.55	0.54	0.0125	2.25	0.56	0.66	-0.1012	-18.06
PB	Night	Chla_RS 3monthlag 100km	0.55	0.54	0.0076	1.38	0.56	0.66	-0.1067	-19.22
PB	Night	Chla_RS 3monthlag 150km	0.55	0.54	0.0045	0.82	0.55	0.66	-0.1101	-19.96
PB	Night	Chla_RS 4monthlag 10km	0.62	0.54	0.0821	13.18	0.63	0.66	-0.0315	-4.99
PB	Night	Chla_RS 4monthlag 20km	0.60	0.54	0.0581	9.70	0.61	0.66	-0.0559	-9.22
PB	Night	Chla_RS 4monthlag 30km	0.59	0.54	0.0446	7.62	0.59	0.66	-0.0695	-11.73
PB	Night	Chla_RS 4monthlag 50km	0.59	0.54	0.0449	7.67	0.59	0.66	-0.0698	-11.78
PB	Night	Chla_RS 4monthlag 75km	0.57	0.54	0.0294	5.15	0.58	0.66	-0.0853	-14.80
PB	Night	Chla_RS 4monthlag 100km	0.56	0.54	0.0223	3.96	0.57	0.66	-0.0925	-16.25
PB	Night	Chla_RS 4monthlag 150km	0.54	0.54	-0.0008	-0.14	0.55	0.66	-0.1158	-21.21
PB	Day	ChlMax	0.62	0.59	0.0242	3.93	0.62	0.65	-0.0230	-3.70
PB	Day	SurfaceChl	0.60	0.59	0.0033	0.55	0.60	0.65	-0.0436	-7.25
PB	Day	IntegratedChl	0.59	0.59	0.0010	0.16	0.60	0.65	-0.0476	-7.96
PB	Day	Chla_RS nolag	0.63	0.59	0.0395	6.25	0.64	0.65	-0.0085	-1.33
PB	Day	Chla_RS 1monthlag	0.60	0.59	0.0090	1.50	0.61	0.65	-0.0382	-6.30
PB	Day	Chla_RS 2monthlag	0.64	0.59	0.0461	7.22	0.64	0.65	-0.0010	-0.15
PB	Day	Chla_RS 3monthlag	0.63	0.59	0.0423	6.66	0.64	0.65	-0.0034	-0.54
PB	Day	Chla_RS 4monthlag	0.66	0.59	0.0647	9.85	0.66	0.65	0.0177	2.67
PB	Day	Chla_RS 5monthlag	0.62	0.59	0.0289	4.65	0.63	0.65	-0.0184	-2.93
PB	Day	Chla_RS 6monthlag	0.61	0.59	0.0134	2.21	0.61	0.65	-0.0343	-5.62
PB	Day	Chla_RS Nolag 10km	0.63	0.59	0.0338	5.39	0.63	0.65	-0.0138	-2.19
PB	Day	Chla_RS Nolag 20km	0.63	0.59	0.0395	6.25	0.64	0.65	-0.0085	-1.33
PB	Day	Chla_RS Nolag 30km	0.63	0.59	0.0389	6.15	0.64	0.65	-0.0093	-1.45

PB	Day	Chla_RS Nolag 40km	0.63	0.59	0.0375	5.95	0.63	0.65	-0.0107	-1.69
PB	Day	Chla_RS Nolag 50km	0.63	0.59	0.0369	5.86	0.63	0.65	-0.0115	-1.81
PB	Day	Chla_RS Nolag 75km	0.62	0.59	0.0323	5.16	0.63	0.65	-0.0162	-2.57
PB	Day	Chla_RS 1monthlag 10km	0.60	0.59	0.0033	0.56	0.60	0.65	-0.0433	-7.20
PB	Day	Chla_RS 1monthlag 20km	0.60	0.59	0.0090	1.50	0.61	0.65	-0.0382	-6.30
PB	Day	Chla_RS 1monthlag 30km	0.62	0.59	0.0237	3.84	0.62	0.65	-0.0241	-3.88
PB	Day	Chla_RS 1monthlag 50km	0.63	0.59	0.0387	6.13	0.64	0.65	-0.0095	-1.50
PB	Day	Chla_RS 1monthlag 75km	0.63	0.59	0.0405	6.40	0.64	0.65	-0.0079	-1.24
PB	Day	Chla_RS 1monthlag 100km	0.63	0.59	0.0415	6.54	0.64	0.65	-0.0071	-1.11
PB	Day	Chla_RS 1monthlag 150km	0.65	0.59	0.0532	8.24	0.65	0.65	0.0044	0.68
PB	Day	Chla_RS 2monthlag 10km	0.65	0.59	0.0578	8.89	0.66	0.65	0.0112	1.70
PB	Day	Chla_RS 2monthlag 20km	0.64	0.59	0.0461	7.22	0.64	0.65	-0.0010	-0.15
PB	Day	Chla_RS 2monthlag 30km	0.64	0.59	0.0430	6.77	0.64	0.65	-0.0043	-0.68
PB	Day	Chla_RS 2monthlag 50km	0.63	0.59	0.0369	5.86	0.63	0.65	-0.0115	-1.81
PB	Day	Chla_RS 2monthlag 75km	0.62	0.59	0.0321	5.14	0.63	0.65	-0.0160	-2.54
PB	Day	Chla_RS 2monthlag 100km	0.62	0.59	0.0288	4.63	0.63	0.65	-0.0194	-3.10
PB	Day	Chla_RS 2monthlag 150km	0.61	0.59	0.0222	3.60	0.62	0.65	-0.0260	-4.19
PB	Day	Chla_RS 3monthlag 20km	0.63	0.59	0.0423	6.66	0.64	0.65	-0.0034	-0.54
PB	Day	Chla_RS 3monthlag 30km	0.63	0.59	0.0376	5.97	0.64	0.65	-0.0086	-1.35

PB	Day	Chla_RS 3monthlag 50km	0.62	0.59	0.0323	5.17	0.63	0.65	-0.0148	-2.34
PB	Day	Chla_RS 3monthlag 75km	0.62	0.59	0.0318	5.10	0.63	0.65	-0.0150	-2.38
PB	Day	Chla_RS 3monthlag 100km	0.62	0.59	0.0280	4.51	0.63	0.65	-0.0192	-3.06
PB	Day	Chla_RS 3monthlag 150km	0.62	0.59	0.0232	3.77	0.62	0.65	-0.0242	-3.89
PB	Day	Chla_RS 4monthlag 10km	0.66	0.59	0.0688	10.40	0.67	0.65	0.0223	3.34
PB	Day	Chla_RS 4monthlag 20km	0.66	0.59	0.0647	9.85	0.66	0.65	0.0177	2.67
PB	Day	Chla_RS 4monthlag 30km	0.66	0.59	0.0638	9.73	0.66	0.65	0.0165	2.50
PB	Day	Chla_RS 4monthlag 50km	0.65	0.59	0.0587	9.01	0.66	0.65	0.0111	1.69
PB	Day	Chla_RS 4monthlag 75km	0.65	0.59	0.0560	8.64	0.65	0.65	0.0084	1.28
PB	Day	Chla_RS 4monthlag 100km	0.65	0.59	0.0531	8.23	0.65	0.65	0.0054	0.83
PB	Day	Chla_RS 4monthlag 150km	0.62	0.59	0.0233	3.79	0.62	0.65	-0.0243	-3.91
PM	Night	ChlMax	0.72	0.71	0.0085	1.18	0.72	0.71	0.0141	1.96
PM	Night	SurfaceChl	0.72	0.71	0.0074	1.03	0.72	0.71	0.0130	1.81
PM	Night	IntegratedChl	0.72	0.71	0.0065	0.90	0.72	0.71	0.0120	1.66
PM	Night	Chla_RS_nolag	0.71	0.71	0.0034	0.48	0.72	0.71	0.0096	1.34
PM	Night	Chla_RS 1monthlag	0.73	0.71	0.0170	2.34	0.73	0.71	0.0233	3.20
PM	Night	Chla_RS 2monthlag	0.69	0.71	-0.0254	-3.70	0.69	0.71	-0.0186	-2.71
PM	Night	Chla_RS 3monthlag	0.70	0.71	-0.0093	-1.32	0.70	0.71	-0.0033	-0.46
PM	Night	Chla_RS 4monthlag	0.75	0.71	0.0378	5.05	0.75	0.71	0.0439	5.85
PM	Night	Chla_RS 5monthlag	0.76	0.71	0.0456	6.03	0.76	0.71	0.0519	6.84
PM	Night	Chla_RS 6monthlag	0.72	0.71	0.0139	1.92	0.73	0.71	0.0204	2.81
PM	Night	Chla_RS Nolag 10km	0.72	0.71	0.0081	1.12	0.72	0.71	0.0145	2.01
PM	Night	Chla_RS Nolag 20km	0.71	0.71	0.0034	0.48	0.72	0.71	0.0096	1.34

263

PM	Night	Chla_RS Nolag 30km	0.70	0.71	-0.0083	-1.18	0.70	0.71	-0.0024	-0.34
PM	Night	Chla_RS Nolag 40km	0.69	0.71	-0.0213	-3.10	0.69	0.71	-0.0153	-2.21
PM	Night	Chla_RS Nolag 50km	0.70	0.71	-0.0154	-2.21	0.70	0.71	-0.0095	-1.36
PM	Night	Chla_RS Nolag 75km	0.70	0.71	-0.0127	-1.82	0.70	0.71	-0.0069	-0.99
PM	Night	Chla_RS 1monthlag 10km	0.72	0.71	0.0063	0.87	0.72	0.71	0.0128	1.78
PM	Night	Chla_RS 1monthlag 20km	0.73	0.71	0.0170	2.34	0.73	0.71	0.0233	3.20
PM	Night	Chla_RS 1monthlag 30km	0.72	0.71	0.0134	1.86	0.73	0.71	0.0195	2.69
PM	Night	Chla_RS 1monthlag 50km	0.69	0.71	-0.0179	-2.58	0.69	0.71	-0.0121	-1.74
PM	Night	Chla_RS 1monthlag 75km	0.70	0.71	-0.0065	-0.92	0.71	0.71	-0.0009	-0.12
PM	Night	Chla_RS 1monthlag 100km	0.71	0.71	-0.0003	-0.05	0.71	0.71	0.0054	0.75
PM	Night	Chla_RS 1monthlag 150km	0.72	0.71	0.0068	0.95	0.72	0.71	0.0124	1.73
PM	Night	Chla_RS 2monthlag 10km	0.66	0.71	-0.0457	-6.88	0.67	0.71	-0.0387	-5.80
PM	Night	Chla_RS 2monthlag 20km	0.69	0.71	-0.0254	-3.70	0.69	0.71	-0.0186	-2.71
PM	Night	Chla_RS 2monthlag 30km	0.70	0.71	-0.0068	-0.97	0.71	0.71	-0.0005	-0.06
PM	Night	Chla_RS 2monthlag 50km	0.70	0.71	-0.0154	-2.21	0.70	0.71	-0.0095	-1.36
PM	Night	Chla_RS 2monthlag 75km	0.72	0.71	0.0098	1.35	0.72	0.71	0.0155	2.15
PM	Night	Chla_RS 2monthlag 100km	0.72	0.71	0.0067	0.94	0.72	0.71	0.0125	1.74
PM	Night	Chla_RS 2monthlag 150km	0.72	0.71	0.0061	0.85	0.72	0.71	0.0118	1.64
PM	Night	Chla_RS 3monthlag 20km	0.70	0.71	-0.0093	-1.32	0.70	0.71	-0.0033	-0.46

PM	Night	Chla_RS 3monthlag 30km	0.70	0.71	-0.0082	-1.17	0.70	0.71	-0.0022	-0.32
PM	Night	Chla_RS 3monthlag 50km	0.71	0.71	-0.0004	-0.06	0.71	0.71	0.0054	0.76
PM	Night	Chla_RS 3monthlag 75km	0.71	0.71	0.0015	0.21	0.71	0.71	0.0072	1.01
PM	Night	Chla_RS 3monthlag 100km	0.72	0.71	0.0089	1.24	0.72	0.71	0.0146	2.02
PM	Night	Chla_RS 3monthlag 150km	0.72	0.71	0.0083	1.16	0.72	0.71	0.0140	1.94
PM	Night	Chla_RS 4monthlag 10km	0.76	0.71	0.0530	6.94	0.77	0.71	0.0593	7.74
PM	Night	Chla_RS 4monthlag 20km	0.75	0.71	0.0378	5.05	0.75	0.71	0.0439	5.85
PM	Night	Chla_RS 4monthlag 30km	0.73	0.71	0.0223	3.05	0.73	0.71	0.0282	3.84
PM	Night	Chla_RS 4monthlag 50km	0.73	0.71	0.0218	2.98	0.73	0.71	0.0275	3.75
PM	Night	Chla_RS 4monthlag 75km	0.73	0.71	0.0166	2.29	0.73	0.71	0.0222	3.05
PM	Night	Chla_RS 4monthlag 100km	0.73	0.71	0.0174	2.39	0.73	0.71	0.0229	3.14
PM	Night	Chla_RS 4monthlag 150km	0.73	0.71	0.0162	2.23	0.73	0.71	0.0217	2.98
PM	Day	ChlMax	0.77	0.77	0.0042	0.54	0.78	0.78	-0.0081	-1.04
PM	Day	SurfaceChl	0.77	0.77	0.0044	0.57	0.78	0.78	-0.0077	-1.00
PM	Day	IntegratedChl	0.78	0.77	0.0103	1.33	0.78	0.78	-0.0021	-0.27
PM	Day	Chla_RS_nolag	0.77	0.77	-0.0019	-0.25	0.77	0.78	-0.0136	-1.77
PM	Day	Chla_RS 1monthlag	0.75	0.77	-0.0232	-3.10	0.75	0.78	-0.0345	-4.61
PM	Day	Chla_RS 2monthlag	0.73	0.77	-0.0370	-5.06	0.73	0.78	-0.0482	-6.56
PM	Day	Chla_RS 3monthlag	0.77	0.77	-0.0020	-0.26	0.77	0.78	-0.0138	-1.79
PM	Day	Chla_RS 4monthlag	0.80	0.77	0.0354	4.40	0.81	0.78	0.0234	2.91
PM	Day	Chla_RS 5monthlag	0.79	0.77	0.0226	2.85	0.79	0.78	0.0110	1.39
PM	Day	Chla_RS 6monthlag	0.75	0.77	-0.0174	-2.32	0.75	0.78	-0.0287	-3.81
PM	Day	Chla_RS Nolag 10km	0.76	0.77	-0.0119	-1.57	0.76	0.78	-0.0233	-3.07

PM	Day	Chla_RS Nolag 20km	0.77	0.77	-0.0019	-0.25	0.77	0.78	-0.0136	-1.77
PM	Day	Chla_RS Nolag 30km	0.77	0.77	-0.0031	-0.40	0.77	0.78	-0.0149	-1.94
PM	Day	Chla_RS Nolag 40km	0.77	0.77	0.0025	0.32	0.77	0.78	-0.0095	-1.23
PM	Day	Chla_RS Nolag 50km	0.77	0.77	0.0021	0.27	0.77	0.78	-0.0100	-1.30
PM	Day	Chla_RS Nolag 75km	0.77	0.77	0.0028	0.36	0.77	0.78	-0.0094	-1.21
PM	Day	Chla_RS 1monthlag 10km	0.73	0.77	-0.0383	-5.24	0.73	0.78	-0.0491	-6.69
PM	Day	Chla_RS 1monthlag 20km	0.75	0.77	-0.0232	-3.10	0.75	0.78	-0.0345	-4.61
PM	Day	Chla_RS 1monthlag 30km	0.75	0.77	-0.0230	-3.09	0.75	0.78	-0.0347	-4.63
PM	Day	Chla_RS 1monthlag 50km	0.76	0.77	-0.0134	-1.77	0.76	0.78	-0.0253	-3.34
PM	Day	Chla_RS 1monthlag 75km	0.76	0.77	-0.0056	-0.73	0.77	0.78	-0.0176	-2.30
PM	Day	Chla_RS 1monthlag 100km	0.77	0.77	-0.0016	-0.20	0.77	0.78	-0.0137	-1.78
PM	Day	Chla_RS 1monthlag 150km	0.78	0.77	0.0121	1.54	0.78	0.78	-0.0002	-0.03
PM	Day	Chla_RS 2monthlag 10km	0.72	0.77	-0.0496	-6.90	0.72	0.78	-0.0605	-8.37
PM	Day	Chla_RS 2monthlag 20km	0.73	0.77	-0.0370	-5.06	0.73	0.78	-0.0482	-6.56
PM	Day	Chla_RS 2monthlag 30km	0.73	0.77	-0.0348	-4.74	0.74	0.78	-0.0463	-6.29
PM	Day	Chla_RS 2monthlag 50km	0.77	0.77	0.0021	0.27	0.77	0.78	-0.0100	-1.30
PM	Day	Chla_RS 2monthlag 75km	0.76	0.77	-0.0125	-1.65	0.76	0.78	-0.0244	-3.21
PM	Day	Chla_RS 2monthlag 100km	0.77	0.77	0.0021	0.27	0.77	0.78	-0.0100	-1.29
PM	Day	Chla_RS 2monthlag 150km	0.78	0.77	0.0092	1.18	0.78	0.78	-0.0031	-0.39

| PM	Day	Chla_RS 3monthlag 20km	0.77	0.77	-0.0020	-0.26	0.77	0.78	-0.0138	-1.79
PM	Day	Chla_RS 3monthlag 30km	0.77	0.77	-0.0011	-0.14	0.77	0.78	-0.0130	-1.68
PM	Day	Chla_RS 3monthlag 50km	0.77	0.77	0.0011	0.14	0.77	0.78	-0.0109	-1.41
PM	Day	Chla_RS 3monthlag 75km	0.77	0.77	-0.0002	-0.03	0.77	0.78	-0.0122	-1.59
PM	Day	Chla_RS 3monthlag 100km	0.77	0.77	0.0017	0.22	0.77	0.78	-0.0104	-1.35
PM	Day	Chla_RS 3monthlag 150km	0.77	0.77	0.0042	0.54	0.78	0.78	-0.0080	-1.03
PM	Day	Chla_RS 4monthlag 10km	0.81	0.77	0.0391	4.84	0.81	0.78	0.0275	3.39
PM	Day	Chla_RS 4monthlag 20km	0.80	0.77	0.0354	4.40	0.81	0.78	0.0234	2.91
PM	Day	Chla_RS 4monthlag 30km	0.80	0.77	0.0334	4.16	0.80	0.78	0.0213	2.64
PM	Day	Chla_RS 4monthlag 50km	0.79	0.77	0.0220	2.78	0.79	0.78	0.0098	1.24
PM	Day	Chla_RS 4monthlag 75km	0.79	0.77	0.0155	1.98	0.79	0.78	0.0033	0.41
PM	Day	Chla_RS 4monthlag 100km	0.78	0.77	0.0151	1.93	0.79	0.78	0.0029	0.36
PM	Day	Chla_RS 4monthlag 150km	0.78	0.77	0.0111	1.43	0.78	0.78	-0.0011	-0.14
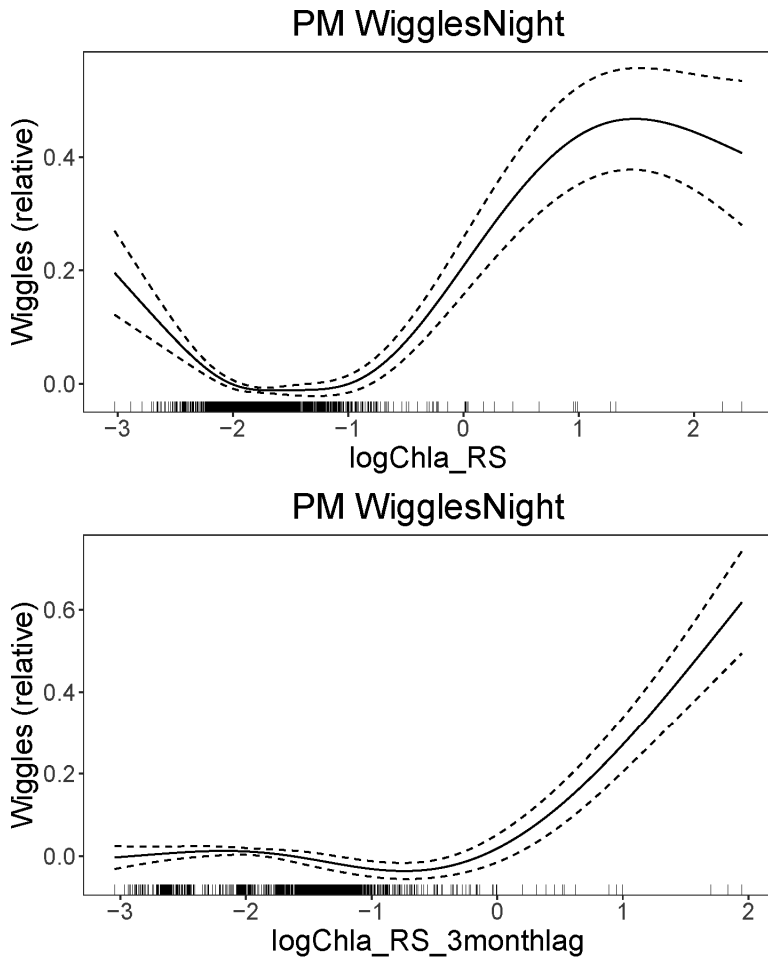
Figure 3.4. Higher number of mean daily wiggles were associated with elevated chlorophyll concentrations at night during the PM trip.
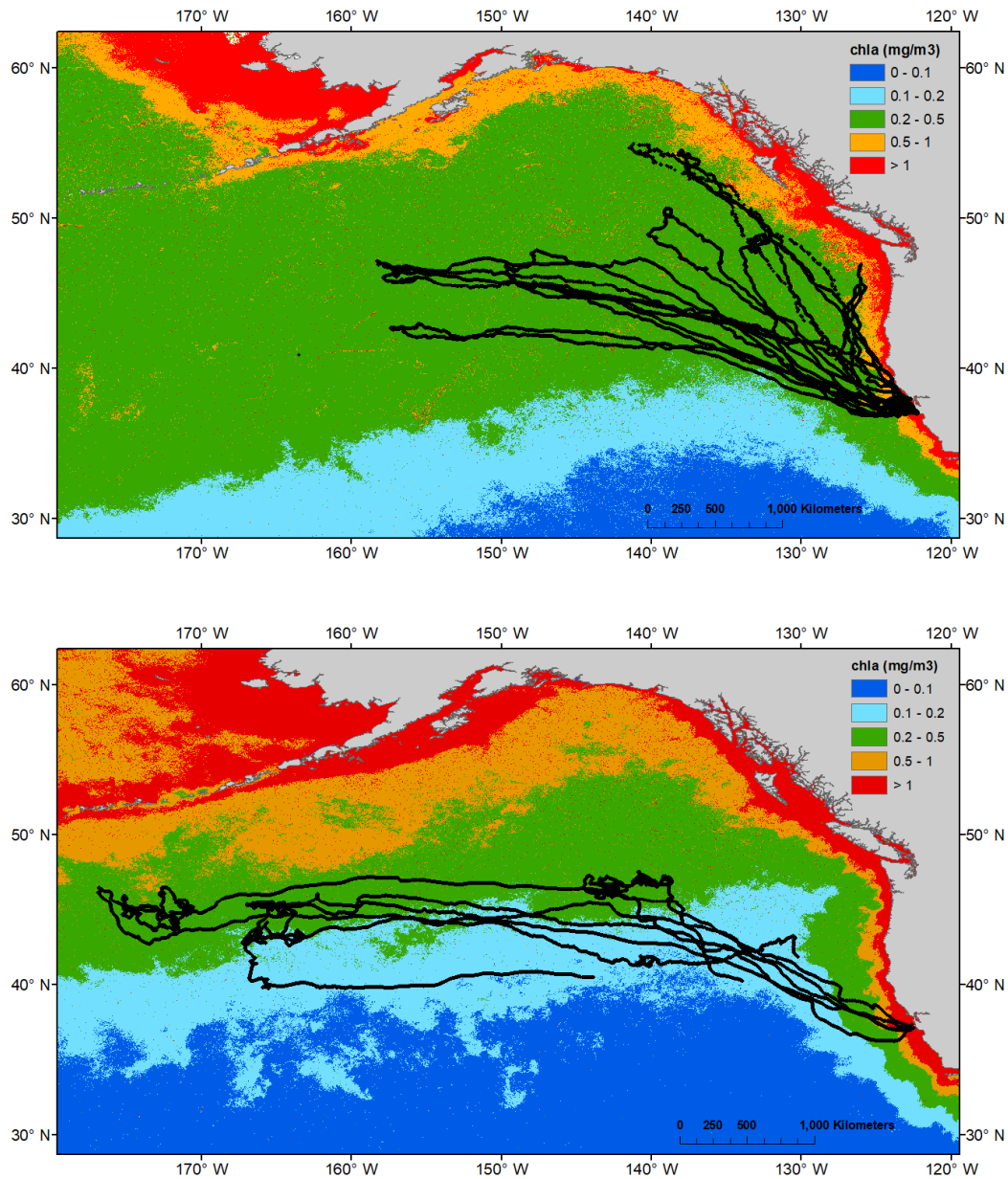
Figure 3.5. Tracks of northern elephant seals during their post-breeding trip (top panel) and post-molt trip (bottom panel) overlaid on mean monthly chlorophyll 2015-2021 for the approximate mid-point of each trip (March-April for PB, September-October for PM). The Transition Zone Chlorophyll Front is operationally defined at the 0.2 mg/m3 isopleth, shown here as the boundary between green and light blue. Chlorophyll data are 750 m resolution from VIIRS, downloaded from NOAA CoastWatch ERDDAP dataset ID erdVHNchlamday.

Conclusion

Understanding the relationship between dynamic oceanographic features and the abundance and distribution of higher trophic levels is important to predicting ecosystem responses to a changing world. To test the influence of oceanography on a mesopelagic predator whose prey is especially poorly understood, this dissertation leverages behavioral and *in situ* oceanographic data from long-term tracking of elephant seals during their long offshore migrations. The influence of eddies and of primary productivity on northern elephant seal foraging behavior in the northeast Pacific were tested to investigate physical and biological drivers of mesopelagic prey abundance and distribution, as inferred by seal behavior. Analogous tracking and hydrographic data from a closely related species in the Southern Ocean, the southern elephant seal, enabled a comparison of oceanographic influence of temperature, salinity, and mixing on mesopelagic predators in two different ocean basins.

Dynamic oceanographic features such as mesoscale eddies (Chapter 1), temperature and salinity boundaries (Chapter 2), and elevated primary productivity (Chapter 3) often triggered elevated foraging behavior. All effects on movement behavior were strongest at mesoscales, about 100 – 300 km. However, the relationship between these features and seal behavior is influenced also by internal influences on seal behavior. Intrinsic influences on seal behavior were significant, with the timing within a trip the largest predictor of seal behavior. Individual seals' experiences and personality in terms of risk taking vs. site fidelity affect decision

making and complicate these relationships. In addition, their two distinct foraging trips, post-breeding and post-molt, differ in length and physiological needs to regain body condition before returning to the colony to give birth or to molt. While it is difficult to fully separate intrinsic and extrinsic influences, environmental influences remained when accounting for internal factors and individuals in our statistical models.

While seals experience different internal pressures between their post-breeding and post-molting foraging trips, there are also seasonal differences in their environment when these trips occur. This is especially well-documented for the surface ocean with the effects on the mesopelagic zone more poorly understood. Seals showed faster, more directed movement post-breeding and greater exploitation of mesoscale features, especially horizontal physical variability, during the longer post-molt trip. The main habitat differences relevant to seals inferred from these chapters are higher primary productivity during the post-breeding trip and a patchier prey field during the post-molt trip. These patterns emerged in both northern and southern elephant seals.

We found the influence of oceanographic environment to be particularly strong at mesoscales, but the temporal scales were additionally important to consider, requiring the use of modeled and remotely sensed data in addition to *in situ* data collected by instruments carried by seals. We found a 2-4 month time lag between elevated primary productivity and increased seal foraging behavior in Chapter 3, giving an approximation of the time required for increased phytoplankton abundance near the

surface to translate to mesopelagic depths and to mid-trophic level prey such as myctophid fish. This time frame is consistent with other studies considering shallower and/or lower trophic level responses.

These patterns in elephant seal behavior relative to oceanographic features illustrate the importance of considering spatiotemporal scale in bottom-up ecosystem processes and the relevance of a predator's behavioral context when making inferences based on reactions to their environment. Life in the mesopelagic zone is linked to surface processes but due to time required for translation to depth and through trophic levels, the relationship between dynamic oceanographic features and a predator's behavior may be spread over space and time and therefore challenging to detect. While oceanographic data collected *in situ* by the predators themselves enables valuable documentation of subsurface conditions at the scale at which the predator experiences them, incorporating oceanographic data that can resolve larger spatiotemporal context, modeled and remotely sensed data, created a more well-rounded representation of a seal's relationship to its dynamic environment at the scales examined. Combining animal tracking and oceanographic data, we gained insight into the ecological relevance of dynamic ocean processes. We found that mesoscale features influenced elephant seal behavior, especially during their post-molt trip. These relationships were better detected by supplementing with modeled and remotely sensed data than using *in situ* data alone. We inferred that physical prey aggregation at temperature and salinity boundaries was a likely mechanism for creating rich foraging opportunities in association with such mesoscale features. For

ecological bottom-up processes to be relevant to foraging seals, several months of time elapsing after elevated primary productivity may be required for a biological response in the mesopelagic zone. Quantifying spatial and temporal scales of these relationships improve our ability to infer subsurface biological effects of near-surface phenomena that are easier to detect across large scales, which can be used to predict ecosystem consequences of a changing environment. Further work examining the influence of oceanography at various scales on seals' responses over larger time periods, from foraging success across a full foraging trip to reproductive success throughout a seal's lifetime, will help us understand the influence of a warming ocean on the population of this marine predator. This will allow us to infer changes occurring to elephant seals' mesopelagic prey and to other pelagic predators occupying a similar ecological niche.